Nitrogen removal using partial nitritation-anammox process

by **Songkai Qiu** MEng.Sc., BEng.

Civil Engineering, College of Engineering & Informatics, National University of Ireland, Galway, Ireland

Research Supervisor:

Prof. Xinmin Zhan, Civil Engineering, NUI Galway

Professor of Civil Engineering: Padraic E. O'Donoghue

A thesis submitted in fulfillment of the requirements for the degree of

Doctor of Philosophy,

in the College of Engineering and Informatics, National University of Ireland, Galway, Ireland

July 2019

Abstract

The partial nitritation-anammox (PN-A) process is a promising biological nitrogen-removal process. Compared with the conventional autotrophic nitrification-heterotrophic denitrification process, it requires no organic carbon and a less aeration demand. However, it has limitations: the main functional microbes, anammox bacteria, are slow-growing and sensitive to operating conditions (dissolved oxygen, temperature, etc.); it is challenging to suppress undesired nitrite oxidizing bacteria (NOB), especially for mainstream wastewater treatment; greenhouse gas nitrous oxide (N_2O) is produced and emitted. These limitations lead to the following research questions for the application of PN-A process: 1) start-up from conventional activated sludge when no anammox sludge is available; 2) understanding of pathways and mechanisms controlling the N_2O generation in PN-A process; 3) reliable and accurate oxygen input control to maintain NOB suppression, and 4) long-term stable nitrogen removal in mainstream wastewater treatment at around 20 °C.

This research aimed to address these research questions by 1) starting up the PN-A process using return sludge in an intermittently aerated sequencing batch reactor (IASBR); 2) investigating the main N_2O generation pathways and the mechanisms of operable factors in regulating N_2O generation in the IASBR; 3) developing a novel system (a Simple Process for Autotrophic Nitrogen-removal, SPAN) to achieve accurate oxygen input control and NOB suppression; and 4) investigating the long-term nitrogen removal performance of SPAN reactor in mainstream wastewater treatment at around 20°C.

The results proved that the PN-A process was able to start up from return sludge in a partial nitritation IASBR by reducing the aeration rate. Anammox bacteria, with the dominant genus *Candidatus Kuenenia*, were enriched in the PN-A IASBR. *Nitrosomonas* and *Candidatus Nitrososphaera* were the main ammonium-oxidizing microbes. *Nitrospira* was effectively restrained (abundance <1.6%). Nitritation accounted for 69% of the N_2O generation. N_2O generation via nitritation was governed by both nitritation activity and oxygen transfer: when oxygen transfer was the limiting factor, a higher oxygen transfer rate led to a higher nitritation activity, and increased the peak value of the N_2O generation rate (PVG); when nitritation was the limiting factor, the increase of the oxygen transfer

rate led to slightly reduced PVG; a higher oxygen transfer rate always led to a shorter duration of the peak N_2O generation rate. Lower initial ammonium concentration reduced the N_2O generation mainly by reducing the PVG.

The novel SPAN system precisely delivers oxygen to meet the oxygen demand of PN-A process by simply circulating the wastewater instead of using conventional aeration systems. With the negligible contribution of heterotrophic denitrification, > 99% of NH_4^+-N and > 81% of TN were removed. Anammox bacteria were efficiently enriched with an abundance of 8.17%, while AOB were well controlled and NOB were effectively suppressed.

The long-term stable nitrogen removal of SPAN in mainstream wastewater treatment was verified in a lab-scale reactor at around 20 °C. Using suspended sludge, long-term stable nitrogen removal was maintained. Using biofilm configuration, anammox capacity was effectively enhanced while the NOB activity in the reactor was suppressed. Stable nitrogen removal was achieved with TN removal efficiency of 61.8 ± 5.4% and nitrogen removal rate of 53.8 ± 4.7 mg N /L/d.

The results indicate that it's possible to overcome the challenges limiting PN-A process from wider applications. With the SPAN technology developed, the realization of long-term, stable nitrogen removal in the mainstream wastewater treatment moves towards the application of the conceptual energy-positive municipal wastewater treatment.

Table of contents

List of tables

List of figures

Declarations

This thesis or any part thereof, has not been, or is not currently being submitted for any degree at any other university.

Author

The work reported herein is as a result of my own investigations, except where acknowledged and referenced.

Author

Acknowledgments

It’s time to express my very great appreciation to many people, who have generously contributed to the work presented in this thesis.

I would like to express my deepest appreciation to my supervisor, Prof. Xinmin Zhan. I thank Prof. Zhan wholeheartedly not only for his tremendous research support and his encouragement over four years, but for so much entertain prepared by him, his wife Jin Xu and his children. The yummy food and fun at his home were always a boost to help me pass the rough road to finish this thesis. During the most difficult times when doing the experiments and writing this thesis, Prof. Zhan was always available to give guidance with his wisdom and his academic insights. This work would not have been possible without his supervision.

Special mention goes to my graduate research committee, Prof. Padraic E. O'Donoghue, Dr. Bryan McCabe, and Dr. Stephen Nash, who have guided me through all four years. Thanks to them for their valuable advice. I am also hugely indebted to Prof. Lvjun Chen at Tsinghua University and Prof. Rui Liu at Yangtze Delta Region Institute of Tsinghua University for their guidance and support.

I wish to acknowledge the financial support of the China Scholarship Council (Ref: 201408330180).

I would like to thank Dr. Alexandre Barretto de Menezes at National University of Ireland, Galway (NUIG), Dr. Maria Barrett at NUIG, Dr Enrico Tatti at NUIG, and Dr. Cindy Smith at University of Glasgow for their assistance in providing training, experimental facilities, and academic suggestions. I must also thank Dr. Jianping Li at CNP Water and Environmental Limited for providing seeding sludge, company AnoxKaldnes for providing biofilm carriers, as well as Dr. Dinesh Kumar and Prof. Anne Marie Healy at Trinity College Dublin for their assistance in the analysis.

I would like to express my sincere thanks to the colleagues in our group and in the lab, who have helped me made this work happen. Special thanks go to Dr. Yuansheng Hu, who gave many valuable suggestions on the draft, Mr. Qingfeng Yang, who helped me a lot with the sludge collection, as well as Mr. Shun Wang and Mr. Zhongzhong Wang, who took good care of my reactors for me when I was away. Great thanks also go to all the staff and technicians of Civil Engineering. I would like to offer my special thanks to my great friends in Ireland.

Finally, my deepest thanks go to the most basic source of my life strength, my family: my parents, my siblings, and my wife Xiaolin Sheng. They have unconditionally supported me all these years whenever I needed it. Their unwavering and unselfish love and support to me make this work possible.

List of Abbreviations

3OC6-HSL	3-oxohexanoyl-homoserine lactone
Anf	Iron (Fe)-containing nitrogenases
A/O	Anoxic/oxic process
AAO	Aerobic ammonium oxidation rate
AHLs	Acyl-homoserine lactones
Amo	Ammonium monooxygenase
Anammox	Anaerobic ammonium oxidation
ANITA™Mox	PN-A process using MBBR technology
ANO	Aerobic nitrite oxidation rate
AOA	Ammonium oxidizing archaea
AOB	Ammonium oxidizing bacteria
ATP	Adenosine triphosphate
ATU	Allylthiourea
BNR	Biological nitrogen removal
BOD	Biological oxygen demand
C12-HSL	N-dodecanoyl homoserine lactone
C6-HSL	N-hexanoyl homoserine lactone
C8-HSL	N-octanoyl homoserine lactone
CANON	Completely autotrophic nitrogen-removal over nitrite
COD	Chemical oxygen demand
CY	Cumulative N_2O yield
DEMON	Deammonification, pH-based intermittent aeration, and feed control
DIB	Deammonification in interval-aerated biofilm
DNA	Deoxyribonucleic acid
DO	Dissolved oxygen
DPG	Duration of the peak N_2O generation rate
ELAN	PN-A process with granular biomass
EPS	Extracellular polymeric substances

FNA	Free nitrous acid
Hao	Hydroxylamine oxidoreductase
HD	Heterotrophic denitrification
HRT	Hydraulic retention time
IASBR	Intermittently aerated sequencing batch reactor
IFAS	Integrated fixed-film activated sludge reactor
KEGG	Kyoto encyclopedia of genes and genomes
K_La	Volumetric oxygen transfer coefficient
MBBR	Moving bed biofilm reactor
MBR	Membrane bioreactor
MWTP	Municipal wastewater treatment plant
Nrf	Nitrite reductase (cytochrome c-552)
Nir	Nitrite reductase (NO-forming)
Nap	Periplasmic nitrate reductase
NAR	Nitrite accumulation rate
Nar	Cytoplasmic nitrate reductase
Nif	Molybdenum (Mo)-containing nitrogenases
NLR	Nitrogen loading rate
NOB	Nitrite oxidizing bacteria
Nor	Nitric oxide reductase
Nos	Nitrous oxide reductase
NRR	Nitrogen removal rate
ODR	Oxygen demand rate
OLAND	Oxygen-limited autotrophic nitrification-denitrification
ORF	Open reading frame
ORP	Oxidation reduction potential
OTA	Oxygen transfer amount
OTE	Oxygen transfer efficiency
OTR	Oxygen transfer rate
OTU	Operational taxonomic units
PCR	Polymerase chain reaction

PICRUSt	Phylogenetic investigation of communities by reconstruction of unobserved states
PN-A	Partial nitritation-anammox
PVG	Peak value of the N_2O generation rate
SAM	S-adenosylmethionine
SBR	Sequencing batch reactor
SNAD	Simultaneous partial nitrification, anammox and denitrification
SNAP	Single stage nitrogen removal using anammox and partial nitritation
SPAN	A simple process for autotrophic nitrogen-removal
SRT	Sludge retention time
TN	Total nitrogen
UASB	Up-flow anaerobic sludge blanket reactors
VSS	Volatile suspended sludge

Chapter 1
Introduction

1.1 Research background

Increasing population, food production (agriculture, animal operations, and aquaculture), and energy production lead to significant losses of nitrogen (organic nitrogen, ammonium-nitrogen (NH_4^+-N), nitrate-nitrogen (NO_3^--N), and nitrite-nitrogen (NO_2^--N)) to the water environment [1]. Municipal wastewater treatment plants (MWTPs) that receive domestic wastewater, and sometimes industrial and agricultural wastewater, are important sinks of the lost nitrogen. Too much nitrogen in the water bodies causes a serious worldwide environmental problem: eutrophication. Eutrophication refers to the excessive growth of plants and algae [2], and causes adverse environmental impacts, including 1) the deterioration of the water quality of water bodies (reduced transparency, increased odor, and toxicity, etc.), and 2) reduction of biodiversity due to the depletion of dissolved oxygen (DO), resulting from the decomposition of the dead algae [3]. The economic loss due to eutrophication in the U.S. alone is approximately $2.2 billion annually [2]. Thus, nitrogen in the wastewater must be reduced to a required level in the MWTPs to avoid nitrogen over-load to the receiving aquatic environments.

Nitrogen pollutants entering the MWTPs, mostly in the form of ammonium, are removed in the mainline (mainstream) wastewater treatment facilities through biological nitrogen removal (BNR) process with two successive steps: 1) aerobic (autotrophic) nitrification in which ammonium is oxidized to nitrite mainly by ammonium oxidizing bacteria (AOB) and then oxidized to nitrate by nitrite oxidizing bacteria (NOB), but AOB and NOB demand oxygen which is introduced by aeration, and 2) anoxic and heterotrophic denitrification in which nitrate is stepwise reduced to nitrite, nitric oxide (NO), nitrous oxide (N_2O), and nitrogen gas by heterotrophic denitrifiers; in this step, organic carbon (measured as chemical oxygen demand, COD) is needed to serve as the electron donors. Part of the nitrogen, together with organic carbon and phosphorus, is consumed by the microorganisms and metabolized to new biomass (i.e., sludge) which must be separated from the treated wastewater and properly handled through a series of processes such as thickening, anaerobic digestion, dewatering, etc. Side-stream wastewater, characterized by high ammonium concentrations and moderate temperature, mainly comes from the sludge-

handling process, and includes the supernatant from anaerobic digesters, the centrate/filtrate from dewatering units, and sometimes the reject stream from advanced membrane treatment units. The side streams which usually account for 15% - 20% of the total nitrogen (TN) entering the MWTPs [4, 5], are conventionally returned to the headworks of the MWTPs and are treated together with the mainstream wastewater. Some industrial wastewaters have high ammonium and need proper treatment. These wastewaters come from the food-production industry (such as meat processing, potato processing, yeast production, starch production, and monosodium glutamate production), the manufacturing industry (such as tannery and semiconductor), and waste disposal (such as landfill leachate) [6].

The BNR process is, however, energy and resource intensive, due to aeration and the extra organic carbon addition. In 1995, a new nitrogen-removal process, anaerobic ammonium oxidation (anammox), was discovered as a promising energy-efficient alternative [7]. The responsible microorganisms, anammox bacteria, convert ammonium together with nitrite to nitrogen gas, and they are both anaerobic and autotrophic, which means neither aeration or extra organic carbon addition is required (Equation 1-1) [8]. Partial nitritation, through which only about 37% of the oxygen-input demanded by BNR is needed to oxidize about half of the ammonium to nitrite by AOB, is needed to serve nitrite for the anammox bacteria. These two processes, partial nitritation and anammox, can be combined in one single reactor to allow the application of the partial nitritation-anammox (PN-A). The application of PN-A process in the MWTPs makes it possible for energy-neutral or even energy-positive wastewater treatment. It has been demonstrated that only 0.8 - 2 kWh/kg N is needed for the side-stream PN-A compared to the BNR energy requirement of about 4.3 kWh/kg N [6, 9].

$$NH_4^+ + 1.32NO_2^- + 0.066HCO_3^- + 0.13H^+ \rightarrow 1.02N_2 + 0.26NO_3^- + 2.03H_2O + 0.066CH_2O_2N_{0.15} \quad 1\text{-}1$$

However, several major challenges remain on the way of PN-A process to wider applications. Firstly, compared with microorganisms involved in BNR, only a small

amount of anammox bacteria, which have low growth rates, exist in the natural environments and the units in the MWTPs. When no anammox-containing inoculum is available, the startup of PN-A process will be a problem. Secondly, the long-term suppression of the undesired NOB, while maintaining AOB and anaerobic anammox bacteria, is still challenging as nitrate build-up has been reported as one of the main operational difficulties in full- scale side-stream PN-A installations [6]. One reason of the failure is the delivery of oxygen to the biomass via conventional aeration (i.e., passing air through water by means of aeration blowers, aeration diffusers, and gas dispersion) is inaccurate, not always reliable and difficult to control. Aeration control has been reported as one of the main operational difficulties for side-stream PN-A [6, 10]. Another major drawback of the conventional aeration is its low oxygen transfer efficiency (OTE, the ratio of the mass of oxygen transferred to the liquid to the mass of oxygen supplied), which varies between 4% and 25% depending on the aeration rate, diffuser type and water quality, etc. [11, 12]. This severely deteriorates the energy savings of the PN-A process which largely depends on the OTE of the aeration system [6]. Thirdly, the PN-A application for the treatment of mainstream wastewater which accounts for most of the nitrogen load is still challenging because of lower temperature, lower ammonium concentration, and high hydraulic load. These conditions lead to difficulties in NOB-suppression and anammox bacteria retention, thereby poor and unstable nitrogen removal performance during long-term operation, particularly at low temperatures. And finally, the release of a greenhouse gas, N_2O, in PN-A process may offset the sustainability brought by anammox. N_2O is 265 - 298 times stronger than carbon dioxide in terms of global warming potential (265 and 298 indicates the global warming potential without and with the inclusion of climate-carbon feedbacks); it has been reported that N_2O was released at a larger amount when PN-A process was applied in a MWTP (0.78 mg N_2O-N/m^3) than during the conventional operation, i.e., when only BNR was applied (0.17 mg N_2O-N/m^3) [9]. N_2O is produced during nitritation through nitrifier denitrification and hydroxylamine oxidation, and during heterotrophic denitrification [13]. Factors influencing the N_2O emission during heterotrophic denitrification have been well studied and high DO, high nitrite concentration, and low COD/nitrogen ratio have been reported to be the most relevant

factors leading to N_2O emission. But the factors affecting nitritation-related N_2O production pathways are not fully understood, and further studies are required.

1.2 Objectives

This thesis investigates the startup of PN-A process from return sludge in an intermittently aerated sequencing batch reactor (IASBR), the development of a novel system with innovative oxygen delivery control for the application of PN-A process into ammonium-rich wastewater and mainstream wastewater treatment, and the key factors governing nitritation-related N_2O production pathways in PN-A process.

By targeting the difficulties in the application of PN-A process, the objectives of this study were to:

1) justify IASBR technology to start up the PN-A process with return sludge as the initial inoculum and the efficiency of this system in achieving TN removal.

2) investigate key factors governing the nitritation-related N_2O production in the PN-A IASBR.

3) develop a novel system with precise oxygen-input control, i.e., a Simple Process for Autotrophic Nitrogen-Removal (SPAN), for the application of PN-A process in the treatment of ammonium-rich wastewater.

4) investigate the nitrogen removal from mainstream wastewater using the developed SPAN technology.

1.3 Methodologies

The roadmap of this Ph.D. research work is outlined in Figure 1-1.

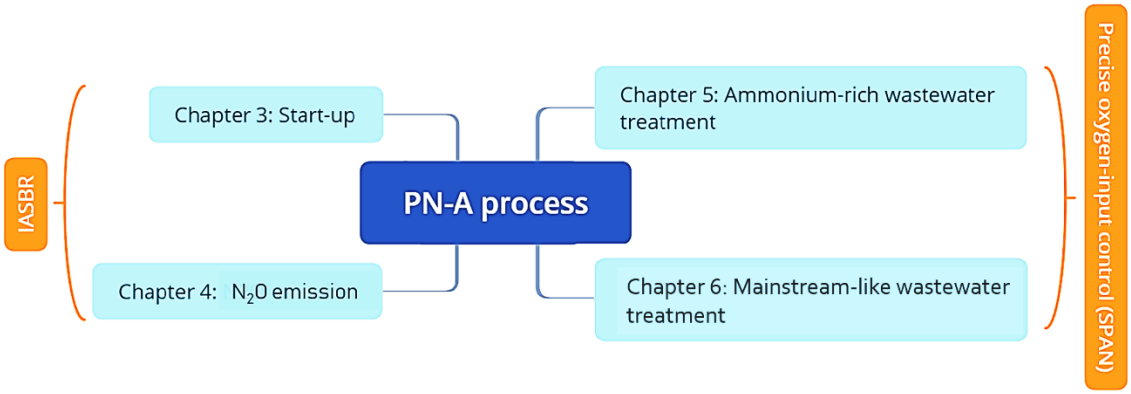

Figure 1-1. Roadmap of this Ph.D. research work.

The research objectives were achieved with intensive laboratory-scale research work. To start up the PN-A process in IASBR, the partial nitritation was first established using return sludge taken from an anaerobic/anoxic/aerobic process as the inoculum in a lab-scale 8L IASBR. Strategies adopted to establish the partial nitritation included initial transient high free ammonia (FA) and high rate continuous aeration (400 mL/min) to achieve a high AOB/NOB ratio, and then low rate intermittent aeration (200 - 100 mL/min) to maintain the partial nitritation process. The presence of ammonium, nitrite, and oxygen-limited conditions in the IASBR allowed the anammox bacteria to develop in the return sludge. By reducing the aeration rate to a further lower level of 30 mL/min, anammox bacteria were enriched to a practically high level, and thereby the PN-A process was successfully started up. The PN-A IASBR was further operated for several months to investigate the nitrogen removal performance. 16s rDNA high-throughput sequencing analysis was carried out to monitor the microbial dynamics of the reactor.

Then, the contribution of nitritation-related pathways to N_2O emission in the PN-A IASBR was evaluated. This was conducted by comparing the N_2O emission during the absence of COD supply (only nitritation-related pathways were responsible for the N_2O production) with N_2O emission during the normal feed when both nitritation-related pathways and heterotrophic denitrification were responsible for the N_2O production. The investigation of factors governing nitritation-related N_2O production was conducted in batch tests using the

biomass cultured in the IASBR. The nitritation-related N_2O production rate was investigated under various conditions to find the impacting factors.

In the SPAN system, oxygen was precisely delivered by circulating water other than air blowers, diffusers, and complex online aeration control strategies and facilities used by conventional aeration methods. If necessary, the oxygen transfer rate can be enhanced by introducing a disturbance to the water surface by installing a shower to spray water to the water surface. The oxygen-supply rate, which is a function of the water circulation rate and shower rate, can be precisely measured and calculated. In this way, the oxygen input can be precisely controlled by adjusting the circulating rate and shower rate to meet the oxygen demand for oxidizing about half of the incoming ammonium by AOB. At the same time, NOB overgrowth and oxygen inhibition on anammox are minimized while the nitrogen removal is maximized. The SPAN technology was first applied to ammonium-rich wastewater in two identical 2.6 L sequencing batch reactors. The reactors were operated at various nitrogen loading rates, circulation rates, and shower rates to investigate the reliability and effectiveness of the SPAN technology. Then, at ambient temperature, the application of SPAN technology for the mainstream wastewater treatment was examined.

1.4 Thesis structure

This dissertation consists of seven chapters:

Chapter 2 reviews the main challenges of the PN-A process (growth rate and activity of anammox bacteria, NOB suppression, and mainstream application of PN-A process), the possible solutions and the practical potential of these solutions.

Chapter 3 comprises a published paper, “Start up of partial nitritation-anammox process using intermittently aerated sequencing batch reactor: Performance and microbial community dynamics” (Science of The Total Environment, 2019, 647: 1188-1198). This

chapter describes the start-up of the PN-A process from return sludge in an IASBR and investigates the nitrogen removal performance in the PN-A IASBR.

Chapter 4 investigates the proportion and impacting factors of the N_2O production via the nitritation-related pathway in PN-A IASBR.

Chapter 5 develops the SPAN technology for reliable nitrogen removal from ammonium-rich wastewater using PN-A process.

Chapter 6 examines the application of the SPAN technology to nitrogen removal from mainstream wastewater at ambient temperatures.

Chapter 7 then summarizes the conclusions drawn from the studies described above and gives future research work that should be concerned about.

Chapter 2
Literature review

2.1 Introduction

The conventional BNR processes, which were developed based on the activated sludge process that was invented more than 100 years ago, are the earliest and still most prevalent nitrogen removal methods [14-16]. BNR processes are accomplished in two separate steps (Figure 2-1A): aerobic (autotrophic) nitrification in which NH_4^+ -N is oxidized to nitrite nitrogen (NO_2^- -N) by ammonium oxidizing bacteria or archaea (AOB or AOA) and then oxidized to nitrate nitrogen (NO_3^- -N) by NOB, and anaerobic (heterotrophic) denitrification, in which NO_3^- -N is reduced to NO_2^- -N before finally reduced to nitrogen gas by heterotrophic denitrifiers. Oxygen introduced by aeration is needed for both AOB and NOB, while a large amount of organic substrates are needed for heterotrophic denitrification [4]. BNR also produces greenhouse gasses such as N_2O and excess biomass that need to be treated with intensive energy input [17]. With the increasing attention to global climate change and concerns for sustainability, scientists and engineers around the world are making more and more efforts to seek cost-effective and environment-friendly nitrogen removal technologies as alternatives to the energy and chemical-intensive BNR processes [18].

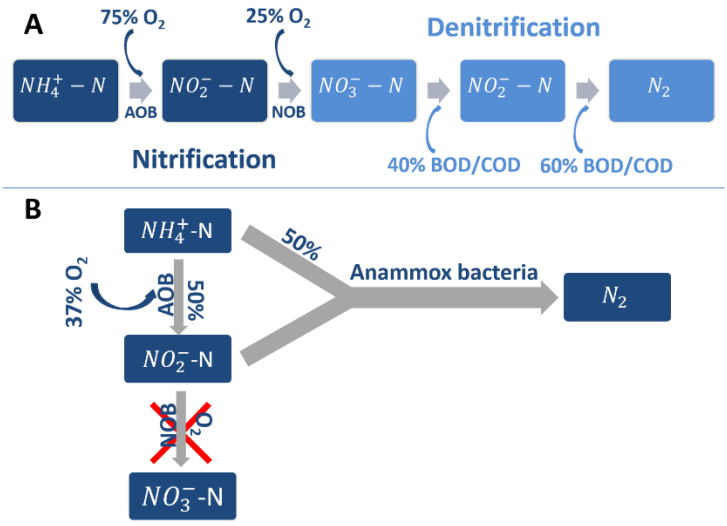

Figure 2-1. Simplified BNR process (A) and PN-A process (B).

The discovery of anaerobic ammonium oxidation (anammox) process in 1995 [7], which has been seen as one of the most innovative biological nitrogen removal processes in recent years,

sheds light on the dreamed energy-efficient BNR alternatives. The anammox process is conducted by a group of anoxic, autotrophic, yet slow-growing bacteria through the conversion of ammonium to dinitrogen gas together with nitrite [19]. The anammox process must be combined with preceding partial nitritation in which around half of the ammonium nitrogen is oxidized to nitrite nitrogen (Figure 2-1B). The combined process can be achieved in two separate reactors forming the two-stage systems (SHARON process), or in single reactor partial nitrification-anammox (PN-A) system (Table 2-1) [20]. Compared with the two-stage systems, PN-A systems (in this thesis, PN-A represents such single-stage systems) can significantly reduce the investment cost and avoid the difficulty to control and attune two reactors [21], so that they are more intensively studied. PN-A systems account for 88% of the total full-scale anammox-based installations [22]. In the PN-A process (Equation 2-1 [23]), AOB oxidize about half of the ammonium to nitrite (Equation 2-2 [24]), and simultaneously, anammox bacteria convert nitrite together with the rest ammonium to nitrogen gas (Equation 2-3 [25]). Compared to BNR processes, the advantages of PN-A processes are significant: 1) reduction by 63% in oxygen demand; 2) nearly 100% reduction in extra organic matters requirements; and 3) reduction by 80% in the sludge yield [22, 26]. Furthermore, the unique cell structure and metabolic pathways of anammox bacteria make anammox process efficient in achieving a high nitrogen removal rate of up to 76.7 kg N/ m^3/day in the lab-scale systems operated under ideal conditions [27] and up to 9.5 kg N/ m^3/day in the full-scale systems [20]. If PN-A processes are used to treat mainstream wastewater in MWTPs, these advantages will provide a unique chance to achieve efficient nitrogen removal and more importantly energy-neutral/positive MWTPs by reducing the energy input for aeration and sludge handling and allowing the separation of nitrogen removal and carbon removal so organic carbon can be recovered in the form of methane [26, 28]. It has been estimated that if using mainstream PN-A as the nitrogen removal process, 24 Watthours per person per day (Wh/pe/d) can be produced compared to a consumption of 44 Wh/pe/d in the conventional BNR process [28].

$$NH_4^+ + 0.85O_2 \rightarrow 0.435N_2 + 0.13NO_3^- + 1.4H^+ + 1.3H_2O \quad (2\text{-}1)$$

$$NH_4^+ + 1.5O_2 \rightarrow NO_2^- + 2H^+ + H_2O \quad (2\text{-}2)$$

$$NH_4^+ + 1.32NO_2^- + 0.066HCO_3^- + 0.13H^+ \rightarrow 1.02N_2 + 0.26NO_3^- + 2.03H_2O + 0.066CH_2O_2N_{0.15} \quad 2\text{-}3$$

Table 2-1. Single stage PN-A processes

Processes	Details	References
CANON	Completely Autotrophic Nitrogen-removal Over Nitrite	[23]
OLAND	Oxygen-limited autotrophic nitrification-denitrification	[29, 30]
DEMON	Deammonification, pH-based intermittent aeration, and feed control	[6, 31, 32]
ELAN	PN-A process with granular biomass	[33]
ANITA™Mox	PN-A process using MBBR technology	[10]
SNAP	Single stage Nitrogen removal using Anammox and Partial nitritation	[34, 35]
DIB	Deammonification in Interval-aerated Biofilm	[34]
SNAD	Simultaneous partial Nitrification, Anammox and Denitrification	[36]

Though extensive studies on the application of PN-A process have been carried out in the last two decades, three main challenges still remain: 1) the low growth rates of anammox bacteria and reduction of anammox activity or population under unfavorable conditions; 2) the suppression of the NOB, failure of which leads to nitrate build-up – one of the main operational difficulties even for the side-stream applications [22]; and 3) the demonstration of efficient and reliable mainstream applications. Other problems such as long start-up, poor effluent water quality, and vulnerable to high COD/N ratio are also reported [26, 37], but they more or less result from the above-mentioned three challenges. Though extensive studies have been done to address these challenges, a critical summarization of the research status and the evaluation of possible solutions are still needed to explore future research directions.

This review critically summarizes the state-of-art of the three major challenges mentioned above, based on which the possible solutions and their potential (e.g., effectiveness, practical availability, etc.) are assessed. Finally, a roadmap for the application of PN-A process into the MWTPs is proposed depending on the technological readiness, so that the benefits of PN-A can be made best of, the cost and energy-input reduction can be maximized, and energy-neutral/positive MWTPs can be achieved.

2.2 Growth rate and activity of anammox

The low growth rate of anammox bacteria is considered as the biggest challenge of PN-A processes and all other anammox-based processes. Besides, anammox bacteria are sensitive to operating conditions such as temperature, pH and DO, and will lose activity under unfavorable conditions[38]. These cause the reduction of anammox activity or anammox populations in the full-scale applications of PN-A process confronting low temperature, high carbon/nitrogen ratio and difficulty in NOB suppression, etc. Therefore, methods including use of anammox with a higher growth rate, enhancement of anammox activity, and efficient maintenance of biomass are researched and developed.

2.2.1 Growth rate of anammox bacteria

Typical doubling times of anammox bacteria are reported as 11 - 32 days at their optimum growth temperature [39], much longer than 0.3 - 1.5 days of AOB and 0.5 - 1.8 days of NOB (Table 2-3). The low growth rate and long doubling time of anammox bacteria probably result from the low activity of a key enzyme – hydrazine synthase – which catalyzes the forging of N-N bond in the key intermediate hydrazine [40]. The low growth rate of anammox bacteria results in the long process start-up time, necessities for either a very large bioreactor volume or highly effective biomass retention, and poor competitivity with other undesired microbial guilds [39].

Studies in the past several years have suggested that anammox bacteria have higher growth rates than widely reported (Table 2-2). The encouraging results indicate the doubling time of anammox bacteria can be as low as 2.1 days at 30 °C, which means anammox might not be regarded as slow-growing microorganisms [39]. So far, six anammox genera have been observed, including *Ca*. *Brocadia*, *Ca*. *Anammoxoglobus*, *Ca*. *Jettenia*, *Ca*. *Kuenenia*, *Ca*. *Scalindua* and *Ca*. *Anammoximicrobium* [41]. The physiological characteristics of *Ca*. *Kuenenia* and *Ca*. *Anammoxoglobus* are less reported than others (Table 2-2). The current results show that *Ca*. *Kuenenia* has a moderate doubling time of 8 - 11 days (38 °C) and a low half-saturation

constant of 0.2 - 3 μM NO_2^-- N (2.8 - 42 μg N/L) [42], while *Ca. Anammoximicrobium* has a long doubling time of 32 days and a high half-saturation constant of 27 μM NO_2^--N (378 μg N/L) [43]. *Ca. Jettenia* is reported to have a wide range of doubling times of 3.9 - 28 days mostly at 37 °C. The growth physiologies of *Ca. Brocadia* are the most well studied. The reported doubling times of *Ca. Brocadia* species are 2.1 - 6.9 days and the reported shortest doubling time is 2.1 days. However, *Ca. Brocadia* has relatively higher half-saturation constants especially compared with *Ca. Kuenenia*.

Ca. Scalindua is the only reported marine anammox genus that may lose activity in the absence of salinity. It has a doubling time of 4.1 - 14.4 days (22 - 28 °C) and low substrate affinity [44, 45]. The growth rate of *Ca. Scalindua* may be higher than other anammox bacteria at the same culturing temperature. For example, the doubling time of *Ca. Scalindua* sp. was reported to be 4.1 days at 22 °C, while that of *Ca. Brocadia* TKU 1 & 2 was 630 days at 20 °C [46]. The optimal temperature range of *Ca. Scalindua* genus (10 - 30 °C for *Ca. Scalindua* sp., and 15 - 45 °C for *Ca. Scalindua* profunda) is lower than that of other anammox species (25 - 45 °C for *Ca. Brocadia* sinica, 20 - 43 °C for *Ca. Brocadia* anammoxidans, and 25 - 37 °C for *Ca. Kuenenia* stuttgartiensis) [44]. This means that *Ca. Scalindua* is more capable of dealing with the low temperature than other anammox species. However, *Ca. Scalindua* is a halophilic genus and anammox activities can be observed under salinity of 0.8% to 4.0%, while no activity can be detected in the absence of salinity [44].

Table 2-2 shows that the growth rates vary a lot within different anammox genera, possibly due to different metabolic strategies within various anammox genera. For example, it has been hypothesized that *Ca. Brocadia* is an r-strategist while *Ca. Kuenenia* be a K-strategist[40, 42, 47-49]. The r-strategist *Ca. Brocadia* has relatively low substrate affinity but high growth rate and would prefer environments rich in ammonium and nitrite. On the other hand, K-strategist *Ca. Kuenenia* usually has high substrate affinity but low growth rate and would survive better at low substrate concentrations [47]. Previous reports support this hypothesis as *Ca. Brocadia* has been mainly detected in reactors with high substrate (ammonium and nitrite) loading rates [48]; a population shift was observed from *Ca. Brocadia* to *Ca. Kuenenia* in an anoxic anammox

moving bed biofilm reactor (MBBR) with nitrite limitation (more suitable for K-strategists) [42].

The remaining question is whether the fast growth rate of some anammox bacteria is intrinsic or can be improved using engineering methods. Lotti et al. [39] reported a high maximum specific growth rate of 0.33/d (doubling time of 2.1 days) at 30 °C. The authors suggested that the maximum growth rate be not an intrinsic process property and can be increased by imposing adequate growth conditions such as maximizing the electron transfer capacity. This was contrary to our general understanding that the maximum specific growth rate is an intrinsic factor for microorganisms. This was proved by Zhang et al. [45] two years later, who reported the same maximum specific growth rate of 0.33/d for the same anammox genera *Ca. Brocadia* without special cultivation and selection pressures. Nevertheless, the growth rate of anammox bacteria can still be improved by optimizing the culturing conditions. The specific growth rate of *Ca. Brocadia* anammoxidans. KSU-1 strain was significantly increased from 0.118/d to 0.172/d by increasing the dosage of Fe (II) from 0.03 mM to 0.09 mM (see section 2.2.2 for the importance of iron) [38]. A substrate inhibition relationship between Fe (II) concentration and the specific anammox growth rate was also found, indicating the important role of Fe (II) in the energy generating process and cell growth process in anammox cells. The growth rate of *Ca. Brocadia fulgida* was reported to be 28% and 32% higher when dosing 30 mg/L exogenous N-hexanoyl homoserine lactone (C6-HSL) and N-dodecanoyl homoserine lactone (C12-HSL), respectively [50]. This was attributed to the quorum sensing effect as C6-HSL and C12-HSL are two kinds of acyl-homoserine lactones (AHLs) that induce quorum sensing effects.

Ca. Brocadia may be capable of achieving a higher growth rate than other anammox genera, but this may be because of the lack of study for other anammox genera. Ca. Scalindua is another promising genus capable of achieving high growth rates, especially at low temperatures, and for saline wastewater treatment. However, even the lowest reported doubling time of anammox (2.1 days) is still higher than those of autotrophic AOB and NOB (Table 2-3) let alone heterotrophic bacteria, and this makes them less competitive to other

Table 2-2. Growth parameters of anammox bacteria

Anammox species	T_d	μ_{max}	K_S (NO_2^--N)	K_S (NH_4^+-N)	Biomass	Operation methods	Reference
Ca. Kuenenia stuttgartiensis	8 - 11	0.06 - 0.08	0.2 - 3	–	Suspended cells	38 °C	[42]
Ca. Scalindua sp.	14.4	0.048	0.45	3	free-living cells	MBR, 28 °C	[44]
Ca. Scalindua sp.	4.1	0.17	–	–	Planktonic cells	22 °C	[45]
Ca. Anammoximicrobium moscowii	32	0.02	27	29	–	–	[43]
Ca. Jettenia moscovienalis	28	0.02	–	–	–	–	[43]
Ca. Jettenia caeni	6.3	0.11	–	–	Planktonic cells	37 °C	[45]
Ca. Jettenia caeni	3.9	0.18	–	–	Immobilized cells	37 °C	[45]
Ca. Jettenia caeni	13.9	0.05	36	17	Suspended free-cells	MBR 37 °C	[41]
Ca. Brocadia anammoxidans	11	0.07	< 5	< 5	–	–	[43]
Ca. Brocadia sincia	2.1	0.33	–	–	Immobilized cells	37 °C	[45]
Ca. Brocadia sincia	4.1	0.17	–	–	Planktonic cells	37 °C	[45]
Ca. Brocadia sinica	6.9	0.1	34	28	Granules	MBR 37 °C	[41]

Ca. Brocadia caroliniensis	6.9	0.098	370	530	flocculent sludge	Batch tests, 30 °C	[47]
Ca. Brocadia fulgida	–	–	350	640	Granular sludge	Batch tests, 30 °C	[47]
Ca. Brocadia sp.40	2.1	0.33	–	–	Suspended cells	Reducing SRT, MBR 30 °C	[39]
Ca. Brocadia sp.	3.3	0.2	2.5	–	Suspended free-living cells	MBR 30 °C	[51]
Ca. Brocadia anammoxidans. KSU-1 strain	5.9	0.118	–	–	–	Batch tests, 30 °C, dosing 0.03 mM Fe (II)	[38]
Ca. Brocadia anammoxidans. KSU-1 strain	4	0.172	–	–	–	Batch tests, 30 °C, dosing 0.09 mM Fe (II)	[38]
Ca. Brocadia TKU 1 & 2	2.1	0.33	–	–	Suspended free-living cells	MBR 30 °C	[46]
Ca. Brocadia TKU 1 & 2	630	0.0011	–	–	Suspended free-living cells	MBR 20 °C	[46]
Ca. Brocadia fulgida	11.6	0.06	–	–	–	37 °C	[50]

Ca. Brocadia fulgida	9	0.0768	–	–	–	37 °C, adding 30 mg/L exogenous C6-HSL	[50]
Ca. Brocadia fulgida	7.6	0.0912	–	–	–	37 °C, adding 30 mg/L exogenous C12-HSL	[50]

Note: T_d: doubling time = $\ln 2/\mu_{max}$, day; μ: growth rate, d^{-1}; K_S: half-saturation constants, μmol N /L; MBR: membrane bioreactor; SRT: sludge retention time; C12-HSL: N-dodecanoyl homoserine lactone; C6-HSL: N-hexanoyl homoserine lactone; –: not available

microorganisms in PN-A process such as NOB and heterotrophic denitrifying bacteria. Further studies are needed to practically make use of the fast-growing anammox bacteria, investigate the physiological kinetics of less-studied anammox bacteria and find promising methods to boost the growth of anammox bacteria such as dosing Fe (II). Therefore, a number of strategies have been applied to boost anammox activity in PN-A process.

2.2.2 Methods to enhance anammox activity

Strategies such as applying an electric/magnetic field, ultrasound, etc. have been assessed to enhance anammox activity, but the application of these methods is confined due to their high operation cost and low feasibility [38, 52]. Anammox activity can also be enhanced by dosing trace elements such as iron (Fe), manganese (Mn), zinc (Zn), nickel (Ni) and copper (Cu), which have been found to be essential for the metabolism and growth of anammox bacteria. Fe (II) is an essential element for the generation of ferredoxin and heme c, which play an important role in the energy generating process, and is considered as an indispensable part of some key enzymes for the growth of anammox bacteria [38]. Manganese oxides can be used with formate as the electron donor by *Ca*. *Kuenenia stuttgartiensis,* Cu is an important element of nitrite reductase in anammox bacteria, and Zn is a key element of 21 ATP-dependent zinc metal-loprotease FtsH 1 and zinc-containing dehydrogenase [52]. Ni contributes to the synthesis of dehydrogenation coenzymes [53]. It was reported that the absence of Ni led to the decrease of anammox activity by 6 %, and 2 mg/L Ni enhanced the activity by 9% but 10 mg/L Ni decreased the activity by 87% [54]. The anammox activity remained unchanged with 0.06 - 2 mg/L Cu and 0.1 - 5 mg/L Zn addition, while reduced by 65% and 79% with 7.5 mg/L Cu and 15 mg/L Zn addition [54]. The nitrogen removal rates of a PN-A reactor were improved by 54.62%, 45.93%, and 44.09% by applying Mn (II), Zn (II) and Cu (II) at optimal concentrations of 2.0 mg/L, 2.0 mg/L, and 0.5 mg/L, respectively [52]. The anammox activity of marine anammox bacteria was enhanced by 57.88% with optimal Ni (II) addition at 0.025 mM and the Ni (II) dosage was suggested to be controlled within 0.075 mM [55]. The specific anammox activity of a PN-A reactor was enhanced by 41.0%, 63.5% and 533.2% with the addition of less than 1 mg/L Cu (II), less than 1.74 mg/L Ni (II) and 3.68 mg/L Fe (III) [53]. Some of these elements such as Zn, Mn, Cu, etc. are among the frequently detected metals in

some nitrogen-rich wastewater, e.g., swine wastewater, landfill leachate and steel manufacturing wastewater [52] and should be carefully handled when PN-A process is applied. For the of trace elements-dosing methods, the key is to find the optimal concentration range of these trace elements as the shortage of these elements leads to low anammox activity while excessive trace elements are toxic and may inhibit anammox activity.

Besides the above-mentioned methods, another promising way to enhance anammox activity is quorum sensing-based methods. The term "quorum sensing" refers to the process that quorum-sensing bacteria communicate with one another to synchronize particular behaviors on a population-wide scale through detecting a minimal concentration of external small hormone-like signal molecules (autoinducers) that are produced and released by themselves (or other species for interspecies quorum sensing) [56]. The quorum sensing-controlled behaviors include cell growth, antibiotic production, biofilm, and granule formation, virulence factor expression and sporulation, etc. [57, 58]. For gram-negative and gram-positive bacteria, two predominant autoinducers AHL and modified oligopeptides, are used [57]. The activity of anammox bacteria which are gram-negative bacteria [59], was first confirmed to be cell density-dependent, but whether this process resulted from quorum sensing was unclear [60]. Later, in a PN-A reactor (OLAND), the specific anammox activity at high biomass concentrations was found to be 1.5 times higher than that at low biomass concentrations, and one specific AHL, N-dodecanoyl homoserine lactone (C12-HSL) was detected in anammox bacteria-enriched community while absent in AOB-enriched community [61]. In another study, N-hexanoyl homoserine lactone (C6-HSL) and N-octanoyl homoserine lactone (C8-HSL) were detected in two anammox reactors [62]. The addition of 30 mg/L C12-HSL significantly increased the anoxic ammonium removal rate with a factor of 1.4. In an anammox reactor, the release of three AHLs, C6-HSL, C8-HSL and C12-HSL, was confirmed, among which the exogenous C6-HSL and C8-HSL significantly increased the ammonium removal rate by 35% and 20%, respectively, while C6-HSL significantly increased the anammox bacteria growth rate from 0.0025 /h to 0.0032 /h [50]. The specific anammox activity can be significantly increased by 8%, 11%, and 7% ($p < 0.05$) by dosing exogenous 3-oxohexanoyl-homoserine lactone (3OC6-HSL), C6-HSL, and C8-HSL, respectively, while the biomass yield rate of the anammox consortia can be significantly improved by 38% ($p < 0.05$) by dosing 3OC6-HSL [63]. The

presence of S-adenosylmethionine (SAM) radical enzyme genes, which regulate the synthesis of AHLs [57], has been confirmed in the genome of one of the anammox species *Kuenenia Stuttgartiensis* [64]. Thus, it can be concluded that anammox bacteria are also quorum-sensing bacteria. Recently, Tang et al [63] have reported the metabolic pathways of how AHLs regulate the activity, growth rate, and extracellular polymeric substances (EPS) production of the anammox consortia: three AHLs, 3OC6-HSL, C6-HSL, and C8-HSL control the electron transport carriers that influence the bacterial activity; 3OC6-HSL regulates lysophosphatidylcholine (20:0) metabolism which affects bacterial growth; AHLs selectively regulate aspartate and leucine to affect the production of extracellular proteins; OC6-HSL, OC8-HSL, and C6-HSL particularly enrich the uridine diphosphate-N-acetylglucosamine pathway to promote exopolysaccharides production and affect the aggregation of the anammox consortia. In conclusion, by dosing exogenous AHLs, the specific anammox activity and anoxic ammonium oxidation can be enhanced; and more importantly, the growth rate can be improved, which is very attractive for relatively slow growing anammox bacteria. However, from the engineering point of view, the improvement in the specific anammox activity with AHLs is still a question during application, let alone the AHL chemicals are very expensive and difficult to dissolve in water. Further research is needed to achieve more applicable results. In terms of improving anammox activity, results from different studies are discrepant, sometimes even opposite. The reason may be that different AHLs induce different behaviors of various anammox species. Upon achieving detailed and comprehensive results, another potential method to improve the anammox activity and growth rate is the construction of genetically engineered anammox bacteria carrying genes for the synthesis of particular AHLs that are capable of improving nitrogen removal performance.

2.2.3 Engineering solutions for biomass retention

Anammox activity has been reported to be strongly correlated with the abundance of anammox bacteria [4]. As anammox bacteria are relatively slow-growing bacteria, maintaining biomass retention is the key to achieving stable and efficient anammox performance. From the engineering point of view, this can be achieved by employing biomass in the form of biofilms or granules instead of suspended /free-living biomass and by utilizing equipment to collect and

return anammox bacteria-containing biomass in the effluent, such as hydrocyclone separation devices for granular sludge [65] and retention sieves for biofilm carriers [10]. Anammox bacteria tend to grow in the form of biofilm or granule/aggregate together with other microorganisms, glued by EPS (including polysaccharides, DNA, and proteins, etc.), so that undesirable washing out of these bacteria from the reactor can be prevented [40, 43]. The biofilm can be formed under hydrodynamic shear force [66] using rotating biofilm reactors or on biofilm carriers made from non-woven fabrics, polymeric plastics, etc., while the formation of granules/aggregates is encouraged by applying selective pressure for faster settling cells in reactors such as SBR and upflow-anaerobic sludge blanket reactors (UASB) [40].

The sessile lifestyle of the relatively slow-growing anammox bacteria enables them to maintain a higher biomass quantity and abundance, nitrogen removal rates, and resistance against less favorable milieu conditions such as low temperatures [46, 67-69]. The biomass concentration increased from 3570 to 5250 mg TSS/L in MBBRs, and decreased from 4370 to 2870 mg TSS/L in suspended growth reactors under the same conditions [67]. By adding zeolite particles as the biofilm carriers to an anammox reactor, the biomass concentration increased significantly from 0.2 g VSS/L to 1.2 g VSS/L and the specific anammox activity of the biomass was enhanced from 0.35 up to 0.5 g N/g VSS/d [68]. In a study comparing the microbial communities of different aggregates taken from anammox bioreactors, the anammox bacteria showed much higher relative abundance (qPCR results) in both the biofilm (87.8%) and granule sludge (94.3%) than in floccular sludge (2.4%) [69]. MBBRs were found to display significantly higher nitrogen removal rates (NRRs), significantly lower propensity for nitrite accumulation against transient temperature perturbation, and more abundant anammox bacteria than the suspended growth reactors [67]. Under unfavorable conditions such as decreasing temperature, biofilms tend to maintain more stable anammox bacteria than those of suspended and granular biomass according to a report [70]: at 20 ºC, anammox bacteria constituted fractions (qPCR results) 16%, 25.5%, 32% and 45% of the total bacteria in the suspended biomass, granulated biomass, biofilm grown on 2 mm-carriers, and biofilm grown on 10 mm-carriers, respectively, but with decreasing temperature to around 10 ºC, the fractions dramatically decreased to 0.8% and 2.7% in the suspended and granulated biomass while remained relatively steady in the biofilms. In different PN-A reactors when the temperature

was decreased from 20 ºC to 10 ºC, the anammox activity of suspended biomass suffered from drastic decrease at 15 ºC, while it persevered in granular biomass and biofilms even when temperatures were < 13 ºC; at the same time, acceptable effluent quality was only achieved in the reactor with the bigger carriers (10 mm) but not in the reactors with the smaller carriers (2 mm), suspended biomass and granular biomass [70].

2.3 NOB suppression

Effective NOB suppression is critical to successful PN-A process. NOB compete with AOB for oxygen and compete with anammox bacteria for nitrite. Failure to maintain efficient NOB repression will lead to nitrate build up. The current NOB-repression strategies are developed based on the control of oxygen, sludge retention time (SRT), and ammonium-inhibition (FA and residual ammonium) [26, 71].

2.3.1 Oxygen-based control strategies

The oxygen-based control strategies suppress NOB by controlling DO concentrations or aeration rate, and are the mostly used NOB-suppression approaches. These strategies require the installation of online sensors, solenoid valves, and aeration control protocols. Sensors are used to monitor DO concentration, pH, temperature, ammonium concentration, nitrate concentration, and potassium concertation (for ammonium sensor correction), etc. The control protocol system receives signals from sensors and sends commands to valves and air blowers.

2.3.1.1 Fixed-DO control

The fixed-DO control approach is based on the general understanding that AOB have higher DO affinities (i.e., lower half-saturation constant values, $K_{S, [DO]}$ in this case) than NOB (Table 2-3), and thus low DO concentration or oxygen-limited conditions can provide advantages for the growth of AOB over NOB, thus providing the possibility of washing NOB out of the PN-

A reactor [72]. DO setpoints of 0.2 - 0.3 mg/L (mean values) are applied into the DEMON process and higher setpoints of up to 1.5 mg/L are applied into the biofilm-based PN-A systems [6]. However, the reported $K_{S, [DO]}$ values vary significantly. The measured $K_{S, [DO]}$ values for AOB are not always lower than those for NOB (Table 2-3). During long-term operation under low DO conditions, the number of the K-strategists (high substrate affinity and low specific growth rate) *Nitrospira* NOB may increase significantly in the bioreactors [4]. Thus, the effectiveness of the DO-based control strategies has to be evaluated on a case-to-case basis [72]. In addition, given the fluctuating nature of the influent ammonium concentrations, alkalinity,

Table 2-3. Growth parameters of AOB and NOB.

	Culture	Doubling time	$K_{S, [S]}$	$K_{S, [EA]}$	References
AOB	Ammonia oxidizers	0.3 - 1.5	50 - 70	–	[73]
	Nitrosomonas sp. ML1	1.4	11.6	0.24	[74]
	Nitrosomonas sp. NL7	1.2	34.3	1.22	
	Nitrosomonas	0.7 - 1.1	42.9 - 257.1	–	
	AOB	0.29 - 0.33	–	–	[75]
	AOB	< 1	0.8 - 112	0.032 - 0.48	[76]
	Suspended PN biomass	–	–	1.16	[72]
	Suspended PN biomass	–	–	0.03	
	Biofilm PN biomass	–	–	0.18	
NOB	Nitrite oxidizers	0.5 - 1.6	15 - 178	–	[73]
	Nitrobacter (28 °C)	0.5 - 1.8	49 - 544	–	[77]
	Ca. Nitrospira defluvii (28 °C)	1.5	9	–	
	Nitrospira	1.3 - 1.5	9 - 27	–	
	Ca. Nitrotoga arctica (17 °C)	1.8	58	–	
	Nitrospira spp	0.76	37	0.33	[78]
	NOB	0.42 - 0.54	–	–	[75]
	NOB	< 1	9 - 544	0.7 - 5.3	[76]
	Suspended PN biomass	–	–	0.16	[72]
	Suspended PN biomass	–	–	0.43	
	Biofilm PN biomass	–	–	0.54	

Note: doubling time: days; K_S: half-saturation constants; [S]: substrate; [EA]: electron acceptor; $K_{S\ [S]}$: μM; $K_{S\ [EA]}$: mg O_2/L; –: not available

and oxygen demand in the bioreactor, manual DO-setpoint adjustment is needed for the fixed-

DO-based control strategies to maximize ammonia removal and avoid alkalinity limitation [71]. Complete NOB suppression was reported to be achievable by combining low DO concentration with FA inhibition for ammonium-rich wastewater (side-stream), but this combination didn't work in mainstream conditions [79]. It is necessary to combine fixed-DO-based control strategies with other methods to maintain long-term NOB suppression.

2.3.1.2 Flexible aeration control

Flexible DO/aeration control through the airflow valve can be realized based on nitrogen concentrations (NH_4^+-N and NO_3^--N) or pH profiles. For the nitrogen-based aeration control, the DO/aeration setpoint is incrementally increased or decreased so that the ammonium removal efficiency and the ratio of nitrate production/ ammonium removal can be maintained at optimum levels (80 - 90% of ammonium removal for the purpose of maintaining a certain concentration of residual ammonium, and ratio of nitrate production/ ammonium removal of 0.13 according to Equation 2-1) [71]. The PN-A process is a net proton producing process (Equation 2-1) and comprises proton-producing aerobic ammonium oxidation (Equation 2-2) and proton-consuming anammox (Equation 2-3). This allows the application of the pH-based aeration control strategy, where DO/airflow is adjusted according to pH setpoints [71]. In continuously aerated reactors, this strategy is based on the linear correlation between the pH and the ammonium removal [80, 81]. When this approach is applied into intermittently aerated PN-A systems, the aeration will be terminated when a minimum pH value is reached during the aeration period in which pH decreases. The aeration will be turned on when a maximum pH value is reached during the non-aeration period in which pH increases. The pH-based aeration control method alone, which relies on stable pH of the target wastewater and can be interfered by pH control operation (to maintain stable pH), is not reliable to prevent DO from increasing to a high level and subsequent NOB overgrowth, especially when ammonium is a limiting factor [82]. The high DO can be prevented by combining pH-based control with DO-control (pH-DO-aeration control) in two ways: 1) setting up a fixed upper DO setpoint; or 2) decreasing the air flowrate/DO setpoint when the pH feedback is less than the pH setpoint, and increase the air flowrate/DO setpoint when the pH feedback is greater than the pH setpoints. pH-based strategy can also be combined with the nitrogen-based control strategy (pH-

ammonium-aeration control) so that the alkalinity depletion can be prevented, and the nitrogen concentrations can be controlled [71].

These control strategies rely on the robustness and reliability of the control system and extensive online sensors. The pH sensors are regarded as the most robust sensors, followed by conductivity sensors and ammonium sensors [71]. The pH-based control strategy is based on the assumption that the target wastewater has enough alkalinity and buffering capacity to maintain a stable pH, which is not guaranteed in reality, thus it is not always reliable. It can be applied as a back-up system for ammonium-based aeration control system [6, 80]. However, the ammonium sensors are not as reliable as pH sensors, especially at low ammonium concentrations.

2.3.1.3 Intermittent aeration

To suppress NOB, the oxygen supply can also be realized by means of intermittent aeration. This is based on the understanding that AOB and NOB have different strategies for managing energy demand and different starvation recovery dynamics, causing AOB to recover earlier than NOB when the anaerobic condition is switched to the aerobic condition [82]. However, to guarantee long-term NOB suppression, other conditions such as pre-established high AOB/NOB ratio, oxygen-limited conditions, and ammonium-based aeration control to prevent the deplete of ammonium are still essential [13, 82]. This strategy has been used alone or combined with other methods to achieve successful side-stream and mainstream PN-A applications [13, 83-85]. A major drawback of intermittent aeration is that it would promote N_2O emissions. In PN-A systems, N_2O is produced through three known biological pathways: nitrifier denitrification, hydroxylamine (NH_2OH) oxidation, and heterotrophic denitrification if COD is present (Figure 2-2) [86, 87]. In intermittently aerated reactors, the N_2O emission has the potential to increase from 0.07% to 27% N_2O-N per mole of oxidized ammonium nitrogen by nitrifying activated sludge [88] and accounts for 0.9 - 2.7% of the removed ammonium in PN-A process [85]. The possible reasons include (Figure 2-3): the sudden AOB-metabolism shift from a low activity to a high activity during the switch from the anoxic condition to the aerobic condition; the longer lag phase of nitrous oxide reductase synthesis and achieving

maximal activity than those of nitrite reductase during the transition from the aerobic condition to the anoxic condition, and nitrite accumulation during aerobic intervals [89, 90]. It's generally agreed that the aeration rate and DO levels significantly affect the N_2O generation and emission, but the guidance for the operable process control cannot be drawn as the suggested DO values to minimize N_2O generation and emission vary a lot depending on wastewater characteristics and operational conditions [89]. Even contrary conclusions have been drawn. A higher aeration rate was reported to be effective in reducing N_2O emission while a lower DO concentration enhanced N_2O generation in the aeration periods [91]. Sun et al. agreed that increasing aeration rates or DO concentrations during aeration periods would reduce N_2O emission [89]. However, Castro et al. reported that intense aeration led to higher N_2O formation rates and emission rates (due to the enhanced N_2O stripping) than low aeration [92]. Other potential methods to reduce N_2O emission in intermittently aerated PN-A include the use of the step feed mode and biofilm systems [89].

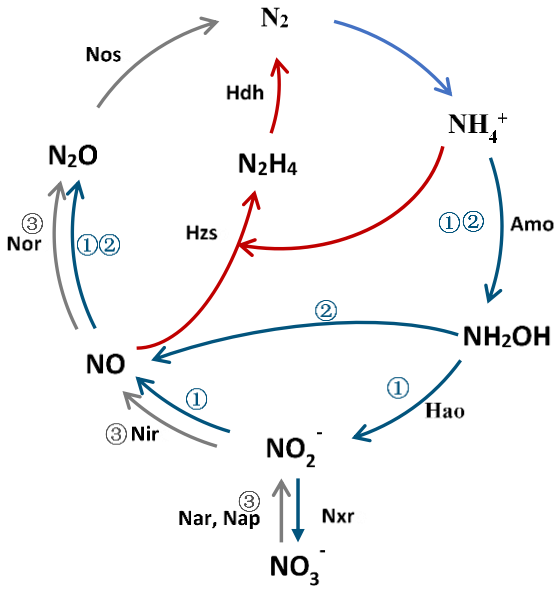

Figure 2-2. Major nitrogen-converting pathways and key enzymes involved. Biological N_2O production pathways: ①, nitrifier denitrification; ②, NH_2OH; and ③, heterotrophic denitrification. The dark blue arrows indicate the nitrification pathways, the grey arrows indicate heterotrophic denitrification pathways, and the dark red arrows indicate anammox pathways. Amo, ammonium monooxygenase; Hao, hydroxylamine oxidoreductase; Nxr, nitrite oxidoreductase; Nar, membrane-bound dissimilatory nitrate reductase; Nap, periplasmic dissimilatory nitrate reductase; Nir, nitrite reductase (NO-forming); Nor, nitric oxide

reductase; Nos, nitrous oxide reductase; Hzs, hydrazine synthase; and Hdh, hydrazine dehydrogenase.

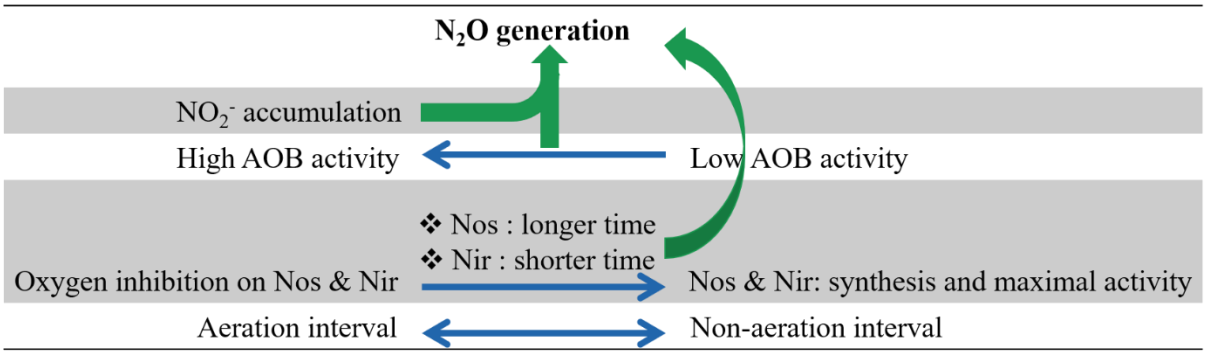

Figure 2-3. Mechanisms of N_2O generation during intermittent aeration. The green arrows indicate the N_2O production.

2.3.2 SRT control

SRT is a crucial controlling parameter for the PN-A process due to the relatively slow-growing anammox bacteria. Controlling SRT has been suggested as an approach to suppress and wash out NOB, as growth rates of AOB are generally considered to be higher than those of NOB at high temperature [26]. This has been reported to be effective at high temperatures of 30 - 40 °C with a short SRT of 1.5 days. But as temperature is lower than 20 °C the growth rate of NOB will be higher than that of AOB, making this control strategy ineffective [93]. Thus, the temperature must be considered when using SRT control method. The doubling time of AOB is not always lower than, but rather close to, that of NOB (Table 2-3). This makes the SRT control method not always reliable. Most important of all, even the fastest-growing anammox bacteria grow slower than most NOB (Table 2-3), which means the application of SRT control strategy in PN-A process will inevitably lead to the loss of anammox bacteria. However, this strategy can be applied if the anammox bacteria exist in the form of biofilms. Because the nitrifiers tend to grow in the suspended sludge, the control of the aerobic SRT and therefore selective wash-out of NOB while retaining anammox is possible. Overall, SRT control is

appropriate for two-stage anammox systems (like SHARON process) and biofilm-based PN-A process, but its effectiveness depends on temperature.

2.3.3 Ammonium inhibition

AOB are more tolerant than NOB against FA inhibition, so NOB can be outcompeted under certain FA concentrations of 0.1 - 1.0 mg/L to 10 - 150 mg/L [94]. FA concentration is determined by pH, total ammonium concentration and temperature (Equation 2-4 [13]). FA control strategy can be effective when the pH and ammonium concentration are high in the target wastewater, but it is no longer effective for the mainstream wastewater which has low concentrations of 15 - 100 NH_4^+-N mg/L [26, 95]. As NOB may get acclimated to FA levels as high as 40 mg NH_3-N/L, FA-inhibition control strategy may not work for long-term NOB suppression [71, 94]. A too high FA concentration also inhibits anammox bacteria. It has been reported that 38 mg NH_3- N/L resulted in 50% anammox activity decrease; during long-term operation, nitrogen removal became unstable at 20 - 25 mg NH_3- N/L and failed at 35 - 40 mg NH_3- N/L [96]. Overall, FA-inhibition control strategy is an effective strategy for temporarily controlling NOB proliferation, and only when high FA concentration is achievable.

$$\text{FA as } NH_3 \text{ (mg/L)} = \frac{17}{14} \times \frac{total\ ammonium\ nitrogen\ (mg\ NH_4^+ - N\ /L)}{1+(K/10^{pH})}, \qquad 2\text{-}4$$

where $K = e^{6344/(273+T)}$.

It is necessary to maintain a residual ammonium concentration, i.e. 2 - 5 mg NH_4-N/L, to suppress NOB in PN-A process [97, 98]. According to Monod equation, the higher the ammonium concentration is, the closer the growth rates of AOB and anammox bacteria to the maximal growth rates [99]. With the presence of residual ammonium, AOB can compete with NOB for oxygen and anammox bacteria are able to compete with NOB for nitrite. PN-A process can fail under ammonium limitation even in side-stream conditions [98]. The residual ammonium also allows the establishment of oxygen-limited conditions which also helps suppress NOB and protect anammox bacteria. It has been demonstrated that NOB suppression

was changed to NOB proliferation when the residual ammonium concentrations were less than 2 - 5 mg NH_4-N/L (DO < 4 mg/L, 20 °C) [97]. The residual ammonium concentration is essential to maintain NOB suppression especially in mainstream conditions where high FA is not available. It can be applied combining with other control strategies to achieve effective NOB suppression.

2.3.4 Summary

As summarized above, extensive studies have been conducted to effectively suppress NOB. However, in practical applications, it is still challenging to achieve this goal, because nitrate build-up has been reported as one of the main operational difficulties, according to a survey on full-scale PN-A installations [6]. Fifty percent of the surveyed full-scale PN-A plants reported this problem which generally lasted up to several weeks. One reason is the effectiveness of the developed NOB suppressing strategies are conditional and are effective only in given conditions, which are summarized in Table 2-4. The other reason is the failure of the control strategies, for instance, failing to keep low DO concentration, which not only leads to the overgrowth of NOB but also the inhibition on anammox bacteria. DO at concentrations as low as 0.032 mg/L reversibly inhibit anammox bacteria [4], but irreversibly inhibit anammox bacteria at higher DO concentrations (> 18% air saturation) [96]. Though a higher DO concentration is usually needed for the biofilm PN-A system to overcome the diffusion limitation, for suspended-growth and hybrid PN-A systems a low DO concentration is needed for the purpose of reducing oxygen inhibition on anammox, suppressing NOB and reducing energy input. Therefore, a good control strategy must not only be able to address the NOB suppression challenge but also able to maintain low DO concentrations and maximize ammonium removal. In practical applications, the control strategies must also be compatible with the fluctuating incoming wastewater, in terms of hydraulic loads, ammonium concentrations and alkalinity concentrations.

Table 2-4 indicates that the single control strategies cannot address the four questions simultaneously. To overcome these limitations, the combined aeration control methods,

Table 2-4. Comparison of the NOB-suppression strategies in PN-A.

Control strategies	Maintaining low DO concentration?	Maximizing ammonium removal?	Preventing nitrate build up?	Compatible with fluctuation?	Other limitations
SRT	No	No	Mostly yes	No	Not always effective; suitable for two-stage anammox process and biofilm PN-A process.
Fixed-DO setpoints	Yes	No	No	No	Need to be combined with other strategies.
Nitrogen-based aeration control	Yes	Yes	Yes	No	Ammonium sensors are not as reliable as pH sensors and their accuracy is affected by the presence of potassium; pH sensors are also needed to monitor the alkalinity dynamics.
pH-based aeration control	No	May not	May not	Yes	Rely on stable pH of the target wastewater and may be interfered by pH control operation (to maintain stable pH); pH variation may not reflect ammonium and nitrate concentrations.
Intermittent aeration	No	No	May not	No	Promote nitrous oxide production and need to be combined with other methods to ensure long-term NOB suppression.

Control strategies	Maintaining low DO concentration?	Maximizing ammonium removal?	Preventing nitrate build up?	Compatible with fluctuation?	Other limitations
FA-inhibition	Possibly	No	Mostly yes	No	Suitable when high FA concentration is available; NOB may get acclimated to high FA; high FA inhibits AOB and anammox bacteria.
pH-DO-aeration control	Yes	May not	May not	Yes	Extensive online instruments are needed.
pH-nitrogen-aeration control	Yes	Yes	Yes	Yes	Extensive online instruments are needed.
DO-nitrogen-aeration control	Yes	Yes	Yes	No	Extensive online instruments are needed; the alkalinity dynamics is unknown.

especially the pH-nitrogen-aeration control, may be promising alternatives. Most of these strategies rely on automated control instruments such as rapid response control systems and online sensors, thus the robustness and accuracy of the instruments need to be considered. Besides, whatever the control strategy is, maintaining a minimum concentration of residual ammonium is a prerequisite to encourage the growth of AOB over NOB.

2.4 Mainstream application

2.4.1 State of the art

The practical application of mainstream PN-A is the crowning glory of the PN-A process. Around 20% of the influent nitrogen is incorporated in the sludge biomass and goes to the side-stream wastewater in a typical MWTP [4, 5, 100]. To make the best of the PN-A process and move it towards the energy-neutral/positive MWTP requires the application of PN-A to remove the bulk nitrogen in the mainstream wastewater [100]. However, it's still a big challenge to achieve this goal and currently, no full-scale mainstream PN-A installations have been reported to achieve long-term stable nitrogen removal. The mainstream wastewater usually has the characteristics as follows: high and variable hydraulic loads, low and varying ammonium concentrations (ca. 30 - 100 mg/L), high C/N ratios (ca. 7 - 12), and low temperature in moderate climates (20 °C in summer and 10 °C in winter) [26]. These characteristics lead to the commonly reported difficulties in implementing PN-A in mainstream conditions [10, 26, 93, 101]: (1) low temperatures reduce the activity and growth rate of AOB and anammox, and make AOB lose the growth advantage over NOB (< 20 °C); (2) the low ammonium concentration and high COD/N ratio may cause heterotrophic bacteria outcompeting anammox bacteria which prefer COD/N ratio < 2 - 3 or even <0.5; (3) poor retention of anammox bacteria at a high loading rate; (5) instability over long-term operation without reliable automatic control of the oxygen-supply, and (6) too poor effluent quality to meet the requirement (i.e., TN concentrations (< 10 mg N/L) and removal efficiencies of 70% - 80% [102]).

Intensive efforts have been made to address these challenges at lab-scale, pilot-scale, and full-scale installations (Table 2-5 and Table 2-6). As shown in Table 2-5, under "warm" conditions (≥ 25 °C), some studies achieved 51 - 81% of nitrogen removal with high NRRs of 190 - 434 mg N/L/d, some got higher nitrogen removal efficiency (NRE) of 62 - 89% with lower NRRs of 55 - 130 mg N/L/d, but some got low NREs with low NRRs. The poor nitrogen removal performance was improved by increasing the COD/N ratio which had no negative effect on anammox (activity and growth rate) when the ratio was < 1.5 [103]. The achieved results are comparable with those of conventional BNR in full-scale MWTPs, of which the NREs range from 40% to 70% [104] and the NRRs range from 80 mg N/L/d to 1360 mg N/L/d (40 - 420 mg N/g VSS/d) for pre-anoxic denitrification, and ranged from 20 mg N/L/d to 120 mg N/L/d (10 - 30 mg N/g VSS/d) for post-anoxic denitrification without exogenous carbon addition [105, 106]. But, the effluent quality complying with the discharge limits is not guaranteed.

However, when it comes to the application at temperatures < 20 °C, especially at low temperature < 15 °C, three major problems remain (Table 2-6): low TN removal efficiency, poor effluent quality, and long-term process instability. The reported mainstream PN-A suffered a lot from the low temperature and mostly could not maintain long-term stable nitrogen removal. The reported NREs and NRRs vary a lot between 4 - 94% and 20 - 1100 mg N/L/d, respectively. The low NRRs and NREs result in high effluent nitrogen concentrations which do not comply with the requirements.

These problems are mainly caused by the adverse effect of low temperature on the activity and growth rate of anammox bacteria as well as the balance among the functional microorganisms. To maintain anammox biomass and activity is a key to mainstream PN-A process. Low temperature reduces both the activity and growth rate of anammox bacteria, as they have much higher cell maintenance activities at low temperature [93]. The anammox activity decreases by about ten times when the temperature drops from 30 °C to 10 °C [26] and decreases by about 70% when the temperature drops from 13 °C to 10 °C [107]. Li et al. found that anammox activity was significantly, but reversibly, suppressed when the temperature was < 11 °C [93]. It seems that a temperature below 10 °C is an insurmountable obstacle for mainstream PN-A, but this

Table 2-5. Nitrogen removal performance of mainstream PN-A process at ≥ 25°C.

Reactor configuration	Temperature (°C)	COD/N	NRE	NRR	SDNR	Reference
Up-flow membrane-aerated biofilm reactor, 2.5L	25	0.6	70 - 89	80	10	[108]
Up-flow granular reactor, 1.35L	24	0.8	75 - 85	84	11	[5]
Aerobic-anoxic activated sludge reactor simulating a 200,000 m^3 step-feed activated sludge process, 8.5L	30	11	62 [a]	130	-	[109, 110]
IFAS, 200L	25	1.8	70	55	-	[80]
Auto-recycling integrated reactor, 11.6L	About 27	0	29	100	-	[111]
Hybrid IASBR (granular anammox), 10L	30	1.1	31	39	14	[103]
Hybrid IASBR (granular anammox), 10L	30	1.5	63	72	20	[103]
Hybrid IASBR (granular anammox), 10L	30	2	74	84	19.5	[103]
Hybrid IASBR (granular anammox), 10L	30	2.5	77	95	22	[103]
IFAS, 8L	25	0.5	47	-	-	[112]
IFAS, 8L	25	1	75	-	-	[112]
IFAS, 8L	25	2	0 - 17	-	-	[112]
MBR, 4L	34	0.8	81	190	-	[113]
Granular SBR, 10L	25	0	54	330	-	[83]
Air-lift microgranule-based reactor, 2.4L	25	0	72	432	160	[114]
IFAS, 60L	28	6.1	63	265	-	[114]
OLAND RBC, 3.6L	25	0	51	434	-	[114]

Note: TN: total nitrogen; NRE: nitrogen removal efficiency, %; NRR: nitrogen removal rate, mg N/L/d; SDNR: specific denitrification rate, mg N/g VSS/d; MBR: membrane bioreactor; IASBR: intermittently aerated sequencing batch reactor; IFAS: integrated fixed-film activated sludge reactor; OLAND: oxygen-limited autotrophic nitrogen denitrification; RBC: rotating biofilm contactor; -: not available.
[a] 62% by PN-A out of more than 85% TN removal.

is not an issue for full-scale applications as the wastewater temperature is normally more than 10 °C [115]. Therefore, effective anammox biomass retention will be critical to successful mainstream PN-A. The growth rate of anammox bacteria can be decreased from 0.33 d^{-1} at 30°C to 0.0011 d^{-1} at 20°C [46], together with the high hydraulic loads (short hydraulic retention time, HRT) making it a major challenge to maintain sufficient anammox biomass in the reactor. The low temperature also reduces the activity of AOB and NOB, but it affects AOB more severely than NOB: NOB begin to have higher growth rates than AOB at temperatures < 20 °C and the lower the temperature is, the higher the difference is [101]. The activity ratio of AOB/NOB was reported to be less than 1 when the temperature was 17 °C [116]. On the other hand, the low anammox activity at low temperatures also worsens the suppression of NOB through nitrite-competition, so low temperature and low ammonium concentrations make it difficult to maintain NOB suppression. Thus, at low temperatures, without efficient maintenance of anammox activity and biomass, the long-term process stability cannot be achieved. If the NLR is higher than the nitrogen removal capacity of the anammox biomass, the removal of ammonium will either lead to the accumulation of nitrite (when NOB are properly suppressed) or nitrate (when NOB suppression fails), resulting in poor nitrogen removal performance and effluent quality.

Despite these challenges, recent studies have reported some encouraging results. In one of the studies, efficient nitrogen removal (ammonium removal efficiency > 90%, NRE 73 ± 6%) with satisfactory effluent quality (TN < 6 mg/L, nitrate production ratio of 16% (NPR, nitrate production over nitrogen removed)) were achieved in a lab-scale MBBR over 5 months at 15 °C, though the NRR was low around 30 mg N/L/d and heterotrophic denitrification contributed to the nitrogen removal [102]. Another exciting news is the occurrence of anammox in the anoxic tank (HRT 3.6 hours, MBBR) and anaerobic tank (HRT 1 hour, MBBR) in a full-scale MWTP in Xi'an (250,000 m^3/d) where the wastewater temperature is 11 - 20°C. The non-peer-reviewed report shows that anammox bacteria accounted for almost 10% of the microbial community in the biofilm and anammox process accounted for about 15% of the TN removal [117]. Though the mechanism and some of the results are still in dispute (e.g., the nitrite production pathway and the percentage of anammox bacteria, etc.), the phenomenon indicates

Table 2-6. Implementation of mainstream PN-A at low temperatures.

Influent (mg/L)	NRR	NRE	Effluent (mg/L)	Operating conditions	Remaining challenges	Reference
NH_4^+-N: 34; COD: 62	64 - 84	40 - 94	NH_4^+-N:1 - 18; NO_3^--N: 4 - 9; NO_2^--N < 2 After re-inoculation: NH_4^+-N:2 - 8; NO_3^--N: 4; NO_2^--N < 1	Lab-scale 1.35 L up-flow granular PN-A; aeration controlled based on DO and performance; HRT 8-9 hours; high COD/N ratio of about 2.5; 20 °C; operation duration 150 days.	Temperature decreased from 24 °C to 20 °C and deductive sulfide (produced by preceding COD- removal anaerobic reactor) inhibition deteriorated the performance; part of the biomass was replaced to recover the performance.	[5]
NH_4^+-N: 21 ± 5; COD: 69 ± 19	30± 10	73 ± 6	NH_4^+-N: 2; TN < 6; nitrate production ratio (NPR, nitrate production over nitrogen removed, %): 16 ± 5 %	Lab-scale 12 L MBBR ran as SBR; NLR 40 mg N/L/d; fixed-DO-ammonium aeration control (350 mL/min); DO 0.18 mg /L; residual ammonium 2 mg N/L; HRT 14 hours; 15 °C; operation duration 5 months.	Significant suppression of anammox activity with a sudden temperature drop to 11 °C.	[102]
NH_4^+-N: 21 ± 5; COD: 69 ± 19	26 ± 14	63 ± 8	NH_4^+-N: 2; TN < 10; NPR: 27	Lab-scale 12 L hybrid MBBR run as SBR; NLR 38 mg N/L/d; fixed-DO-ammonium aeration control (100 mL/min); DO 0.15 mg/L; residual ammonium 2 mg N/L; SRT of the suspended biomass was not	Same problem with MBBR when the temperature dropped to 11 °C. Compared with those of MBBR, the hybrid MBBR had less stable and lower NRR, lower NRE, and higher NPR. This was partially caused by	[102]

Influent (mg/L)	NRR	NRE	Effluent (mg/L)	Operating conditions	Remaining challenges	Reference
				controlled; HRT 14 hours; 15 °C; operation duration 5 months.	uncontrolled SRT and the biomass washout when short HRT was applied to deal with low nitrogen concentration.	
NH_4^+-N: 50 - 60	380 - 700 [a]	36 - 42	NH_4^+-N:2 - 23; NO_3^--N:5 - 10; NO_2^--N:10 - 20 [a]; NPR:16 – 21%	2.5 L lab-scale OLAND RBC; DO 1.7 - 3.1 mg/L; immersion level 55%; HRT 1.1 - 1.9 hours; temperature stepwise decreased from 16 °C to 14 °C; operation duration 94 days	The accumulation of nitrite and nitrate resulted in lower nitrogen removal efficiencies.	[118]
NH_4^+-N: 74.5 ± 3.2	0 - 152 ± 17	4 - 60	NH_4^+-N: 32.8 ± 5.00; NO_3^--N: 18 - 62 [a]	10 L SBR, granular sludge; continuous aeration; NLR: 40 - 387 mg N/L/d [a]; 15 °C; operation duration 63 days.	Last for 63 days, then the system crashed (specific NRRs decreased from 45 to 6.6 mg N/ g VSS/d)	[83]
NH_4^+-N: 70 [a]	20	10 - 45	NH_4^+-N: 20 - 50; NO_3^--N: 10 - 20 [a]	10 L SBR, granular sludge; intermittent aeration; 15 °C; operation duration 40 days.	NRE gradually decreased to about 13%	[83]
NH_4^+-N: 30 - 60; sCOD:60 - 90; TSS: 80 - 120	0.8 [b]	Increased from 22 to 70 [a]	NH_4^+-N < 10; NO_3^--N < 5; NO_2^--N < 2 NPR: 15% [a]	2 m^3 IFAS; continuous feeding and continuous aeration; fixed DO-ammonium aeration control (DO 0.2 - 1.0 mg/L, residual NH_4-N 5 - 10 mg/L, NO_3-$N_{production}$/NH_4-$N_{comsumption}$ < 11%); SRT 3 days to wash out NOB; K5 carriers (800 m^2/m^3, 40% filling degree); MLSS 3 g/L; temperature	An effluent polishing step was needed; long-term performance remains unknown.	[10]

Influent (mg/L)	NRR	NRE	Effluent (mg/L)	Operating conditions	Remaining challenges	Reference
				naturally dropped from 20 °C to 17 °C; operation duration 50 days.		
NH_4^+-N: 40 - 60 [d] to 700 - 1000	200 - 300 [e]	50 - 82	NH_4^+-N: 20 to 100 - 200	Semi-industrial scale 50 m^3 IFAS; bioaugmentation (biofilm carriers recirculation); alternating feed strategy (2 days side-stream+ 5 days mainstream) to boost anammox activity and supress NOB activity; Biofilme ChipM carriers (1200 m^2/m^3, 37% filling degree); DO 0.2 - 0.8 mg/L; 15 - 18 °C (mainstream), 25 - 28 °C (side-stream); operation duration about 90 days.	The NRR was not optimized due to the strict NOB-suppression control operation; the alternating feed strategy led to the variation of the effluent quality; an effluent polishing step was needed.	[10]
NH_4^+-N: 45; COD:44	0.03 [f]	25	NH_4^+-N:20; NO_3-N:4; NO_2^--N:0.4	Pilot-scale 0.2 m^3; MBBR with side-stream bioaugmentation; K1 carriers (500 m^2/m^3, 40% filling degree); online DO control; intermittent aeration; HRT 1.7 days; 15 - 17 °C; operation duration about 130 days	NOB activity and nitrate concentration increased when ammonium concentration decreased to about 20 mg N/L; an effluent polishing step was needed.	[84]

Influent (mg/L)	NRR	NRE	Effluent (mg/L)	Operating conditions	Remaining challenges	Reference
NH_4^+-N: 47; COD:71	0.05 [f]	44	NH_4^+-N:6.5; NO_3^--N:19.1; NO_2^--N:0.3	The above-mentioned MBBR was run as IFAS by inoculating 70 L of activated sludge; a clarifier and a recirculation pump was installed to return sludge to the IFAS; HRT 1.6 days; 15 - 17 °C; operation duration about 100 days	An effluent polishing step was needed.	[84]
NH_4^+-N: 26.8; NO_3-N: 1.7; NO_2-N: 1.0; COD: 62	158 - 191	33 - 46	NH_4^+-N: 6.8; NO_3^--N: 9.1; NO_2^--N:2.3	Pilot-scale 4 m^3 plug-flow granular sludge reactor equipped with an integrated tilted plate settler; without bioaugmentation; DO 0 - 2 mg/L; HRT 1.5 - 2 hours; 19 ± 1°C; operation duration >10 months.	Nitritation was the rate-limiting process; a better and stable effluent quality and attention for suspended solids handling were needed.	[119]
-	500 - 1100	-	NH_4^+-N: 2 - 3; NO_2^--N:1 - 3	Strass full-scale MWTP Carousel type aeration tank DO varied between 0~0.55 mg/L along the flow path; ammonia-based aeration control; side-stream bioaugmentation; NLR 550 - 1600 mg N/L/d; 9 - 19 °C;	Higher N_2O emission than conventional operation.	[110] a

Influent (mg/L)	NRR	NRE	Effluent (mg/L)	Operating conditions	Remaining challenges	Reference
NH_4^+-N: 60 - 80	Decreased from 150 to 0	Decreased from 60 to 5	NH_4^+-N: 10 - 40; NO_3^--N: increased from 10 to 60; NO_2^--N: < 1	10 L SBR with granular sludge; continuous aeration; 15°C; operation duration 100 days.	System collapsed after 63 days of operation (NO_3-$N_{production}$/NH_4-$N_{comsumption}$ to 0.95).	[83]
NH_4^+-N: 65 - 80	Decreased from 10 to 5	Decreased from 40 to 10	NH_4^+-N: 20 - 50; NO_3^--N: 10 - 20; NO_2^--N: < 10	10 L SBR with granular sludge; intermittent aeration; 15°C; operation duration of about 150 days.	NRE decreased from 40% to 10% after 30 days of operation then again decreased from 30% to 10% after recovery (increased NO_3-$N_{production}$/NH_4-$N_{comsumption}$ to 0.7).	[83]

Note: NRR: nitrogen removal rate, mg N/L/d; NRE: nitrogen removal efficiency, %; NLR: volumetric nitrogen load, mg N/L/d; NPR: nitrate production ratio, i.e., nitrate production over nitrogen removed, %; OLAND: oxygen-limited autotrophic nitrification/denitrification; RBC: rotating biofilm contactor; pollutants concentration: mg/L; -: not available.

[a]: estimated data based on the given information.

[b]: NRE, g NH_4-N/m^2/day;

[c]: data during non-disturbed periods.

[d]: the mixture of mainstream wastewater (NH_4^+-N: 23 mg/L; sCOD: 65 mg/L; TSS:30 mg/L) with 5% of reject water (NH_4^+-N: 756 mg/L; sCOD: 310 mg/L; TSS: 1770 mg/L) to make a target NH_4^+-N level of 50 mg/L.

[e]: NH_4^+-N removal rate.

[f]: g N/m^2/day.

the feasibility of the mainstream anammox application in full-scale MWTP at low temperatures. Further work is needed to figure out the reasons leading to the occurrence of anammox, the operational boundaries, and the methods to improve the contribution of anammox so that the results can be replicable. Overall, with the current technology, it's still challenging for the application of mainstream PN-A at low temperatures in terms of achieving efficient long-term stable nitrogen-removal performance and satisfactory effluent quality. While using proper control approaches, there are chances to overcome these challenges.

2.4.2 What should we do next?

To address the remaining challenges, further research work can be conducted in four aspects: cultivation of anammox bacteria with higher growth rate and anammox activity enhancement (section 2.2), suppression of NOB, biomass control, and effluent polishing. The detailed NOB-suppression information can be found in section 2.3. But not all of the strategies are suitable to mainstream PN-A, such as the FA-inhibitory strategy which needs high ammonium concentration and the pH-based aeration control strategy which needs stable pH [80]. The currently reported strategies include residual ammonium, fixed-DO setpoints, and oxygen-supply control (intermittent aeration, DO-ammonium-aeration control) (Table 2-6). Some of the results [10, 102, 107, 118, 119] indicate that with proper control, it is possible to effectively suppress the NOB activity in mainstream PN-A reactors. By combining the strategies of residual ammonium, low fixed-DO setpoints, and nitrogen based-aeration control, NOB can be suppressed (in terms of relative abundance) for over 5 months at 15 °C [102], which suggests that reliable low-temperature NOB suppression in mainstream conditions requires the combination of several rather than single control strategies. But more practically available and more reliable methods need to be developed. More attention should also be paid to biomass control (retaining AOB and anammox while washing out NOB) and effluent polishing methods which are more practically accessible.

2.4.2.1 Biomass control

Efficient biomass control can retain anammox bacteria and AOB and wash out undesired NOB and heterotrophs. The highest priority should be given to efficient anammox biomass

retention, in particular when treating mainstream wastewater which is characterized with high hydraulic loads, low temperature, and low ammonium concentrations. As mentioned in section 2.3, biofilm-based and granule-based biomass is more efficient in retaining anammox biomass. However, the anammox-containing granules still have chances to be washed out of the reactor, especially under the high hydraulic loading conditions. The necessitation of hydrocyclones to retain anammox granules at a MWTP also indicates this [65]. Separation of the granules from the effluent remains as one of the main challenges in a pilot-scale granular mainstream PN-A reactor at another MWTP [120]. Therefore, biofilm-based PN-A seems to be a better choice for anammox retention. For the mainstream PN-A, both anammox activity and anammox biomass can be stably maintained in the biofilm at 15 °C for over 5 months [102], and the reactor with larger carriers displayed better overall performance at low temperatures [70]. The case of the MWTP in Xi'an also demonstrates it is feasible to retain anammox bacteria in the form of biofilm under "real" mainstream conditions (in anoxic and anaerobic tanks).

Bioaugmentation is another choice to maintain sufficient anammox biomass and AOB within the reactor. This approach has been adopted in several studies (Table 2-6) and can also be used to accelerate start-up and recover failing PN-A process [93]. The bioaugmentation can be realized in two ways [10, 65, 121]: 1) delivering part of the anammox biomass from a side-stream reactor to the mainstream reactor, and 2) separating anammox biomass from the mainstream effluent and flocculant sludge (containing mainly AOB) from the side-stream effluent and returning both of them to the mainstream reactor. Besides the bioaugmentation methods, the anammox growth can be enhanced by periodically feed the multi-cell mainstream PN-A, one cell after another, with side-stream wastewater (temporary side-stream PN-A). At the Strass MWTP, the bioaugmentation (the first method mentioned-above) was carried out at the rate of 40 m^3/week to the mainstream reactor from a 500 m^3 side-stream reactor [65]. This also assisted the NOB suppression in the mainstream PN-A without affecting the performance (in terms of ammonium removal efficiency) of the side-stream reactor, but surprisingly improved the anammox abundance (in terms of granule volume) of the side-stream reactor [65].

More and more evidence shows that a hybrid system accommodating both suspended-growth and biofilm biomass is a better choice to realize efficient biomass control and is more advantageous than the pure biofilm-based system. The nitritation process (the

oxidation of ammonium to nitrite) rather than the anammox process was reported to be the main bottleneck in pilot-scale mainstream PN-A reactors [10, 119]. The suspended sludge has the potential to have a higher nitritation capacity than biofilm-based sludge as AOB are usually highly enriched in suspended growth reactors (6.0% - 7.3%) compared to biofilm in MBBRs (0.5% - 0.8%) while anammox bacteria are more abundant in biofilm in MBBRs (29.6% - 55.6%) than in suspended growth reactors (15.6% - 24.2%) [67]. Thus, the nitritation capacity and therefore nitrogen removal performance can be improved by maintaining a certain amount of suspended-growth activated sludge flocs. Therefore, a hybrid system may take advantage of the two biomass configurations with regard to process stability. Besides, the hybrid system has lower oxygen requirements than the biofilm systems because of the reduced diffusion limitations for nitritation in suspended-growth sludge. In the hybrid system, a short enough flocculent SRT can be applied to selectively wash out undesired NOB and heterotrophs while retaining anammox in the biofilm [98]. It has been proved that by introducing suspended biomass into MBBR (integrated fixed film activated sludge, IFAS), the NRE was increased from 36 ± 3% to 70 ± 4% with a simultaneous three-fold increase of NRR [80]. Taken together, with proper biomass control (control of SRT (suspended-growth biomass) and segregation of conditions and microbial activities (anoxic condition in biofilm for anammox and aerobic condition in flocs for AOB)), the hybrid configuration bears the potential in achieving higher volumetric rates with lower oxygen requirements, more versatile control of NOB, and possibly more flexible operation towards varying influent loadings compared with pure biofilm configuration [102].

2.4.2.2 Effluent polishing

Theoretically, presuming the NOB activity is completely inhibited, the maximum NRE of PN-A is 87% (Equation 2-1). So far, the most encouraging long-term stable results are NRR of 30 mg N/L/d with NRE of about 73% at 15 °C (COD/N of 3.3) [102]. This means at best, the influent ammonium concentration of more than 37 mg/L (compared with the common range of 15 - 100 mg/L) will have the effluent nitrogen concentrations exceeding 10 mg/L, which is over the discharge limit of most countries. Therefore, to achieve satisfactory effluent quality, an effluent-polishing step, either combined with PN-A process or as a separate subsequent step, is a prerequisite for the application of mainstream PN-A. Further study is needed to investigate the polishing of the effluent from mainstream PN-A.

As nitrate and nitrite are the main nitrogen components in the effluent from PN-A, the processes capable of removing nitrate and nitrite can be used to polish the effluent (Table 2-7). The most obvious option is heterotrophic denitrification. Even though an up-front stage (e.g., anaerobic digestion, etc.) is established to remove the COD prior to the mainstream PN-A step (Figure 2-5 B), organic carbon can hardly be completely removed, especially at low temperatures. For example, 71% of the COD in the mainstream wastewater was removed in an anaerobic digestion reactor at 13 °C with 140 - 160 mg COD/L (COD/N ratio of 2.3) in the effluent [122]. This amount of COD is more than enough to remove nitrate and nitrite in the effluent of PN-A via the heterotrophic denitrification (5.72 g COD/ g NO_3^--N [123, 124]). The presence of higher COD/N ratio may increase the NRE (Table 2-5) and benefit anammox bacteria due to oxygen-depletion, but may also lead to the overgrowth of heterotrophic denitrifiers, which compete with anammox bacteria [26]. In a mainstream PN-A SBR, NRE increased from 18% to 66% (anammox process contributed to 50 - 60%) when the COD/N ratio was increased from 1.4 to 2.7, but the specific anammox activity decreased from 170 mg N/g VSS/d to 58 mg N/g VSS/d [125]. Biofilm and hybrid PN-A system can be used in this case, as it has been reported heterotrophic biomass grew preferentially in the suspended-growth sludge and was washed out efficiently in a pilot-scale hybrid PN-A reactor (granular anammox biomass and suspended-growth biomass) [26, 119].

Methane is one of the main products of anaerobic digestion and exists in the effluent of the anaerobic digestion of mainstream wastewater (can be up to 91 mg of COD/L) [24]. When methane serves as the electron donor, the nitrate and nitrite can be removed by newly discovered denitrifying anaerobic methane oxidation (DAMO) process [13]. Two kinds of microorganisms are currently known to carry out this process: archaeal *Candidatus Methanoperedens nitroreducens* reducing nitrate to nitrite and bacterial *Candidatus Methylomirabilis oxyfera* reducing nitrite to dinitrogen gas [126]. It has been proved that at 22 °C (influent 400 mg NH_4^+-N /L, influent 1000 mg NO_3^--N /L, HRT 1.5 days), a DAMO-anammox reactor can reach a nitrate reduction rate of 330 ± 9 mg NO_3^--N /L/d and 268 ± 2 mg NH_4^+-N /L/d, in which anammox removed 354 ± 3 mg NO_2^--N /L/d [127]. By combing with anammox process at 20.8 °C (influent NH_4^+-N 22 mg N/L, influent NO_2^--N 29.5 mg N/L, HRT 4 h), an NRR of 275 mg-N /L/d was achieved with satisfactory effluent quality (TN concentration below 5 mg N/L) and 30 - 60% of the nitrate produced by anammox was

reduced to nitrite by DAMO archaea [126]. The major challenges for the application of DAMO process are the consumption of methane, which is a renewable energy source, and the long doubling time of bacterial DAMO cultures (1 - 2 weeks for *Candidatus Methylomirabilis oxyfera* [128]), which results in relatively long start-up time.

Electrons required for the removal of nitrate and nitrite can also originate from the autotrophic /bio-electrochemical processes as listed in Table 2-7. The selection of these process can be made on the case-by-case basis depending on the availability of the electron donors and the local conditions. In terms of the availability of the electron donors, trace amount of H_2 and H_2S are common products of anaerobic digestion (about 62 mg COD/L equivalent sulfide in the anaerobic digestion effluent of mainstream wastewater [24]), iron is the fourth most abundant element in the Earth's crust (primarily exists as solid phase minerals when pH>7 and ferrous iron primarily exists as an aqueous species when pH < 4) [129], and pyrite (FeS_2) and pyrrhotite ($Fe_{1-x}S$)) are two ubiquitous iron sulphide minerals [130].

The nitrate-dependent oxidation of ferrous iron can be either abiotic, biotic, or both [131]. This process is energetically favorable at neutral pH and should yield enough energy to support the growth of microorganisms such as a hyperthermophilic archaeon, *Ferroglobus placidus*, and a mesophilic *Betaproteobacterium*, strain 2002 [129]. The microbial nitrate reduction by ferrous iron has been found to take place depending on pH (maximum rates at pH 8) in different types of activated sludge treatment plants and if conditions are suitable, it may be as important as the heterotrophic denitrification in terms of denitrification [132]. However, energy conservation directly coupled to the nitrate-dependent oxidation of ferrous iron could not be demonstrated without an additional electron donor, even in the case of a known ferrous iron-oxidizing chemolithoautotrophic bacterium, *Thiobacillus denitrificans* [129]. This means ferrous iron-bearing minerals containing other electron donors such as iron sulfide minerals pyrite and pyrrhotite [130] may be better choices for nitrate removal. Pyrrhotite has been demonstrated very effective in almost complete nitrate removal (NLR 55 - 332 mg NO_3-N/L/d) and simultaneous phosphorus removal [130]. For the sulfur-based nitrate removal, high NRR can be achieved (2258 - 4500 mg NO_3-N/L/d) when thiosulfate is used as the electron donor, while lower NRR of 0.4 - 560 mg NO_3-N/L/d can be achieved when elemental sulfur is used (usually combined with lime to maintain pH and alkalinity) [133]. The application of hydrogen-based nitrate removal can be

Table 2-7. Microbial nitrate/nitrite removal processes.

Processes	Reactions	Identified microorganisms	μ	NLR	NRE	Cost	References
Heterotrophic denitrification	$5CH_3COO^- + 8NO_3^- + 13H^+ \rightarrow 4N_2 + 10CO_2 + 14H_2O$	*Paracoccus denitrificans*, *Paracoccus ferrooxidans*, *Paracoccus pantotrophus*, *Ochrobactrum anthropi*, *Azospirillum brasilense*, *Bradyrhizobium japonicum*, *Ralstonia metallidurans*, *Rhodocyclus* sp., *Azospira oryzae*, and *Acidovorax BoFeN1*	-	20 - 1360 [a]	40 - 70	7.9	[24, 104-106, 134]
	$CH_3OH + 0.926 NO_3^- + 0.926H^+ \rightarrow 0.060 C_5H_7O_2N + 0.703 CO_2 + 2.26 H_2O + 0.432 N_2$					1.8 - 2.3	
Sulphur-based denitrification	$1.10 S + NO_3^- + 0.76 H_2O + 0.4 CO_2 + 0.086 NH_4^+ \rightarrow 0.04 C_5H_7NO_2 + 0.48 N_2 + 0.98 SO_4^{2-} + 0.96 H^+$	*Thiobacillus denitrificans*, *Thiomicrospira CVO*, and *Sulfurimonas paralvinellae*	-	2680 (20°C)	> 98	0 - 0.26 [d]	[133, 134]
	$0.84 S_2O_3^{2-} + NO_3^- + 0.43 H_2O + 0.35 CO_2 + 0.87 HCO_3^- + 0.087NH_4^+ \rightarrow 0.087 C_5H_7NO_2 + 0.5 N_2 + 1.69 SO_4^{2-} + 0.7 H^+$	*Paracoccus denitrificans*, *Paracoccus ferrooxidans*, *Paracoccus pantotrophus*, *Thiobacillus thiophilus*, *Thioalkalivibrio denitrificans*, *Thialkalivibrio nitratireducens*, *Thiohalomonas denitrificans*, *Thioalkalivibrio thiocyanodenitrificans* , *Thiohalophilus thiocyanoxidans*, *Thioalkalispira microaerophila*,	-	280 - 3250 (30°C)	100	1.4 - 1.7	

Processes	Reactions	Identified microorganisms	μ	NLR	NRE	Cost	References
		Thiohalorhabdus denitrificans, *Alkalilimnicola ehrlichi strain MLHE-1*, *Sulfurimonas denitrificans*, *Thiobacillus denitrificans*, *Thiomicrospira CVO*, and *Sulfurimonas paralvinellae*					
	$3HS^- + 5H^+ + 8NO_2^- \rightarrow 3SO_4^{2-} + 4N_2 + 4H_2O$	*Paracoccus denitrificans*, *Paracoccus pantotrophus*, *Thiohalomonas denitrificans*, *Thioalkalispira microaerophila*, *Alkalilimnicola ehrlichi strain MLHE-1*, *Sulfurimonas denitrificans*, *Thiobacillus denitrificans*, *Thiomicrospira CVO*, and *Sulfurimonas paralvinellae*	3.24	50 - 90 (30°C)	> 98	0.25	[24, 134]
	$5HS^- + 3H^+ + 8NO_3^- \rightarrow 5SO_4^{2-} + 4N_2 + 4H_2O$						
	$3HS^- + 5H^+ + 2NO_2^- \rightarrow 3S + N_2 + 4H_2O$						
	$5HS^- + 7H^+ + 2NO_3^- \rightarrow 5S + N_2 + 6H_2O$						
Hydrogen-based denitrification	$3.03\ H_2 + NO_3^- + H^+ + 0.23\ CO_2 \rightarrow 0.05\ C_5H_7NO_2 + 0.48\ N_2 + 3.37\ H_2O$	*Paracoccus denitrificans*, *Paracoccus ferrooxidans*, *Paracoccus pantotrophus*, *Ochrobactrum anthropi*, *Azospirillum brasilense*, *Bradyrhizobium japonicum*, *Ralstonia metallidurans*, *Rhodocyclus* sp., and *Alkalilimnicola ehrlichi strain*	-	1970 - 6200 (27°C)	> 97.5	1.1 - 2.1	[133, 134]

Processes	Reactions	Identified microorganisms	μ	NLR	NRE	Cost	References
Hydrogen (bio-electro denitrification)	$2\ NO_3^- + 6\ H_2O + 10e^- \rightarrow N_2 + 12\ OH^-$ (cathode) $2\ NO_3^- + H_2O \rightarrow N_2 + 2.5\ O_2 + 12\ OH^-$ (overall)	-	-	-	-	-	[133]
Iron-based denitrification	$10Fe^{2+} + 2NO_3^- + 24H_2O \rightarrow 10Fe(OH)_3 + N_2 + 18H^+$	*Thiobacillus denitrificans*, *Azospira oryzae*, *Acidovorax BoFeN1*, *Pseudogulbenkiania sp. strain 2002*, and *Acinetobacter* sp. *SZ28*	-	41 - 117 (30°C)	>99	6.0	[132, 134]
	$Fe + 0.4\ NO_3^- + 1.2\ H_2O \rightarrow Fe^{2+} + 0.2\ N_2 + 2.4\ OH^-$		-	-	-	0	[134]
Iron sulphide mineral-based denitrification	$5FeS_2 + 14NO_3^- + 4H^+ \rightarrow 7N_2 + 10SO_4^{2-} + 5Fe^{2+} + 2H_2O$	*Thiobacillus denitrificans*	-	-	-	1.2	[131, 134]
	$10Fe_{1-x}S + 2(9-3x)\ NO_3^- + (28-36x)\ H^+ \rightarrow 10SO_4^{2-} + (9-3X)\ N_2 + 10(1-x)\ Fe^{3+} + (14-18x)\ H_2O$	*Thiobacillus* and *Sulfurimonas*	-	-	-	-	[130, 135]
Thiocyanate-based denitrification	$SCN^- + 1.6\ NO_3^- + 0.2\ H_2O + 1.6H^+ + HCO_3^- \rightarrow SO_4^{2-} + NH_3 + 2\ CO_2 + 0.8\ N_2$	-	-	1200 (21°C)	>90	0	[134]
Denitrifying anaerobic methane oxidation	$CH_4 + 4NO_3^- \rightarrow CO_2 + 4NO_2^- + 2H_2O$ (archaea)	*Candidatus Methanoperedens nitroreducens*	0.8	10 [b] (21°C)	-	-	[24, 126]
	$3CH_4 + 8NO_2^- + 8H^+ \rightarrow 3CO_2 + 4N_2 + 10H_2O$ (bacteria)	*Candidatus Methylomirabilis oxyfera*	0.035	17.5 [c] (21°C)	-	-	

Note: μ: growth rate of the responsible microorganisms, /day; NLR: nitrogen loading rate, mg N/L/d; NRE: nitrogen removal rate, %; Cost: USD/kg NO_3^--N; Fe, SCN^-, and S (biogenic) were assumed free of the cost being waste products and/or contaminants; -: not available.

[a] nitrogen removal rate, mg N/L/d.

[b] nitrate removal rate, mg N/L/d.

[c] nitrite removal rate, mg N/L/d.

[d] 0.26 for chemical S, 0 for biogenic S.

realized in the fluidized reactor, hollow-fiber membrane biofilm reactor, etc., with NRR of 110 - 2420 mg NO_3-N/L/d, or in bioelectro-reactors where microorganisms on the cathode remove nitrate together with hydrogen produced on the cathode by electrolysis, achieving NRR of about 343 mg NO_3-N/L/d [133]. The hydrogen-based nitrate removal process has several drawbacks: the high cost of production and handling of hydrogen, the low solubility of hydrogen gas and potential safety problems. The extremely low aqueous solubility and dissolution rate of H_2 and solid phase electron donors such as elemental sulfur, FeS_2, and $Fe_{1-x}S$ are the factors limiting their availability to denitrifying microorganisms and the denitrification kinetics. Membrane biofilm reactors establishing counter fluxes between nitrate and gaseous electron donors such as H_2 and methane may be a better approach to enhance the dissolution [136]. Biofilm systems are recommended for the solid phase electron donors as they allow direct contact between electron donor and microorganisms [134].

2.4.2.3 Partial denitrification providing nitrite for anammox

In the PN-A process, the aerobic partial nitritation process which produces nitrite, is combined with the anaerobic anammox process in a single reactor. As the practical application of mainstream PN-A process turns difficult, combining the anoxic/anaerobic partial denitrification (the reduction of nitrate to nitrite) and anammox has been proposed. In this process, nitrite generated from heterotrophic nitrate reduction is removed with ammonium by the anammox process (Equation 2-5) [137], and a preceding full nitrification step is needed to oxidize about half of the ammonium to nitrate. This process, which is termed partial denitrification-anammox, can be applied to the existing anoxic heterotrophic denitrification units of the MWTPs to reduce the operating cost (reducing extra organic carbon addition and the aeration cost). The key for this process is the realization of partial denitrification which can be achieved through two ways (Table 2-8): 1) selectively enriching microorganisms only capable of reducing nitrate to nitrite, or 2) maintaining a lower reduction rate for nitrite than nitrate, which is the result of the lower nitrite reductase (Nir) activity than nitrate reductase (Nar and Nap) activity (Figure 2-2) [138], by controlling the types of carbon sources, COD/NO_3^--N ratio, pH, temperature, nitrate concentration, and DO level.

Table 2-8. Factors impacting partial denitrification.

Impacting factors	Details	References
Type of carbon sources	• Acetate, glycerol, methanol, glucose, and ethanol lead to partial denitrification providing as long as the nitrite sink was available (e.g., enough competition for nitrite by anammox); • Glucose caused higher nitrite accumulation and production rate than acetate and methanol; • Long-term performance indicated reactors fed with acetate and glycerol achieved a higher partial denitrification efficiency; • Methanol was easy for full denitrification during long-term operation.	[138, 139]
COD/NO_3^--N ratio	Controversial opinions: • COD/NO_3^--N ratio did not directly affect the partial denitrification efficiency and should be used to balance partial denitrification rates and anammox rates; • Higher COD/ NO_3^--N ratios (1, 6, 10, 15, 25) resulted in greater peak values of nitrite concentration (peaked at 1 h); • Poor/insufficient carbon sources (COD/NO_3^--N ratio of 3, 6, 12, 30) were more prone to produce nitrite; • Optimal COD/NO_3^--N ratio existed: low ratios meant low nitrate reduction efficiency while high ratios led to low NTR.	[138-141]
pH	• A high pH of 9.0 (compared with 7, 8, and 10) facilitated the start-up of the partial denitrification process; • Higher pH led to higher nitrite accumulation rate.	[141, 142]
DO	• High DO was prone to nitrite accumulation.	[140]
Nitrate concentration	• Slightly influenced nitrite production.	[140]
Potential functional microbes	• *Thauera*, *Pseudomonasstutzeri* D6, *Competibacter*, *Paracoccus denitrificans*, *Pseudomonas fluorescens*, *Pseudomonas stutzeri*, *Alcaligenes species*,	[139]

Impacting factors	Details	References
	Flavobacterium species, *Staphylococcus species*, *Pseudomonas pseudoalcaligenes*, and *Bacillus niacin*.	

Note: NTR: nitrate-to-nitrite transformation ratio, i.e., nitrite production/nitrate consumption.

Table 2-9. Performance of partial denitrification integrated with anammox process.

Reactor	Carbon sources	Performance	Operating conditions	Microbes responsible for partial denitrification	References
Single-stage, SBR, 6L	Acetate	NRE 93.6%, NTR 95.8%; contribution of anammox in nitrogen removal: 95%.	The ratio of seeding granular anammox biomass/partial denitrification biomass was 3; 50 mg NO_3^--N/L; 50 mg NH_4^+-N/L; COD/ NO_3^--N 2.6; HRT 24 h; NLR 100 mg N/L/d; 29.2 - 12.7 °C; operation for180 days.	*Thauera* (61.5%)	[137]
Single-stage, SBR, 6L	Ethanol	With decreasing temperature from 22.7 °C to 16.6°C, NRE decreased from 90% to 85%; the contribution of anammox in nitrogen removal decreased from 95% to 89%.	The ratio of seeding granular anammox biomass/partial denitrification biomass was 3; 50 mg NO_3^--N/L; 50 mg NH_4^+-N/L; COD/ NO_3^--N 3; HRT 24 h; NLR 100 mg N/L/d; 22.7 - 16.6 °C; operation for 180 days.	*Thauera* (45.2%)	[137]
Two-stage, 11L partial	Municipal wastewater	Partial denitrification: NTR 63.5%; 22.5 mg NO_2^--N/L;	The partial denitrification SBR was sequentially run as	*Competibacter* (6.4 - 5.8%)	[143]

Reactor	Carbon sources	Performance	Operating conditions	Microbes responsible for partial denitrification	References
denitrification SBR, 10L anammox SBR		NO_2^--N/ NH_4^+-N 1.3; NRE about 69%; phosphorus removal efficiency: 98%; Anammox stage: 95% nitrogen removal; contributed to about 30% of the TN removal	anaerobic/anoxic/aerobic for 150min/180min/10min; influent of partial denitrification SBR: 3 L municipal wastewater (about 45 mg NH_4^+-N/L, 262 - 311 mg COD/L 3.4 - 6.9 mg PO_4^{3-}-P /L) during anaerobic phase, then 3.5 L synthetic wastewater (121 mg NO_3^--N /L) during anoxic phase; the effluent of partial denitrification SBR was fed to anammox SBR; 15–24 °C.		
Partial denitrification, 1L	Acetate	NAR: 21%, 38%, and 57% with pH of 5, 7, and 9, respectively	30 mg NO_3^--N/L; 90 mg COD/L; pH: 5, 7, and 9; HRT 1 h; 29.2 - 12.7 °C; operation for 420 days.	*Thauera* [a]	[142]
Single-stage, UASB, 2 L	Acetate	NRE: 89%; NTR>90%; NRR: 640 mg N/L/d; contribution of anammox in nitrogen removal: 92%.	30 mg NO_3^--N/L; 30 mg NH_4^+-N/L; COD/ NO_3^--N 3.4; NLR 560 - 720 mg N/L/d; HRT 2.55 - 2.0 h; 15.5 - 17.6 °C; operation for 60 days.	-	[144]
Single-stage, UASB, 2 L	Acetate	NRE: around 70%; NH_4^+-N removal efficiency: 60 - 80%; NTR: about 50%; NRR: about 600 mg N/L/d; contribution of anammox in nitrogen removal: 90%.	30 mg NO_3^--N/L; 30 mg NH_4^+-N/L; COD/ NO_3^--N 2.8; NLR 850 mg N/L/d; HRT 1.7 h; 17.6 °C; operation for 109 days.	-	[144]

Reactor	Carbon sources	Performance	Operating conditions	Microbes responsible for partial denitrification	References
Partial denitrification, SBR, 10L	Sodium acetate	Difference between nitrate reduction rate and nitrite reduction rate: 0.24, 1.29, 1.99, and 0.75 mg / g VSS/h at pH of 7, 8, 9, and 10, respectively.	Batch tests; four reactors operated at pH of 7, 8, 9, and 10; stirred at 100 rpm; seeding sludge: secondary sedimentation tank of a MWTP (anaerobic/anoxic/oxic process); 30 mg NO_3^--N/L; 150 mg COD/L; 25 °C; operation for 180 min.	-	[141]
Partial denitrification, SBR, 100L	Sodium acetate	NTR: 93% (with pH controlled at 8.9 - 9.3) and < 40% (pH 7.8 - 8.5); 84%, 81%, 87%, and 66% at COD/ NO_3^--N of 1.5, 2, 2.5, and 3, respectively. Nitrate removal efficiency: 57%, 75%, 85%, and 97% at COD/ NO_3^--N of 1.5, 2, 2.5, and 3	Stirred at 120 rpm; seeding sludge: secondary sedimentation tank of a MWTP (anaerobic/anoxic/oxic process); 60 mg NO_3^--N/L; COD/ NO_3^--N 1.5, 2, 2.5, and 3; cycle duration 58 min; 25 °C; operation for 240 cycles.	*Thauera* (65%)	[141]

Note: NRE: nitrogen removal efficiency, %; SBR: sequencing batch reactor; NTR: nitrate-to-nitrite transformation ratio, i.e., nitrite production/nitrate consumption; NAR: nitrite accumulation rate, %; HRT: hydraulic retention time; NLR: nitrogen loading rate, mg N/L/d; UASB: up-flow anaerobic sludge blanket; -: not available.
[a] higher NAR was correlated with the enrichment of *Thauera*.

$$NO_3^- + 0.519CH_3COO^- + 1.026NH_4^+ \rightarrow 0.926N_2 + 0.56HCO_3^- + 0.064H^+ + 0.083C_5H_7NO_2{}_{(denitrifying)} + 0.062CH_2O_{0.5}N_{0.15(anammox)} + 2.164H_2O \quad 2\text{-}5$$

Table 2-9 indicates that apart from the aerobic partial nitritation, partial denitrification is a promising process providing nitrite for anammox process even at low temperatures. However, the success relies on strict control over operating conditions as this process prefers certain types of organic carbon sources, prefers high pH, and requires both optimal COD/NO_3^--N ratio and NO_3^--N/NH_4^+-N ratio to ensure the balance between partial denitrification and anammox process. Besides, the role of COD/ NO_3^--N ratio which balances partial denitrification rates and anammox rates or directly affects partial denitrification remains controversial and further study is needed to find the optimal COD/ NO_3^--N ratio for real wastewater. How to simultaneously control the NO_3^--N/NH_4^+-N ratio and COD/NO_3^--N ratio is another operational difficulty. For example, when using the real municipal wastewater (containing about 45 mg NH_4^+-N/L, 262 - 311 mg COD/L), the COD/N ratio was too high to produce enough nitrite for anammox so that external NO_3^--N (121 mg NO_3^--N/L) had to be added to achieve nitrate-to-nitrite transformation ratio (NTR, nitrite production/nitrate consumption) of 63.5% [143]. But the achieved NO_2^--N/NH_4^+-N ratio was still less than 1.3, thus, an aerobic phase had to be added to consume part of the ammonium to increase the NO_2^--N/NH_4^+-N ratio to 1.3 for the subsequent anammox process. Though operating difficulties present, the results show that with proper control, it is possible to combine the anammox process with the heterotrophic denitrification process. The case of Xi'an fourth MWTP also demonstrates the feasibility of the coexistence of anammox and heterotrophic denitrifiers in anaerobic and anoxic units. Thus, before the mainstream PN-A is practically available, a temporary, but more realistic way would be adding anammox biomass (in the form of biofilm) to the current anaerobic and anoxic units in the MWTPs so that part of the nitrogen can be removed by anammox and the operating cost can be reduced.

2.4.3 Summary

Mainstream PN-A process can achieve comparable nitrogen removal performance under "warm" conditions, but the effluent quality cannot be guaranteed to comply with the discharge

limits. It's much more challenging for the application of mainstream PN-A at temperatures < 20 °C. The main problems are long-term process instability, low TN removal efficiency, and poor effluent quality. Partial denitrification may serve as a temporary nitrite-supply alternative to partial nitritation. Figure 2-4 provided a roadmap to operable mainstream PN-A application and the availability of the potential solutions based on the current understanding of PN-A process. It can be concluded that approaches to gain a higher growth rate and activity of anammox bacteria are still a matter of concept, and engineering solutions for anammox retention are currently most available choices. Among the NOB suppression methods, the residual ammonium control and fixed-DO control is feasible, but needs to be combined with other methods; flexible aeration control (aeration control based on pH or nitrogen concentrations) and the combined aeration control strategies have been well studied in laboratory but are not ready for practical application. SRT control is suitable for the hybrid system and its feasibility in practical applications needs to be demonstrated. Biofilm-based hybrid system is suggested efficient for the purpose of reducing anammox biomass loss and maintaining nitritation capacity, but the successful full-scale application hasn't been proved; the bioaugmentation methods (adding exogenous biomass) are currently available and has been proved at both pilot-scale and full-scale systems. Finally, an effluent-polishing step, which can be realized by heterotrophic or autotrophic denitrification is prerequisite for the high-quality effluent. Overall, the road to successful mainstream PN-A application requires the integration of multiple, instead of single strategies.

2.5 Roadmap of the PN-A applications in future MWTPs

The current energy-negative MWTP accounts for approximately 3-5% of the electricity consumption in a country [145]. The BNR process requires extensive energy-input for aeration (oxidizing ammonium to nitrate) and a large amount of external organic carbon (usually methanol, glucose, ethanol, etc.). The anammox-based PN-A process is currently one of the most promising energy-efficient nitrogen removal alternatives. Though some operational difficulties (e.g., incoming solids, aeration control, and nitrate build up) still remain and require further research [6], the application of PN-A process for nitrogen removal from side-stream and

other ammonium-rich wastewater with low COD/N ratio is considered to be well-established [70]. For example, more than 76% of TN removal is achieved in full-scale and lab-scale PN-A systems treating real landfill leachate (Table 2-10). The installation of around 100 full-scale PN-A systems treating side-stream wastewater by 2014 and the proved energy savings demonstrate the importance and acceptance of the PN-A process [6, 22, 37]. Much more PN-A process applications for the treatment of side-stream and similar wastewater can be expected in the future.

Table 2-10. Nitrogen removal performance of partial nitritation combined with anammox (single-stage and two-stage) for the treatment of landfill leachate.

Reactor	Temperature (°C)	Influent	NLR	NRE (%)	References
Two-stage, SBR-hybrid biofilm reactor, 66.5 - 5 L	-	Diluted aged leachate; NH_4^+-N: 500 mg/L; BOD: 55 mg/L	4.2	93	[146]
Two-stage, A/O-UASB, 10.5- 5 L	-	Mature leachate; NH_4^+-N: 1330 mg/L; COD: 2250 mg/L	0.5	94	[147]
Single-stage, SNAD, 384 m^3	30 - 33	Real leachate; NH_4^+-N: 634 mg/L; COD: 554 mg/L	0.19	76	[148]
Single-stage lab-scale biofilm PN-A	35	Synthetic secondary-treated leachate; NH_4^+-N: 240 mg/L; COD: 554 mg/L	0.6	78.5	[149]

Note:

NLR: nitrogen loading rate, kg N/L/d;
NRE: nitrogen removal efficiency, %;
SBR: sequencing batch reactor;
A/O: anoxic/oxic process;
UASB: up-flow anaerobic sludge bed;
SNAD: simultaneous partial nitrification, anaerobic ammonium oxidation and denitrification;
-: not available.

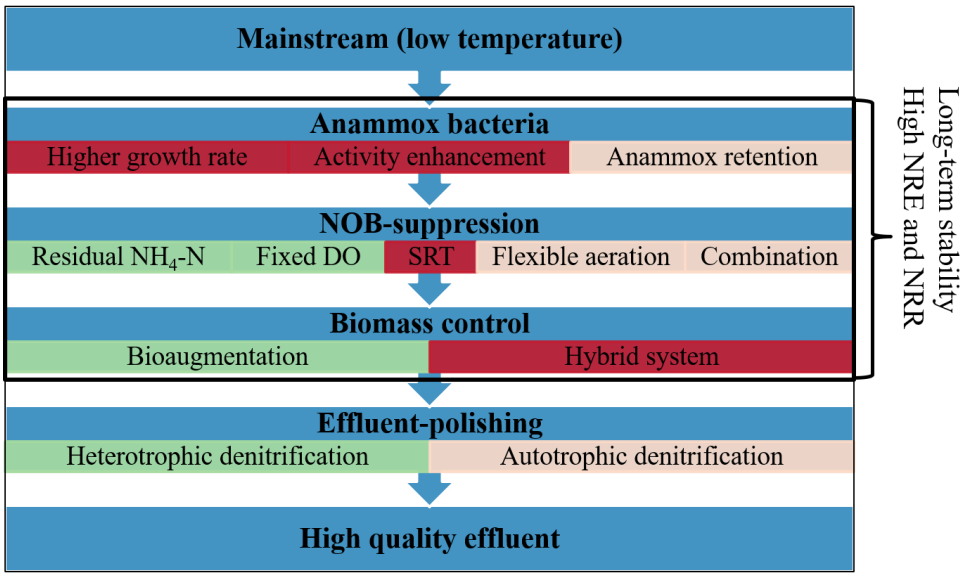

Figure 2-4. Roadmap to operable low-temperature mainstream PN-A. NRE: nitrogen removal efficiency. NRR: nitrogen removal rate.

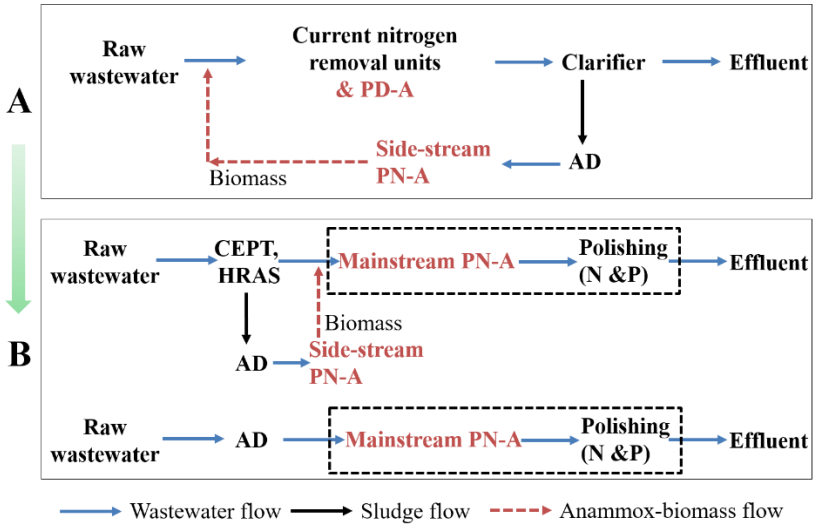

Figure 2-5. Simplified roadmap for the application of PN-A in MWTPs. Dash boxes indicate that the indicated processes can be integrated or separate. PD-A: partial denitrification-anammox; AD: anaerobic digestion; N: nitrogen; P: phosphorus; CEPT: chemically enhanced primary treatment; HRAS: high rate activated sludge.

Considering the challenging issues of the mainstream PN-A process, the application of PN-A in MWTPs is proposed to be realized in two steps (Figure 2-5). Firstly, the temporary

application of side-stream PN-A and mainstream partial denitrification integrated with anammox process is proposed (Figure 2-5 A) for the purpose of reducing energy-input and operational cost as well as improving nitrogen removal performance. This can be achieved by integrating PD-A with the current nitrogen removal system as already realized in Xi'an Fourth MWTP, and implementing side-stream PN-A at the same time. Anammox biomass from side-stream PN-A can be added to the mainstream reactors. With the breakthrough in the future, the application of mainstream PN-A can be expected which will promisingly maximize the energy recovery in the MWTP (Figure 2-5 B). This requires up-front carbon-capture that can be achieved through two ways: direct anaerobic digestion or concentration (such as chemically enhanced primary treatment (CEPT), high-rate activated sludge (HRAS), etc.) followed by anaerobic digestion [10, 95, 119]. The carbon-capture step converts most of the organic carbon to methane and thus reduces the COD/N to the required level for the subsequent mainstream PN-A. An effluent-polishing step, either combined with PN-A process or as a separate subsequent step, is required to reduce phosphorus and further reduce remaining nitrogen.

Chapter 3
Start up of partial nitritation-anammox process using intermittently aerated sequencing batch reactor: performance and microbial community dynamics

This chapter has been published as:

Songkai Qiu, Yuansheng Hu, Rui Liu, Xiaolin Sheng, Lujun Chen, Guangxue Wu, Hongying Hu, Xinmin Zhan., Start up of partial nitritation-anammox process using intermittently aerated sequencing batch reactor: Performance and microbial community dynamics. Science of The Total Environment, 2019, 647: 1188-1198.

3.1 Introduction

The most commonly used methods to start up the One-stage PN-A process are either inoculating an anammox reactor with nitrifying biomass or the other way around, or directly inoculating biomass from another PN-A system [35]. If there is no such inoculum available, it is also possible to start up the PN-A process using the more easily available activated sludge, because anammox bacteria are widespread in natural ecosystems, aerobic, and anaerobic sludges of MWTPs [150]. This is usually achieved by initiating the partial nitritation process firstly, followed by further process optimization (dissolve oxygen control, dosing of chemicals, etc.) to enrich the anammox bacteria in the partial nitritation system. For example, Jeanningros et al. triggered anammox activity in a continuously aerated partial nitritation SBR by maintaining low DO of 0.3-0.8 mg/L using on-line probes (DO, pH, conductivity, ammonium and nitrate concentrations, etc.) [21]. Another PN-A system was started up from a partial nitritation reactor by reducing DO from 0.9 to 0.4 mg/L, but efficient TN removal (74-80%) could only be maintained for 10 days [151]. Zhang et al. started up a PN-A sequencing batch biofilm reactor with around 30% of TN removal by applying salt stress to inhibit NOB and dosing hydrazine and hydroxylamine (0.1 mM) to induce the anammox process [152].

These studies demonstrate that it is challenging to start up the PN-A process without anammox inoculum and to maintain long-term efficient TN removal performance so sophisticated process control and/or specific chemicals addition are required. The challenges lie on 1) the difficulty in achieving stable partial nitritation; 2) the low growth rate of anammox bacteria and their vulnerability to oxygen inhibition, and 3) the difficulty in maintaining the balanced microbial community. IASBRs have proved to be a robust process to achieve stable partial nitritation [82]. In addition, the alternate aerobic/anoxic conditions are beneficial to preventing anammox from oxygen inhibition and to achieving balanced microbial activities. These features make IASBR a promising technology to address all these challenges, thus providing a robust method to start up and maintain the PN-A process.

Another gap in PN-A studies is that there is still no detailed microbial community analysis revealing the phylogenetic and functional traits of the microbes during the shifting from partial nitritation to PN-A process. Only the AOB genus *Nitrosomonas* was reported in the overwhelming majority of PN-A related studies, while the role of another important group of ammonium-oxidizing microorganisms – AOA – was rarely mentioned. The growth of AOA can be encouraged by low DO [153, 154] and thus may thrive in PN-A systems operated under oxygen-limited conditions [155]. AOA have an extremely high affinity towards ammonia which makes them capable of achieving higher ammonia oxidation rates. Therefore, they can be a better partner with anammox bacteria compared with AOB [153, 155]. Obviously, a thorough understanding of the microbial community is of great importance to the PN-A systems for optimizing reactor design and performance.

Therefore, the primary goal of this study was to justify IASBR technology to start up the PN-A process with return sludge as the initial inoculum and the robustness of this system in achieving long-term efficient TN removal. The following four objectives were pursued: 1) evaluating the long-term partial nitritation performance of IASBR; 2) assessing the feasibility of starting up PN-A process using IASBR and the long-term TN removal performance; 3) investigating the dynamics of functional microorganisms including AOB, anammox bacteria, NOB and particularly the evolution and role of AOA during the shift from partial nitritation to PN-A, and 4) investigating the dynamics of other major bacteria and archaea in the IASBR. Attempts were also made to link reactor operating conditions and reactor performance to functional microorganism populations and predicted functional genes.

3.2 Materials and methods

3.2.1 Experimental set-up

An SBR with a working volume of 8 L and height/diameter ratio of 1.4, made from acrylic plastic cylinder, was used in this study. Two peristaltic pumps were used, feeding the SBR

with synthetic landfill leachate and the other withdrawing the effluent. An air pump was used to supply air to the reactor through an air diffuser located at the bottom of the reactor, and the air flow rate was controlled by a flowmeter. Mixing of the bulk liquid during the SBR reaction phase was carried out by a submerged pump. The duration of the whole operational cycle was 360 min, which consisted of a reaction phase of 270 min and a settling phase of 90 min, giving four cycles per day. In each cycle, 700 mL of the synthetic landfill leachate was fed to the reactor in the first 5 min of the react phase, and the same amount of effluent was drawn out of the reactor during the last 15 min of the settle phase, giving a hydraulic retention time of 2.9 days. The sequential operation of the reactor was controlled by timers. The reactor was placed in a thermostatic cabinet to maintain the temperature at 30 ℃. A schematic diagram of the system is shown in Figure 3-1.

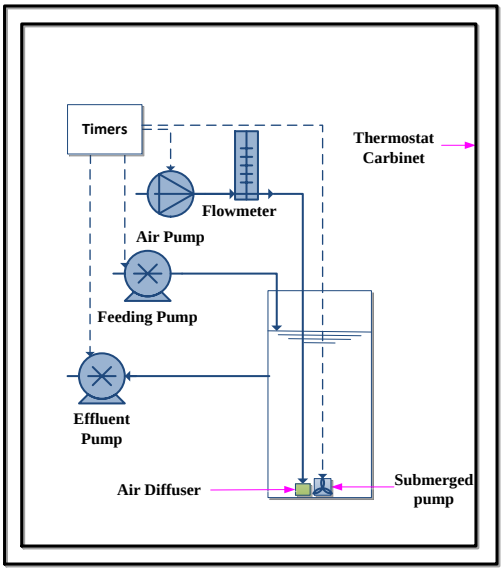

Figure 3-1. Schematic diagram of the reactor.

Aged landfill leachate is often characterized by high ammonium concentration and low COD/N ratio, which is an ideal wastewater for PN-A process. In order to exclude other potential influencing factors, synthetic wastewater simulating ammonium-rich aged landfill leachate was fed to the IASBR. The synthetic landfill leachate was made from tap

water and consisted of 300-900 mg/L NH_4^+-N (ammonium sulfate), 100 mg/L chemical oxygen demand (COD) (glucose), 58 mg/L $MgSO_4 \cdot 7H_2O$, 111 mg/L KH_2PO_4 and 170 mg/L $CaCl_2 \cdot 6H_2O$. Trace elements were supplied according to Van De Graaf et al. [156] $NaHCO_3$ was added to maintain the mole ratio of NH_4-N to HCO_3^- between1.55-2.0 and the pH value of the bulk liquid (Table 3-1). Four liters of return sludge collected from a local municipal MWTP was inoculated into the reactor, giving an initial sludge concentration of 1000 mg VSS /L. No sludge was discharged during the operation of the reactor except for that in the effluent.

3.2.2 Control strategies

The operation of the reactor consisted of three stages (Table 3-1). In Stage I and Stage II, control strategies developed previously by Li et al [82] were adopted. Briefly, in Stage I, to start up nitritation, continuous high rate aeration (to encourage the growth of AOB) and high level of free ammonia (FA, to temporarily inhibit NOB) were applied so that a high AOB:NOB ratio could be established quickly. A high nitrite accumulation ratio (NAR, the percentage of nitrite nitrogen to total oxidized nitrogen) would suggest successful start-up of the nitritation process. Then in Stage II, the aeration mode was switched to intermittent aeration (six successive 15 min non-aeration-30 min aeration intervals in the reaction phase) with a low aeration rate to maintain the partial nitritation process.

Specifically, in Stage I, free ammonium (FA) concentrations were maintained between 8.5-42 mg/L by keeping high NH_4^+-N concentrations (> 80 mg/L) in the reactor and adjusting the pH value (using 3 M KOH solution) of the synthetic leachate to more than 7.9; the aeration rate (continuous) was set at 400 mL/min. The high NH_4^+-N concentration in the reactor was achieved by increasing NH_4^+-N concentration of the synthetic leachate and additional operation of manually replacing certain amount of the supernatant of the reactor with fresh synthetic leachate during the settling phase. A high nitrite accumulation rate (NAR, the percentage of nitrite nitrogen to total oxidized nitrogen) would suggest successful start-up of the nitritation process. In Stage II, the reactor was run as a partial

Table 3-1. Operational strategies during various stages.

Stages	Processes	Time (day)	Aeration mode	Aeration rate (mL/min)	Influent NH_4^+-N (mg/L)	Free ammonia concentration	pH	DO (mg/L)
Stage I	Start-up	0 - 22	Continuous	400	600 - 900 [b]	High	7.95 - 8.42	0.08 - 0.7
Stage II A	PN	23 - 152	Intermittent	200	300	Uncontrolled	6.6 - 8.3	0.08 - 0.21
Stage II B		153 - 205		100			7.5 - 7.9	0.05 - 0.1
Stage III A	PN-A	205 - 227	Intermittent	0 - 100	300	Uncontrolled	7.9 - 8.3	N.A.
Stage III B		228 - 237	Continuous	400	600		7.4 - 8.4	N.A.
Stage III C		238 - 367	Intermittent	30 - 100 [a]	300		7.8 - 8.5	0 - 0.05

[a]100 mL/min during day 238 - 247, 30 mL/min during day 248 - 278, 50 mL/min during day 278 - 367. [b] Additional operation was carried out by manually replacing certain amount of the supernatant of the reactor with fresh synthetic leachate during the settling phase. N.A.: not available

nitritation (PN) reactor. NH4+-N concentration in the synthetic leachate was maintained at 300 mg/L, giving a COD: N ratio of 1:3, a low nitrogen loading rate of 0.105 g N /(L·d) and COD loading rate of 0.035 g COD/(L·d). In the reacting phase, instead of continuous aeration, intermittent aeration consisted of six successive 15 min non-aeration-30 min aeration intervals in the reaction phase was applied, which means the reactor was run as an IASBR. FA concentrations were uncontrolled, and the aeration rate was decreased to 200 mL/min and then 100 mL/min.

In Stage III, the reactor encountered a low aeration rate after day 205 caused by the blocking of the air diffuser after long-term use. The start-up strategies including 400 mL/min continuous aeration and high FA concentration were applied again during day 228 to 237. After the confirmation of the existence of anammox bacteria (day 247), the aeration rate was reduced to 30- 50 mL/min.

3.2.3 Ex-situ activity test procedures

On day 247 (Stage III), biomass was taken from the reactor, washed twice and diluted to the original volume with potassium phosphate buffer (0.01 mol/L, pH 8.0). Trace element stock solutions were added at the dosage of 1 mL/L. All the batch activity tests were carried out in triplicate in a water bath shaker at a shaking speed of 200 rpm and 30 ºC. Water samples were taken every 30 min over 2 h to monitor the dynamics of nitrogen species. For maximum anammox activity test, the washed biomass was sparged with N_2 gas until no DO was detected. 100 mL portions of the washed biomass were transferred to 160 mL serum bottles which were flushed with N_2 gas and contained 1 mg of inorganic carbon ($NaHCO_3$), 1 mg N of NH_4^+-N (NH_4Cl) and 1 mg N of NO_2^--N ($NaNO_2$). The bottles were then sealed with rubber stoppers and aluminum crimp seals. For maximum heterotrophic denitrification (HD) activity test, the biomass from the anammox activity tests were continually incubated until no NH_4^+-N could be detected. Afterward, 1 mg NO_3^--N ($NaNO_3$) and 10 mg COD (sodium acetate) were injected into the serum bottles.

Allylthiourea (ATU) was used to discriminate the contribution to nitritation between ammonium-oxidizing bacteria (AOB) and ammonium-oxidizing archaea (AOA). The tests were carried out in duplicate in 250 mL Erlenmeyer flasks. The methods were the same with the activity tests mentioned above, except the DO wasn't removed and the flasks were left open. Only 8 mg N of NH_4^+-N (NH_4Cl) was added to the flasks. ATU was added to the flasks with a range of final concentrations of 0, 0.4, 0.8, 1.6, 2.0 and 50 uM.

Anammox (TN consumption), nitritation (NH_4^+-N consumption) and HD activities were calculated as the slopes from the linear regression curve of five data points. The measurement uncertainties were given as the standard error of the calculated slopes. The corresponding activities were determined by dividing the calculated values in mg N/ (L· d) by the volatile suspended solids (VSS) concentration measured in the reactor on the same day.

3.2.4 Analytical procedures

Effluent water samples of the reactor were taken regularly to monitor the performance of the reactor. Water samples were filtered using syringe filters with pore size of 0.45 µm (Sarstedt Ltd, Germany) before being measured for NH_4^+-N, NO_2^--N and NO_3^--N concentrations using a nutrient analyzer (Konelab 20, Thermo Clinical Labsystems, USA). DO and pH were determined with a portable meter (Multi3620, WTW, Germany). COD and VSS were measured according to the standard methods [157]. FA concentration was calculated according to Equation 3-1.

$$\text{FA as } NH_3 \text{ (mg/L)} = \frac{17}{14} \times \frac{total\ ammonium\ nitrogen\ (mg\ NH_4^+ - N\ /L)}{1+(K/10^{pH})}, \qquad 3\text{-}1$$

where $K = e^{6344/(273+T)}$; T=30 °C.

3.2.5 Molecular analysis

One milliliter biomass samples were collected in Stage I (on day 0 and 22), Stage II (on day 117 and 190) and Stage III (on day 250 and 280). The samples were stored at -70 ºC before DNA extraction. The DNA extraction, PCR (polymerase chain reaction) amplification, and high-throughput sequencing were completed by commercial service (Sangon Biological Engineering Co., China). Hypervariable V3-V4 regions of the bacterial and archaeal 16S rDNA were amplified. The primers were: 341F (CCTACGGGNGGCWGCAG) and 805R (GACTACHVGGGTATCTAATCC) for bacterial 16S rDNA; 349F (GYGCASCAGKCGMGAAW) and 806R (GGACTACVSGGGTATCTAAT) for archaeal 16S rDNA. The amplicons were sequenced on an Illumina MiSeq platform. For sequences processing, barcodes were removed from sequence reads, followed by filtering and denoising to eliminate ambiguous and low-quality reads (sequence lengths <200 bp, or average sequence quality <20). The chimeric sequences were removed using UCHIME. The remaining high-quality sequences were clustered into operational taxonomic units (OTUs) using Usearch (version 5.2.236), with a sequence identity threshold of 97%. Taxonomic classification of the bacterial sequences was referred to the Silva database.

Metagenomes were predicted from the high-throughput sequencing data using Phylogenetic Investigation of Communities by Reconstruction of Unobserved States (PICRUSt) [158], according to the online protocol (http://huttenhower.sph.harvard.edu/galaxy/). The functional genes were identified at hierarchy level of 3 based on Kyoto Encyclopedia of Genes and Genomes (KEGG) database. The nitrogen-conversion related functional categories were assigned to the Nitrogen metabolism pathway map (map00910, http://www.genome.jp/kegg-bin/show_pathway?map00910) to locate their positions in the nitrogen conversion pathways. Based on the results, a full-view map of the distribution of the key nitrogen-conversion functional genes was drawn to investigate the dynamics of the nitrogen pathways along the three stages.

3.2.6 Statistical analysis

Statistical analysis was performed using SPSS (version 24, IBM, USA). The normality ($P > 0.05$) of the data was checked using Shapiro-Wilk test. Correlation analyses among the quantity of bacterial 16S rDNA genes, predicted functional genes and the physicochemical parameters of the IASBR were conducted using two-tailed Spearman's rho correlation test at a significance level of 0.05.

3.3 Results and discussion

3.3.1 Performance of the reactor and occurrence of PN-A

3.3.1.1 Partial nitritation performance of the IASBR

In Stage I (Figure 3-2 A), high concentration of NH_4^+ -N (600-900 mg/L) was fed to the reactor to achieve high FA concentrations with the purpose of temporarily inhibiting NOB as NOB was reported to be more sensitive to FA (inhibition concentration 0.1-1 mg/L) than AOB (inhibition concentration 10-150 mg/L) [159]. Correspondingly, the effluent NH_4^+ -N concentration was high between 73 and168 mg/L. The NO_2^- -N concentration gradually increased from 0 to 520 mg/L. The NO_3^- -N concentration was 78 mg/L at the end of day 1 and gradually decreased to 1-25 mg/L at the end of this stage. NAR gradually increased from 0 to 94-100%, suggesting the successful start-up of the nitritation process. Under high FA concentrations of 8-42 mg/L (Figure 3-2 B), NOB was gradually inhibited while AOB growth was encouraged under a high rate of continuous aeration, and thus a high ratio of AOB: NOB was established (Figure 3-8). So, the strategies used by Li et al. [82] were proved to be effective to start up the partial nitritation process.

In Stage II (Figure 3-2 A), the influent NH_4^+ -N concentration was reduced to a normal level of 300 mg/L, and the intermittent aeration pattern was applied. During day 23- 103, the aeration rate was decreased to 200 mL/min on day 23. NH_4^+ -N concentration gradually decreased and then maintained mostly below 20 mg/L. NO_2^- -N concentration increased to about 250 mg/L, and NO_3^- -N concentration was stable at about 10 mg/L, with NAR of 90-

100%, indicating that efficient and stable partial nitritation was achieved in the IASBR. The low rate intermittent aeration enabled the establishment of oxygen-limited conditions with the DO concentration of below 0.2 mg/L. Due to their different strategies for managing energy demand and recovering from starvation, AOB recover faster than NOB when the anaerobic condition is switched to the aerobic condition [82]. AOB is regarded as a more competent oxygen competitor than NOB under oxygen-limited conditions, provided that NH_4^+ -N is sufficient. The oxygen-limited conditions and the intermittent aeration strategy made it possible for the AOB to suppress the growth of NOB and maintain the stable partial nitritation performance. On days 91, 146, and 195 the IASBR encountered high-rate overnight aeration caused by malfunction of the timer. As a result, the NO_3^--N concentration increased to 50 - 65 mg/L since day 103, and the NO_2^--N concentration decreased to around 205 mg/L. Correspondingly, the NAR dropped to around 80%. To reduce the over-aeration impact, the aeration rate was further decreased to 100 mL/min on day 153. This caused the increase of effluent NH_4^+ -N concentration to about 56 mg/L. However, a high NAR of about 80% was still maintained. In conclusion, regardless of the negative effect of over-aeration, efficient and stable partial nitritation performance was achieved in the IASBR, indicating the effectiveness and robustness of the partial nitritation strategies used.

3.3.1.2 Occurrence of anaerobic ammonium oxidation

The TN removal efficiency was below 5% during most of the time in Stage II (Figure 3-2 A). In Stage III, the reactor encountered an unexpected decrease of aeration rate since day 205. As a result, both the effluent NH_4^+-N and NO_3^--N concentrations rose slightly (possibly caused by the thriving of anammox bacteria during this period, which converted part of nitrite to nitrate), but the NO_2^--N concentration dramatically decreased to 11 mg/L, and the NAR decreased to as low as 14%. NO_2^- -N accumulation could not be recovered even though the aeration rate was adjusted back to 100 ml/min. To recover the AOB activity, the start-up strategies were employed again during day 228-237, but the accumulation of NO_2^--N was still not achieved. Instead, the nitrogen mass balance showed that around 50% of the TN, i.e. 150 mg N/L, was lost on day 240 (Figure 3-2 A).

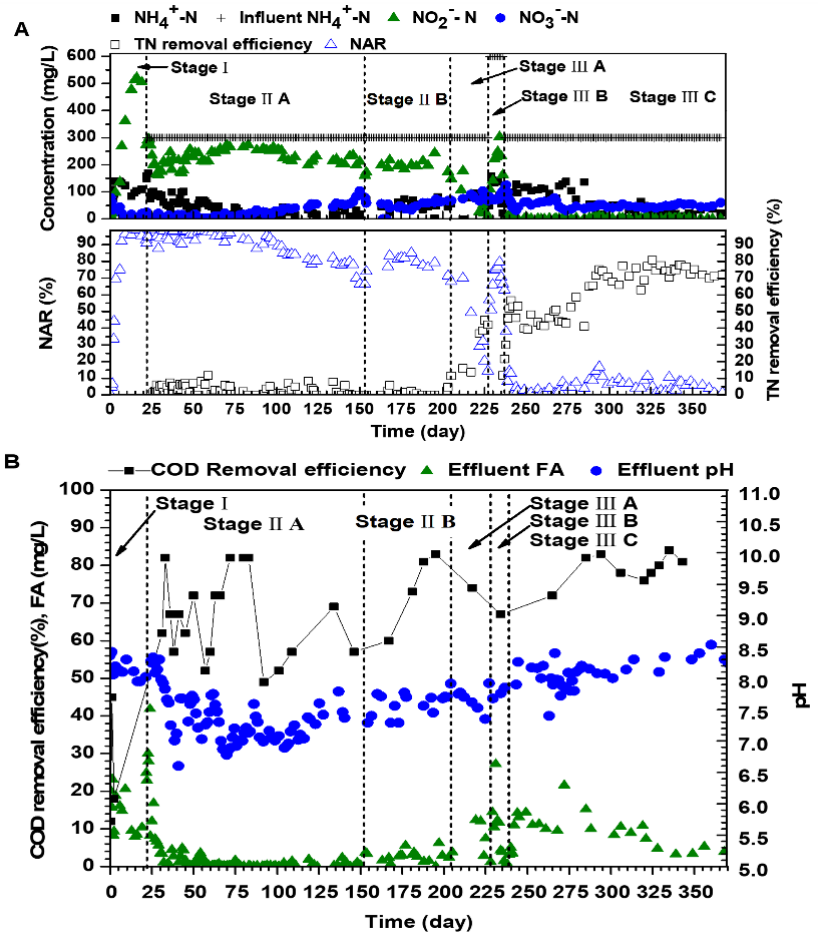

Figure 3-2. Performance of the reactor: (A) influent and effluent nitrogen concentrations, profiles of NAR and TN removal efficiency; (B) profiles of COD removal efficiency, effluent pH and FA concentration. NAR: nitrite accumulation rate; FA: free ammonia.

Considering the operational conditions of the reactor, the TN loss was most likely caused by two biological processes: heterotrophic denitrification and anammox. Taking NO_2^--N as the electron acceptor, the ratio of readily biodegradable organic meters (S_F) to nitrate plus nitrite nitrogen (S_{NO_2-N}) was calculated based on yield coefficient (Y_H, 0.6g COD/g COD with oxygen as the electron acceptor, 0.5 g COD/g COD with nitrate or nitrite as the electron acceptor): $S_F/S_{NO_2-N} = 1.71/(1-Y_H) = 1.71/(1-0.5) = 3.42$ g COD/ g NO_2^--N, which means 3.42 g COD is needed for the complete denitrification of NO_2^--N [5, 100, 119]. The COD removal efficiency on day 240 was around 60% (Figure 3-2 B) with 60 mg/L COD removed, which meant heterotrophic denitrification could potentially remove 18 mg N /L

if all the removed COD was used for heterotrophic denitrification. However, the nitrogen removed by heterotrophic denitrification would be less than 18 mg N /L as certain amount of the COD would be consumed by other processes such as aerobic respiration. Indeed, only around 5% (15 mg N /L) of the influent TN was removed before day 205 with the same influent COD concentration and similar COD removal efficiency. Thus, heterotrophic denitrification was very limited, making anammox the only possible major route for the substantial TN removal.

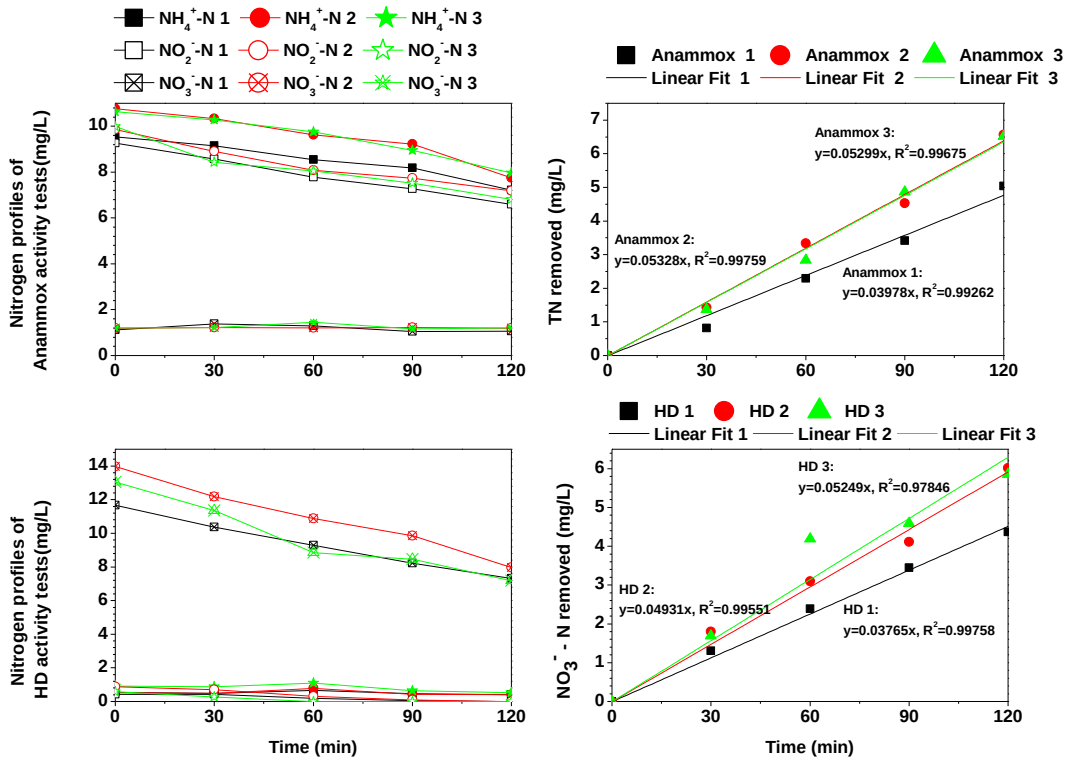

Figure 3-3. Profiles of nitrogen species and linear fit of the batch maximum activities (Anammox activities and HD activities) tests.

To confirm the existence of anammox and to evaluate the maximum nitrogen removal potential of heterotrophic denitrification and anammox, on day 247, ex-situ maximum activity tests (anammox and heterotrophic denitrification) were carried out under optimal conditions and non-limiting substrate concentrations. In the anammox activity tests, simultaneous removal of NH_4^+-N and NO_2^--N was observed without the existence of COD

and oxygen (Figure 3-3) which confirmed the existence of anammox bacteria in the reactor. The maximum anammox activity was calculated to be 0.142 ± 0.023 mg N/mgVSS/d. The maximum heterotrophic denitrification activity was 0.136 ± 0.023 mg N/mgVSS/d under a COD/TN ratio of 10. These results indicated that even under organics-replete condition, the heterotrophic denitrification was still slightly lower than the anammox activity. In the actual case of the reactor, the ammonium and nitrite were always sufficient to sustain high anammox activity, while the heterotrophic denitrification activity would be significantly reduced due to the very low influent COD/TN ratio (0.33). As mentioned above, only around 5% of the influent TN could be removed by heterotrophic denitrification in Stage 2. Therefore, the substantial TN removal in Stage 3 was mainly caused by anammox.

Then, the aeration rate was reduced to 30 mL/min from day 247 and the IASBR was run as a PN-A reactor. During the period of day 247-278, the TN removal efficiency was around 45% and the NAR dropped to less than 5% (Figure 3-2 A). The effluent NH_4^+-N was about 108 mg/L, indicating insufficient oxygen supply, so the aeration rate was increased to 50 mL/min on day 279. The TN removal efficiency gradually rose to up to 81.5% (Figure 3-2 B). Effluent NO_3^- -N concentration was stable at around 45 mg/L, of which 57-73% was produced by anammox bacteria, as calculated based on NH_4^+-N consumption as per the stoichiometric equation of PN-A (Equation 3-2) [5]. The nitrogen removal rate of 86 mg N /d /L was comparable to the reported result of 72 mg N/d/ L [152], but lower than 475 mg N/d/ L [35] and 490 mg N/d/ L [151] which resulted from the low nitrogen loading rate of 105 mg N /d /L. A higher nitrogen removal rate can be expected if a higher nitrogen loading rate was applied. Overall, the above results indicated that using the IASBR configuration, stable and efficient partial nitritation, start-up of the PN-A process from return sludge and efficient long-term TN removal can be achieved. However, it's worthy to note that the real landfill leachate may contain high concentration of ammonium and inhibitory components [159] and may vary widely in terms of leachate amount and ammonium concentration depending on the landfill age, operation of the landfill, seasonal weather variations, etc. [160]. Longer HRT and on-line monitoring and controlling equipment are recommended when using PN-A IASBR system to treat real leachate.

$$NH_4^+ + 0.85O_2 \rightarrow 0.13NO_3^- + 0.435N_2 + 1.4H^+ + 1.3H_2O \quad 3\text{-}2$$

3.3.2 Cyclic performance before and after the occurrence of anammox

The typical cyclic analysis was conducted on day 171 in the partial nitritation stage (Stage II) and day 293 in the PN-A stage (Stage III). In Stage II (Figure 3-4 A), after 5 min of filling phase, NH_4^+-N concentration increased from 32.7 mg/L to 56.4 mg/L and then decreased linearly to the original level because of nitritation. The consumed NH_4^+-N was oxidized to NO_2^--N indicated by a linear increase of NO_2^--N concentration during the reaction phase. NO_3^--N concentration first dropped from 53.8 mg/L to 50.4 mg/L due to the dilution effect of the influent feeding, and then slightly increased to 54.4 mg/L at the end of the cycle. The pH value of the influent was about 8.0, and the influent caused an increase of the reactor's pH from 7.5 to 7.7. As the ammonium oxidation by AOB produced H^+, the pH value gradually decreased to 7.48 at the end of the cycle. The DO concentration was around 0.05 - 0.10 mg/L during the cycle.

The cyclic performance was different after the occurrence of anammox (Figure 3-4 B). There was also a linear decrease of NH_4^+-N concentration, and NO_3^- -N concentration remained stable in the whole cycle. But there was no NO_2^--N accumulation observed due to the consumption by anammox bacteria. Instead of a declining trend, the pH value gradually increased to a higher level because of the H^+ - consuming metabolism of anammox bacteria [161]. The aeration rate was turned down to 50 mL/min on day 293, so the DO concentration was lower than that in Stage II. DO concentration remained at 0.02 mg/L in most of the aeration periods and 0.01 mg/L during the non-aeration periods.

The IASBR and control strategies not only created oxygen-limited conditions that allowed AOB to out-compete NOB but also created a suitable environment for the growth of anammox bacteria: efficient biomass retention, oxygen-limited conditions, sufficient NH_4^+-N and NO_2^- -N. Anammox bacteria are not only widespread in natural ecosystems such as marine ecosystems, freshwater wetland ecosystems, but also in various units of

municipal MWTPs including anaerobic/anoxic/oxic units, oxidation ditch units, SBR units, and even aerobic zones (DO > 2 mg/L) [150, 162]. The seed sludge of the IASBR was return sludge taken from a local MWTP, which probably contained a small number of anammox biomass already. The suitable conditions in the IASBR stimulated the enrichment of anammox bacteria during long-term operation. Li et al. [163] observed the presence of anammox in IASBR with FISH technique. Lv et al [151] reported the enrichment of anammox bacteria from a partial nitritation reactor after more than 1-year operation by reducing the DO concentration, indicated by "positive" FISH results. In another report [152], 0.1 mM hydrazine and hydroxylamine were dosed twice a day to start up the anammox process in a partial nitritation reactor, which was also detected by FISH analysis. However, no further detailed microbial community analysis was available in these studies.

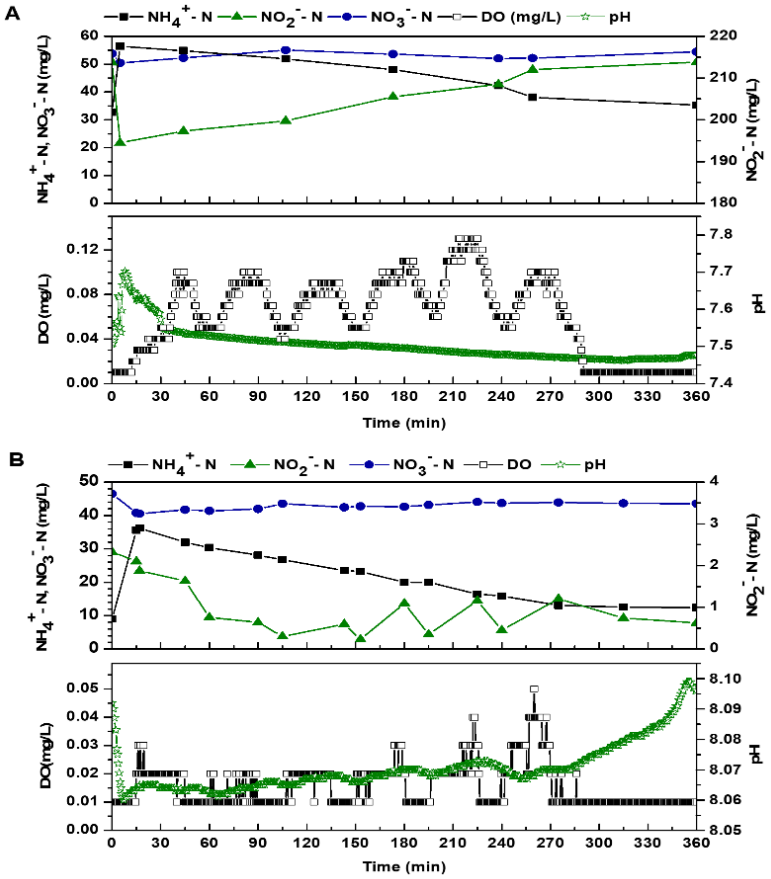

Figure 3-4. Performance of the IASBR in one typical cycle during (A) Stage II, the partial nitritation stage, and (B) Stage III, the PN-A stage.

3.3.3 Microbial community structure in the IASBR

To gain insights into the microbial community in the IASBR during the shift from PN to PN-A process, six amplicon libraries were constructed from biomass taken during the three stages: Stage I (on day 0 and 22); Stage II (on day 117 and 190), and Stage III (on day 250 and 280). Higher diversity and richness were observed in bacterial community than in archaeal community (Table 3-2). The results of correlation tests showed that both the richness and diversity of the bacterial community were negatively affected by the FA concentration.

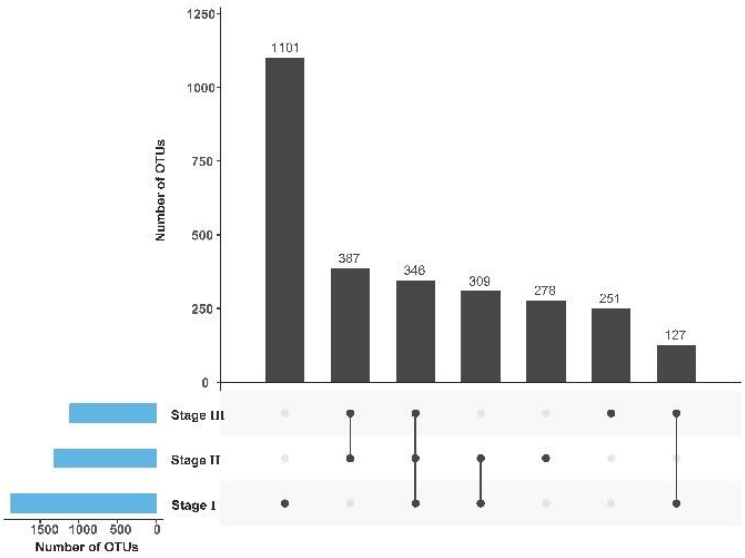

Figure 3-5. The number of detected OTUs in the bacterial community during the three stages.

The numbers of detected OTUs in various stages are shown in Figure 3-5 and Figure 3-6. Much higher OTU numbers were observed in the bacterial community than in the archaeal community. However, the bacterial community experienced an arresting decrease at the end of Stage I (day 22). These results agreed with the alpha diversity indexes as shown in Table 3-2. The Shannon index and Simpson index indicated a higher diversity of the bacterial community than the archaeal community. The ACE index and Chao1 index, on

the other hand, suggested that the bacterial richness was much higher than that of the archaeal community. The diversity and richness of archaeal community remained stable. The notable decrease from Stage I to Stage II in both bacterial community diversity and richness could also be concluded from Table 3-2. Two-tailed Spearman's rho correlation tests were conducted between the operating parameters and the alpha diversity indexes (Table 3-3). The results indicate that the FA concentration and alpha diversity of the bacterial community significantly and negatively correlated with each other (the absolute value of the coefficient r ranged between 0.812 - 0.886, $P<0.05$), which in turn means that high FA concentration was the main reason for the decreased community diversity and richness at the end of Stage I.

Table 3-2. Alpha diversity indexes during various stages.

		Sample ID	Shannon index	Simpson index	ACE index	Chao1 index
Bacterial community	Stage I	Day 0	5.95	0.01	1713	1674
		Day 22	3.10	0.22	985	951
	Stage II	Day 117	4.08	0.04	1485	1370
		Day 190	4.05	0.04	1021	973
	Stage III	Day 250	3.88	0.05	970	981
		Day 286	4.40	0.03	1161	1102
Archaeal community	Stage I	Day 0	2.47	0.15	224	212
		Day 22	2.24	0.17	239	213
	Stage II	Day 117	2.30	0.15	186	189
		Day 190	2.43	0.19	272	249
	Stage III	Day 250	2.08	0.20	240	222
		Day 286	2.50	0.14	230	214

Table 3-3. Two-tailed Spearman's rho correlation tests between the operating parameters and the alpha diversity indexes (diversity indexes and richness indexes).

		Shannon index	Simpson index	ACE index	Chao1 index
Bacterial community	Aeration Rate	-0.771	.812*	-0.429	-0.657
	FA concentration	-.829*	.812*	-.886*	-.829*
Archaeal community	Aeration Rate	-0.600	0.319	0.143	-0.086
	FA concentration	-0.543	0.406	0.543	0.429

*$P<0.05$

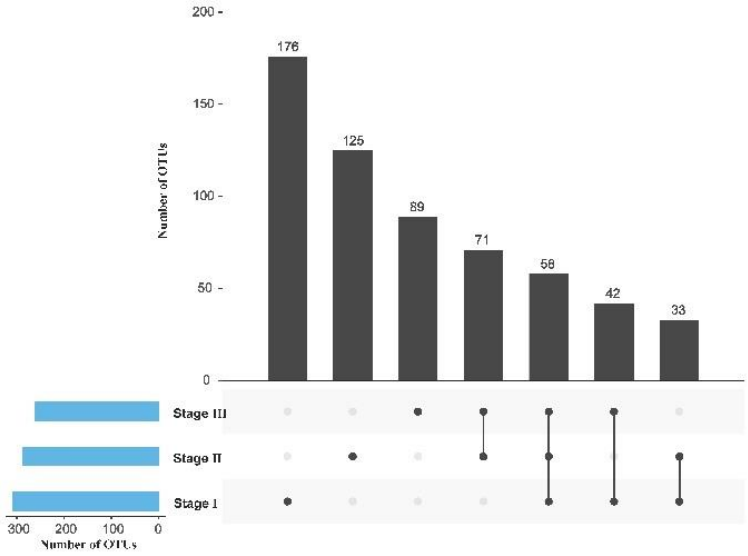

Figure 3-6. The number of detected OTUs in the archaeal community during the three stages.

3.3.3.1 The bacterial community in the IASBR

Proteobacteria, which is a major phylum of gram-negative bacteria [164], was the most dominant bacterial phylum in all the samples (Figure 3-7A). Its abundance increased from 42.8% to 64.8% on day 22 (the end of Stage I) and then dropped to 31-36% during Stage II and Stage III. *Proteobacteria* is a common dominant phylum with relative abundance of 30-43.1% in PN-A system [5, 165], and has always been found regardless of the characteristics of reactors – the configurations, biomass growth mode, operational parameters and inoculum types [166]. The sharp increase of *Proteobacteria* abundance on day 22 was mainly caused by the enrichment (from 0.5% to 46.2%) of the AOB genus *Nitrosomonas* (Figure 3-7 B) within the *Proteobacteria* phylum (Figure 3-7 C). The following dominant phyla were *Bacteroidetes* (9.2-35.1%), *Verrucomicrobia* (3.2-17.2%), *Firmicutes* (1.6-18.2%), *Chloroflexi* (0.9-13.0%) and *Planctomycetes* (0.3-10.1%). Other phyla with low detected abundance were *Actinobacteria* (<4%), *Acidobacteria* (<3%), *Chlorobi* (<3%) and *Gemmatimonadetes* (<5%). Among these phyla, *Bacteroidetes,* which is a phylum that widely distributes in the environment and branches very closely with the

phylum *Chlorobi*, together with *Chloroflexi*, *Actinobacteria*, *Acidobacteria* and *Chlorobi*, are the frequently detected phyla in PN-A system [167] [165, 168, 169].

At genus level, 43 major (relative abundance >1% in at least one sample) bacteria genera were detected, which were classified into 4 groups according to their dynamic behaviors in the three operational stages (Figure 3-7 B). Twelve genera (Group a), which included 8 genera from the phylum *Proteobacteria*, only dominated in Stage I (day 0 and day 22). It can be deduced that these 12 genera were less tolerant of the IASBR conditions such as high FA concentration in Stage I and high nitrite concentration in Stage II, etc. Based on their very low (almost zero) abundance in Stage II and III, they might have a very minor contribution to either the partial nitritation process or the PN-A process. Nine genera were classified into Group b as they only dominated in Stage II, i.e. the partial nitritation stage (Figure 3-7 B). Among them, *Thermomonas*, a genus within the phylum *Proteobacteria*, achieved a high abundance of 5.1- 5.3% during Stage II. Their high abundance was probably associated with their aerobic and non-motile characteristics and ability to reduce nitrite or nitrate [170]. The bacteria in Group c (Figure 3-7 B) dominated in both stages II and III with relative abundances of 3-11%. The bacteria in Group d were minor genera in the partial nitritation stage but became dominant genera in the PN-A stage (Figure 3-7 B). Bacteria in Group c and Group d dominated in Stage III suggesting that they might play an important role in PN-A system, but the reason for their thriving was unknown and further studies on the interactions among these bacteria are needed.

3.3.3.2 Archaeal community in the IASBR

The archaeal community, which was dominated by methanogens, consisted of nine major (relative abundance >1% in at least one sample) genera including eight methanogens and one AOA genus – *Candidatus Nitrososphaera* (Figure 3-7 C). *Methanosaeta* was the most dominant genus with a relative abundance of 22.7-52.3% to the total Archaeal community. The relative abundance of *Methanobacterium, Methanoregula, Methanospirillum*, and *Methanosarcina* were all low and between 0.3-5.1% in the inoculum, but in Stage II and Stage III, all of them increased to higher levels of 10.6-27.4%, 5.1-32.7%, 5-39% and 0.3-

3.8% (to the total archaeal community), respectively. The abundance of *Methanobrevibacter*, *Methanolinea*, and *Methanomassiliicoccus* were high at 26-27.8 %, 4.9-6.5% and 0-1.3% in Stage I, but all decreased to less than 0.6% in Stage II and Stage III.

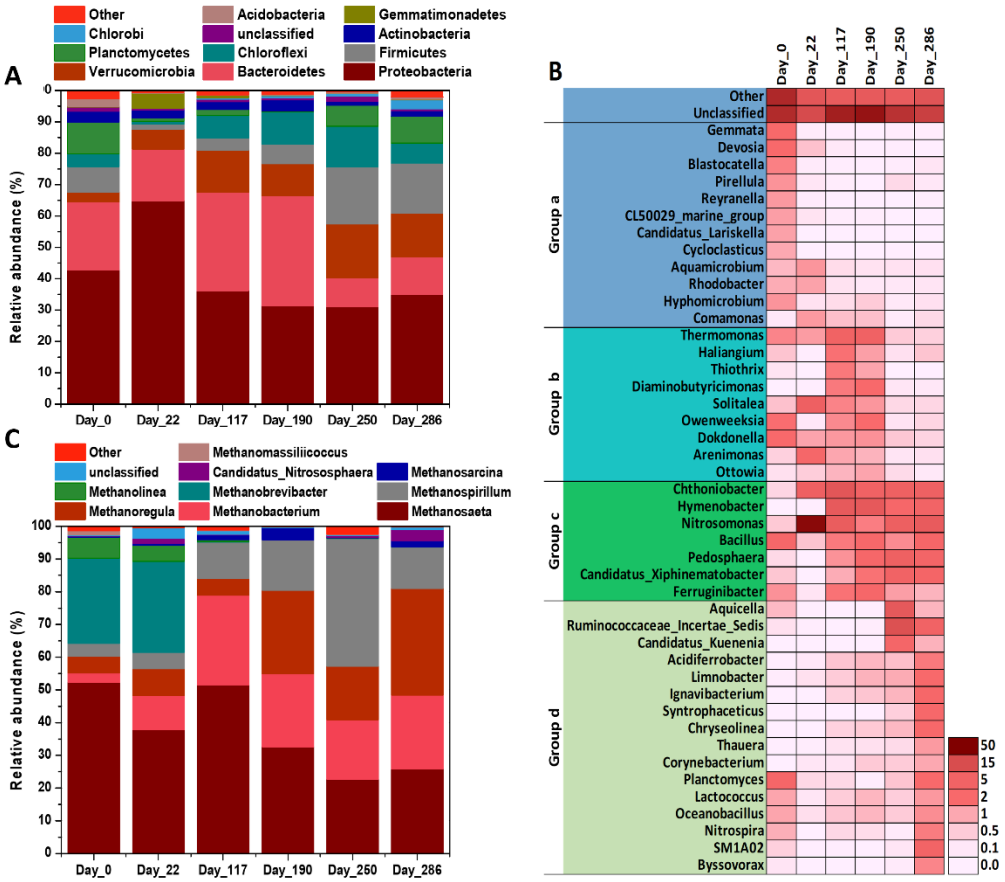

Figure 3-7. Microbial community structure in the IASBR: (A) relative abundance of the bacterial community at phylum level; (B) relative abundance of the bacterial community at genus level, and (C) archaeal community at genus level. "Other" represents all classified taxa with relative abundance <1%.

Methanogenic archaea are thought to be very sensitive to oxygen. The reasons for their survival in the current study could be the COD supply in the influent, the oxygen-limited conditions and the unique intermittent aeration mode. The phenomenon that methanogens co-existed with both aerobic and anaerobic nitrogen-conversion microorganisms suggests

that CH_4 could be an important COD sink in PA-N system when COD was present. However, dissolved CH_4 was not detectable in the bulk liquor in the IASBR using the salting-out method [171] followed by a gas chromatography measurement. Methane can be oxidized by methanotrophs. One explanation could be the produced methane was oxidized by methanotrophs. However, only two genera of methanotrophs, *Methylocella* and *Methylocystis*, were identified with abundances < 0.01%. Methane could also be consumed by newly discovered nitrite/ nitrate-dependant anaerobic methane-oxidizing microorganisms such as *Candidatus Methylomirabilis* and *Candidatus Methanoperedens* [86], but these two genera were not detected in the IASBR. Therefore, the undetectable CH_4 in this study could result from the low influent COD concentration (100 mg/L) and its partial consumption by heterotrophic bacteria. To our best knowledge, the measurement of methane in PN-A systems hasn't been reported. The existence of methanogens suggests that it is worthy to investigate the methanogenic community dynamics and potential CH_4 production in PN-A systems, especially under higher influent COD concentration and COD/N ratio conditions since CH_4 is a prominent greenhouse gas.

3.3.3.3 Dynamics of nitrogen-conversion microorganisms during the three stages

Five groups of nitrogen-conversion microorganisms were found in the IASBR: the relatively well-studied aerobic AOB, aerobic NOB, anammox bacteria, other potential denitrifiers (apart from anammox bacteria), and rarely reported archaeal AOA genera (Figure 3-8). The other potential denitrifiers detected might have played only a minor role in TN removal in the current study (Table 3-4). Following the activity tests (section 3.1.2), the molecular evidence confirmed again the occurrence of anammox bacteria in the IASBR. Two well-known anammox genera *Candidatus Kuenenia* and *Candidatus Brocadia* and a newly discovered yet less reported anammox genus *Candidatus Anammoximicrobium* [172, 173] were identified in the IASBR. *Candidatus Kuenenia* was the most abundant anammox genus detected, with a relative abundance of 3.6% on day 250 and 0.9% on day 286 (Figure 3-7 B). The decrease of its abundance on day 286 could be attributed to the low aeration rate which caused the accumulation of NH_4^+ -N and FA (Figure 3-2). *Candidatus Brocadia* and *Candidatus Anammoximicrobium* were detected

since day 250 and day 117 respectively, with much lower relative abundance (<0.32%) and read numbers (Figure 3-8). Both *Candidatus Kuenenia* and *Candidatus Anammoximicrobium* showed strong and positive (r = 0.955 and 0.941 respectively, P<0.01) correlation with the TN removal efficiency (Figure 3-11). This indicates that *Candidatus Kuenenia* was the main contributor to the TN removal, considering its higher relative abundance. Overall, it can be concluded that the PN-A process could be started up from partial nitritation IASBR using return sludge as the inoculum.

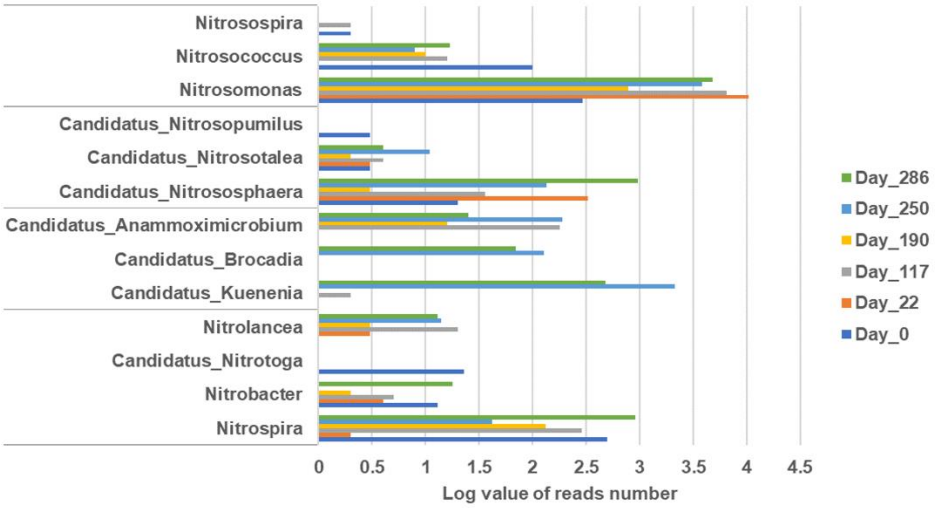

Figure 3-8. Log value of read numbers of AOB, AOA, anammox bacteria and NOB (from top to bottom) on various sampling date.

Three AOB genera *Nitrosomonas*, *Nitrosococcus* and *Nitrosospira* with *Nitrosomonas* as the most abundant genus and four NOB genera *Nitrospira*, *Nitrobacter*, *Candidatus Nitrotoga* and *Nitrolancea* with *Nitrospira* as the most abundant genus were detected. In Stage I, *Nitrosomonas* was enriched from 0.5% to 46.2% while the abundance of *Nitrospira* was reduced from 0.9% to 0, which was consistent with the establishment of partial nitritation (Figure 3-2). The abundance of *Nitrosomonas* remained at a prominent level of 6.4-8.6% except on day 190, which dropped to 1.6% when the aeration rate was reduced to 100 mL/min. The quantity of *Nitrosomonas* was significantly correlated with the NAR (r = 0.829, P <0.05), suggesting the main contribution of this genus in converting NH_4^+-N to NO_2^--N. The abundance of *Nitrospira* maintained below 0.3% between day 22 and day

250 and increased to 1.6% on day 286. But the NO_3^--N concentration was stable at around 45 mg/L (Figure 3-2 A).

Table 3-4. The relative abundance of the potential denitrifiers.

Potential denitrifier genera	Relative abundance (%)					
	Day_0	Day_22	Day_117	Day_190	Day_250	Day_286
Bacillus	3.19	0.61	1.67	2.49	1.41	3.49
Corynebacterium	0.01	0.14	0.16	0.53	0.51	1.01
Hyphomicrobium	1.29	0.19	0.27	0.5	0.09	0.2
Pseudomonas	0.3	0.06	0.08	0.05	0.07	0.15
Alcaligenes	0	1.29	0.12	0	0	0
Rhizobium	0.62	0.04	0.01	0	0	0.02
Flavobacterium	0.81	0.14	0.02	0	0.02	0.01
Acinetobacter	0.24	0	0.01	0	0.02	0.2
Paracoccus	0.02	0.01	0.03	0.05	0.06	0.1
Propionibacterium	0	0	0	0.01	0	0.05
Streptomyces	0.06	0	0.02	0.26	0.02	0
Flavobacterium	0.81	0.14	0.02	0	0.02	0.01
Bradyrhizobium	0.07	0.01	0	0	0	0
Mesorhizobium	0.28	0.12	0.1	0.03	0.05	0.01
Pseudochrobactrum	0.03	0	0	0	0	0
Rhodobacter	0.95	1.09	0.18	0.11	0.11	0.15
Acidovorax	0.18	0.32	0.06	0.05	0.05	0.11
Azospira	0.29	0.02	0.18	0.32	0.29	0.57
Azoarcus	0.49	0.12	0.01	0.02	0.08	0.08
Achromobacter	0.01	0.01	0	0	0.02	0.09
Comamonas	0.1	1.22	0.68	0.67	0.07	0.31
Denitratisoma	0	0	0	0.01	0.16	0.43
Ottowia	0.21	0.48	0.83	1.06	0.29	0.09
Thauera	0.02	0.04	0.18	0.21	0.29	1.21
Halomonas	0.09	0	0	0	0	0
Luteimonas	0.01	0.1	0.04	0.05	0.01	0.03
Pseudoxanthomonas	0.06	0.05	0.03	0.02	0.04	0.08
Shewanella	0	0	0.01	0	0.01	0.05
Stenotrophomonas	0.04	0	0	0	0.01	0

Three genera assigned to AOA were also detected: *Candidatus Nitrososphaera*, *Candidatus Nitrosotalea*, and *Candidatus Nitrosopumilus*. *Candidatus Nitrososphaera*

was the predominant genus with a high relative abundance (to the total archaeal community) of 1.42% on day 22 and the highest abundance 3.44% on day 286. The abundances of the other two AOA genera were less than 0.05%. These results showed that along with AOB, AOA could also be boosted by the start-up strategies and enriched to a high abundance in IASBR. AOA are pervasive in marine environments that are critical for the global nitrogen cycle, such as the coastal sediments and the base of the euphotic zone. Their abundance in the North Pacific Gyre and Monterey Bay was found to be up to two orders of magnitude higher than that of AOB [174]. Certain lineages of AOA contribute to a large extent to the nitrogen cycle in the ocean [175]. AOA are also widespread in municipal conventional (not anammox bacteria-driven) wastewater treatment units [176]: in three municipal MWTPs, AOA were reported to be 17-90 times more abundant than AOB; the AOA's relative abundance to total archaeal genes ranged from 0.3% to 3.3%. Compared with AOB, AOA have an extremely high affinity towards ammonia (Ks = 133 nM) [153]. Factors including low DO concentrations, relatively long solids retention time (SRT $\geq$ 15 days) and low residual NH_4^+ -N were reported to contribute to stimulating the growth of AOA [153, 154].

AOA are likely a better partner with anammox as they often thrive at low DO levels of 0.1 mg/L and can achieve higher ammonia oxidation rates under oxygen-limited conditions [155]. In a modeling study, Liu et al demonstrated that the AOA-anammox system required less oxygen supply and had higher TN removal capability than AOB-anammox system [177]. The cooperation between AOA and anammox was only reported in one study [153] in which the AOB/AOA ratio of 2 (based on AmoA gene copy numbers) was measured. However, the system was a model system: pre-cultivated pure marine AOA culture was inoculated into an anammox reactor; and the influent also contained both ammonium (10-11 mM) and nitrite (10-12.5 mM). In practical wastewater treatment systems, the bacterial and archaeal communities are much more complex. In actually operated anammox systems, the successful identification of AOA has only been reported in one study [178] which investigated the effect of feed starvation on anammox activity in a demonstration-scale one-stage anammox SBR. The AOB quantity in that study was approximately 3-4 orders of magnitude higher than that of AOA (almost negligible), suggesting that AOB played a

much more significant role in comparison with AOA. No AOA were detected in other anammox-based wastewater treatment units, neither in one-stage anammox systems, 2-stage anammox systems [179], nor anaerobic up-flow granular bed anammox reactor [180]. In this study, besides the high relative abundance, the sequence counts of AOA genus *Candidatus Nitrososphaera* were 964 on day 286, accounting for 16.7% of the total aerobic ammonium oxidizing microorganism population (the sequence counts of AOB genus *Nitrosomonas* was 4806) (Figure 3-8). Thus, for the first time, this study showed that AOA could be enriched to a relatively high abundance in IASBR PN-A system, but their contribution to partial nitritation needs further study.

3.3.3.4 Metabolic dynamics of the microbial community in the IASBR

In order to gain further insights into the metabolic dynamics of the microbial community during the three stages, PICRUSt was used to predict functional genes encoding the key nitrogen-conversion enzymes, and the abundances were mapped against the nitrogen cycle pathways (nitritation, denitrification, nitrogen fixation and dissimilatory nitrate reduction) (Figure 3-9). Unfortunately, anammox bacteria-related functional genes (hydrazine dehydrogenase and hydrazine synthase) were not available due to the lack of KEGG annotations on anammox process. The correlations among the quantity of bacterial16S rDNA, predicted functional genes and the physicochemical parameters of the IASBR were performed using two-tailed Spearman's rho correlation test (Figure 3-11). The enzymes encoded by AmoABC genes (genes encoding ammonium monooxygenase subunit A, B, and C) and Hao genes (genes encoding hydroxylamine oxidoreductase) are the two successive key enzymes involved in the nitritation process, so it was conceivable that there was a strong correlation ($r=1.000$, $P< 0.01$) between them (Figure 3-11). The abundance of the AmoABC and Hao increased remarkably during the start-up stage, then dropped to the lowest level on day 190 and finally recovered to a higher level during the PN-A stage, which was in accordance with the partial nitritation performance (Figure 3-2). Strong correlations were also observed between these two genes and both *Nitrosomonas* ($r=0.943$, $P<0.01$) and *Candidatus Nitrososphaera* ($r=0.829$, $P<0.05$), suggesting that both the two ammonium oxidizers acted during the nitritation process.

It has been reported that AOB were more sensitive to nitrification inhibitor ATU than AOA [181, 182], which means AOB can be totally inhibited at certain ATU concentration while AOA are not. Figure 3-10 showed that the nitritation rate was not further inhibited with the increasing ATU concentration from 1.6 uM to 2.0 uM, which means AOB were inhibited while AOA were not. Therefore, the nitritation rate of 4.95 mg N/mg VSS/d at ATU concentration of 1.6-2.0 uM was contributed by AOA accounting for 13.9% of the full nitritation ability, which agreed with the proportion of AOA to the total aerobic ammonium oxidizing microorganism population of 16.7%. Hence, it can be concluded that AOA were not only enriched to high abundance but also contributed significantly to the partial nitritation process in the IASBR PN-A system.

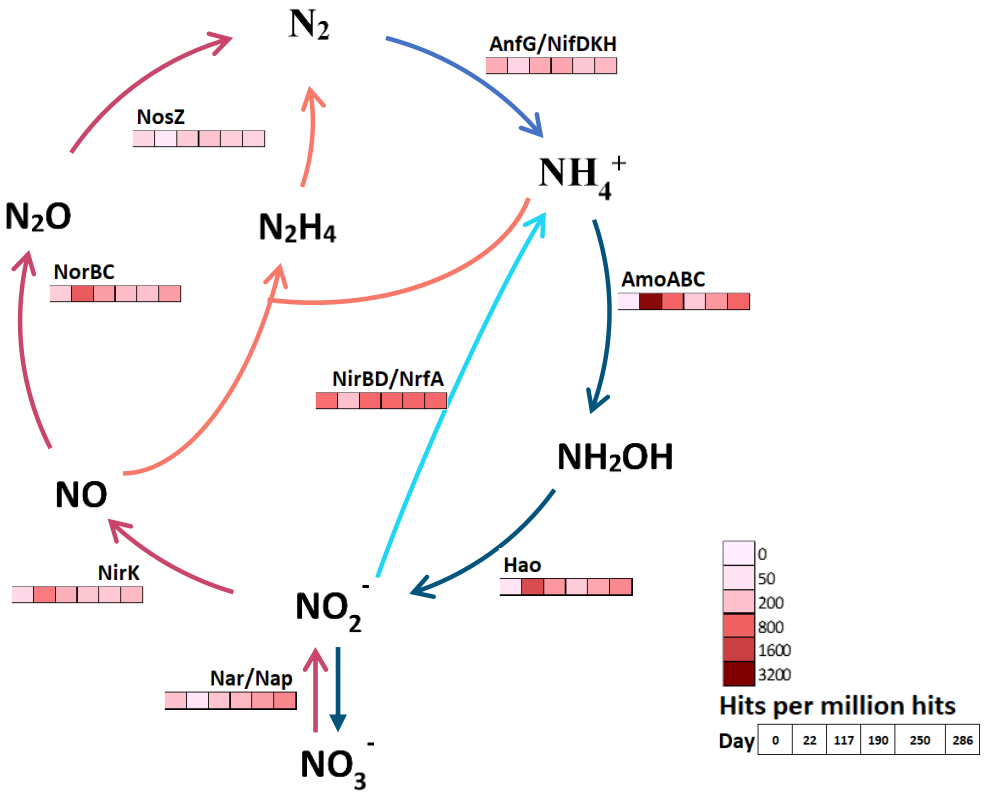

Figure 3-9. Distribution of the predicted functional genes encoding the key nitrogen-metabolic enzymes in the three stages. The abundances of the functional genes were

calculated as hits per million hits. The abundance of the functional genes in each sample was shown in the color bars. AmoABC, genes encoding ammonium monooxygenase subunit A, B and C; Hao, genes encoding hydroxylamine oxidoreductase; Nap, genes encoding periplasmic nitrate reductase; Nar, genes encoding cytoplasmic nitrate reductase; NirK, genes encoding nitrite reductase (NO-forming); NorBC, genes encoding nitric oxide reductase cytochrome b-containing subunit I and cytochrome c-containing subunit II; NosZ, genes encoding nitrous oxide reductase; AnfG, genes encoding nitrogenase; NifDHK, genes encoding nitrogenase molybdenum-iron protein alpha chain, beta chain and nitrogenase iron protein; NirBD, genes encoding nitrite reductase large and small subunit; NrfA, genes encoding nitrite reductase (cytochrome c-552).

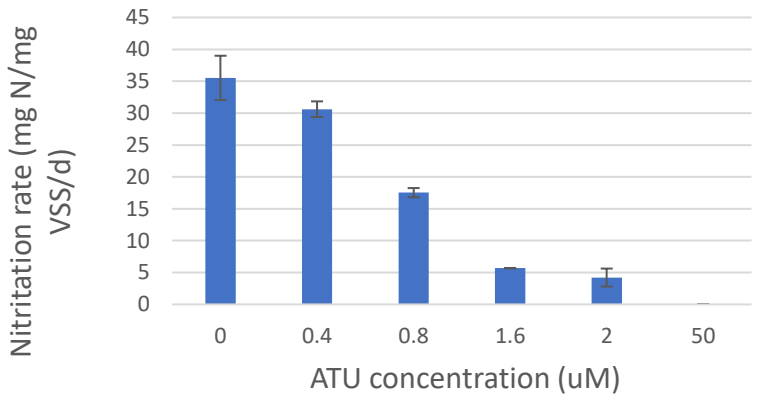

Figure 3-10. The inhibition of ATU on nitritation rate.

Enzymes encoded by Nar/Nap (Nar: genes encoding cytoplasmic nitrate reductase, Nap: genes encoding periplasmic nitrate reductase), NirK (genes encoding nitrite reductase (NO-forming)), NorBC (genes encoding nitric oxide reductase cytochrome b-containing subunit I and cytochrome c-containing subunit II) and Nosz (genes encoding nitrous oxide reductase) are the key enzymes in heterotrophic denitrification, which stepwise catalyze the reduction of NO_3^- to NO_2^-, NO, N_2O and finally to N_2 (Figure 3-9). Among these functional genes, both NirK and NorBC were positively correlated with AmoABC genes, Hao gens, the abundance of AOB genus *Nitrosomonas* and partial nitritation performance indicator NAR (Figure 3-11). However, no significant correlations were observed between

NirK-Nar/Nap and NorBC-Nar/Nap. All these results indicate that the dynamic of NO and N_2O production over the three stages was highly coincident with the performance of the *Nitrosomonas* - driven partial nitritation process. Key microbial pathways regulating N_2O production include [183-185]: Pathway 1, the conventional heterotrophic denitrification, in which N_2O is a by-product of reduction of NO_3^- and NO_2^- by heterotrophic denitrifiers; Pathway 2, termed as nitrifier denitrification, in which the sequential reactions of $NH_4^+ \rightarrow NH_2OH \rightarrow NO_2^- \rightarrow NO \rightarrow N_2O$ are carried out by AOB such as *Nitrosomonas* europaea under oxygen-limiting conditions; and Pathway 3, NH_2OH oxidation, in which N_2O is produced as the byproduct in the oxidation of NH_2OH to NO_2^-. The correlation between potential N_2O production and the partial nitritation performance could indicate that a certain amount of N_2O was produced by the "non-conventional" pathway 2 or pathway 3. However, further studies are needed to give a clearer explanation.

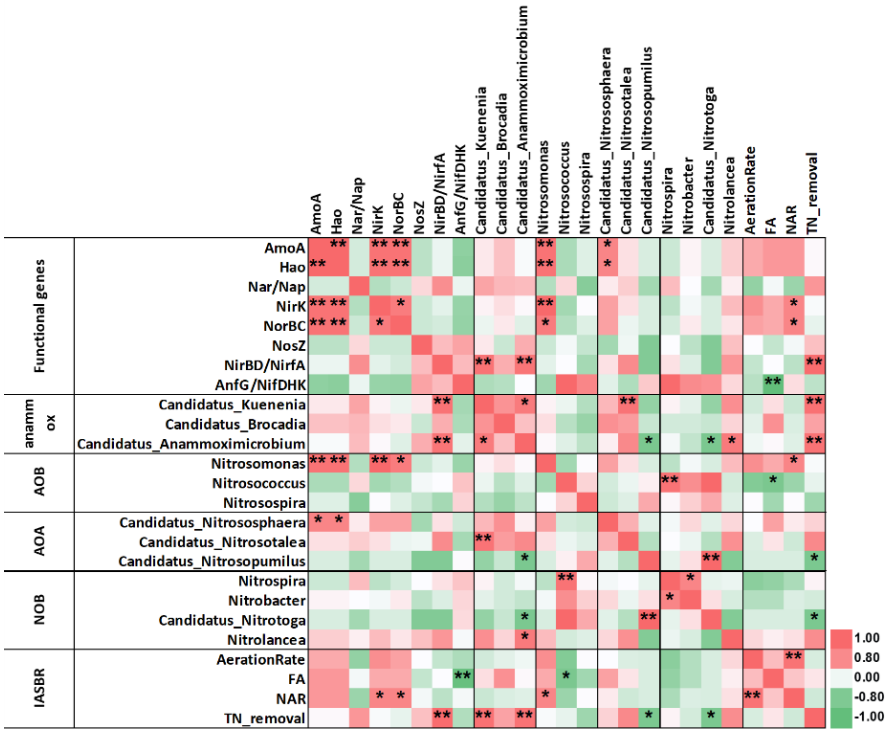

Figure 3-11. Correlations among the quantity of bacterial16S rDNA, predicted functional genes and the IASBR's physicochemical parameters. Correlation tests were performed using two-tailed Spearman's rho correlation test, *$p < 0.05$, **$p < 0.01$. The color code indicates the correlation coefficients between two variables.

3.4 Conclusions

This study demonstrated that the IASBR configuration was efficient in starting up PN-A process with return sludge as the initial inoculum and achieving long-term efficient TN removal. *Nitrosomonas* and *Candidatus Kuenenia* were the predominant AOB genus and anammox bacteria genus, respectively. AOA genus *Candidatus Nitrososphaera* was also enriched to a high abundance of 3.44% and contributed significantly to the partial nitritation in the PN-A stage. NOB genus *Nitrospira* was effectively restrained throughout the whole experiment. Methanogens could co-exist with both aerobic and anaerobic nitrogen-conversion microorganisms in PN-A systems.

Chapter 4
Regulation of the N_2O generation via nitritation by the oxygen transfer rate, nitritation activity, and initial ammonium concentration

4.1 Introduction

The PN-A process is a promising energy-efficient nitrogen removal alternative. However, a high amount of N_2O might be emitted from PN-A reactors. N_2O is a greenhouse gas with a global warming potential of 265- 298 over 100 years (265- 298 times higher than that of CO_2; 265 and 298 indicate the global warming potential without and with the inclusion of climate-carbon feedbacks, respectively) and an important stratospheric ozone-depleting substance [87, 186, 187]. According to the current understanding, in the PN-A system treating low COD/N ratio wastewater, the biological N_2O production is from three pathways (Figure 4-1) [13, 188]. Nitrifier denitrification and NH_2OH oxidation are the two pathways associated with nitritation that is mainly conducted by AOB. Nitrifier denitrification refers to the sequential process that NH_4^+ is oxidized to NH_2OH and NO_2^- followed by the reduction to NO and N_2O, while NH_2OH oxidation is the short-cut process in which NH_2OH is directly oxidized to NO followed by reduction to N_2O. The third pathway is the incomplete heterotrophic denitrification in which N_2O is an intermediate. It has been reported that 0.1% to 12.2%, and on average about 1% of the nitrogen loading was released from the PN-A systems as N_2O [9, 189]. One of the most significant advantages of PN-A process is the significant energy saving, but the resultant reduction of CO_2 footprints may be offset by the increase of CO_2 footprint caused by N_2O emission [9]. Therefore, it's important to investigate the factors governing the generation of N_2O in the PN-A systems so as to mitigate N_2O emission.

The results of Chapter 3 indicate that the N_2O generation might be highly coincident with the nitritation process driven by an ammonium-oxidizing bacteria genus *Nitrosomonas* [13]. This deduction was drawn based on the significant positive correlations between the abundance of the functional genes regulating N_2O production (nitric oxide reductase, Nor) and the nitritation-related factors: the abundance of two functional genes regulating NH_4^+ oxidation and NH_2OH oxidation (ammonium monooxygenase subunit, Amo and hydroxylamine oxidoreductase, Hao, respectively), the abundance of *Nitrosomonas*, and the nitritation performance. No significant correlation was observed between the abundance of Nor and the abundance of genes regulating NO_3^- reduction (nitrate reductase,

Nar and Nap) which is the first step of heterotrophic denitrification. Thus, the N_2O generation and the contribution of nitritation to N_2O generation in the PN-A IASBR need to be studied to examine this deduction.

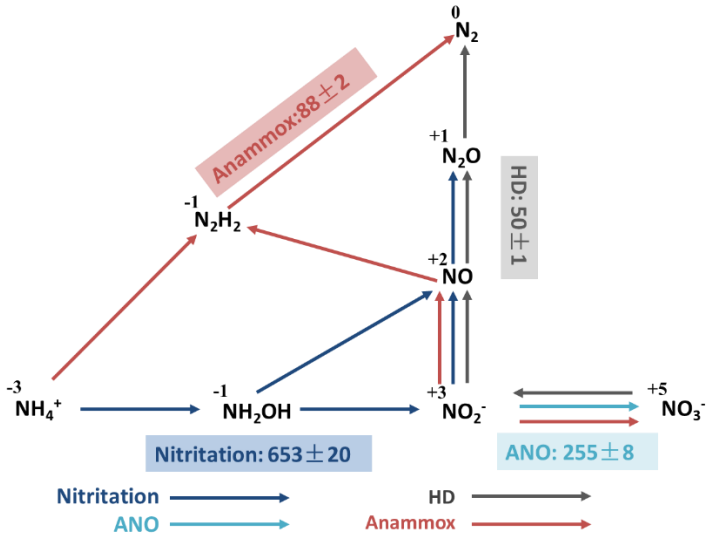

Figure 4-1. Main nitrogen conversion pathways and maximum specific nitrogen conversion capacities of biomass in the IASBR. The shaded numbers indicate the relative maximum specific nitrogen conversion capacities (mg N/L/d), and the naked numbers indicate the valences of nitrogen. ANO: aerobic nitrite oxidation. HD: heterotrophic denitrification.

It is important to find the factors governing the N_2O generation via nitritation so that measures can be taken to mitigate N_2O emission during real applications. Many studies have been carried out and ammonium concentration/loading, DO concentration and nitritation activity are identified among the most important impacting factors [184, 190, 191]. However, these factors were mostly investigated separately and on a single-factor basis. It has been proposed that the N_2O production by classical AOB is related to an imbalance in electron flow or metabolism of the two-step nitritation which may be caused by the accumulation of ammonium, the accumulation of intermediates such as nitrite, and intermittent aeration [188, 191, 192]. Fundamentally, the nitration and the resultant N_2O production are the results of the ammonium concentration, oxygen transfer rate (OTR)

which determines how fast oxygen is delivered to the biomass, and nitritation activity which determines how fast AOB oxidize ammonium. Yet how these factors regulate the N_2O generation via nitritation remains unclear.

Therefore, the first objective of this Chapter was to investigate the N_2O production and emission in the PN-A IASBR for the identification of the main pathway (nitritation or heterotrophic denitrification). Then, batch tests using biomass taken from the IASBR were carried out to investigate the mechanisms of initial ammonium concentrations, nitritation activities, and OTR in regulating N_2O production via nitritation, which was identified as the dominant N_2O production pathway of the IASBR.

4.2 Material and methods

4.2.1 Reactor operation

The PN-A process was applied in an IASBR as previously described in Chapter 3 [13]. In general, the IASBR with a working volume of 8 L, was operated at 30 °C. The IASBR was intermittently aerated at an aeration rate of 50 mL/min and was operated at a cyclic duration of 360 min giving four cycles per day (Figure 4-2). The synthetic wastewater mainly containing 300 mg NH_4^+-N/L and 100 mg COD/L mimicking low COD/N wastewater was fed to the reactor at a hydraulic retention time of 2.9 days.

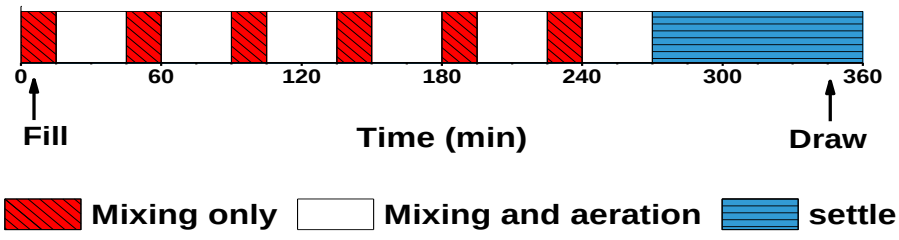

Figure 4-2. Sequencing operation of the IASBR.

4.2.2 N_2O measurement

The dissolved N_2O concentration was measured and recorded online using a system (Figure 4-3) consisting of a sensitive N_2O micro-sensor (N_2O-500, Unisense, Denmark) with a detection range of 0.1- 500 μM, a picoammeter (PA2000, Unisense, Denmark), and an A/D-converter (to convert the analogue signal from the picoammeter to digital signals for the computer, ADC-216USB, Unisense, Denmark). The online data were recorded on a computer every 5 seconds using a software (Sensor Trace Logger v3.1.150, Unisense, Denmark). Every time before use, the sensor was calibrated with solutions containing 0 and 0.28 mg N_2O-N/L dissolved N_2O.

The N_2O generation rate (R_g, mg N_2O-N/L/h) was calculated according to Equation 4-1 [193]:

$$R_g = R_a - R_e \qquad 4\text{-}1$$

where R_a (mg N_2O-N/L/h) is the accumulation rate in the aquatic phase and R_e (mg N_2O-N/L/h) is the N_2O emission rate from the liquid phase to the atmosphere.

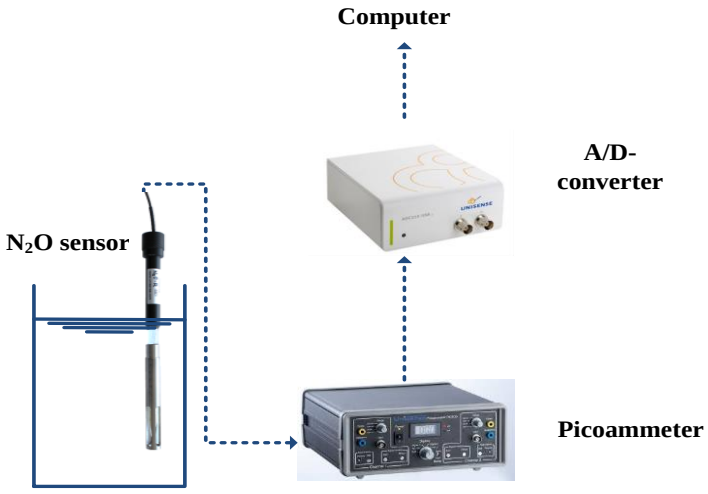

Figure 4-3. Setup for the measurement of dissolved N_2O concentration.

The cumulative N_2O yield (Y, mg N_2O-N) during the period of t_1 to t_2 was calculated according to Equation 4-2.

$$Y = V \times \int_{t_1}^{t_2} R_g \, dt \qquad 4\text{-}2$$

where V was the volume of the reactor (L). The accumulation rate R_a was calculated based on the measured dissolved N_2O concentration (Equation 4-3):

$$R_a = \frac{dC}{dt} \qquad 4\text{-}3$$

where C is the measured dissolved N_2O concentration at time t.

The N_2O emission is caused by mixing and air stripping in the IASBR and by shaking of the liquid during the batch tests. The N_2O emission rate R_e is proportional to the dissolved N_2O concentration C, and the relationship can be described by Equation 4-4:

$$R_e = -KC \qquad 4\text{-}4$$

where K is the N_2O transfer coefficient, s^{-1}. K value can be determined using clear water tests without biomass inoculation. As no N_2O generation during the clear water test, the N_2O emission rate R_e is equal to the N_2O accumulation rate R_a which was calculated based on Equation 4-3. Then, based on Equation 4-4, the K value can be calculated as the slope of the linear fit curve of R_e against the dissolved N_2O concentration C.

The cumulative N_2O emission (E, mg N_2O-N) during the period of t_1 to t_2 was calculated according to Equation 4-5:

$$E = -V \times \int_{t_1}^{t_2} R_e \, dt \qquad 4\text{-}5$$

where V is the volume of the reactor (L).

4.2.3 Contribution of nitritation on N_2O generation and emission in the IASBR

The microbiological N_2O generation in the PN-A IASBR was mainly caused by nitritation and heterotrophic denitrification. The N_2O generation and emission in one operating cycle were first evaluated with synthetic wastewater containing 300 mg /L NH_4^+-N and 100 mg /L COD. N_2O was produced via both nitritation and heterotrophic denitrification in this case (defined as "Experiment 1"). COD was no longer supplied in the feed, and the N_2O generation and emission in one operating cycle were investigated when no COD was detected in the bulk liquid of the IASBR. In this case, N_2O was only produced via nitritation under these conditions (defined as "Experiment 2"). The contribution of nitritation on N_2O generation and emission can be assessed by comparing the two results of the two tests (Experiment 1 and Experiment 2).

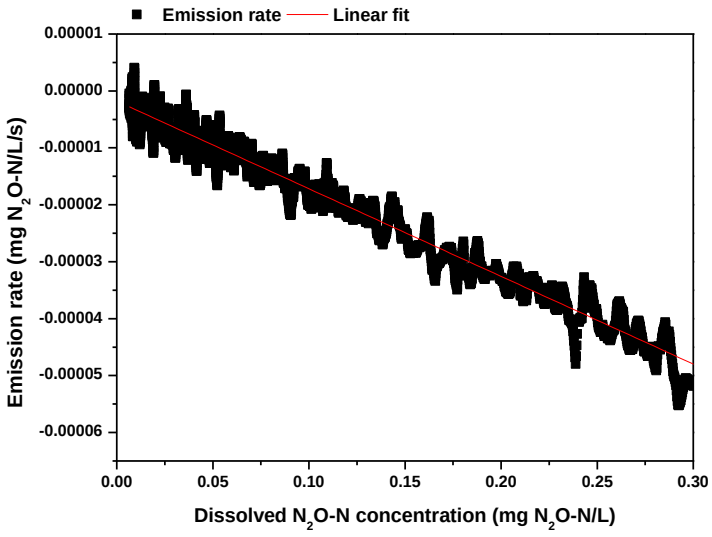

Figure 4-4. Determination of N_2O transfer coefficient *K* in the IASBR under the conditions of mixing and 50 mL/min aeration. The N_2O transfer coefficient *K* was the slope of the linear fit line, 1.54×10^{-4} s^{-1} (R^2=0.97) in this case.

The *K* values during the mixing phase and mixing-aeration phase of the IASBR were determined in an identical reactor. An N_2O solution made from saline water (the same salinity of 0.25% with that in the IASBR reactor) was added to an identical reactor without biomass. The reactor was mixed or mixed and aerated under the conditions (mixing rate, temperature, and aeration rate (50 mL/min)) identical to those in the IASBR. The dissolved N_2O concentration was recorded online using the N_2O sensor mentioned above. The measured *K* values were 1.54×10^{-4} s^{-1} (R^2=0.91) during the mixing-aeration phase (Figure 4-4) and 3.48×10^{-5} s^{-1} (R^2=0.87) during the mixing phase (Figure 4-5).

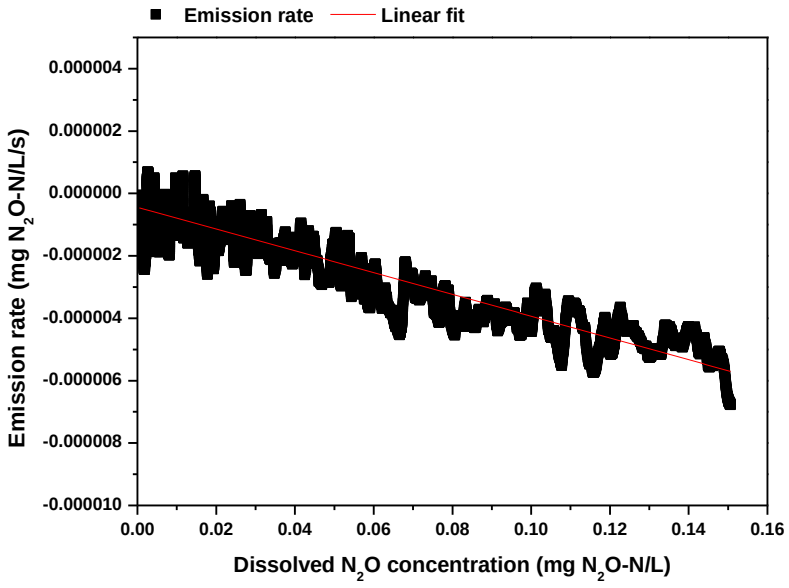

Figure 4-5. Determination of N_2O transfer coefficient *K* in the IASBR under the conditions of mixing. The N_2O transfer coefficient *K* was the slope of the linear fit line, 3.48×10^{-5} s^{-1} (R^2=0.87) in this case.

4.2.4 Batch tests: N_2O generation via nitritation

Ex-situ batch tests were carried out to investigate how the OTR, nitritation activity, and initial ammonium concentrations would impact the N_2O generation via nitritation. The tests were conducted in a wide-mouth 500 mL Erlenmeyer flask incubated at 30 °C in a shaking

bath (FBS3D, TECHNE, UK). 200 mL biomass (865 mg VSS/L) taken from the IASBR was added into the flask after being washed three times and dispersed with 200 mL potassium phosphate buffer (0.01 mol/L, pH 8.0). Trace element stock solutions [13] were added at the dosage of 1 mL/L. In the first batch (Batch 1), ammonium chloride (NH_4Cl) was added to the flask to achieve an initial NH_4^+-N concentration of 30 mg NH_4^+-N /L which was similar to that in the IASBR (initial concentration of 26.3 mg NH_4^+-N /L with complete NH_4^+-N removal), and a lower level of 20 mg NH_4^+-N /L in the second batch (Batch 2). For each of the batches, OTR was controlled by adjusting the shaking speed (i.e., 122, 144, 167, and 200 stroke/min). The N_2O generation rates and cumulative yields were determined as per section 2.2. DO was monitored and recorded using a portable meter (Multi3620, WTW, Germany) and a DO sensor (FDO925, WTW, Germany). Water samples were taken regularly to monitor the concentrations of NH_4^+-N, NO_2-N, and NO_3^--N. The nitritation activity, which was influenced by OTR and initial NH_4^+-N concentration, was calculated as the slope of the linear regression curve of the NH_4^+-N consumption against time.

The N_2O *K* values at various shaking speeds were determined under the same conditions in the batch tests without biomass inoculation. *K* values at the shaking speeds of 122, 144, 167, and 200 stroke/min were determined using the same methods used to measure *K* values in the IASBR. OTR (mg O_2/L/h) was calculated based on Equation 4-6 [194]. The measurement of volumetric oxygen transfer coefficient K_La values at various shaking speeds was conducted under the same conditions (30 °C) in the batch tests except no addition of biomass. Firstly, DO was completely removed from the 200 mL potassium phosphate buffer by flushing with N_2 gas until no DO was detected in the Erlenmeyer flask. Then the flask was shaken at speeds of 122, 144, 167, and 200 stroke/min, respectively, to allow oxygen in the air being transferred into the solution, and at the same time, DO was monitored and recorded. The K_La was calculated according to Equation 4-6 and Equation 4-7 [194]:

$$OTR = \frac{dC_{O_2}}{dt} = K_La(C_s - C_{O_2t}) \quad \text{4-6}$$

$$\ln\left(\frac{C_s - C_t}{C_s - C_0}\right) = -k_L a \times t \quad 4\text{-}7$$

where OTR is the oxygen transfer rate, mg O_2/L/h, C_{O_2} is the DO concentration, $C_{O_2 t}$ or C_t in Equation 4-7 is the DO concentration at time t, C_S is the saturated DO concentration which was 7.47 mg/L under the conditions of the tests, and C_0 is the DO concentration at time 0. The oxygen transfer amount (OTA, mg O2/L) was calculated as per Equation 4-8. The theoretical oxygen demand rate for aerobic ammonium oxidation and nitrite oxidation (ODR, mg O_2/L/h) was calculated based on aerobic ammonium oxidation rate (AAO, nitritation rate, mg NH_4^+-N/L/h) and aerobic nitrite oxidation rate (ANO, NO_3^--N production rate, mg NO_3^--N/L/h), as shown in Equation 4-9, Equation 4-10, and Equation 4-11.

$$\text{OAT} = \int_0^t k_L a \times (C_s - C_t) \times dt \quad 4\text{-}8$$

$$\text{ODR} = 3.43 \times \text{AAO} + 1.14 \times \text{ANO} \quad 4\text{-}9$$

$$NH_4^+ + 1.5O_2 \rightarrow NO_2^- + 2H^+ + H_2O \quad 4\text{-}10$$

$$NO_2^- + 0.5O_2 \rightarrow NO_3^- \quad 4\text{-}11$$

4.2.5 Analytical methods

The concentrations of NH_4^+-N, NO_2-N, and NO_3^--N of the water sample were measured using a nutrient analyzer (Konelab 20, Thermo Clinical Labsystems, USA) after being filtered through 0.45 um syringe filters (Sarstedt Ltd., Germany). COD and VSS were measured as per the standard methods [157]. The nitrogen removal capacities of the biomass (865 mg VSS/L) for the main nitrogen-conversion pathways, i.e., nitritation, aerobic nitrite oxidation, anammox, and heterotrophic denitrification, were determined following the previous activity methods in Chapter 3 except that higher nitrogen concentrations were used to achieve maximum activities (80 mg NH_4^+-N/L in nitritation tests, 20 mg NO_2^--N/L

in aerobic nitrite oxidation tests, 20 mg NH_4^+-N/L together with 40 mg NO_2^--N/L in anammox tests, and 30 mg NO_3^--N/L in heterotrophic denitrification tests).

4.3 Results and discussion

4.3.1 Nitrogen conversion capacities in the IASBR

N_2O production depends on the activity of the nitrogen-conversion pathways. Therefore, preceding the investigation of N_2O generation and emission in the IASBR, the capacities of the main nitrogen-conversion pathways were first measured to serve as background information (Figure 4-1). The nitritation, which was mainly carried out by two groups of microorganisms, *Nitrosomonas* and *Candidatus Nitrososphaera* (Chapter 3), had a nitritation capacity of 653 mg N/L/d, ranking the highest among the main nitrogen-conversion pathways. The aerobic nitrite oxidation capacity of 255 mg N/L/d was 2.6 times lower than that of the nitritation, indicating the efficient suppression of NOB. The main nitrogen removal pathway, anammox, was mainly conducted by *Candidatus Kuenenia* and had a capacity of 88 mg N/L/d, which was lower than that of the nitritation. This agrees with the findings that in the suspended sludge, AOB usually are more abundant than anammox bacteria [69]. The presence of a small amount of COD (100 mg/L, COD/N ratio of 1/3) led to the heterotrophic denitrification capacity of 50 mg N/L/d. N_2O was produced in both the nitritation and heterotrophic denitrification process and was only consumed by heterotrophic denitrification process. To the current best knowledge, aerobic nitrite oxidation and anammox are not directly involved in the N_2O generation and consumption, but affect the N_2O generation by consuming NH_4^+, NO_2^-, and NO.

4.3.2 Contribution of nitritation to N_2O generation and emission in the IASBR

For Experiment 1, the IASBR was ran with normal COD supply, i.e., 100 mg/L COD and COD/N ratio of 1/3. Both the heterotrophic denitrification process and nitritaion process generated N_2O. The dissolved N_2O concentration in one operating cycle experienced a

slight decrease at the beginning of the cycle followed by a gradual increase to the highest level of 0.09 mg N_2O-N/L at 280 min, and then gradually decreased to 0.01 mg N_2O-N/L at the end of the cycle (Figure 4-6). The generation and emission of N_2O were shown in Figure 4-7, in which the negative emission rate indicates the emission of N_2O (Equation 4-4) and the negative generation rate indicates the net consumption of N_2O. The N_2O generation rate showed a sharp decrease at the beginning of the cycle followed by a general increasing period with the highest value of 0.12 mg N_2O-N/L/h in which there were six peak intervals roughly coincident with the aeration intervals. After the termination of the reaction phase, the N_2O generation rate quickly decreased to - 0.13 mg N_2O-N/L/h and then gradually increased to 0 at the end of the cycle (Figure 4-7, top part). The N_2O generation rate in this study was calculated as the difference between the N_2O accumulation rate and the N_2O emission rate, so the net consumption of dissolved N_2O together with almost negligible N_2O emission rate resulted in the sharp decrease or even negative N_2O generation rates as shown at the beginning and the end of the cycle (Figure 4-7). The N_2O emission rate had peak values during the aeration intervals; otherwise, it remained almost zero.

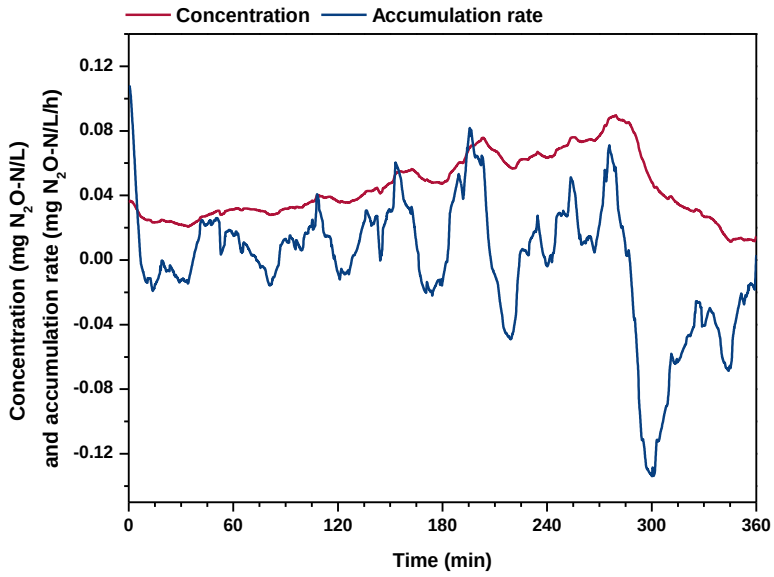

Figure 4-6. Dissolved N_2O concentration and N_2O accumulation rate in one typical operating cycle of the IASBR at the COD/N ratio of 1/3.

In line with the profile of the N_2O generation rate, the cumulative N_2O yield during aeration intervals initially saw a slow increase and then a faster increase to 0.816 mg N_2O-N at the end of the reaction phase, while a stable increase to the highest value of 0.384 mg N_2O-N was observed in non-aeration intervals (Figure 4-7, bottom part). At the end of the cycle, the cumulative N_2O yield during non-aeration decreased to -0.16 mg N_2O-N, indicating a net-consumption of N_2O by heterotrophic denitrification process during this period. Overall, in one operating cycle, the total net N_2O production was 1.2 mg N_2O-N (1.89 mg N_2O) accounting for 0.57% of the nitrogen loading, and 68% of which was produced during aeration periods, and 45% of the produced N_2O was consumed during the settling phase (Table 4-1). A total amount of 0.688 mg N_2O-N which was equal to 53% of the total produced N_2O and 0.33% of the nitrogen loading, was released from the IASBR in one operating cycle. This is within the reported range of 0.1% to 12.2% and lower than the average value of 1% [9, 189]. 0.624 mg N_2O-N of the N_2O emission occurred during aeration periods, accounting for 91% of the total N_2O emission (Table 4-1).

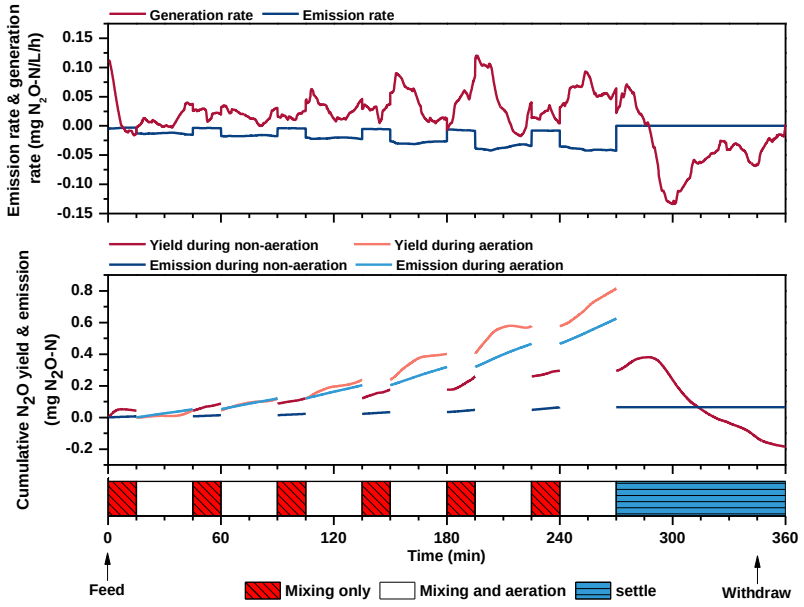

Figure 4-7. N_2O generation rate, emission rate, cumulative yield, and emission in one typical operating cycle of the IASBR with normal COD supply (COD/N of 1:3). Cumulative N_2O yield $= \sum_{n=1}^{6}(N_2O \text{ yield during nth aeration intervals})$ and N_2O yield was calculated as $V \times \int_0^t r_g \, dt$, where V was the volume of the reactor. Cumulative

N_2O yield during non-aeration intervals, N_2O emission during aeration, and N_2O emission during non-aeration were calculated in the same way. N_2O emission= $V \times \int_0^t r_e \, dt$, where V was the volume of the reactor.

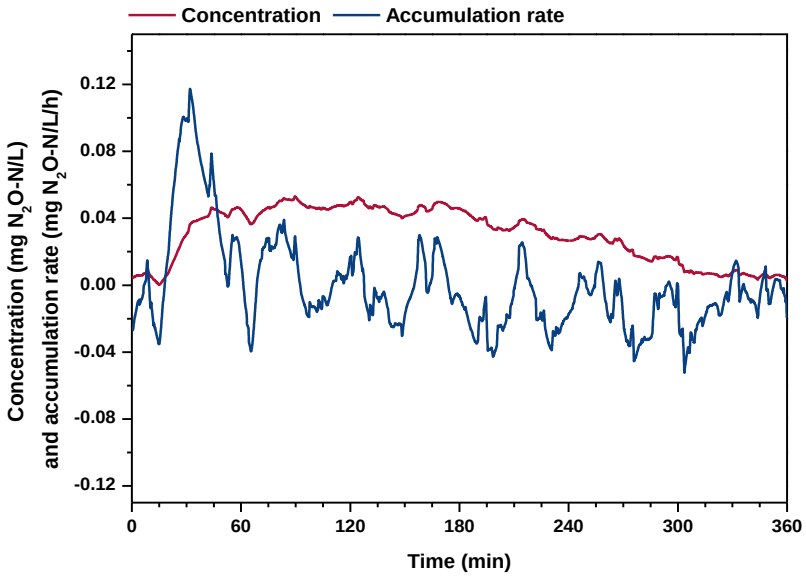

Figure 4-8. Dissolved N_2O concentration and N_2O accumulation rate in one typical operating cycle of the IASBR without COD supply.

In Experiment 2, the COD was no longer supplied to the IASBR and the nitritation process should be the most significant biological N_2O generation pathway. Different from the profiles of Experiment 1, the dissolved N_2O concentration first showed a rapid increase at the beginning of the reaction phase and then leveled off at around 0.046 mg N_2O-N/L until about 180 min, followed by gradual reduction to the lowest level at the end of the cycle (Figure 4-8). For the profile of N_2O generation rate, six peak intervals during the aeration intervals were also observed (Figure 4-9, top part, the negative emission rate indicates the emission of N_2O (Equation 4-4) and the negative generation rate indicates the net consumption of N_2O). But contrary to results of Experiment 1, the highest value of 0.12 mg N_2O-N/L/h appeared at the beginning of the cycle and then gradually decreased to almost 0 at the end of the reaction phase. Similarly, negative but much smaller (absolute

value) N_2O generation rate (-0.05 mg N_2O-N/L/h) appeared during the initial settling phase and then gradually increased to about 0. This is because without external COD supply, N_2O produced by nitritation was consumed at a much lower rate by heterotrophic denitrification process with a limited amount of organic matters from the lysis of cells, etc. N_2O emission rate also had peak values of about -0.025 mg N_2O-N/L/h during the aeration periods and remained almost zero during non-aeration intervals.

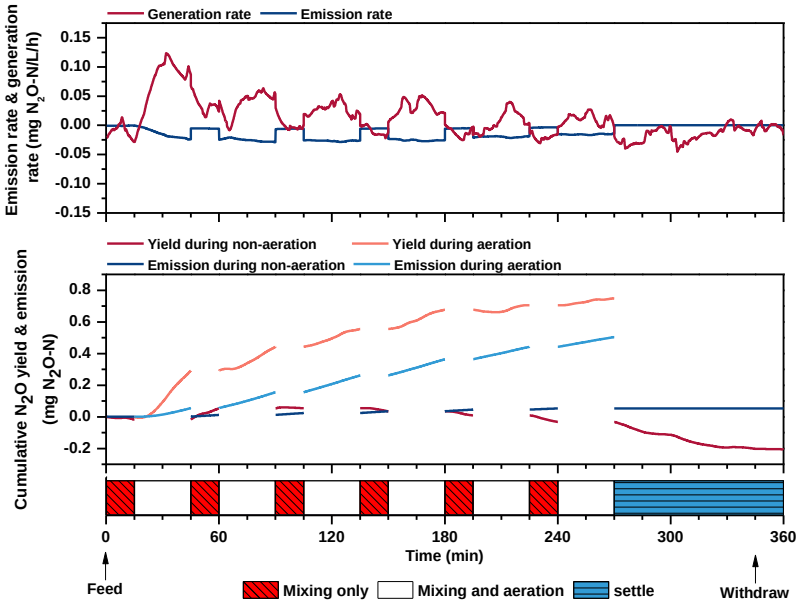

Figure 4-9. N_2O generation rate, emission rate, cumulative concentration, and emission in one typical operating cycle of the IASBR without COD supply. Cumulative N_2O yield $= \sum_{n=1}^{6}(N_2O \text{ yield during nth aeration intervals})$ and N_2O yield was calculated as $V \times \int_0^t r_g \, dt$, where V was the volume of the reactor. Cumulative N_2O yield during non-aeration intervals, N_2O emission during aeration, and N_2O emission during non-aeration were calculated in the same way. N_2O emission= $V \times \int_0^t r_e \, dt$, where V was the volume of the reactor.

During aeration, a total N_2O yield of 0.748 mg N_2O-N was produced at higher generation rates at the beginning of the cycle and lower generation rates at the end (Figure 4-9). During non-aeration periods, the peak value of 0.064 mg N_2O-N occurred at 90 min, and began to

decrease since then which means the occurrence of net-consumption of N_2O thereafter. During the settling phase, 0.208 mg N_2O-N was consumed at lower rates than that in Experiment 1. The reason for the extremely small N_2O consumption without external COD supply was that only 1 mol electrons are needed for the reduction of 1 mol N_2O-N compared to 5 mol electrons for the complete heterotrophic denitrification (Figure 4-1); this COD supply can be supported by organic matters from the lysis of cells, etc. Overall, when the nitritation process was the only N_2O generation pathway, the total net N_2O production was 0.812 mg N_2O-N (1.276 mg N_2O) accounting for 0.39% of the nitrogen loading, and 92% of which was produced during aeration periods (Table 4-1). 33% of the produced N_2O was consumed during the whole cycle and 69% (0.56 mg N_2O-N) was released to the atmosphere mainly during aeration periods when 90% (0.504 mg N_2O-N/L) N_2O was emitted. The result was similar to that in Experiment 1 and agreed with the reported results of 80% N_2O emission during aeration periods in an intermittently aerated PN-A reactor [85].

The common opinion is that low COD/N ratio induces N_2O emission [190, 195]. In this study, by comparing the results of Experiment 1 and Experiment 2, the presence of COD at a COD/N ratio of 1/3 did lead to the increase of the N_2O generation from 0.39% to 0.57% to the nitrogen load mainly by enhancing the N_2O generation during non-aeration periods, as summarized in Table 4-1. But this only led to a slight N_2O emission increase from 0.27% to 0.33% to the nitrogen load. While the presence of COD, on the other hand, also improved the N_2O consumption from 0.13% to 0.26% to the nitrogen load, which happened mainly during the settling phase when DO was almost 0 (Figure 2 B [13]). This means the N_2O emission caused by low COD/N ratio can be minimized by properly managing the DO concentration which is important for the mitigation of N_2O emission in PN-A systems. Further study is needed to determine the optimal conditions to reduce the generated N_2O.

Table 4-1. Comparison between the results of Experiment 1 and 2.

		Generation				Emission			Consumption	
		Amount	Proportion (%)	Total amount	Factor	Amount	Proportion (%)	Factor	Amount	Factor
Experiment 1	Aeration	0.816	68	1.20	0.57	0.624	91	0.33	0.544	0.26
	Non-aeration	0.384	32			0.064	9			
Experiment 2	Aeration	0.748	92	0.812	0.39	0.504	90	0.27	0.272	0.13
	Non-aeration	0.064	8			0.056	10			

Note: amount: mg N_2O-N; factor: amount of N_2O-N/nitrogen load×100%, %; The nitrogen load in one cycle was 210 mg NH_4^+-N.

Based on the results of Experiment 1 and Experiment 2, it can be calculated that the nitritation process accounted for 69% of the N_2O generation and 81% of the N_2O emission, making it the dominant pathway for both N_2O generation and emission in the IASBR. Some of the reported studies investigating the N_2O production in PN-A systems also confirmed that nitritation was the dominant N_2O producing pathway [196, 197]. Thus, it's important to investigate the factors affecting the N_2O generation via this pathway so that corresponding measurements can be taken to minimize the N_2O emission.

4.3.3 Factors governing the generation of N_2O via nitritation

Understanding the mechanisms of some of the most important factors such as OTR, initial NH_4^+-N concentration, and nitritation activity in regulating the nitritation-induced N_2O generation rate is crucial for effective mitigation of N_2O emission from PN-A systems. The measured N_2O *K* values at the shaking speeds of 122, 144, 167, and 200 stroke/min, based on which the generation and emission of N_2O were calculated, were 5.73×10^{-4} s^{-1} (R^2=0.97), 0.00106 s^{-1} (R^2=0.98), 0.00186 s^{-1} (R^2=0.98), and 0.0105 s^{-1} (R^2=0.99), respectively (Figure 4-10). The measured K_La values at shaking speed of 122, 144, 167, and 200 stroke/min, based on which the OTR was calculated, were 2.5 h^{-1} (R^2=0.99), 6.0 h^{-1} (R^2=0.99), 11.4 h^{-1} (R^2=0.99), and 41.3 h^{-1} (R^2=0.99), respectively (Figure 4-11).

Two batch tests were carried out to investigate the combined effect of these three factors on N_2O generation via nitritation. Batch test 1 were conducted under various K_La and OTR at the initial NH_4^+-N concentration of 30 mg N/L (similar to that in the IASBR with complete NH_4^+-N removal), while the initial NH_4^+-N concentration was set at a lower level of 20 mg N/L in batch tests 2. Nitritation activity varied with the initial NH_4^+-N concentration and OTR. Two terms were defined to describe the profiles of N_2O generation rate, i.e., the peak value of the N_2O generation rate (PVG) and the duration of the peak N_2O generation rate (DPG).

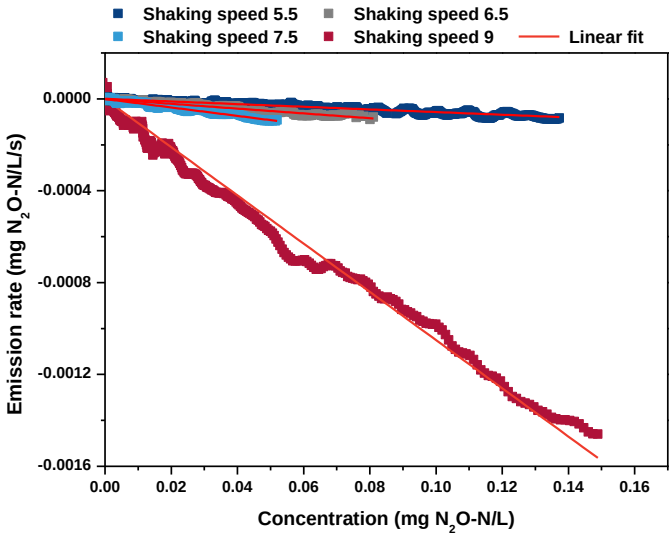

Figure 4-10. Determination of N_2O transfer coefficient *K* at shaking speeds of 122, 144, 167, and 200 stroke/min. *K* values were calculated as the slopes of the linear fit lines and the corresponding values were 5.73×10^{-4} s^{-1} (R^2=0.97), 0.00106 s^{-1} (R^2=0.98), 0.00186 s^{-1} (R^2=0.98), and 0.0105 s^{-1} (R^2=0.99).

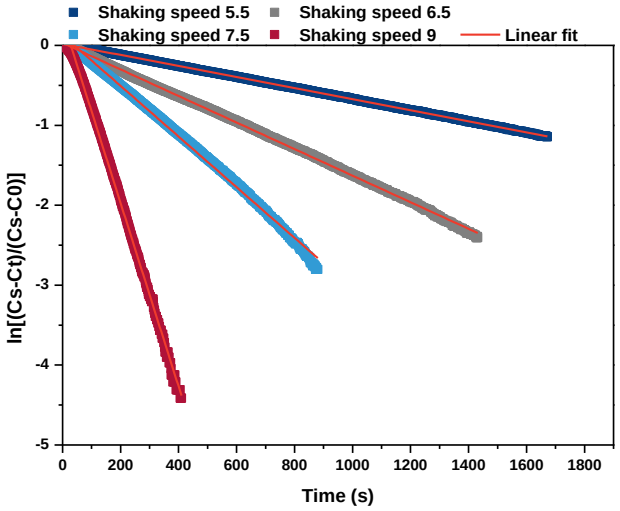

Figure 4-11. Determination of oxygen transfer coefficient K_La at shaking speeds of 122, 144, 167, and 200 stroke/min. The K_La was calculated as the slope of the linear fit line and the corresponding values were 2.5 h^{-1} (R^2=0.99), 6.0 h^{-1} (R^2=0.99), 11.4 h^{-1} (R^2=0.99), and 41.3 h^{-1} (R^2=0.99), respectively.

4.3.3.1 Regulation of nitritation activity and OTR in N_2O generation

In Batch 1, with K_La of 2.5 h^{-1}, the addition of 30 mg N/L NH_4^+-N caused an immediate increase of the dissolved N_2O concentration to a peak value of 0.46 mg N_2O /L (Figure 4-12) and the increase of N_2O generation rate to a PVG of 0.121 mg N_2O-N/L/h and a DPG of 150 min (Table 4-2). The resultant cumulative N_2O yield was 0.208 mg N_2O-N/L with an N_2O yield factor (cumulative N_2O yield ÷ nitrogen load×100%) of 3.5% (Figure 4-13). Simultaneously, NH_4^+-N was consumed at a nearly constant rate, resulting in a constant nitritation activity, which was indicated by NH_4^+-N conversion rate of 5.4 mg N/L/h (Figure 4-14). It was observed that N_2O generation rate was dynamic rather than constant even under constant nitritation activity. These results suggested that simply linking the N_2O generation rate with the nitritation activity, which is often mentioned in other research [85, 198, 199], is not comprehensive enough to reflect the whole situation. The NO_2^--N concentration gradually increased to a relatively low level of 4.0 mg N/L (equivalent free nitrous acid (FNA) of 0.0001 mg HNO_2-N/L) when the N_2O generation rate displayed a rising trend but the further increase of the NO_2^--N concentration to a higher level of 6.8 mg N/L (equivalent FNA of 0.0004 mg HNO_2-N/L) was coincident with a declined trend of N_2O generation rate. These results suggest that N_2O was mainly produced by NH_2OH oxidation rather than nitrifier denitrification as NH_2OH oxidation is favored at high ammonium and low nitrite concentrations while nitrifier denitrification shows a reverse behavior [195]. DO concentration first sharply decreased from around 7.47 mg/L to 0.38 mg/L due to the oxygen consumption, and then slowly increased to 1.32 mg/L at a nearly constant rate (Figure 4-12). The OTR increased to 18 mg O_2/L/h within 10 min and then remained relatively unchanged (Figure 4-12). The slightly higher ODR (for aerobic ammonium oxidation and nitrite oxidation) of 21 mg O_2/L/h than OTR indicated that the oxygen transfer was the limiting factor (Table 4-2). The reason for the slightly lower OTR than ODR was the initial bulk DO (7.47 mg/L) prior to the test provided extra oxygen for nitrogen conversion. In this test, the DO concentration was a parameter that resulted from the oxygen input and oxygen consumption. No obvious relationship between the DO concentration and N_2O generation rate was observed which indicates that solely using either nitritation activity or DO concentration as an indicator to the N_2O generation rate was not inclusive.

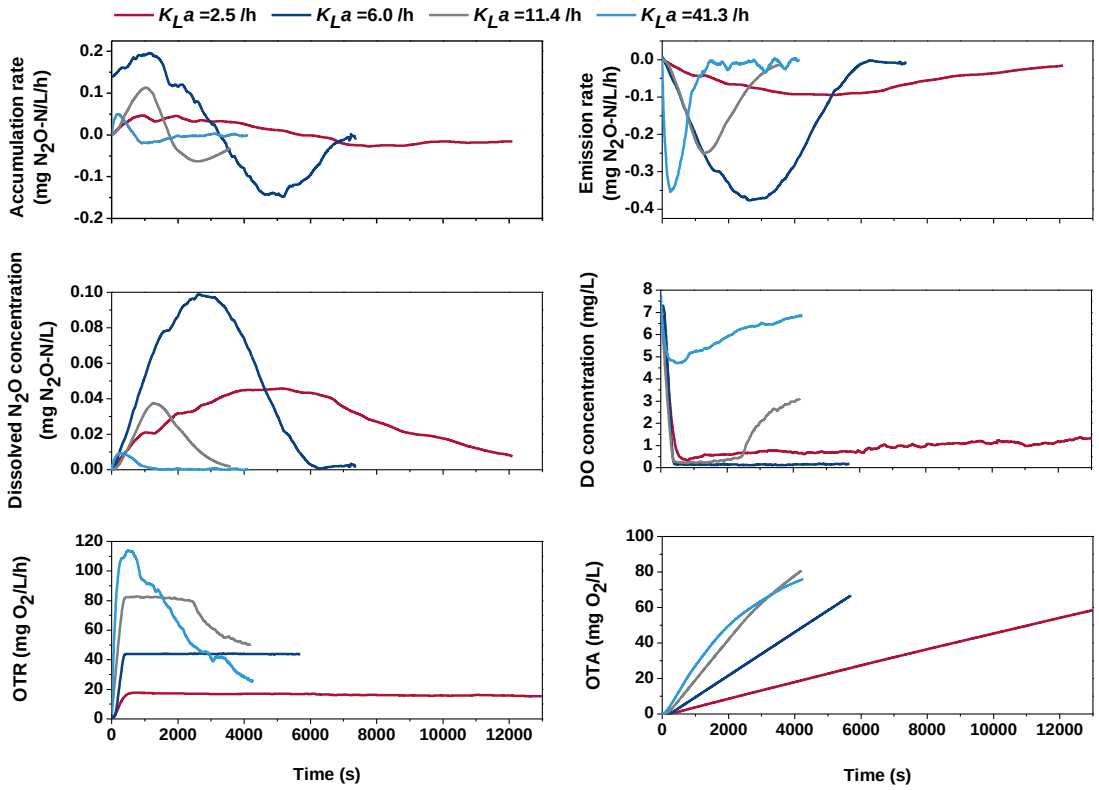

Figure 4-12. N_2O accumulation rates, N_2O emission rates, dissolved N_2O concentration, DO concentration, oxygen transfer rate (OTR), and oxygen transfer amount (OTA) at various K_La in Batch 1, in which the initial NH_4^+-N concentration was 30 mg N/L.

When the K_La was increased to 6.0 h^{-1}, the highest OTR increased to 44 mg O_2/L/h and the profiles of dissolved N_2O and N_2O generation rate displayed a similar pattern with those at 2.5 h^{-1}, but the peak values remarkably increased to 0.099 mg N_2O /L (Figure 4-12) and 0.414 mg N_2O-N/L/h (Figure 4-13), respectively. The N_2O yield factor rose to 6.2% (cumulative N_2O yield of 0.374 mg N_2O-N/L) though the increase of OTR reduced the DPG from 150 min to 91 min. ODR increased to the same level with OTR but the oxygen consumption of 69.5 mg O_2/L for nitrogen conversion during the 1.58 h test was still higher than the oxygen transfer amount of 67 mg O_2/L (Table 4-2), indicating that oxygen transfer was still the limiting factor. Both the nitritation activity and the DO concentration (about 0.15 mg/L, Figure 4-12) remained

constant during the whole test which again clearly confirmed that solely link the two factors with the N_2O generation rate was not comprehensive.

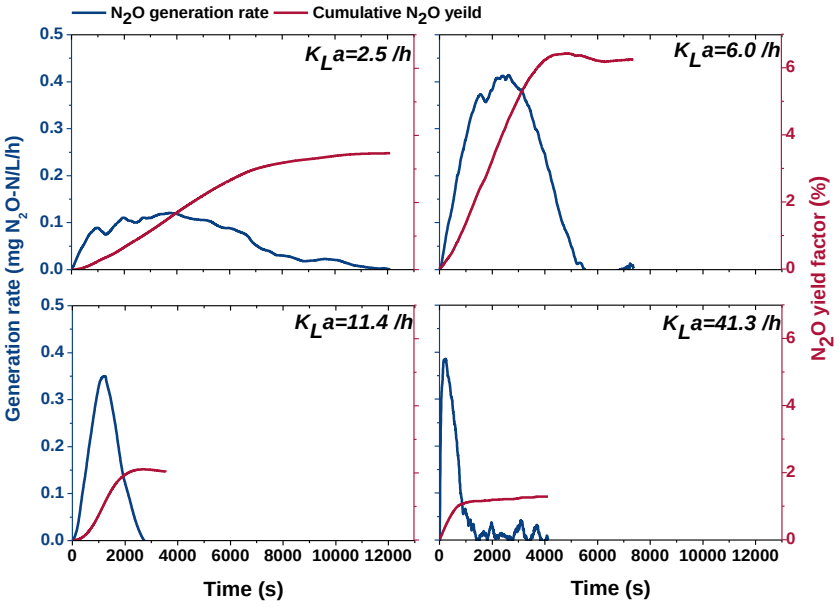

Figure 4-13. N_2O generation rates and N_2O yield factor of the batch tests with initial NH_4^+-N concentration of 30 mg N/L at various volumetric oxygen transfer coefficients. N_2O yield factor = cumulative N_2O yield ÷ nitrogen load×100%. The nitrogen load was 6 mg N/L in this case.

Further increasing the K_La values to 11.4 h^{-1} and 41.3 resulted in the increase of the peak OTR to 83 mg O_2/L/h and 114 mg O_2/L/h, respectively, but this didn't change the patterns of dissolved N_2O concentration and the N_2O generation rate which all experienced a peak period. The increase of OTR led to PVGs of 0.350 mg N_2O-N/L/h and 0.386 mg N_2O-N/L/h, respectively, which were slightly lower than that at K_La of 6.0 h^{-1} but still higher than that at K_La of 2.5 h^{-1}. The increase of OTR significantly reduced the DPGs to 45 min and 23 min, respectively, which led to the reduction of cumulative N_2O yields to 0.122 mg N_2O-N/L and 0.077 mg N_2O-N/L. The higher OTRs than ODRs (Table 4-2) indicated that nitritation activity,

instead of the oxygen transfer, became the limiting factor which can also be reflected by the profiles of DO concentration (Figure 4-12).

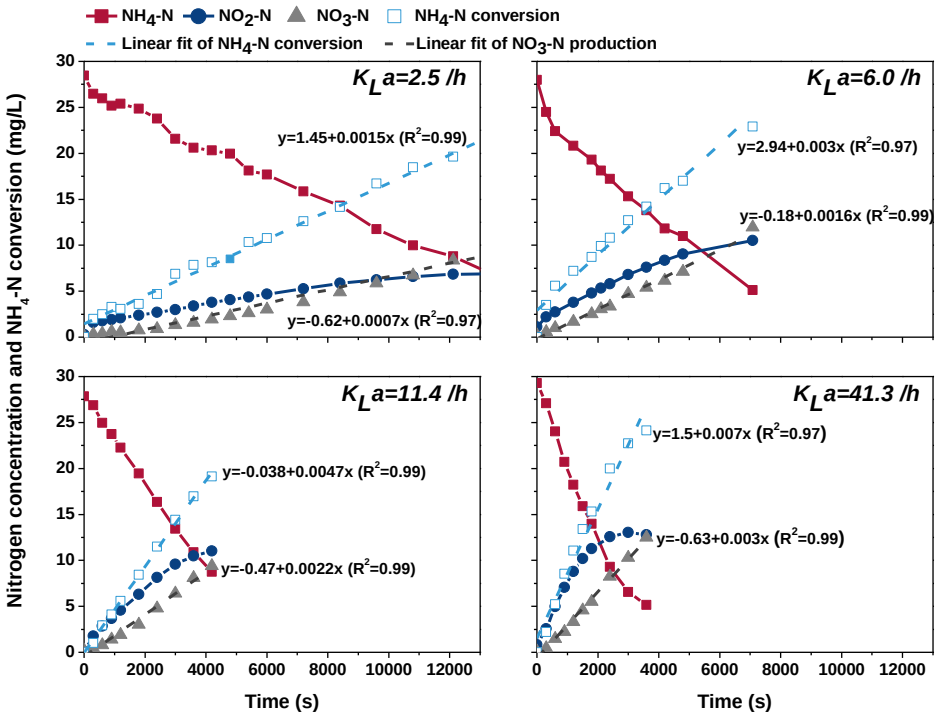

Figure 4-14. Profiles of the nitrogen concentration and nitrogen conversion of the batch tests with initial NH_4^+-N concentration of 30 mg N/L at various K_La. The nitritation activities and aerobic nitrite oxidation rates were calculated from the slopes of the linear fit lines of the NH_4^+-N conversion and linear fit lines of the NO_3^--N production.

These results clearly show that at K_La values of 2.5 h^{-1}, 6.0 h^{-1}, 11.4 h^{-1}, and 41.3 h^{-1}, the profiles of N_2O generation rate was dynamic with time and all experienced a peak period, the DO concentrations showed relative constant or dynamic profiles depending on the K_La values, while the nitritation activities remained constant. The similar trend was also observed in another study [191]. The increase of the N_2O generation rate probably was due to the metabolic process with which that AOB deal with the shock caused by ammonium load and the decrease of the N_2O generation rate may result from the adaption of AOB to the ammonium shock. Currently, the N_2O generation rate is often related to nitritation activity either in a linear

relationship or exponential relationship [85, 198-200]. DO concentration is an indirect parameter that is often suggested as one of the most important factors affecting N_2O generation and it's generally agreed that low DO concentration leads to higher N_2O generation during nitritation [183, 190, 196, 200, 201], though controversial conclusion is also drawn that the increase of DO concentration would stimulate N_2O production via nitritation (due to the activation of ammonia oxidation) [202] or no significant correlation can be observed between DO concentration and N_2O production [203]. However, in this study, the dynamic N_2O generation rate indicates that it's not comprehensive enough to simply link the N_2O generation rate with the nitritation activity which remained constant during the tests or the DO concentration as no obvious relationship was observed.

Nitritation is a two-step process in which ammonium is oxidized to nitrite via NH_2OH (Figure 4-1). N_2O is a by-product of the nitritation process and the result of AOB dealing with imbalanced electron flows which may be caused by the imbalance between ammonium oxidation to NH_2OH and the oxygen transfer, a sudden increase of ammonium concentration, and accumulation of intermediates such as NH_2OH [191, 192]. In this study, the NH_2OH oxidation was the most possible N_2O production pathway as mentioned above. At low K_La, when oxygen transfer was the limiting factor, the increase of OTR (from 18 mg O_2/L/h to 44 mg O_2/L/h) led to the increase of the PVG which might be the result of the enhanced electron-flow imbalance because ammonium was converted at a higher rate (higher nitritation activity) but the oxygen transfer was still limiting. The further increase of the OTR to 83 mg O_2/L/h and 114 mg O_2/L/h made the ammonium oxidation the limiting factor rather than the oxygen transfer (Table 4-2). The sufficiently higher OTR reduced the electron-flow imbalance probably by consuming the accumulated intermediates, thus reduced the PVG. On the other hand, the increase of OTR led to a higher nitritation activity and faster consumption of the intermediates thus reducing the DPG. For the cumulative N_2O yield, when oxygen transfer was the limiting factor, the increase of OTR resulted in the increase of the total produced N_2O. But when nitritation activity was the limiting factor, the increase of OTR led to the reduction of the cumulative N_2O yield mainly by reducing the DPG. These results are in line with a reported study stating that very high and very low DO concentrations were found to result in lower N_2O emissions, while medium DO concentrations led to higher N_2O emissions [204]. In conclusion, N_2O generation via nitritation

would be governed by nitritation activity and the OTR instead of commonly reported single factors such as nitritation activity or DO. The control of N_2O generation during nitritation by nitritation activity and the OTR probably is achieved through regulating the electron-flow imbalance: when oxygen transfer is the limiting factor, higher OTR would lead to higher nitritation activity (enhanced electron-flow imbalance) which can remarkably increase the PVG; when nitritation is the limiting factor, the increase of OTR (reduced electron-flow imbalance) would lead to slightly reduced PVG; higher OTR would always lead to shorter DPG regardless of the limiting factors; and when evaluated based on the cumulative N_2O yield, the increase of OTR would increase the N_2O yield when oxygen transfer is the limiting factor while reducing the yield when nitritation is the limiting factor. Thus, using a higher OTR (e.g., higher aeration rate, more efficient diffusers, etc. [205], while avoid inhibiting anammox activity) to make sure nitritation is the limiting factor (higher OTR than ODR for aerobic nitrogen oxidation), instead of merely creating high DO concentrations is recommended for the practical operation to mitigate N_2O generation. Otherwise, to maintain a low nitritation activity will benefit the reduction of N_2O generation.

4.3.3.2 Effect of initial ammonium concentration

In Batch 2, the initial NH_4^+-N concentration was reduced to a lower level of 20 mg N/L to investigate the N_2O generation under a lower concentration of ammonium. The dissolved N_2O concentration, N_2O generation rate, cumulative N_2O yield and N_2O yield factor were significantly lower than those in tests of Batch 1. With the K_La of 2.5 h^{-1}, 6.0 h^{-1}, and 41.3 h^{-1} (corresponding OTR of 17 mg O_2/L/h, 43 mg O_2/L/h, and 89 mg O_2/L/h, respectively), the addition of 20 mg N/L ammonium resulted in the peak dissolved N_2O concentrations of 0.004 mg N_2O /L, 0.022 mg N_2O /L, and 0.003 mg N_2O /L, respectively (Figure 4-15); the PVGs of 0.018 mg N_2O /L/h, 0.109 mg N_2O /L/h, and 0.011 mg N_2O /L/h, and the N_2O yield factor of 0.24%, 1.09%, and 0.16% (cumulative N_2O yields of 0.010 mg N_2O /L, 0.044 mg N_2O /L, and 0.007 mg N_2O /L, respectively, Figure 4-16, Table 4-2). The DPGs at K_La of 2.5 h^{-1} and 6.0 h^{-1} were 27 min and 45 min, respectively, which were remarkably lower than those in Batch 1, while the DPG at K_La of 41.3 h^{-1} was comparable with that in Batch 1 (Table 4-2). Ammonium was also consumed at constant rates of 5.0 mg N/L/h, 10.8 mg N/L/h, and 10.8 mg N/L/h

(Figure 4-17). The comparison of OTR and ODR showed that the oxygen transfer was the limiting factor at OTR of 17 mg O_2/L/h and 43 mg O_2/L/h while nitritation was the limiting factor at OTR of 89 mg O_2/L/h (Table 4-2). With the increase of OTR, the PVGs and cumulative N_2O yields showed similar trends with those in Batch 1, but with prominently lower values.

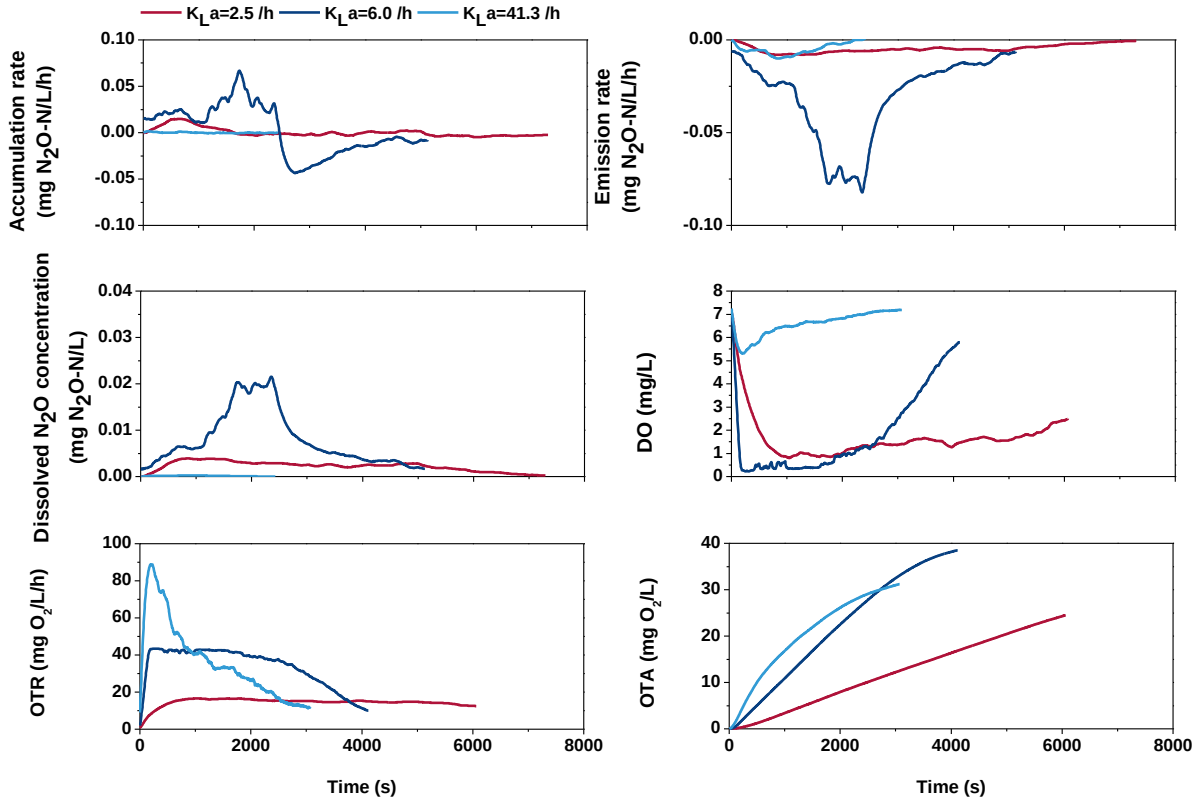

Figure 4-15. N_2O accumulation rates, N_2O emission rates, dissolved N_2O concentration, DO concentration, oxygen transfer rate (OTR), and oxygen transfer amount (OTA) at various K_La in Batch 2, in which the initial NH_4^+-N concentration was 20 mg N/L.

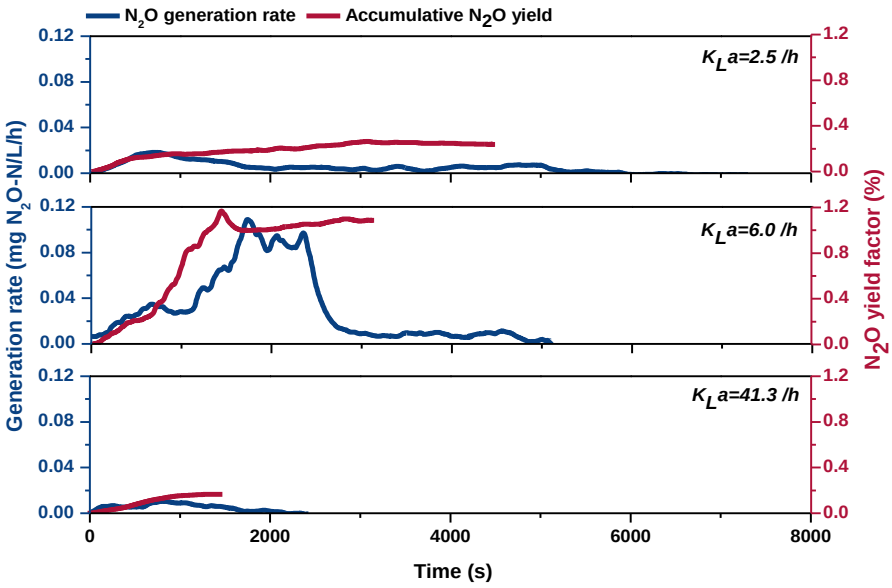

Figure 4-16. N_2O generation rates and cumulative N_2O yields of the batch tests with initial NH_4^+-N concentration of 20 mg N/L at various volumetric oxygen transfer coefficients. N_2O yield factor = cumulative N_2O yield ÷ nitrogen load×100%. The nitrogen load was 4 mg N/L in this case.

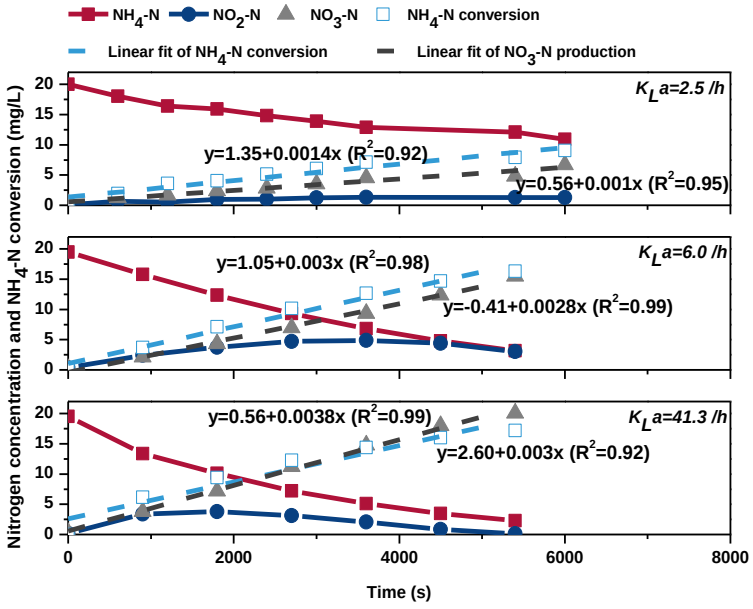

Figure 4-17. Profiles of the nitrogen concentration and nitrogen conversion of the batch tests with initial NH_4^+-N concentration of 20 mg N/L at various K_La. The nitritation activities and

aerobic nitrite oxidation rates were calculated from the slopes of the linear fit lines of the NH_4^+-N conversion and linear fit lines of the NO_3^--N production.

With the increasing OTR, the profiles of N_2O generation rate showed the same trends with those in Batch 1: the increase of OTR increased the N_2O generation when oxygen transfer was the limiting factor while reducing the generation when nitritation was the limiting factor. This also supports the conclusion that N_2O generation via nitritation would be regulated by ammonium oxidation (nitritation activity) and OTR rather than any single one of them. However, compared with the results of Batch 1, both the cumulative N_2O yield and N_2O yield factor decreased to a significantly lower level, mainly resulting from the reduced PVG. This suggests that the initial ammonium concentration would be another major factor affecting the N_2O generation and lower initial ammonium concentration leads to lower N_2O production. This agrees with the reported results that higher ammonium concentration increased N_2O emission via nitritation no matter in the PN-A reactor [204] or from the soil [206, 207]. The effect of ammonium concentration on N_2O generation was attributed to the resultant nitritation activity or the accumulation of nitrite (higher ammonium concentrations usually lead to higher nitrite concentrations) [196, 199, 208]. But in this study, the results clearly don't support the hypothesis of nitrite-accumulation oriented N_2O generation as the N_2O generation rate increased at lower nitrite concentrations while decreased at higher nitrite concentrations (Figure 4-16, Figure 4-17). On the other hand, both the PVGs and cumulative N_2O yields were significantly reduced with the decreased initial ammonium concentration from 30 mg NH_4^+-N/L to 20 mg NH_4^+-N/L while the nitritation activities remained unchanged (K_La of 2.5 h^{-1} and 6.0 v, respectively, Table 4-2). These results demonstrate that the production of N_2O is the result of initial ammonium concentration, nitritation activity, and OTR instead of a single one of them.

Based on the results of this study, practical strategies to mitigate the N_2O generation and emission are recommended:

1) High ammonium load to the reactor or fluctuating bulk ammonium concertation should be avoided. This can be achieved by applying strategies such as gradual feeding, step feeding,

Table 4-2. Key traits of the N_2O generation rate, nitrogen conversion rate, and oxygen transfer in Batch 1 and Batch 2.

Initial NH_4^+-N (mg/L)	Nitrogen conversion rate		N_2O generation			Oxygen transfer			
	AAO	ANO	PVG	DPG	CY	K_La	OTR	ODR	OTA
30	5.4	2.52	0.121	150	0.208	2.5	18	21	59
	10.8	5.76	0.414	91	0.374	6.0	44	44	67
	16.9	7.92	0.350	45	0.122	11.4	83	67	81
	25.2	10.8	0.386	23	0.077	41.3	114	99	76
20	5.0	3.6	0.018	27	0.0095	2.5	17	21	25
	10.8	10.1	0.109	45	0.044	6.0	43	49	39
	10.8	13.7	0.011	35	0.0066	41.3	89	53	31

Note: AAO: aerobic ammonium oxidation rate (nitritation rate), mg N/L/h; ANO: aerobic nitrite oxidation rate, mg N/L/h; K_La: volumetric oxygen transfer coefficient, h^{-1}; PVG: peak value of the N_2O generation rate, mg N_2O-N/L/h; DPG: duration of the peak N_2O generation rate, min; CY: cumulative yield, mg N_2O-N/L; OTR: peak value of oxygen transfer rate, mg O_2/L/h; ODR: theoretical oxygen demand rate for aerobic ammonium oxidation and nitrite oxidation, ODR=3.43×AAO+1.14×ANO, mg O_2/L/h; OTA: oxygen transfer amount, mg O_2/L.

conditioning tank/equalization tank, and sufficient mixing which has been reported to be effective in reducing N_2O emission via nitritation [89, 209, 210].

2) Applying higher OTR (e.g., higher aeration rate, more efficient diffusers, etc. [205]) to make sure OTR is higher than ODR, instead of merely creating high DO concentrations is recommended.

3) Because higher OTR, which may lead to inhibition on anammox or encourage the undesired NOB, is not applicable for PN-A process, maintaining low nitritation activity is recommended for the mitigation of N_2O production in PN-A systems.

4.4 Conclusions

In this study, the dominant N_2O production pathway in the PN-A IASBR was identified and the regulation of nitritation activity, OTR, and initial ammonium concentration in N_2O production during nitritation was investigated. Nitritation was found to be the dominant N_2O production pathway accounting for 69% of the total N_2O generation in PN-A IASBR. The presence of COD at a COD/N ratio of 1/3 led to the increase of the N_2O generation but only resulted in a slight N_2O emission increase because the presence of COD also improved the N_2O consumption during the settling phase when DO was almost 0. N_2O generation via nitritation would be the result of the electron-flow imbalance governed by nitritation activity and OTR: when oxygen transfer was the limiting factor, higher OTR led to higher nitritation activity (enhanced electron-flow imbalance) which remarkably increased the peak value of the N_2O generation rate (PVG); when nitritation was the limiting factor, the increase of OTR (reduced electron-flow imbalance) led to slightly reduced PVG; higher OTR always led to shorter duration of the peak N_2O generation rate (DPG). Lower initial ammonium concentration reduced the N_2O generation mainly by reducing the PVG.

Chapter 5
A novel system with precise oxygen input control: application of the partial nitritation-anammox process

5.1 Introduction

One-stage PN-A process relies on stable interactions between AOB and anammox bacteria as described in previous chapters as described with Equation 5-1. The activity of undesirable NOB, which compete with AOB for oxygen and anammox bacteria for NO_2^- [98], must be well suppressed. Oxygen is one of the most vital controlling parameters in PN-A process: it not only serves as a necessary electron acceptor for both AOB and undesirable NOB, but also acts as an inhibitor for anaerobic anammox bacteria. Thus, in practical application, the stability of PN-A systems relies on the reliable and accurate control of oxygen input; improper oxygen input control leads to the imbalance of microbial communities (overgrowth of NOB and inhibition of anammox bacteria) and deterioration of nitrogen removal performance (accumulation of NH_4^+, NO_2^- or NO_3^-).

$$NH_4^+ + 0.85O_2 \rightarrow 0.435N_2 + 0.13NO_3^- + 1.4H^+ + 1.3H_2O \qquad 5\text{-}1$$

However, reliable and accurate oxygen input control via conventional aeration methods remains as one of the main operational difficulties in the application of PN-A process into side-stream wastewater treatment [6], let alone the even more challenging mainstream wastewater treatment. The main reason for this is the delivery of oxygen to the biomass via conventional aeration (i.e., passing air through the liquid by means of aeration blowers and gas dispersion) is not always reliable and difficult to control; this largely results in a big gap between the oxygen demand and the actual oxygen input. The efforts to reduce this gap via conventional aeration methods rely on "feedback loop" control [211] based on monitoring the indicators such as the aeration flow rate, DO, oxidation reduction potential (ORP), nitrogen concentrations, and pH. This can be misleading as these parameters alone cannot directly reflect the actual oxygen input and may not always provide a good correlation with biomass activity or substrate depletion (for instance, DO concentration could still fall in the target control level when excessive oxygen is supplied beyond the requirement of AOB because of the oxygen consumption by NOB or other aerobic bacteria) [6, 108], thus a gap between the oxygen demand and the oxygen input always remains. On the other hand, the incapability of precise oxygen input control necessitates complex online

aeration control strategies including fixed-DO control, ammonia-based aeration control, and pH-based aeration control, etc. [71], and complex aeration control instruments such as online probes (probes measuring NH_4^+, NO_2^- and NO_3^- concentrations, DO probe, pH probe, and specific conductivity probe, etc.), distributed control systems (to receive signals and send commands) and modulating control valves [6, 21, 212, 213]. But still, according to a survey on full-scale PN-A application, aeration control remains as one of the main operational difficulties for the application of PN-A process in side-stream wastewater treatment: 30% of the surveyed plants have experienced NH_4^+ accumulation (oxygen input < oxygen demand) for several days to three weeks, and 50% of the surveyed plants have experienced NO_2^- and NO_3^- build-up (oxygen input > oxygen demand) generally lasting for up to several days for NO_2^- accumulation and several weeks for NO_3^- accumulation [6]. Thus, establishment of a more reliable, easily accessible, and precise oxygen input control method is required for the oxygen-sensitive PN-A process.

Therefore, in this study, a novel, yet extremely simple system with precise oxygen input control (a Simple Process for Autotrophic Nitrogen-removal, SPAN) was developed to treat ammonium-containing wastewater via PN-A process. In SPAN reactors, the oxygen transfer from air to the wastewater is realized through diffusion, which is enhanced through creating disturbance at the air-water interface by circulating/showering the wastewater instead of blowing air into the wastewater using air blowers and diffusers. The SPAN system consists of a cylindrical reactor, three pumps for filling, drawing, and wastewater circulation, and timers for controlling the pumps. In the SPAN reactor, biomass is located at the bottom to achieve efficient biomass retention. DO in the wastewater at the top of the reactor is delivered to the biomass at the bottom of the reactor via wastewater circulation. DO is consumed by AOB in the biomass to oxidize NH_4^+ to NO_2^- and the DO-depleted wastewater is circulated back to the top of the reactor thus creating an oxygen gradient difference to allow the natural diffusion of oxygen from the air into water. If necessary, the oxygen transfer rate can be enhanced through creating disturbance at the air-water interface by creating water spray on the water surface (like a shower). The oxygen input is precisely controlled to meet the oxygen demand for oxidizing about half of the NH_4^+ to NO_2^- by adjusting the water circulation rate/shower rate. The oxygen input at various circulation

rates/shower rates can be measured aforehand using clear water without biomass in an identical reactor. The oxygen demand is calculated according to Equation 5-1 based on the incoming NH_4^+-N. Therefore, the oxygen input is precisely controlled to accurately meet the demand by controlling the water circulation rate and the shower rate. The oxidized NO_2^-, together with the rest NH_4^+, is converted to N_2 by anammox bacteria in the biomass. Because the delivered oxygen is advantageously consumed by AOB over NOB so that the NOB overgrowth is suppressed, oxygen-inhibition on anammox is minimized, and the nitrogen removal is maximized.

In this study, two identical lab-scale SPAN reactors (R1 and R2) were set up and operated to verify the effectiveness of SPAN. The research aims were to investigate: 1) the empirical, quantitative correlation among oxygen input, the circulation rate, and shower rate so that oxygen input can be predicted accurately; 2) the long-term nitrogen removal performance at various oxygen inputs; 3) capacities of the key nitrogen-conversion pathways to monitor the evolution of the key nitrogen-converting guilds; and 4) the dynamics of the microbial communities in one of the reactors (R1) through metagenomic analysis.

5.2 Materials and methods

5.2.1 Design and operation of SPAN

In this study, two identical reactors previously operated using conventional aeration methods, R1 and R2, were set up as SPAN reactors and run parallelly to confirm the effectiveness of the novel SPAN technology (Figure 5-1). The SPAN system consisted of a cylindric reactor with a working volume of 2.6 L and height/diameter ratio of 11.5. Three peristaltic pumps were used, i.e., an influent pump, an effluent pump and a pump for circulating water and creating shower via a by-pass line if necessary (Figure 5-1 B); all pumps were controlled by programmable timers. The reactors were used to treat synthetic wastewater and were run as SBR. The SBR cyclic operation consisted of a fill phase of 5

min, a reaction phase of 340 min, a settling phase of 10 min and a draw phase of 5 min, giving four cycles per day. The temperature was maintained at 30 ℃ by placing the reactors in a light-blocked thermostatic cabinet. As shown in Table 5-1, the operation of the reactors was divided into three stages depending on the increasing nitrogen loading rate (NLR). In Stage 1, the nitrogen removal performance of SPAN reactors with precise oxygen input control to meet the oxygen demand was investigated. In Stage 2, the reactors were operated under various water circulation rates to examine the nitrogen removal performance with less or more oxygen input than oxygen demand. In Stage 3, the reactors were operated to examine the effectiveness of the SPAN technology with shower.

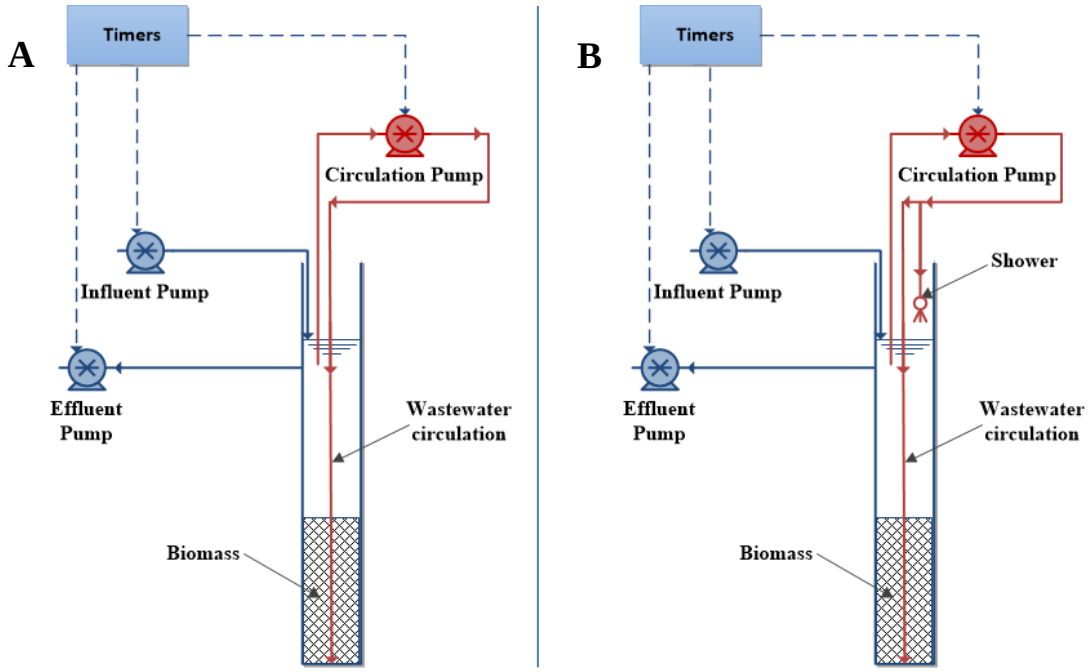

Figure 5-1. Simplified scheme of the SPAN system. A： SPAN system without shower; B: SPAN system with shower.

Table 5-1. The operating conditions of R1 and R2.

Day	1-82	83-358	359-431
Stages	1	2	3
Influent NH_4^+-N concentration (mg/L)	200	300	300
NLR (mg N/L/d) [a]	77	115	231
Circulation rate/shower rate (mL/min / mL/min)	70/0	70/0, 150/0, 300/0 [b]	200/88
Oxygen input (mg O_2/d)	314	314, 454, 858	1290

[a]: nitrogen loading rate.
[b]: day 83-158: 70/0; day 159-260: 150/0; day 261-358: 300/0.

5.2.2 Determination of oxygen input

Oxygen input (mg O_2/d) was calculated according to Equitation 5-2 [214].

$$\text{Oxygen input} = \int_0^t k_L a \times (C_s - C_t) \times V \times dt \quad \text{5-2}$$

where, k_La is the volumetric oxygen transfer coefficient (s^{-1}), C_s is the oxygen saturation concentration in wastewater, C_t is the DO concentration at time t, V is the volume of the reactor, and D is the duration (one day). C_t was measured and recorded using a portable meter (Multi3620, WTW, Germany) and a DO sensor (FDO925, WTW, Germany). At the bottom of the reactor where the biomass resided, C_t was constant at 0 (Figure 5-14), so C_t was set as 0 during the calculations. C_s was measured using saline water (the same salinity of 0.22% as that in the reactor) at 30 °C. k_La was determined using the dynamic method according to Equitation 5-3 and the integrated Equitation 5-4 [194].

$$\frac{\mathrm{dC}}{\mathrm{dt}} = k_L a \times (C_s - C_t) \quad \text{5-3}$$

$$\ln\left(\frac{C_s - C_t}{C_s - C_0}\right) = -k_L a \times t \quad \text{5-4}$$

where C is the DO concentration, and C_0 is the DO concentration at time 0.

k_La under various circulation rates and shower rates was determined in an identical reactor using saline water (0.22%, same with that in the reactors) with the absence of biomass. Firstly, DO in the saline water was removed by flushing dinitrogen gas, and then the saline water was circulated at the set circulation rate and shower rate. The DO concentrations during the tests were recorded and were used to calculate k_La. Because the temperature of the saline water was inevitably reduced to lower than 30 °C by the cold dinitrogen gas, k_La was determined at 20 °C and adjusted to at 30 °C as per Equitation 5-5 [215, 216].

$$K_L\mathrm{a}(T) = k_L a_{20}\theta^{T-20} \qquad 5\text{-}5$$

where $k_La(T)$ is k_La at temperature T, k_La_{20} is k_La at temperature 20 °C, and θ is the theta factor (1.008 was used in this study [216]).

5.2.3 Prediction of oxygen demand for nitrogen removal and calculation of oxygen consumption by nitrogen conversion

The oxygen demand (mg O_2/d) for nitrogen removal was calculated based on the stoichiometry of Equation 5-1, i.e., 1.94 mg O_2 needed to remove 1 mg NH_4^+-N. The oxygen consumption (mg O_2/d) by PN-A and by the production of NO_3^- -N via full nitrification were considered. The oxygen consumption (mg O_2/d) by PN-A was calculated based on Equation 5-1: the production of 1 mg N_2-N from NH_4^+-N requires 2.23 mg O_2. The calculation was made based on the TN removal instead of NH_4^+-N removal or NO_3^--N production because part of NH_4^+-N was converted to NO_3^--N via nitrification. The oxygen consumption (mg O_2/d) by full nitrification was calculated based on Equation 5-6: the production of 1 mg NO_3^--N requires 4.57 mg O_2 (NO_3^--N formation due to nitrification was calculated as the difference between the measured NO_3^--N and the NO_3^--N produced by PN-A which was calculated based on Equation 5-1).

$$NH_4^+ + 2O_2 \rightarrow NO_3^- + 2H^+ + H_2O \qquad 5\text{-}6$$

5.2.4 Synthetic wastewater and seeding sludge

Synthetic wastewater mimicking the ammonium-rich wastewater with high N/COD ratio was made from tap water according to Qiu et al [13] mainly containing 200 - 300 mg/L NH_4^+-N (ammonium chloride), 40 - 60 mg/L COD (glucose) with N/ COD ratio of 4, $NaHCO_3$ at the mole ratio of NH_4^+-N to HCO_3^- of 1.7, 58 mg/L $MgSO_4 \cdot 7H_2O$, 111 mg/L KH_2PO_4, 170 mg/L $CaCl_2 \cdot 6H_2O$ and trace elements. The two reactors were originally inoculated with one liter of suspended sludge collected from a full-scale PN-A reactor. On day 1, when the two reactors were operated as SPAN reactors, the sludge concentrations were 1340 ± 28 mg VSS /L in R1 and 1230 ± 14 mg VSS /L in R2 (the small difference was due to the previous operation using conventional aeration methods).

5.2.5 Analytical procedures

Prior to analysis, effluent water samples were filtered through syringe filters with pore size of 0.45 μm (Sarstedt Ltd, Germany). NH_4^+-N, NO_2^--N and NO_3^--N concentrations were measured using a nutrient analyzer (Konelab 20, Thermo Clinical Labsystems, USA). pH was determined with a portable meter (Multi3620, WTW, Germany). VSS and COD were measured according to the standard methods [157]. The salinity was determined using a salinity electrode and a portable meter (Extech DO700, FLIR Commercial Systems, USA). To evaluate the maximum nitrogen conversion potential of the main pathways, the nitrogen-conversion capacities of aerobic ammonium oxidation (AAO, mainly by AOB), aerobic nitrite oxidation (ANO, mainly by NOB), anaerobic ammoniu oxidation (anammox), and HD were tested in triplicate according to Qiu et al [13] (NOB activity tests were the same as those of AOB tests except that only NO_2^- instead of NH_4^+ was supplied).

5.2.6 Metagenomic high throughput sequencing

Five milliliters of biomass samples were collected on day 1, day 57, day 101, day 152, day 256, and day 320 for metagenomic analysis. The samples were stored at -80 ºC prior to

being sent to the commercial service provider (Sangon Biological Engineering Co., China) for DNA extraction and metagenomic sequencing. Genomic DNA extraction was conducted using rapid bacterial genomic DNA isolation Kit (Sangon Biological Engineering Co., China) as per the manufacturer's protocol. DNA concentration was determined using a Qubit Fluorometer (Qubit 2.0, Thermo, USA). DNA quality was checked using 2% agarose gel electrophoresis. Then, the extracted DNA samples were used for shotgun library construction and high-throughput sequencing on the Illumina HiSeq platform to produce 150 bp paired-end reads. The raw reads were quality filtered by trimming the adaptor sequences and ambiguous nucleotides, removing reads shorter than 35 bp, and excluding the sequences with the quality score lower than 20 using Trimmomatic (version 0.36). The cleaned sequences were assembled into contigs using IDBA_UD (version 1.1.2) with default parameters. Open reading frames (ORFs) were predicted from contigs using Prodigal (version 2.60). The predicted ORFs longer than 100 bp were translated into protein sequences. CD-HIT (version 4.6), Bowtie2 (version 2.1.0) and SAMtools (version 0.1.18) were used to remove the redundant sequences and determining gene abundance. Taxonomic annotation was done by searching the reads against NCBI Nr database with the E-value cut-off of 10^{-5}.

5.3 Results and discussion

5.3.1 Determination of the oxygen input

k_La values at various water circulation rates and shower rates were determined (Figure 5-2 and Table 5-2) and based on k_La values the oxygen input was calculated. Then, a non-linear surface regression analysis was conducted to investigate the empirical, quantitative correlation of the oxygen input to the circulation rate and shower rate. This was described by Equation 5-7 (R^2=0.96) and Figure 5-3. Based on the equation, the oxygen input was predicted at various water circulation rates and shower rates.

$$\text{Oxygen input, mg } O_2/\text{d} = -214.6 + 351.1e^{A} + 2.8e^{B} + 1555e^{A+B} \quad \text{5-7}$$

where $A = -e^{\frac{25.8-C}{42.8}}$, $B = -e^{\frac{-15.5-S}{123.3}}$, C is the circulation rate (mL/min), and S is the shower rate (mL/min).

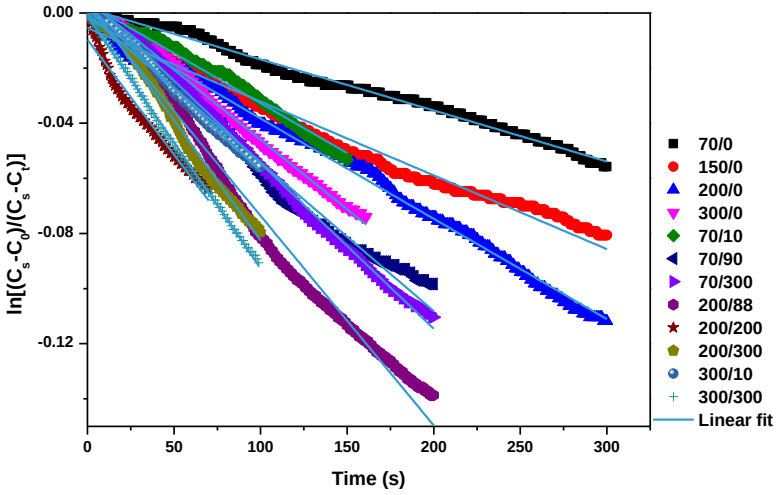

Figure 5-2. Determination of K_La under various scenarios (circulation rate/shower rate). The results were summarized in Table 5-2.

Table 5-2. Summary of the measured K_La values under various scenarios (circulation rate/shower rate).

Circulation rate/shower rate	Measured K_La ($\times 10^{-4}$)	K_La adjusted to 30 °C ($\times 10^{-4}$)	R^2
0/0	0		
0/50	0		
0/150	0		
0/300	0		
70/0	1.85	1.71	0.996
150/0	2.68	2.47	0.989
200/0	3.64	3.36	0.998
300/0	5.06	4.67	0.998
70/10	3.62	3.34	0.991
70/90	5.39	4.98	0.992
70/300	6.00	5.54	0.998
200/88	7.60	7.02	0.994
200/200	8.34	7.70	0.983
200/300	8.72	8.05	0.996
300/10	6.05	5.59	0.997
300/300	9.16	8.46	0.999

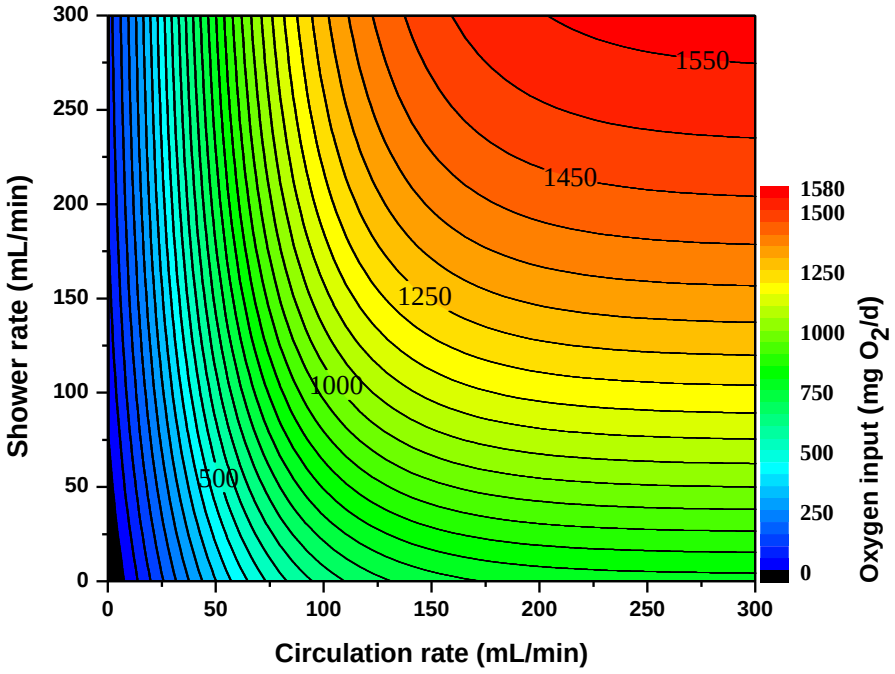

Figure 5-3. Heatmap showing the dependence of the oxygen input on the water circulation rate and shower rate.

Good agreement was observed between the predicted oxygen input and the measured oxygen input, except those at low circulation rates of 70 mL/min and 150 mL/min which may result from measurement errors (Figure 5-4). Equation 5-7 and Figure 5-3 indicate that the increased circulation rate will deliver more oxygen into the SPAN system, and the contribution of shower with water circulation can introduce much more oxygen than simply employing water circulation. For instance, 858 mg O_2/d was delivered at a circulation rate of 300 mL/min while 1290 mg O_2/d was achieved at a circulation rate of 200 mL/min and a shower rate of 88 mL/min (Figure 5-4). The introduction of shower improved the k_La value by creating more disturbance at the water-air interface and thus improved the oxygen transfer rate. Therefore, from the perspective of minimizing the amount of circulated wastewater, circulation-shower mode is a better choice than the circulation-only mode.

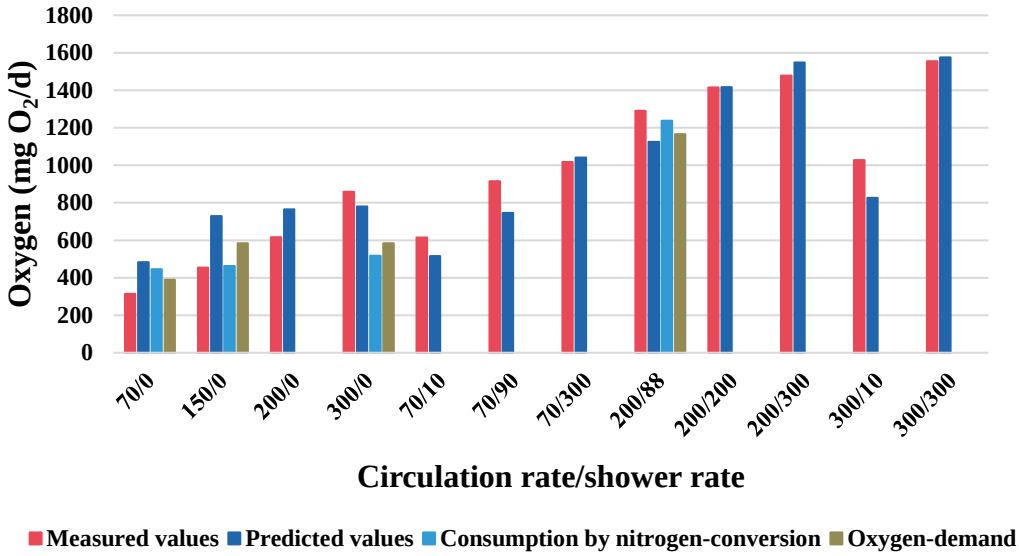

Figure 5-4. Comparison among the measured oxygen input, predicted oxygen input, oxygen consumption by nitrogen-conversion, and oxygen demand for nitrogen-removal. Circulation rate: mL/min. Shower rate: mL/min. Oxygen demand was calculated based on the nitrogen load, i.e., the oxygen required by PN-A to convert all the influent NH_4^+-N. Oxygen consumption was calculated based on the nitrogen conversion.

5.3.2 Performance of SPAN

5.3.2.1 Nitrogen-removal performance of R1 and R2

The nitrogen removal performance of the two SPAN reactors R1 and R2 ran in parallel is shown in Figure 5-5. In Stage 1 (day 1- day 82), the two reactors were operated at the water circulation rate of 70 mL/min (oxygen input of 314 mg O_2/d) and fed with 200 mg NH_4^+-N/L at the NLR of 77 mg N/L/d. At this NLR, the theoretical oxygen demand for PN-A to convert all the NH_4^+-N was 389 mg O_2/d (Figure 5-4). Around 86% and 82% of the NH_4^+-N was removed, leaving 28 mg NH_4^+-N /L and 37 mg NH_4^+-N /L in the effluent of R1 and R2, respectively. NO_2^--N concentrations in both reactors remained almost non-detectable of about 0.2 mg N/L. The average NO_3^--N concentrations in R1 and R2 were 55 mg N/L

and 44 mg N/L, respectively. The TN removal efficiencies gradually increased from about 55% to 68% in R1 and from 55% to 65% in R2.

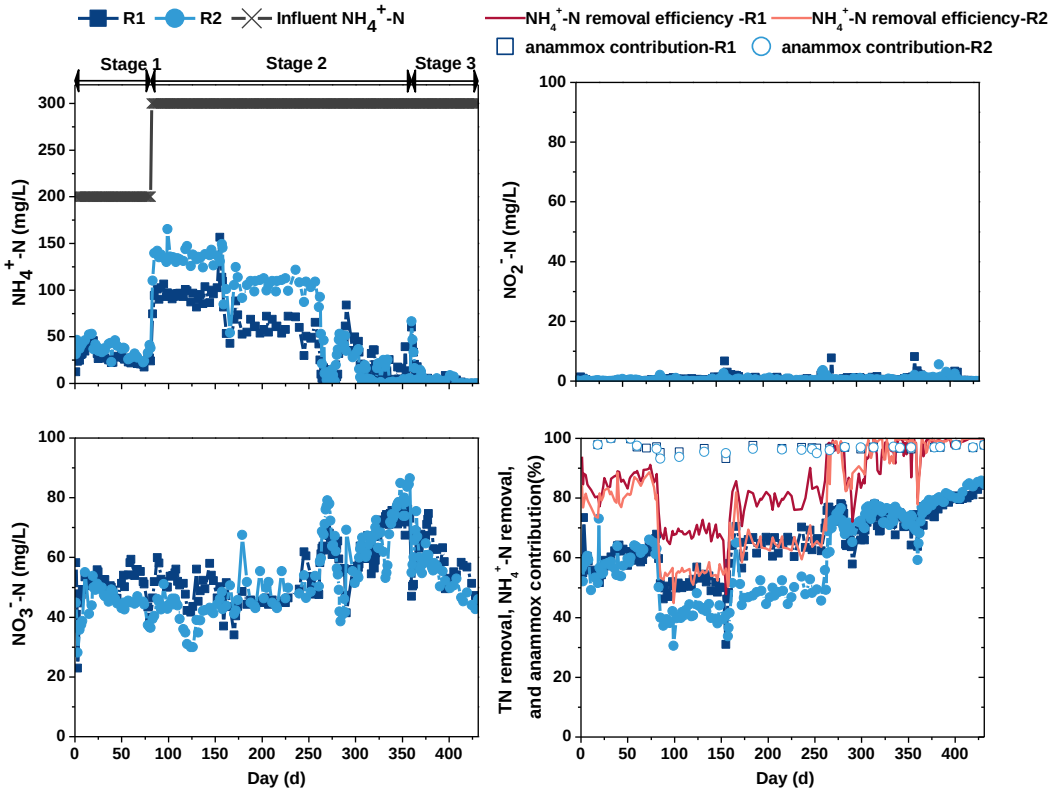

Figure 5-5. Nitrogen removal performances of R1 and R2. The contribution f anammox to TN removal was calculated based on the COD removal, stoichiometry 5.72 g COD/ g NO_3^--N, and the assumption that all the removed COD was used by heterotrophic denitrifiers for the removal of NO_3^--N.

The ratio of NO_3^--N-production/ NH_4^+-N-consumption indicates how well the NOB suppression is controlled: larger than the theoretical value of 0.13 (Equation 5-1) will indicate some of the NO_3^--N is produced by NOB; the larger the ratio is, the more NO_3^--N is produced by NOB. The ratios of the two reactors showed a gradual decline trend to 0.23 (Figure 5-6), indicating a well-controlled NOB-suppression. A small amount of the influent COD (40 mg/L) was removed, with around 23 mg/L and 25 mg/L left in the effluent of R1 and R2, respectively (Figure 5-7). pH in both reactors remained relatively stable at approximately 7.6 (Figure 5-7). The biomass in the two reactors was gradually enriched to

roughly 2000 mg VSS/L from the original level, suggesting the efficient biomass retention of SPAN system (Figure 5-8). During this stage, the initial anammox capacities (55 mg N/L/d and 110 mg N/L/d in R1 and R2) were far less than those of AAO (424 mg N/L/d and 314 mg N/L/d in R1 and R2) and ANO (292 mg N/L/d and 316 mg N/L/d in R1 and R2) (Figure 5-9). The differences in nitrogen conversion capacities between R1 and R2 were caused by previous operation before they were run as SPAN reactors. But still, stable nitrogen removal efficiency was achieved without NO_3^--N build-up. These results proved that regardless of the high NOB capacity, stable nitrogen removal performance was reliably achieved in the SPAN system by controlling the oxygen input to meet the oxygen demand.

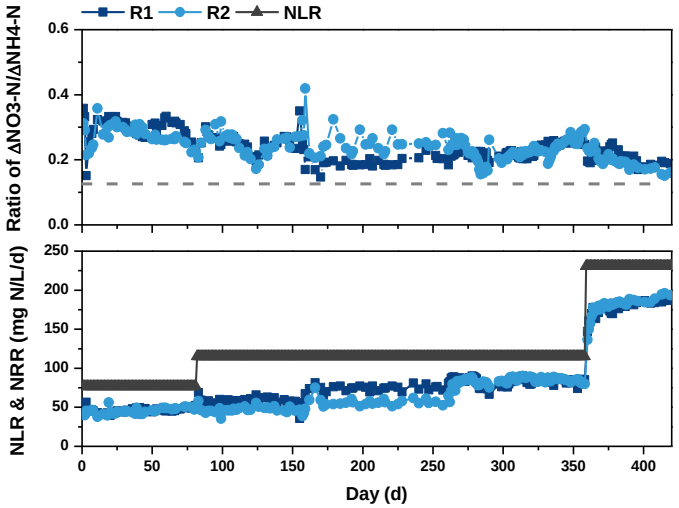

Figure 5-6. Ratio of nitrate produced/ammonium consumed, nitrogen loading rate (NLR) and nitrogen removal rate (NRR) of R1 and R2.

In Stage 2, the influent NH_4^+-N concentration was increased to 300 mg N/L (NLR of 115 mg N/L/d, the theoretical oxygen demand for PN-A to convert all the NH_4^+-N was 583 mg O_2/d). To examine the nitrogen removal performance of SPAN with less or more oxygen input than the oxygen demand, the reactors were operated under various circulation rates: 70 mL/min during day 83-158 (oxygen input 314 mg O_2/d); 150 mL/min during day 159-260 (oxygen input 454 mg O_2/d), and 300 mL/min during day 261-358 (oxygen input 858 mg O_2/d). It is worth pointing out that the water circulation of R1 and R2 was controlled

by one peristaltic pump with a multi-channel pump head. Therefore, there was always a discrepancy between the circulation rates of the two reactors which led to the differences in nitrogen-removal performance between R1 and R2. With a less oxygen input than the oxygen demand (day 83-158), the effluent NO_2^--N concentrations and NO_3^--N concentrations remained at the same level as those in Stage 1, while the effluent NH_4^+-N concentrations increased to 97 mg N/L and 136 mg N/L in R1 and R2, respectively, which led to the deterioration of NH_4^+-N removal efficiency to 68% and 55%, and TN removal efficiency to 50% and 41% in R1 and R2, respectively (Figure 5-5). During day 159-260, the water circulation rate was increased from 70 mL/min to 150 mL/min which enhanced the oxygen input to 454 mg O_2/d. The effluent NO_2^--N concentrations and NO_3^--N concentrations roughly remained unchanged at around 0.5 mg N/L and 47 mg N/L, respectively, but the effluent NH_4^+-N concentrations decreased to 60 mg N/L in R1 and 104 mg N/L in R2, which improved the TN removal efficiency to 64% and 49% (Figure 5-5). These results indicate that with a smaller oxygen input than the theoretical oxygen demand, stable nitrogen removal performance was maintained using SPAN, but the improvement of TN removal efficiency was restricted by the shortage of oxygen to oxidize NH_4^+. The circulation rate was further increased from 150 mL/min to 300 mL/min during day 260-358 so that the oxygen input of 858 mg O_2/d exceeded the oxygen demand of 583 mg O_2/d. With excessive of oxygen input, the effluent NH_4^+-N concentrations immediately reduced to mostly less than 10 mg N/L in the two reactors, achieving NH_4^+-N removal efficiency of more than 96% in R1 and 98% in R2 except during day 280-303 when the circulation rate was not well-controlled due to malfunction of the circulation pump (Figure 5-5). No NO_2^- accumulation was observed with NO_2^--N concentrations remaining stable at around 0.5 mg N/L. NO_3^--N concentrations in R1 increased and then leveled off at about 74 mg N/L (Figure 5-5), which resulted from the increased nitrogen removal by anammox and the enhanced NOB activity due to the excessive oxygen input. The NO_3^--N concentrations in R2 showed an increased trend to about 85 mg N/L at the end of the stage. The possible reason was that more oxygen was delivered into R2, leading to higher NH_4^+-N removal and enhanced NOB activity. Overall, stable TN removal efficiencies of about 75% in R1 and 73% in R2 were achieved even with excessive oxygen input. Around 65% of the influent 60 mg/L COD was consumed in the reactors with an average of 21 mg/L

left in the effluent in Stage 2 (Figure 5-7). Taken together, in SPAN reactors, stable nitrogen removal was achieved with less or more oxygen input than theoretical oxygen demand. When oxygen input was less than theoretical oxygen demand, the TN removal efficiency was low due to the shortage of oxygen to oxidize NH_4^+-N. When the oxygen input (858 mg O_2/d) was more than the theoretical oxygen demand (583 mg O_2/d), TN removal efficiency was immediately improved though NO_3^--N concentration increased to a higher but controllable level.

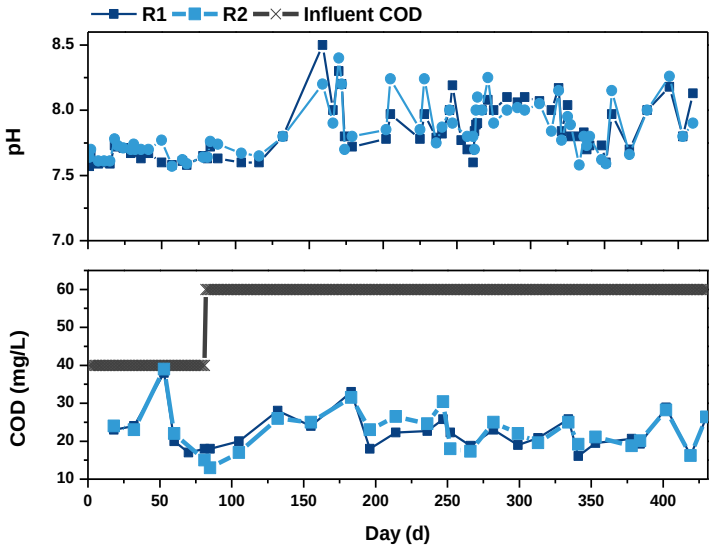

Figure 5-7. Effluent pH and effluent COD concentration of R1 and R2.

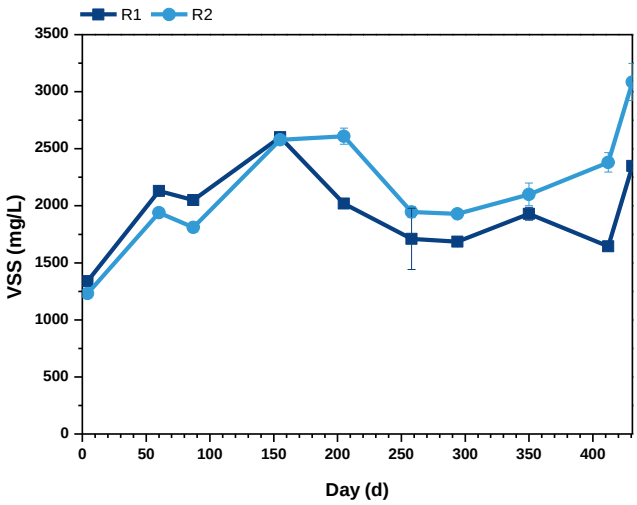

Figure 5-8. Biomass concentration of R1 and R2.

In Stage 3, the NLR was increased to 231 mg N/L/d (Figure 5-6) which meant theoretically 1166 mg O_2/d of oxygen was required for PN-A process to convert all the NH_4^+-N. A by-pass creating shower at the rate of 88 mL/min was introduced together with the water circulation rate of 200 mL/min to provide an oxygen input of 1290 mg O_2/d. The effluent NH_4^+-N gradually decreased to less than 1 mg N/L (more than 99% removal efficiency) and even non-detectable during the last 21 days (Figure 5-5). The effluent NO_2^--N concentrations first slightly increased to about 1 mg N/L and then decreased to 0 until the end of this stage. Impressively, effluent NO_3^--N concentrations significantly decreased in both reactors, from 74 mg N/L to average value of 55 mg N/L in R1 and from 84 mg N/L to average value of 49 mg N/L in R2. At the end of the stage, the effluent NO_3^--N concentration of R2 was even as low as around 45 mg N/L, which meant only 6 mg N/L was produced by NOB (39 mg NO_3^--N /L was produced by PN-A based on Equation 5-1) and the NOB activity was almost completely suppressed. This caused the NO_3^--N-production/ NH_4^+-N-consumption ratio to decrease to 0.18 and 0.15 in R1 and R2, respectively (Figure 5-6). As a result, high TN removal efficiency of 81% and 83% were achieved in R1 and R2, respectively (Figure 5-5). Stable TN removals of 82% and 85%, which were close to the theoretical level of 87%, were maintained in R1 and R2 at the end of this stage. With higher NLR, the biomass concentrations increased to 2350 mg VSS/L in R1 and 3085 mg VSS/L in R2 (Figure 5-8). pH values of the two reactors slightly fluctuated between 7.7 and 8.3 (Figure 5-7). COD removal remained at approximately the same level as that in Stage 2, and 63% was removed (Figure 5-7). According to the stoichiometry in ASM2 [123], the ratio of readily biodegradable organic meters (S_F) to nitrate plus nitrite nitrogen (S_{NO3-N}) was calculated based on yield coefficient (Y_H, 0.6g COD/g COD with oxygen as the electron acceptor, 0.5 g COD/g COD with nitrate or nitrite as the electron acceptor): $S_F/S_{NO3-N} = 2.86/(1-Y_H) = 2.86/(1-0.5)$=5.72 g COD/ g NO_3^- -N, which means 5.72 g COD is needed for the complete denitrification of NO_3^- -N. This value is close to other reported value of 7.6 g COD/g NO_3^- -N [119, 124]. Assuming that all the removed COD was used by heterotrophic denitrifiers for the removal of NO_3^- -N (which is not the case), anammox contributed more than 98%, 96%, and 97% to TN removed in Stage 1, Stage 2, and Stage 3 of both R1 and R2, respectively (Figure 5-5). Thus, it's

convincing to say that almost all the nitrogen-removal was conducted by anammox bacteria. Overall, with precise oxygen input control, NH_4^+-N was almost completely removed and high TN removal efficiency close to the theoretical value was stably achieved in the SPAN reactors. These results proved the extremely high efficiency and reliability of SPAN technology in removing nitrogen from ammonium-rich wastewater.

5.3.2.2 Nitrogen-conversion capacities of the key pathways

Ex situ activity tests were carried out to investigate the capacities of four key nitrogen-conversion pathways (Figure 5-9 for R1, and Figure 5-10 for R2), i.e., AAO (mainly by AOB), ANO (mainly by NOB), anammox, and heterotrophic denitrification. Figure 5-9 (A) and Figure 5-10 (A) evaluate the capacities on the basis of the unit biomass (mg N/ mg VSS/d) which indicates the dynamics of the key nitrogen-converting guilds. Figure 5-9 (B) and Figure 5-10 (B) evaluate the capacities on the basis of the unit volume of the reactor, which suggests the nitrogen-conversion potential. Similar nitrogen-conversion capacities of the four pathways were observed between R1 and R2. ANO capacities showed an initial rapid decrease in both of the reactors, then slightly decreased to 0.16 mg N/ mg VSS/d in R1 and slowly increased to 0.13 mg N/ mg VSS/d in R2. In both of the two reactors, the capacities of AAO first decreased and then gradually increased to the higher levels of 0.22 mg N/ mg VSS/d and 0.17 mg N/ mg VSS/d in R1 and R2, respectively. The AAO capacities gradually exceeded those of ANO in both of the two reactors, suggesting that in SPAN reactors, AOB were not restricted by the oxygen input control and were able to effectively over-compete NOB. These results prove that even with high NOB activity (comparable with AOB activity) in the reactor, stable and efficient nitrogen-removal was still achieved with the oxygen input control in SPAN. Heterotrophic denitrification capacities of the two reactors were much lower than those of other three pathways and slightly increased from 0.01 mg N/ mg VSS/d to about 0.03 mg N/ mg VSS/d in Stage 1 and Stage 2, then increased to 0.07 mg N/ mg VSS/d in Stage 3 due to a higher NLR. In Stage 1, due to the low NLR, the anammox capacities remained stable at 0.04 mg N/ mg VSS/d in R1 and slightly increased from 0.06 mg N/ mg VSS/d to 0.07 mg N/ mg VSS/d. Along with the stepwise increase of NLR to higher levels in Stage 2 and Stage 3, anammox

capacities rapidly exceeded those of all other three pathways and increased to the final levels of 0.35 mg N/ mg VSS/d in R1 and 0.3 mg N/ mg VSS/d in R2. The high anammox capacity together with the oxygen input control accounted for the extremely high nitrogen-removal performance in Stage 3. These results prove that in SPAN reactors, anammox activity was efficiently and rapidly enhanced to the highest one among the key nitrogen-conversion pathways especially with higher NLR; AOB activity was also improved and over-competed the activity of NOB which was effectively suppressed.

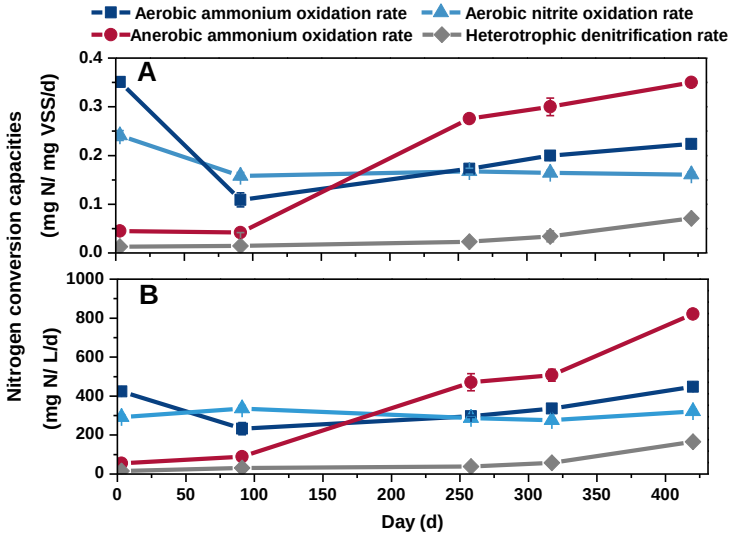

Figure 5-9. Capacities of the key nitrogen-conversion pathways in R1. A: the capacities on the basis of the unit biomass (mg N/ mg VSS/d); B: the capacities on the basis of the unit volume of the reactor (mg N/ mg VSS/L).

Based on the above results, it can be summarized that SPAN technology is outstanding in several ways. Firstly, the oxygen input can be precisely and reliably controlled to meet the oxygen demand by simply adjusting the water circulation rate and shower rate which cannot be guaranteed via conventional aeration methods. Currently, using the conventional aeration methods, the efforts mainly focus on the reduction of the gap between oxygen demand and the oxygen input which depends on the accuracy and robustness of the complexed online control methods and equipment mentioned above. Oxygen input control is among the most critical operational practice for the PN-A process because both too much

and too little oxygen supply lead to the accumulation of nitrogen species, deteriorated nitrogen removal performance and an imbalanced microbial community that needs up to several weeks to restore. Regardless of the installation of various online control systems, the accumulation of NH_4^+ (30% of the surveyed plants), NO_2^- (50% of the surveyed plants) and NO_3^- (50% of the surveyed plants) that for up to several weeks were reported in the full-scale PN-A plants employing conventional aeration methods, mostly due to the failure in oxygen supply control [6]. It is reported 56 days were needed to restore the PN-A reactor that suffered from the NOB overgrowth and NO_3^- accumulation [217]. These scenarios can be avoided with precise oxygen input control in SPAN reactors. Secondly, the reliable and precise oxygen input control can be realized simply by adjusting the wastewater circulation/shower rate without the complexed online control system used by conventional aeration control, and the pumps for water circulation are more easy to maintain and fix than blowers. Thirdly, the activities of the key microbial guilds can be effectively controlled in the way that is required, i.e., to enhance the anammox activity, maintain the AOB activity, and suppress the NOB activity. This is critical for the PN-A application which has not been always controllable using conventional aeration systems [6]. In fact, both the anammox bacteria retention and NOB suppression remain as the major challenges to achieve stable performance in PN-A [217]. Especially the NOB suppression that requires the implementation of control strategies such as above-mentioned aeration control, maintaining a high FA concentration and a certain concentration of residual ammonium, SRT control, and even re-inoculation (replace the sludge) [26, 94, 97, 98, 217, 218]. The NOB suppression was effectively achieved in SPAN simply with precise oxygen input control and the absence of SRT control, residual ammonium or high FA concentration (more than 99% of the NH_4^+-N was removed). Fourthly, high nitrogen removal efficiencies, both NH_4^+-N (>99%) and TN (>81%, up to 85%), can be maintained during long-term operation. These are close to the maximum theoretical removal efficiencies of PN-A process with negligiable contribution of heterotrophic denitrification. Even in Stage 1 when the anammox capacity (55 mg N/ L/d in R1) was far lower than those of AAO (424 mg N/ L/d) and ANO (292 mg N/ L/d), efficient nitrogen removal (>82% NH_4^+-N removal and > 65% TN removal) were achieved in both reactors. Finally, high oxygen utilization efficiency can be achieved in SPAN. Compared with low OTE of 4%-25% for the

conventional aeration methods [11, 12], more than 96% of the supplied oxygen was consumed for nitrogen removal except for 60% in the scenario with 300 mL/min circulation rate (Figure 5-4).

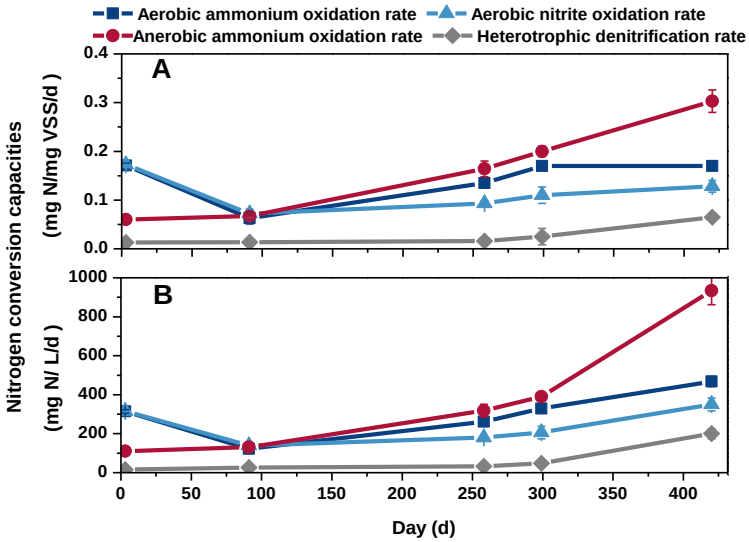

Figure 5-10. Capacities of the key-nitrogen converting pathways in R2. A: the capacities on the basis of the unit biomass (mg N/ mg VSS/d); B: the capacities on the basis of the unit volume of the reactor (mg N/ mg VSS/L).

5.3.3 Microbial community structure in the SPAN

Biomass samples were taken from R1 on day 1, day 57, day 101, day 152, day 256, and day 320 for metagenomic analysis and to gain further insights into the microbial communities in the SPAN reactor.

5.3.3.1 Community structure in the SPAN reactor

Fourteen major phyla were detected with the relative abundance of more than 1% (Figure 5-11). The relative abundance of the most abundant phylum *Proteobacteria*, which is a major phylum of gram-negative bacteria that AOB belong to [5, 164, 165], gradually increased from the initial 25.3% to 38.8%. The relative abundance of the second most abundant

phylum, *Planctomycetes*, also showed a gradually increasing trend from 6.0% to 16.7% except a decrease from 9.2% to 6.3% during day 57 - day 101. Currently, six reported anammox genera including *Candidatus Brocadia*, *Candidatus Anammoxoglobus*, *Candidatus Jettenia*, *Candidatus Kuenenia*, *Candidatus Scalindua*, and *Candidatus Anammoximicrobium*, are all affiliated with the phylum *Planctomycetes* [41]. The relative abundance of three phyla, *Chloroflexi*, *Firmicutes*, and *Verrucomicrobia*, declined from 7.9% to 6.2%, 6.0% to 2.0%, and 5.1% to 1.3%, respectively. The phylum *Nitrospirae* which includes the NOB genera *Nitrospira*, slightly varied between 1.0% and 1.4%. This agrees with the ANO capacities (Figure 5-9) and proves the well-controlled NOB-suppression with precise oxygen input control in SPAN. The relative abundance of other phyla generally remained stable, among which *Bacteroidetes*, *Chloroflexi*, *Actinobacteria*, *Acidobacteria*, and *Chlorobi* are among the frequently detected phyla in PN-A system [165, 167-169].

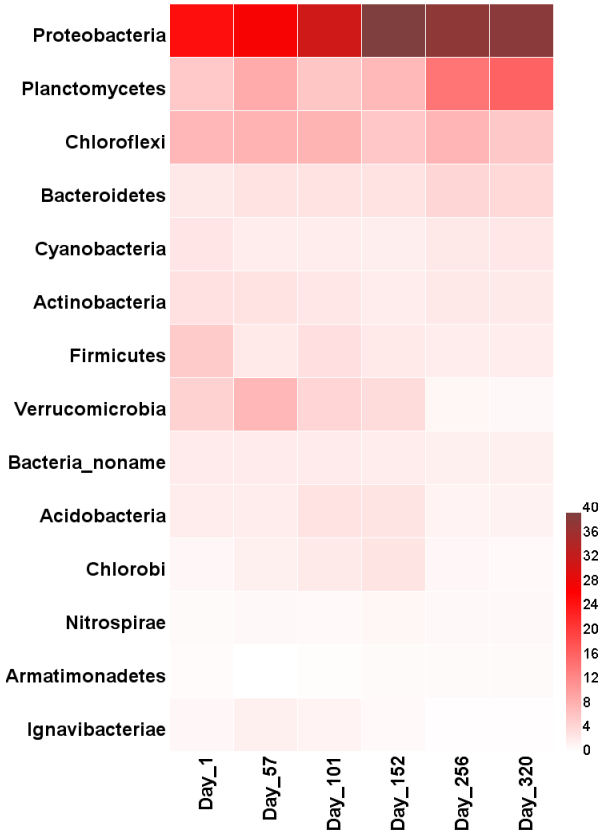

Figure 5-11. Abundance of the major phyla (>1%) in R1.

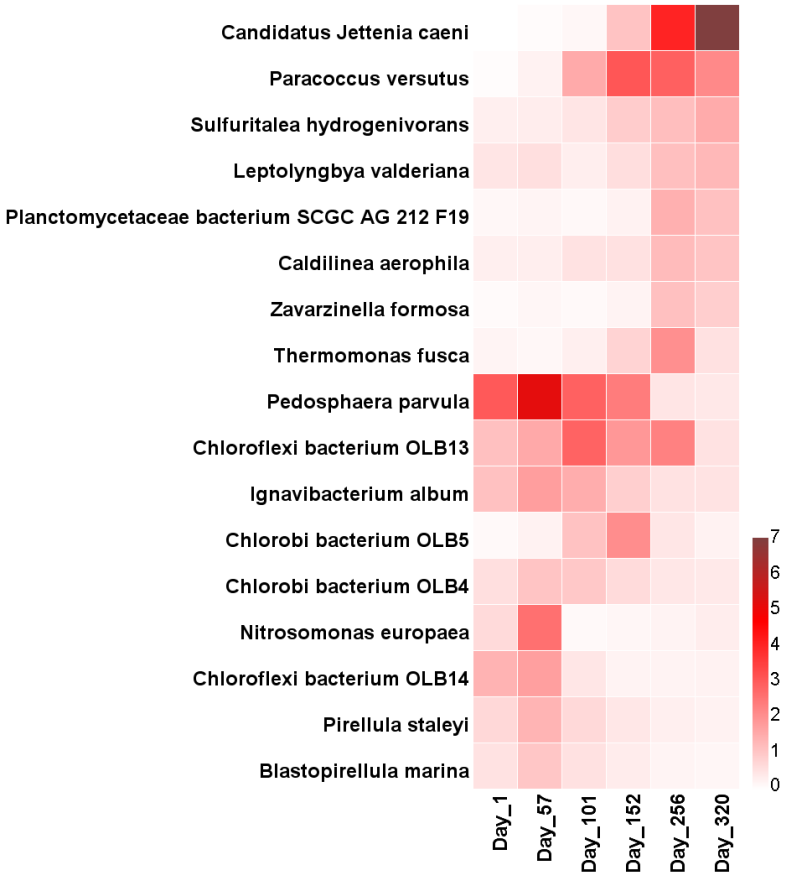

Figure 5-12. Major species (relative abundance >1% in any of the samples) in R1.

At the species level, 17 major species (>1%) were detected in R1 (Figure 5-12). *Candidatus Jettenia* caeni, one of the identified anammox species, gradually increased from 0.06% to the highest abundance of 7.1%. The relative abundance of *Nitrosomonas europaea*, one AOB species, remained 0.16% - 0.74% on day 57 when the relative abundance temporarily increased to 2.70% on day 57. Six species, *Paracoccus versutus*, *Sulfuritalea hydrogenivorans*, *Leptolyngbya valderiana*, *Planctomycetaceae bacterium* SCGC AG-212-F19, *Caldilinea aerophile*, and *Zavarzinella formosa* also displayed a rising trend to 1.0%-2.2%. Among them, *Paracoccus versutus* have the ability to convert NO_3^- into molecular nitrogen [219]. The relative abundance of *Pedosphaera parvula*, *Ignavibacterium album*, *Chlorobi bacterium* OLB4, and *Chloroflexi bacterium* OLB14 all displayed a peak value around day 57, then decreased and leveled off at the level of less than 1% on day 256

and day 320. The other species generally had the highest relative abundance in Stage 1 and gradually reduced to the lowest level on day 320.

5.3.3.2 Dynamics of nitrogen-converting species in the SPAN reactor

Five key nitrogen-converting microbial microorganisms were detected including anammox, AOB, NOB, comammox (complete nitrification by a single microorganism [220]), and AOA (Figure 5-13). Among these guilds, the total relative abundance of anammox bacteria had the most outstanding increase from 0.61% to the highest value of 8.17% and the increase happened mainly after day 101 (Figure 5-13, top-left part), which agrees with the results of the capacity tests (Figure 5-9). This proves that with precise oxygen input control and nearly zero DO in the sludge (Figure 5-14), the slow-growing anammox bacteria were effectively retained and enriched in SPAN reactor which is a big challenge for the reactors equipped with conventional aeration methods, partly due to inhibition caused by DO [4, 96]. Four anammox species were detected (Figure 5-13, bottom-left part) among which *Candidatus Jettenia* caeni was the dominant anammox species achieving the highest relative abundance of 7.13%, *Candidatus Kuenenia* stuttgartiensis remained between 0.22% and 0.48%, and *Candidatus Brocadia* sinica and *Candidatus Brocadia* fulgida increased from 0.12% to 0.61% and from 0.07% to 0.11%, respectively. The relative abundance of NOB, which ranked the second highest guild except in Stage 1 when AOB showed a higher relative abundance, generally remained stable and slightly increased from around 1.08% to 1.88% during day 1 - 152 and then gradually decreased to 1.43% on day 320. This agrees with the results of the ANO capacity and proves the well-controlled NOB-suppression in SPAN reactors. On the other hand, this also means that with precise oxygen input control, NOB were restricted to produce NO_3^--N (only 6 mg N/L was produced by NOB) regardless of their high abundance. For the reactors equipped with conventional aeration methods, the NO_3^--N production is usually suppressed by washing NOB out with strategies such as SRT control, etc. Five NOB species that are phylogenetically affiliated to two genera *Nitrospira* and *Nitrobacter* were detected (Figure 5-13, top-right part). The relative abundance of the most abundant species, *Nitrospira* sp. OLB3, remained between 0.29% and 0.72%. AOB first experienced an increase from

1.14% on day 1 to 3.65% on day 57 and then dramatically decreased to 0.42% which probably resulted from the inhibition of high NH_4^+-N concentrations in Stage 2. Thereafter, the AOB abundance gradually recovered to 0.79% on day 320. Though AOB had low relative abundance, they had high AAO capacities (Figure 5-9) to oxidize NH_4^+-N (indicated by NLR) which means AOB were also well controlled in SPAN reactors. The common *Nitrosomonas* europaea was the most dominant detected AOB species showing a similar trend with that of the total AOB and achieved a final relative abundance of 0.39% (Figure 5-13, bottom-right part). The relative abundance of the other two AOB species, *Nitrosomonas* eutropha, and *Nitrosomonas* communis, mostly remained below 0.1%.

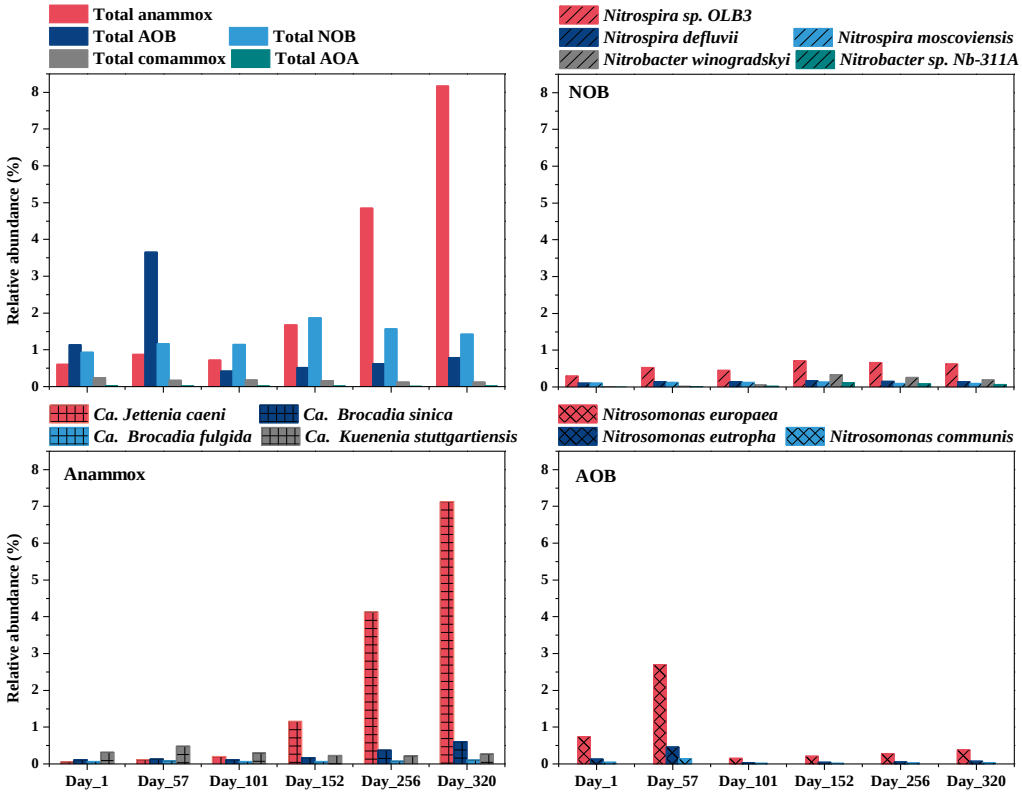

Figure 5-13. Relative abundance of the nitrogen-converting microbial guilds, i.e., anammox bacteria, AOB, NOB, comammox, and AOA. "Total" represents the sum relative abundance of the same functional group.

Three newly discovered comammox species were detected, i.e., *Candidatus Nitrospira* nitrosa, *Candidatus Nitrospira* nitrificans, *Candidatus Nitrospira* inopinata, and *Candidatus Nitrospira* inopinata [220, 221]. But they were less abundant (<0.1%) and the relative abundance of the total comammox gradually decreased from 0.24% to 0.13% suggesting that they were also well-managed along with the NOB. AOA were the least abundant ones among the five key nitrogen-converting guilds with the total relative abundance of around 0.02%. In conclusion, with the precise oxygen input control in SPAN reactor, anammox bacteria were efficiently enriched to the highest abundance than other microorganisms, AOB were well controlled to provided sufficient AAO capacity, and NOB were maintained stable and effectively restricted to produce NO_3^--N.

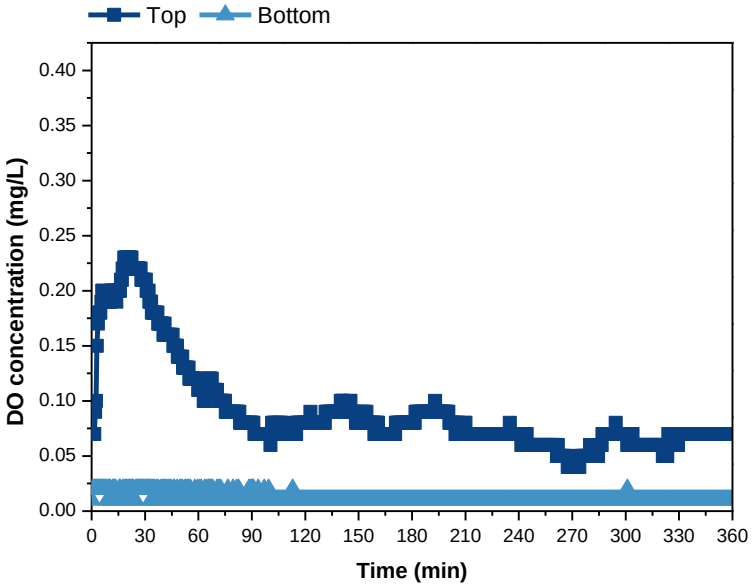

Figure 5-14. DO concentrations at the top and bottom of R1 in a typical cycle.

5.3.4 Outlook

The presented results prove the reliability and high efficiency of SPAN reactor and the effectiveness of precise oxygen input control in removing nitrogen form ammonium-rich wastewater. More than 99% NH_4^+-N and more than 81% TN (up to 85%), which were

closed to the maximum theoretical removal efficiencies, were stably removed during the long-term operation. Energy consumption of SPAN technology is one of the concerns. Besides the energy-input for feeding and withdrawing, the water circulation is the only source of energy consumption for the SPAN system. The maximum upflow velocity of 5.3 m/h in SPAN (at the maximum circulation rate of 300 mL/min) was comparable with those of 2.3 m/h in an upflow nitritation-anammox granular reactor (aeration is still needed) and > 4 m/h for expanded granular sludge bed [5, 222], which means energy-consumption is comparable with these reactor configurations. However, the oxygen is expected to be delivered into the reactor with less energy input with future study on the optimization of the reactor such as the height/diameter ratio and more efficient shower system, etc. NOB suppression which mainly depends on the proper oxygen input control is a prerequisite for the application of PN-A process in mainstream wastewater treatment, and future work is suggested to be conducted to examine the effectiveness of SPAN in the mainstream conditions.

5.4 Conclusions

This study demonstrated the reliability and high efficiency of SPAN and the effectiveness of precise oxygen input control in removing nitrogen from ammonium-rich wastewater. The quantitative correlation among the oxygen input, the water circulation rate, and shower rate was established. The circulation-shower mode was proven to be more efficient than the circulation mode in delivering oxygen. Nitrogen was removed with efficiencies that were closed to the maximum theoretical level: >99% NH_4^+-N removal and >81% TN removal (up to 85%) at high oxygen utilization efficiency of more than 96%. Anammox contributed more than 98%, 96%, and 97% of the TN removal in Stage 1, Stage 2, and Stage 3 of both R1 and R2, respectively. Anammox bacteria were efficiently enriched and were the most abundant microorganisms (8.17%) while AOB were well controlled to provide sufficient AAO capacity. NOB were maintained stable (1.08%-1.88%) and were effectively restricted to produce NO_3^--N

Chapter 6
Partial nitritation-anammox to treat mainstream wastewater with SPAN reactor

6.1 Introduction

The PN-A process has been applied to treat the side-stream wastewater such as reject water, which only accounts for 15%-20% of the TN loading to the municipal wastewater treatment plants [4-6]. PN-A process treating mainstream municipal wastewater has been conceptually proposed as a key component to achieve a more sustainable treatment of municipal wastewater [98], because it not only brings the advantages of PN-A process but allows the separation of the nitrogen removal and carbon removal, so that carbon (characterized as COD) can be recovered in the form of methane in a preceding anaerobic digestion step [6, 102]. It has been estimated that using mainstream PN-A process, 24 Watthours per person per day (Wh/p/d) can be produced compared to a consumption of 44 Wh/p/d for the conventional biological nitrogen removal process [28].

However, achieving long-term stable nitrogen removal remains as one of the major obstacles on the way of PN-A to practical mainstream applications. The PN-A process is oxygen-sensitive because a lower oxygen input than the oxygen demand will lead to ammonium accumulation, while a higher oxygen input will result in the overgrowth of NOB, deteriorated nitrogen-removal performance (accumulation of nitrate), and even collapse of the system. In mainstream conditions, PN-A process is even more vulnerable to disturbance caused by inappropriate oxygen input control because the low temperature (< 20 °C) and the low ammonium concentration (20 - 60 mg/L) [70] impact the tolerance of PN-A process by reducing the anammox activity and imposing less free ammonia inhibition on NOB [93, 101]. More importantly, AOB lose growth advantage over NOB when the temperature drops below 20 °C [101], making mainstream PN-A process liable to NOB overgrowth and nitrate build-up. But the conventional aeration methods, which deliver oxygen through aeration blowers and gas dispersion, have various drawbacks (Chapter 5), and are incapable of precisely and reliably controlling oxygen input to meet the oxygen demand, and thus, often fail to control nitrate build-up and achieve long-term stable nitrogen removal. For example, a PN-A system (SBR with granular sludge) crashed and the NRR decreased from about 150 mg N/L/d to 0 after 63 days of operation [83]. TN removal efficiency decreased from about 80% to 40% when the temperature decreased

from 24 °C to 20 °C and the biomass had to be replaced to recover the performance [5]. In a 2 m^3 integrated fixed-film activated sludge reactor, TN removal efficiency decreased from around 60% to less than 10% due to the aeration issue [10]. When the influent ammonium concentration was gradually decreased from 884 mg N /L to 31 mg N /L in an MBBR (25°C), nitrate began to build up, with nitrate production by NOB gradually rising to 90% of the oxidized ammonium, and nitrogen removal efficiency decreased to 35% [223]. The nitrogen removal efficiency decreased to an even lower level of 19%, and 71% of the oxidized ammonium was converted to nitrate when the continuous aeration was switched to intermittent aeration. In a granular PN-A reactor (temperature was decreased from 25°C to 15°C), the ratio of NO_3^--N production/NH_4^+-N consumption gradually increased to 0.95 and the nitrogen removal efficiency declined from about 54% to <10%, even though the NLR and airflow rate were reduced to deal with the nitrate build up [83]. Though there is one case in which long-term stability was achieved in MBBR and hybrid MBBR treating mainstream wastewater with COD/N of 3.3 (operation conditions: temperature was maintained at 15°C, residual ammonium was controlled at 2 mg NH_4^+-N/L, and DO was controlled at 0.15 and 0.18 mg O_2/L) [102], it can still be concluded that the long-term stability of mainstream PN-A is hard to be guaranteed. This is why the practical application of mainstream PN-A hasn't been realized so far.

Therefore, in this study, the novel SPAN described in Chapter 5 that is capable of precisely controlling oxygen input, was used to treat synthetic mainstream wastewater at temperatures of < 20°C. Oxygen input in mainstream conditions was measured at various water circulation rates. The long-term nitrogen removal performance at various NLR was examined using both suspended sludge and biofilm. Capacities of the key nitrogen-conversion pathways were tested to provide guidelines for the operation of the reactor.

6.2 Materials and methods

6.2.1 Experimental setup

One of the SPAN reactors in Chapter 5 was used to start up the mainstream SPAN process. The set-up of the system was the same as that in Chapter 5, i.e., a cylindric reactor with a working volume of 2.6 L and three peristaltic pumps (influent pump, effluent pump, and circulation pump) controlled by programmable timers. The reactor was also run as a SBR at four cycles per day. One operational cycle consisted of a feeding phase of 10 min, a reaction phase of 330 min, a settling phase of 10 min, and a draw phase of 10 min. Initially, the reactor was taken out of the thermal cabinet (30 °C), placed in a cold room (11 °C) and ran for 7 days. The sudden temperature reduction led to the failure in nitrogen removal. Thus, from day 8 onward, the reactor was taken out of the cold room and operated at ambient temperatures. The reactor was light-blocked to prevent algae growth.

Table 6-1. Operational conditions of the mainstream SPAN.

Day	1-161	172-241
Stages	1	2
Biomass configuration	Suspended sludge	Biofilm
NLR (mg N/L/d) [a]	38.5-76.9 [b]	87.0
HRT (day)	1.3-0.65 [c]	0.57
Circulation rate (mL/min)	10-100 [d]	67

[a]: nitrogen loading rate.
[b]: day 1-43: 38.5; day 44-92: 76.9; day 93-161: 57.7.
[c]: day 1-43: 1.3; day 44-92: 0.65; day 93-161: 0.87.
[d]: day 1-43: 10; day 44-76: 67; day 77-92: 100; day 93-161: 19

The operation of the reactor consisted of two stages depending on the biomass form (Table 6-1). In Stage 1, the biomass in the reactor was suspended-growth sludge and the NLR was increased from 38.5 mg N/L/d to 76.9 mg N/L during day 1 to day 92 by shortening the hydraulic retention time (HRT) from 1.3 days to 0.65 days. The NLR was then decreased to 57.7 mg N/L/d (HRT 0.87 days) during day 93 to day 161 in response to the sludge loss caused by the nitrogen gas bubbles. In Stage 2, 450 K1 biofilm carriers with protected surface area of 500 m^2/m^3 (Anoxkaldes, Sweden) were fixed to strings and added into the

reactor at a filling ratio of 12%, which led to the reduction of the effective working volume to 2.3 L. 1 L of the sludge from another SPAN reactor in Chapter 5 was inoculated into the reactor to recover the system. During day 162 and day 171, measures were taken to culture the biofilm: water was circulated from bottom to the top of the reactor to allow sufficient contact between the sludge and biofilm carriers; the wastewater in the reactor was replaced daily with fresh synthetic wastewater (300 mg N/L), and the reactor was drained and refilled at a frequency of 1 h to provide the hydraulic shear force for biofilm culturing. From day 172 onward, the reactor was run in the same conditions with those in Stage 1 (same synthetic wastewater and sequencing operation) and the NLR was increased to 87.0 mg N/L (HRT 0.58 days).

6.2.2 Synthetic wastewater

Synthetic wastewater was made from tap water and mainly contained 50 mg/L NH_4^+-N (NH_4Cl), 25 mg/L COD (sodium acetate) with COD/N ratio of 0.5, 1.2 g/L $NaHCO_3$, 29 mg/L $MgSO_4 \cdot 7H_2O$, 10 mg PO_4-P/L (KH_2PO_4), and 85 mg/L $CaCl_2 \cdot 6H_2O$, adapted from the literature [107, 114]. Trace element solutions were made according to Qiu et al. [13] and were added at the dosage of 1 mL/L.

6.2.3 Nitrogen-conversion capacities

In Stage 1, the nitrogen-conversion capacities of the main pathways, the nitrogen-conversion capacities of aerobic ammonium oxidation (AAO, mainly by AOB), aerobic nitrite oxidation (ANO, mainly by NOB), anaerobic ammonium oxidation (anammox), and heterotrophic denitrification were tested using the methods described in Chapter 3 except at ambient temperatures. In stage 2, the biofilm didn't grow evenly on biofilm carriers and some biofilm grew on the wall of the reactor, which meant ex-situ capacity measurement using certain numbers of biofilm carriers wouldn't be representative, so the nitrogen-conversion capacities were measured in situ in the reactor. Synthetic wastewater used for the test was made in the same way with that in section 6.2.2, except that the concentrations

of NH_4^+-N, NO_2^--N, NO_3^--N, and COD varied depending on the targeted nitrogen-conversion pathways. Water samples were taken every 30 min during the 2 h test, and the calculation of the nitrogen-conversion capacities was the same as those in Chapter 3 and Chapter 5. The AAO and ANO capacities were measured simultaneously using synthetic wastewater containing 40 mg NH_4-N/L and 20 NO_2-N/L. The water circulation rate and shower rate during the tests were 300 mL/min and 150 mL/min, respectively to provide sufficient oxygen. For the anammox capacity test, after removing DO, synthetic wastewater containing 40 mg NH_4-N/L and 53 NO_2-N/L was fed to the drained reactor. The reactor was circulated at 100 mL/min to allow sufficient substrates diffusion. The headspace of the reactor was continuously flushed with N_2 gas to prevent the air from entering the reactor. For the heterotrophic denitrification capacity test, NO_3^- and COD (sodium acetate) were added at the dosage of 40 mg NO_3^--N/L and 400 mg COD/L, respectively, at the end of the anammox activity test. The heterotrophic denitrification capacity was calculated as the difference between the TN removal rate and the anammox capacity calculated based on Equation 6-1 [8], as shown in Equation 6-2 (HD is the acronym of heterotrophic denitrification).

$$NH_4^+ + 1.32NO_2^- + 0.066HCO_3^- + 0.13H^+ \rightarrow 1.02N_2 + 0.26NO_3^- + 2.03H_2O + 0.066CH_2O_2N_{0.15} \quad 6\text{-}1$$

$$HD\ capacity, mg\ N/L/d = TN\ removal\ rate - 2.04 \times ammonium\ nitrogen\ removal\ rate \quad 6\text{-}2$$

6.2.4 Analytical procedures

The determination of NH_4^+-N, NO_2^--N, NO_3^--N, volatile suspended solids (VSS), COD, DO and salinity was carried out using the same methods with those in Chapter 5. The room temperature was measured with a temperature sensor (HOBO Temperature External Channel Data Logger, Onset Computer Corporation, USA) and recorded using HOBO (version 2.7.3, Onset Computer Corporation, USA). Oxygen inputs at various water circulation rates were measured using the same method as described in Chapter 5 except

the salinity which was controlled at 0.083% (same salinity with that in the reactor). The measured oxygen saturation concentration was 9.15 mg/L.

6.3 Results and discussion

6.3.1 Determination of oxygen input

k_La values at various water circulation rates were determined as shown in Figure 6-1. The calculated oxygen input and the oxygen demand calculated based on the nitrogen loading, are summarized in Table 6-2. The oxygen input was enhanced with a higher circulation rate. Combining shower, even at a small rate, with circulation significantly enhanced the oxygen input (Table 6-2), but for the purpose of easy control, no shower was used in this study.

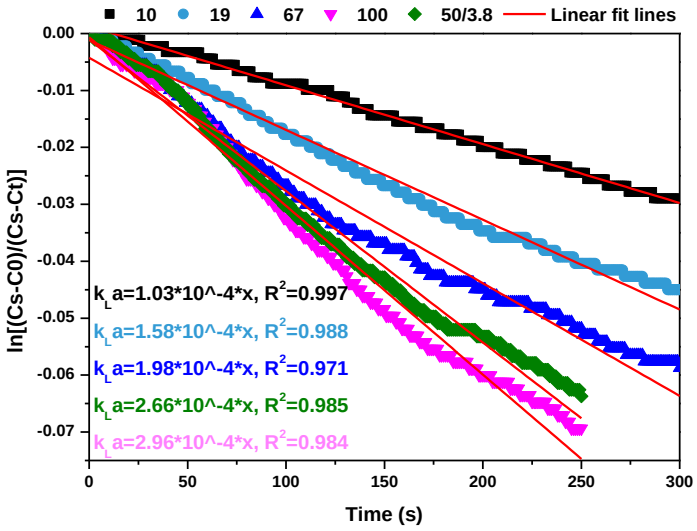

Figure 6-1. Determination of k_La under various water circulation rates (calculated from the slope of the linear fit lines). 50/3.8 indicates the water circulation rates of 50 mL/min and shower rate of 3.8 mL/min. The results are summarized in Table 6-2.

Table 6-2. Summary of the k_La values and the oxygen input under various circulation rates, and the oxygen demand at various nitrogen loading.

Circulation rate (mL/min)	Nitrogen loading (mg N/d)	Effective volume of the reactor (L)	Measured k_La ($\times 10^{-4}$)	Oxygen input (mg O_2/d)	Oxygen demand (mg O_2/d)
10	100	2.6	1.03	212	194
19	150	2.6	1.58	324	291
67	200	2.6	1.98	407	389
67	200	2.3	1.98	360	389
100	-	2.6	2.96	608	-
50/3.8 [a]	-	2.6	2.66	547	-

[a]: circulation rate/shower rate.

6.3.2 Stage 1: application of suspended-growth biomass

In Stage 1 during day 1 - 43, the NLR was set at 38.5 mg N/L/d (oxygen demand was equal to 194 mg O_2/d) and the water circulation rate was set at 10 mL/min (oxygen input was equal to 212 mg O_2/d). In the first 7 days, the reactor was operated at 11 °C to investigate the nitrogen removal performance at low temperature. The sudden temperature decrease from 30 °C to 11 °C led to NO_3^--N accumulation and low TN removal of 3% (Figure 6-3). From day 8, the reactor was run at ambient temperatures with the daily average temperature of 19.8 ± 0.9 °C (Figure 6-2). During day 8 to day 43, the effluent NH_4^+-N was 6.2 ± 3.3 mg N /L (Figure 6-3) achieving NH_4^+-N removal efficiency of 87.6 ± 6.7% (Figure 6-3). The effluent NO_2^--N and NO_3^--N concentrations were 1.0 ± 0.8 mg N /L and 15.0 ± 4.2 mg N /L (Figure 6-3), respectively. The ratio of NO_3^--N production/NH_4^+-N consumption was around 0.3 (Figure 6-4) which was higher than the theoretical value of 0.13 (Equation 6-3) but comparable with the reported value of 0.28 at a higher operating temperature of 25°C [83]. pH value showed a slight increase from 7.4 to around 7.7 (Figure 6-4). During this period, 55.6 ± 12 % TN removal was achieved (Figure 6-3). 22.9 ± 4.1% of COD (5.7 mg/L) was removed in this period (Figure 6-4), indicating less than 1 mg N/L was removed by heterotrophic denitrification based on the value of 5.72 g COD/ g NO_3^--N for complete denitrification [123, 124], provided all the removed COD was used by heterotrophic denitrifiers which was not the case. This proved that nearly all the nitrogen

was removed by anammox bacteria. The biomass concentration rose from 1450 mg VSS/L to 2115 mg VSS/L (Figure 6-5).

$$NH_4^+ + 0.85O_2 \rightarrow 0.435N_2 + 0.13NO_3^- + 1.4H^+ + 1.3H_2O \quad 6\text{-}3$$

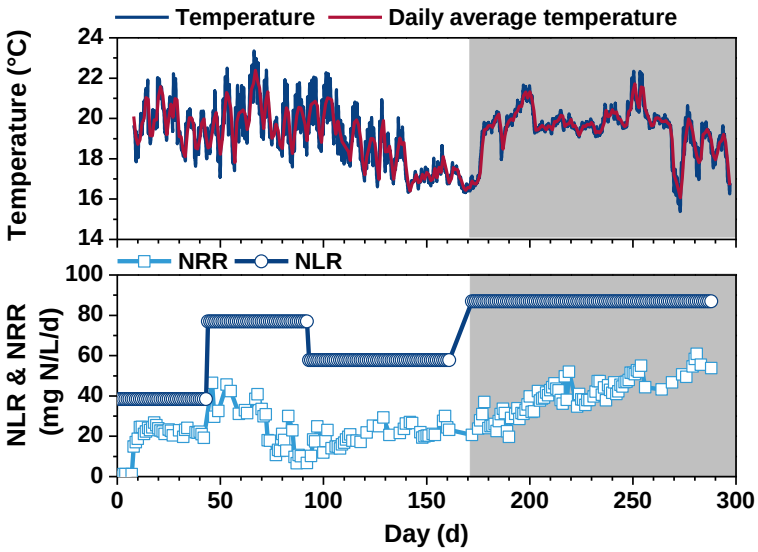

Figure 6-2. Room temperature, nitrogen loading rate (NLR), and nitrogen removal rate (NRR). The white area indicates Stage 1 and the shaded area indicates Stage 2.

The anammox capacities decreased from 155.4 mg N /L/d (day 1) to 109.7 mg N /L/d (day 27) (Figure 6-6). This mainly resulted from the decrease of temperature from 30 °C to 11 °C (for 7 days) and then 19.8 °C without any acclimation of the biomass. The results agree with the reported approximately 53% reduction of the in-situ anammox activity with the temperature decreasing from 28 °C to 18 °C during long-term operation [224]. Anammox bacteria are sensitive to temperature reduction, which could lead to 61% activity reduction with sudden temperature decrease from 30 °C to 20 °C [225] and about ten times decrease when the temperature drops from 30 °C to 10 °C [26]. AAO capacities were stable at 160 mg N /L/d during this period. However, the ANO capacities increased from 125 mg N /L/d to 176 mg N /L/d, which were higher than the AAO capacity. The possible reason was that the 7 days operation at 11 °C led to the dominance of NOB over AOB and other microorganisms. NOB have a similar growth rate (0.788 d^{-1}) with AOB (0.801 d^{-1}) at 20

°C, but with the further decrease of temperature, NOB have higher growth rate than AOB, for example, 0.642 d^{-1} of NOB over 0.523 d^{-1} of AOB at 15 °C, and the lower the temperature is, the more growth advantages NOB have [101]. This was also indicated by the fact that almost all the oxidized ammonium was converted to nitrate by NOB during the initial 7 days. Then since day 8, AOB and NOB had higher growth rates at 19.8 °C than at 11 °C but similar growth rates to each other. This allowed NOB to thrive on a dominant basis established previously and the increase of ANO capacity to a higher level than AAO. In spite of the low-temperature disturbance during the first 7 days, stable NRR of 21.4 ± 4.6 mg N /L/d was achieved (Figure 6-2). More importantly, the nitrogen removal performance was stably maintained at 19.8 °C. This shows that SPAN reactor can maintain the stability of PN-A for mainstream wastewater treatment, which is difficult to achieve using conventional aeration methods. With almost negligible contribution of heterotrophic denitrification, the TN removal efficiency of 55.6 ± 12 % in this study (19.8 ± 0.9 °C) was higher than the reported values of 28.9% (about 27 °C) [111], 30.8% (30 °C, C/N 1.1) [103], and 47% (25 °C, C/N 0.5) [112], and comparable to 66% (around 22 °C) [111] and 77.3% (30 °C, C/N 2.0) [103] reported by other studies while the NRR was comparable to a reported 26 mg N /L/d [102]. In conclusion, stable and efficient nitrogen removal was achieved in the SPAN reactor.

During day 44 to day 92, the NLR was increased to 76.9 mg N /L/d (oxygen demand of 389 mg O_2/d, HRT of 15.6 hours) and the water circulation rate was set at 67 mL/min (oxygen input 407 mg O_2/d) and 100 mL/min (oxygen input 608 mg O_2/d, during day 77-92). The temperature remained at the same level of 19.9 ± 1.0 °C (Figure 6-2). pH and COD removal efficiency remained stable at 7.8 ± 0.1 and 36.8 ± 3.7%, respectively (Figure 6-4). Effluent NO_2^--N and NO_3^--N also slightly rose from 1.7 ± 1.2 mg N /L to 2.3 ± 1.8 mg N /L and from 10.3 ± 2.7 mg N /L to 11.8± 1.8 mg N /L, respectively. Effluent NH_4^+-N rose from 12.4 ± 6.0 mg N /L to about 29 mg N /L, leading to the decrease of NH_4^+-N removal efficiency from 75.2 ± 12.5% to 42%. Further increasing the circulation rate to 100 mL/min (day 77-92) didn't improve the nitrogen removal performance, but led to the increase of the ratio of NO_3^--N production/ NH_4^+-N consumption from 0.27 ± 0.03 to 0.44 ± 0.11, even as high as 0.77 (Figure 6-4). TN removal efficiency also reduced from 51.2 ±

10.1 %, which was maintained for 14 days, to around 11% till day 92 (Figure 6-3). The cause of the poor performance was sludge loss, from 2115 mg VSS/L to 1115 mg VSS/L (Figure 6-5); the high NLR caused a higher volume exchange and higher production of fine N_2 bubbles which floated the sludge out of the reactor. The biomass loss resulted in a sharp decrease of the anammox capacity from 109.7 mg N/L/d to 43.1 mg N/L/d because anammox bacteria have low growth rates of 0.0011/d at 20 °C [46] and could not be enriched to the original level in a short period. AAO capacity and heterotrophic denitrification capacity were not affected by the biomass loss and increased from 160.1 mg N/L/d to 183.7 mg N/L/d and from 24.8 mg N/L/d to 30.7 mg N/L/d, respectively. The reason was that: the corresponding microorganisms (AOB and heterotrophs) have a higher growth rate (0.801/d for AOB at 20 °C) than anammox bacteria. NOB have similar growth rates (0.788/d, 20 °C) with those of AOB [101], but the ANO capacity decreased from 176.2 mg N/L/d to 140.4 mg N/L/d indicating that with precise oxygen input control, the proliferation of NOB was efficiently suppressed. Taken together, efficient nitrogen removal was achieved at higher NLR but couldn't be maintained for a long time due to the reduction of anammox capacities caused by biomass loss.

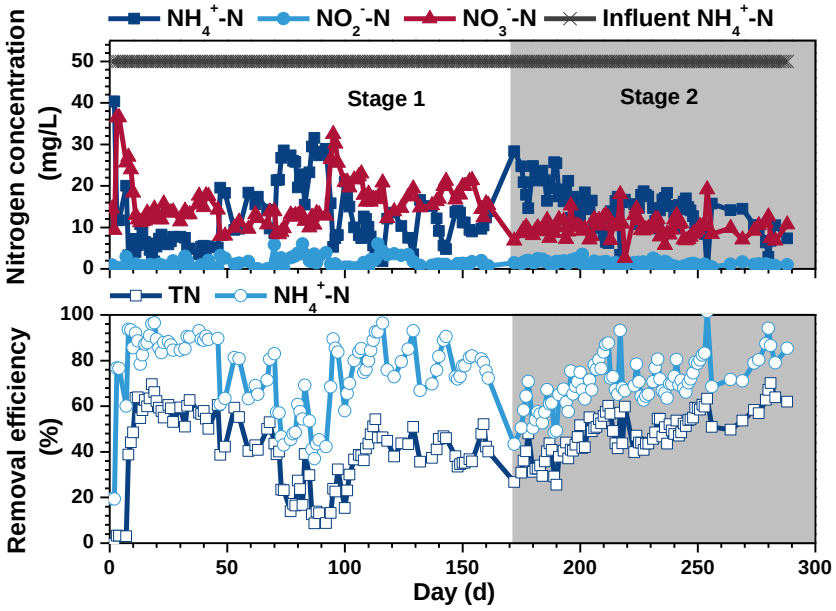

Figure 6-3. Nitrogen removal performances of the reactor.

Therefore, during day 93 to day 161, to reduce the biomass loss the NLR was decreased to 57.7 mg N /L/d (oxygen demand of 291 mg O_2/d, HRT of 15.6 hours) and the water circulation rate was set at 19 mL/min (oxygen input 324 mg O_2/d). Temperatures were 19.1 ± 1.1 °C during day 93 to day 140 and then were 17.1 ± 0.4 °C thereafter (Figure 6-2). With lower NLR, the biomass concentration was maintained stable at 1115 mg VSS/L (Figure 6-5). pH remained stable at 7.7 ± 0.1 (Figure 6-4). COD was removed at a slightly higher efficiency of 42.1 ± 5.7% than in the previous period leaving 14.5 ± 1.4 mg/L in the effluent (Figure 6-4). 79.5 ± 8.5% of NH_4^+-N was removed and 10.3 ± 4.3 mg NH_4^+-N /L remained in the effluent (Figure 6-3). Effluent NO_2^--N was low at 1.5 ± 1.3 mg N /L. NO_3^--N initially increased to a high level of around 30 mg N /L due to the excessive oxygen input during day 77 - 92 and then gradually reduced to about 15 mg N /L. The ratio of NO_3^--N production/ NH_4^+-N consumption decreased from the initial value of 0.7 to about 0.4 indicating the NOB activity in the reactor was gradually suppressed. NRR of 20.5 ± 4.3 mg N /L/d was comparable with that during day 1 to day 43 and the reported 26 mg N /L/d [102]. Though temperatures were at a lower level of 17.1 ± 0.4 °C after day 140, TN removal efficiency was stable at 38.6 ± 9.4% (Figure 6-3) which was lower than that during day 1 to day 43 but was still higher than the reported 28.9%-30.8% at higher temperatures of 25 °C - 30 °C [103, 111].

The main reason for the lower TN removal efficiency was the low anammox capacity which decreased from 43.1 mg N/L/d to 27.1 mg N/L/d (Figure 6-6). One of the reasons for the reduction of anammox capacities was the loss of anammox bacteria. Another possible reason was the lower temperature of 17.8 °C on the day when the capacity test was done. The specific anammox activity was found to slowly decrease during long-term operation at 20 °C and long SRT [46]. The long SRT (no deliberate sludge disposal in this study) would lead to the increase of fast-growing non-active and non-anammox microorganisms in the reactor, and a small amount of the slow-growing anammox bacteria might be washed out of the reactor though the biomass concentration remained stable. AAO capacities and ANO capacities also decreased to 84.3 mg N/L/d and 110.6 mg N/L/d, respectively, but were much higher than anammox capacities. The suppression of NOB not only relies on oxygen input control but the competition of anammox bacteria on nitrite.

When the anammox activity is much lower than NOB activity, higher NO_3^--N production by NOB is hardly avoidable and thus it is diffcult to achieve efficient TN removal. This was the reason that the ratio of NO_3^--N production/NH_4^+-N consumption (0.4) was higher than 0.3 during day 1 to day 43. Possibly caused by the lower temperature, the heterotrophic denitrification capacities decreased from 30.7 mg N/L/d to 22.9 mg N/L/d. To sum up, despite the severe biomass loss during the previous period and the resultant lower anammox capacities, stable TN removal was successfully maintained with lower NLR, but nitrogen removal performance was less efficient than that during day 1 to day 43.

Taken together, with precise oxygen input control in the SPAN reactor using suspended-growth sludge, stable nitrogen removal was maintained and NOB activity in the reactor was suppressed over long-term operation. Using suspended-growth sludge in SPAN, long-term stable nitrogen removal (NRR of 20.5 - 21.4 mg N/L/d) was achieved at the NLR of 38.5 - 57.7 mg N/L/d. At higher NLR of 76.9 mg N/L/d, TN was removed at higher NRR of 39.4 mg N/L/d, but the reactor was vulnerable to the biomass loss and anammox activity reduction when using suspended-growth biomass.

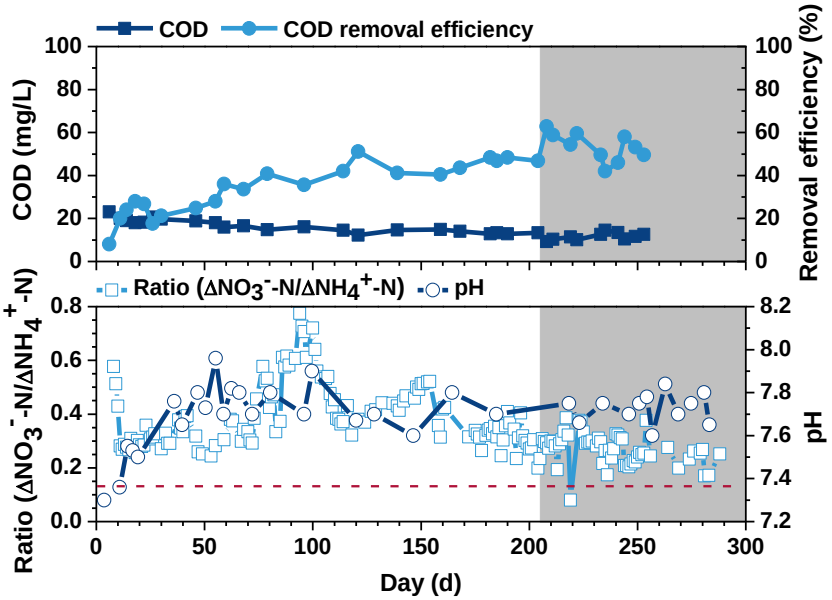

Figure 6-4. COD removal, the ratio of nitrate produced/ammonium consumed, and pH in the reactor. The red dash line indicates the theoretical ratio of nitrate produced /ammonium consumed with complete NOB suppression (0.13).

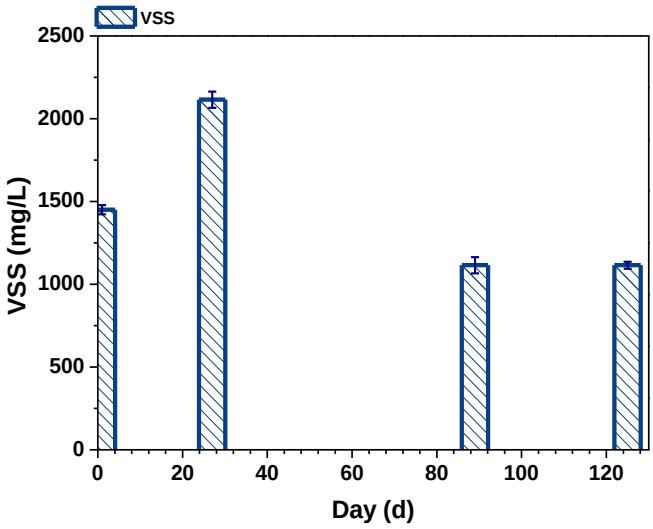

Figure 6-5. Biomass concentration in Stage 1.

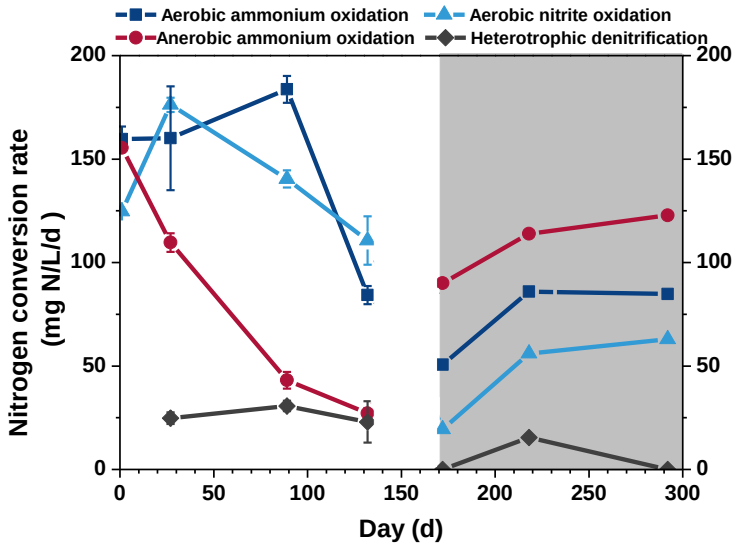

Figure 6-6. Capacities of the key nitrogen-conversion pathways in R1.

6.3.3 Stage 2: application of biofilm

The biofilm enables anammox bacteria to maintain a higher abundance and resistance against less favorable conditions such as low temperatures, thus preventing them from being washed out of the reactor [67-69]. In Stage 2, 1 L of PN-A sludge was inoculated into

the reactor and biofilm was formed (Figure 6-7). The NLR was set at 87.0 mg N/L/d (oxygen demand 389 mg O_2/d) and the water circulation rate was set at 67 mL/min (oxygen input 360 mg O_2/d). The temperature was less than 20 °C during most of the operation period and was 18.6 ± 0.7 °C at the end of the operation (Figure 6-2), while pH remained stable at 7.7 ± 0.2 (Figure 6-4). Higher COD removal efficiency of 51.8 ± 6.4% was achieved than in Stage 1 (Figure 6-4) which meant 2.3 mg NO_3^--N /L was removed by heterotrophic denitrification assuming all the removed COD was consumed by heterotrophic denitrifiers. Effluent NH_4^+-N gradually decreased to 6.8 ± 2.7 mg N /L (82.8 ± 7.0%) while NO_2^--N and NO_3^--N were relatively stable at 1.1 ± 0.3 mg N /L and 9.4 ± 2.2 mg N /L (Figure 6-3). The ratio of NO_3^--N production/ NH_4^+-N consumption also showed a decreasing trend to 0.23 (Figure 6-4), which is lower than the reported value of 0.28 achieved at a higher operating temperature of 25°C [83]. Compared with Stage 1, higher TN removal efficiency of 61.8 ± 5.4% and NRR of 53.8 ± 4.7 mg N /L/d were achieved in Stage 2 (Figure 6-2). The nitrogen removal performance was comparable with that of conventional biological nitrogen removal, i.e., nitrogen removal efficiency of 40% - 70% [104], and NRR of 20 - 120 mg N/L/d (for post-anoxic denitrification without exogenous carbon addition) [105, 106]. Compared with the reported study mentioned above, the nitrogen removal performance was better even at lower temperatures and with an almost negligible contribution of heterotrophic denitrification. More importantly, stable nitrogen removal was achieved during long-term operation.

With regard to the capacities of nitrogen-conversion pathways, the anammox capacities ranked the highest among the four major pathways and increased from the initial value of 90.1 mg N /L/d to122.8 mg N /L/d (Figure 6-6) suggesting anammox bacteria were efficiently retained and enriched even with higher NRR than the suspended-growth sludge in Stage 1. This proved the superiority of biofilm over suspended-growth sludge in keeping anammox bacteria and thereby maintaining stable nitrogen removal performance, especially at higher NLR. AAO capacities and ANO capacities also rose from 50.7 mg N /L/d to 84.8 mg N /L/d and from 19.4 mg N /L/d to 62.9 mg N /L/d, respectively. But the AAO capacities were lower than the NLR of 87.0 mg N /L/d, especially during the initial period, indicating that the nitritation process rather than anammox process was the rate-

limiting step that prevented the SPAN reactor from achieving a better nitrogen removal performance. This explained the higher effluent NH_4^+-N concentration and lower TN removal efficiency at the beginning of Stage 2 (Figure 6-3). This phenomenon was also observed in pilot-scale mainstream PN-A systems [10, 119]. The reason is the major functional microbial group AOB prefer to grow in the suspended sludge (6.0%-7.3%) over biofilm (0.5%-0.8%) while on the contrary, anammox bacteria are more abundant in biofilm (29.6%-55.6%) than in suspended sludge (15.6%-24.2%) [67]. Instead of the current biofilm SPAN system, a hybrid system that accommodates and takes advantage of the two biomass configurations (suspended-growth and biofilm) may be a better choice for future study. Heterotrophic denitrification capacities were low and varied between not detectable and 15.4 mg N /L/d. In conclusion, stable nitrogen removal and NOB suppression were achieved during long-term operation. The nitritation process was the rate-limiting step rather than the anammox process whose capacity was effectively retained using biofilm. Better nitrogen removal performance can be expected with the improvement of AAO capacity.

Figure 6-7. Image of the biofilm sludge in Stage 2.

6.4 Conclusions

This study demonstrated that long-term stable nitrogen removal was achieved in mainstream SPAN at temperatures around 20°C. Using suspended sludge, stable nitrogen removal (TN removal of 55.6% and NRR of 21.4 mg N/L/d) was maintained and NOB activity was suppressed over the long-term operation at NLR of 38.5 mg N/L/d. But at higher NLR of 76.9 mg N/L/d, the nitrogen performance deteriorated due to severe biomass loss and the resultant anammox activity reduction. When the NLR was decreased to 57.7 mg N/L/d to prevent biomass loss, stable nitrogen removal (NRR of 20.5 ± 4.3 mg N /L/d) was maintained despite the biomass loss, low anammox activity, and lower temperatures of 17.1 ± 0.4 °C. Using biofilm, anammox capacity was effectively retained and enhanced while the NOB activity in the reactor was suppressed, which allowed the realization of stable TN removal efficiency of 61.8 ± 5.4% and NRR of 53.8 ± 4.7 mg N /L/d at NLR of 87.0 mg N/L/d.

Chapter 7
Conclusions and Recommendations

7.1 Overview

The application of PN-A process was studied in two reactor configurations: IASBR and newly developed SPAN reactor. The PN-A process was first started up from the partial nitritation process in IASBR using return sludge as the inoculum, and then the emission and generation of the N_2O gas via the nitritation-related pathway in PN-A IASBR were investigated. SPAN technology, which can well control oxygen input in a way different from the conventional aeration methods, was developed. The long-term nitrogen removal performance of PN-A process in SPAN reactors treating ammonium-rich wastewater (30°C) and mainstream wastewater at around 20°C were evaluated.

7.2 Main conclusions

1. The IASBR configuration was efficient in starting up PN-A process with return sludge as the initial inoculum and achieving long-term efficient TN removal. Anammox bacteria *Candidatus Kuenenia* were enriched and acted as the main nitrogen removal contributor. *Nitrosomonas* was the dominant AOB genus and played a major role in the nitritation process, while NOB was effectively restrained.
2. In the PN-A IASBR, nitritation was the dominant N_2O generation pathway. How operating factors regulated N_2O generation via nitritation was revealed. When the oxygen transfer rate was the limiting factor, a higher oxygen transfer rate led to a higher nitritation activity and remarkably increased the PVG; when ammonium oxidation was the limiting factor, the increase of the oxygen transfer rate led to slightly reduced PVG; a higher oxygen transfer rate always resulted in a shorter duration of the peak N_2O generation rate; a lower initial ammonium concentration significantly reduced the N_2O generation mainly by reducing the PVG.
3. The developed SPAN technology was simple, yet highly reliable and efficient in precisely controlling the oxygen input and removing nitrogen from ammonium-rich wastewater. In the SPAN reactors, anammox bacteria were efficiently enriched, AOB

were well controlled, while NOB were maintained stable and effectively suppressed from producing nitrate.

4. SPAN technology was effective in achieving long-term nitrogen removal for the treatment of mainstream wastewater at around 20°C. Using suspended-growth sludge configuration,a long-term stable nitrogen removal was maintained and NOB activity was suppressed at the NLR ranging 38.5 - 57.7 mg N/L/d. Using biofilm configuration, the anammox capacity was effectively enhanced while the NOB activity in the reactor was suppressed, which allowed the realization of stable TN removal.

7.2.1 Summary

Currently, the enrichment of anammox biomass and the start up of PN-A process is drawing little attention from researchers, because the availability of anammox biomass is not a problem for lab-scale installations which only requires a small amount of anammox biomass and can be easily obtained. But with more and more full-scale application of PN-A process worldwide, the availability of anammox biomass is becoming a big problem, especially when no available anammox is present in the vicinity of the installations. For example, anammox sludge has to be imported from the Netherlands at the price of about 2.7 M € (around 1500 €/ton) to seed into a full-scale anammox reactor treating monosodium glutamate manufacturing wastewater in China [226]. Besides, sometimes the import of biomass from other countries is not allowed and has to follow stringent regulations. The study in Chapter 3 focused on starting up PN-A process using easily available conventional activated sludge. The results demonstrated that it is achievable to enrich anammox bacteria and start up PN-A process using return sludge as the inoculum in the IASBR.

N_2O is a potent greenhouse gas. It is estimated that N_2O is the third largest greenhouse gas source in the U.S., accounting for 6% of the total greenhouse gas emissions in 2017 [227]. The PN-A process accommodates all the known biological N_2O producing pathways, providing COD is present in the wastewater to be treated. Many studies have been conducted to investigate the factors impacting N_2O production and emission from PN-A

process, but an operable guideline for the mitigation of N_2O emission is still absent. This is largely due to the relationship between the operable factors and the N_2O production is not fully understood. This PhD research reveals that the oxygen transfer rate and nitritation activity both regulate N_2O generation via nitritation pathway in PN-A reactors, and provides practical suggestions for mitigating N_2O generation.

The development of SPAN technology, which was proved to be capable of treating both ammonium-rich wastewater and mainstream wastewater, provides PN-A design with simplicity and efficiency, especially for the decentralized wastewater treatment installations where complex control systems are not available or effective, such as the manure digestate treatment in Ireland, and rural domestic wastewater treatment in China.

The research results of this thesis will support the efforts to put the energy-efficient PN-A process into wider applications by developing reliable and efficient methods to: start up the PN-A process using the easily available activated sludge, achieve the precise oxygen input control for reliable NOB suppression and high-efficiency nitrogen removal in ammonium-rich wastewater, and realize long-term stable nitrogen removal from municipal wastewater. The revealing of the influencing factors of the N_2O generation via the nitritation pathway provides a deeper insight into the biological N_2O production in wastewater treatment facilities and operable guidance for the mitigation of the emission of this greenhouse gas during BNR practice.

7.3 Recommendations

Further studies are recommended, which may include:

1. The optimization of the methods in starting up PN-A process in IASBR, i.e., to develop methods to shorten the startup duration, and to investigate the effectiveness of different types of seeding sludge such as anaerobic sludge, the mixture of aerobic

and anaerobic sludge, or the mixture of a small proportion of anammox sludge and activated sludge.

2. The contribution of nitrifier denitrification and the NH_2OH oxidation to the nitritation-related N_2O generation and the mechanisms of nitration activity and oxygen transfer in regulating these two pathways; the metabolic activities of AOB, i.e., dynamics of the key intermediates (NH_2OH and nitric oxide (NO)) and gene expression, responding to the N_2O generation regulated by nitration activity and oxygen transfer; the identification of the operational boundaries for mitigating N_2O production and emission.

3. The optimization of the SPAN technology in achieving higher oxygen input with lower energy input; the establishment of mathematic models deciphering the relationship between the oxygen input and the operating conditions including temperature, wastewater characteristic, reactor configuration and dimensions (height, the size of the cross section, the shape of the cross section, etc.), and water circulation rate/shower rate.

4. The treatment of the mainstream wastewater with SPAN concept in the configurations of hybrid systems which accommodate both suspended sludge and biofilm and membrane bioreactors for efficient anammox biomass control and substrate diffusion.

5. The effect of COD/N ratio on the long-term nitrogen removal performance in the mainstream wastewater treatment using SPAN reactors.

6. The nitrogen removal of SPAN reactor treating mainstream wastewater at lower temperatures < 15°C.

References

1. Glibert, P.M., et al., Eutrophication. Oceanography, 2005. **18**(2): p. 198.
2. Chislock, M.F., et al., Eutrophication: causes, consequences, and controls in aquatic ecosystems. Nature Education Knowledge, 2013. **4**(4): p. 10.
3. Cai, T., S.Y. Park, and Y. Li, Nutrient recovery from wastewater streams by microalgae: Status and prospects. Renewable and Sustainable Energy Reviews, 2013. **19**: p. 360-369.
4. Ma, B., et al., Biological nitrogen removal from sewage via anammox: Recent advances. Bioresource Technology, 2016. **200**: p. 981-990.
5. Li, X., et al., Mainstream upflow nitritation-anammox system with hybrid anaerobic pretreatment: Long-term performance and microbial community dynamics. Water Research, 2017. **125**: p. 298-308.
6. Lackner, S., et al., Full-scale partial nitritation/anammox experiences – An application survey. Water Research, 2014. **55**(0): p. 292-303.
7. Mulder, A., et al., Anaerobic ammonium oxidation discovered in a denitrifying fluidized bed reactor. Fems Microbiology Ecology, 1995. **16**(3): p. 177-183.
8. Kuenen, J.G., Anammox bacteria: from discovery to application. Nature Reviews Microbiology, 2008. **6**(4): p. 320-326.
9. De Clippeleir, H., et al., Mainstream partial nitritation/anammox: Balancing overall sustainability with energy savings. Proceedings of the Water Environment Federation, 2012. **2012**(10): p. 5761-5770.
10. Lemaire, R., et al., MAINSTREAM DEAMMONIFICATION WITH ANITA™MOX PROCESS, in IWA World Water Congress and Exhibition. 2016: Brisbane, Australia.
11. Redmon, D., W.C. Boyle, and L. Ewing, Oxygen transfer efficiency measurements in mixed liquor using off-gas techniques. Journal (Water Pollution Control Federation), 1983: p. 1338-1347.
12. Gillot, S. and A. Héduit, Effect of air flow rate on oxygen transfer in an oxidation ditch equipped with fine bubble diffusers and slow speed mixers. Water Research, 2000. **34**(5): p. 1756-1762.
13. Qiu, S., et al., Start up of partial nitritation-anammox process using intermittently aerated sequencing batch reactor: Performance and microbial community dynamics. Science of The Total Environment, 2019. **647**: p. 1188-1198.
14. Wan, J., et al., COD capture: a feasible option towards energy self-sufficient domestic wastewater treatment. Scientific Reports, 2016. **6**: p. 25054.
15. Hoekstra, M., Mainstream anammox, potential & feasibility of autotrophic nitrogen removal. 2017, Delft University of Technology.
16. Mccarty, P.L., What is the Best Biological Process for Nitrogen Removal: When and Why? Environmental Science & Technology, 2018. **52**(7): p. 3835-3841.
17. Kuenen, J.G., B. Kartal, and M.C.M. Van Loosdrecht, Application of anammox for N-removal can turn sewage treatment plant into biofuel factory. Biofuels, 2011. **2**(3): p. 237-241.
18. Gu, Y., et al., The feasibility and challenges of energy self-sufficient wastewater treatment plants. Applied Energy, 2017. **204**: p. 1463-1475.
19. Kartal, B., et al., How to make a living from anaerobic ammonium oxidation. Fems Microbiology Reviews, 2013. **37**(3): p. 428-461.
20. Van Der Star, W.R.L., et al., Startup of reactors for anoxic ammonium oxidation: Experiences from the first full-scale anammox reactor in Rotterdam. Water Research, 2007. **41**(18): p. 4149-4163.

References

21. Jeanningros, Y., et al., Fast start-up of a pilot-scale deammonification sequencing batch reactor from an activated sludge inoculum. Water Science and Technology, 2010. **61**(6): p. 1393-1400.
22. Lackner, S., et al., Full-scale partial nitritation/anammox experiences - An application survey. Water Research, 2014. **55**: p. 292-303.
23. Third, K.A., et al., The CANON system (completely autotrophic nitrogen-removal over nitrite) under ammonium limitation: Interaction and competition between three groups of bacteria. Systematic and Applied Microbiology, 2001. **24**(4): p. 588-596.
24. Vela, J.D., et al., Prospects for Biological Nitrogen Removal from Anaerobic Effluents during Mainstream Wastewater Treatment. Environmental Science & Technology Letters, 2015. **2**(9): p. 234-244.
25. Chen, H., et al., Successful start-up of the anammox process: Influence of the seeding strategy on performance and granule properties. Bioresource Technology, 2016. **211**: p. 594-602.
26. Cao, Y., M.C.M. Van Loosdrecht, and G.T. Daigger, Mainstream partial nitritation–anammox in municipal wastewater treatment: status, bottlenecks, and further studies. Applied Microbiology and Biotechnology, 2017: p. 1-19.
27. Tang, C.-J., et al., Performance of high-loaded ANAMMOX UASB reactors containing granular sludge. Water Research, 2011. **45**(1): p. 135-144.
28. Kartal, B., J.G. Kuenen, and M.C.M. Van Loosdrecht, Sewage Treatment with Anammox. Science, 2010. **328**(5979): p. 702-703.
29. Kuai, L. and W. Verstraete, Ammonium removal by the oxygen-limited autotrophic nitrification-denitrification system. Applied and environmental microbiology, 1998. **64**(11): p. 4500-4506.
30. Windey, K., I. De Bo, and W. Verstraete, Oxygen-limited autotrophic nitrification-denitrification (OLAND) in a rotating biological contactor treating high-salinity wastewater. Water Research, 2005. **39**(18): p. 4512-4520.
31. Wett, B., Development and implementation of a robust deammonification process. Water Science and Technology, 2007. **56**(7): p. 81-88.
32. Wett, B., Solved upscaling problems for implementing deammonification of rejection water. Water science and technology, 2006. **53**(12): p. 121-128.
33. Morales, N., et al., Influence of dissolved oxygen concentration on the start-up of the anammox-based process: ELAN(R). Water Sci Technol, 2015. **72**(4): p. 520-7.
34. Li, J., et al., A critical review of one-stage anammox processes for treating industrial wastewater: Optimization strategies based on key functional microorganisms. Bioresource Technology, 2018. **265**: p. 498-505.
35. Zhang, J., et al., Start-up and bacterial communities of single-stage nitrogen removal using anammox and partial nitritation (SNAP) for treatment of high strength ammonia wastewater. Bioresource Technology, 2014. **169**: p. 652-657.
36. Wang, G., et al., Study of simultaneous partial nitrification, ANAMMOX and denitrification (SNAD) process in an intermittent aeration membrane bioreactor. Process Biochemistry, 2016. **51**(5): p. 632-641.
37. Ali, M. and S. Okabe, Anammox-based technologies for nitrogen removal: Advances in process start-up and remaining issues. Chemosphere, 2015. **141**: p. 144-153.
38. Liu, Y. and B.-J. Ni, Appropriate Fe (II) Addition Significantly Enhances Anaerobic Ammonium Oxidation (Anammox) Activity through Improving the Bacterial Growth Rate. Scientific Reports, 2015. **5**: p. 8204.
39. Lotti, T., et al., Faster through training: The anammox case. Water Research, 2015. **81**: p. 261-268.
40. Kartal, B., et al., Anammox-Growth Physiology, Cell Biology, and Metabolism, in Advances in Microbial Physiology, Vol 60, R.K. Poole, Editor. 2012. p. 211-262.

41. Ali, M., et al., Physiological characterization of anaerobic ammonium oxidizing bacterium 'Candidatus Jettenia caeni'. Environmental Microbiology, 2015. **17**(6): p. 2172-2189.
42. Van Der Star, W.R.L., et al., The membrane bioreactor: A novel tool to grow anammox bacteria as free cells. Biotechnology and Bioengineering, 2008. **101**(2): p. 286-294.
43. Kallistova, A.Y., et al., Role of anammox bacteria in removal of nitrogen compounds from wastewater. Microbiology, 2016. **85**(2): p. 140-156.
44. Awata, T., et al., Physiological Characterization of an Anaerobic Ammonium-Oxidizing Bacterium Belonging to the "Candidatus Scalindua" Group. Applied and Environmental Microbiology, 2013. **79**(13): p. 4145-4148.
45. Zhang, L., et al., Maximum specific growth rate of anammox bacteria revisited. Water Research, 2017. **116**: p. 296-303.
46. Hoekstra, M., et al., Deterioration of the anammox process at decreasing temperatures and long SRTs. Environmental Technology, 2018. **39**(5): p. 658-668.
47. Puyol, D., et al., Kinetic characterization of Brocadia spp.-dominated anammox cultures. Bioresource Technology, 2013. **139**: p. 94-100.
48. Mamoru, O., S. Hisashi, and O. Satoshi, Ecology and physiology of anaerobic ammonium oxidizing bacteria. Environmental Microbiology, 2016. **18**(9): p. 2784-2796.
49. Isanta, E., et al., Microbial community shifts on an anammox reactor after a temperature shock using 454-pyrosequencing analysis. Bioresource Technology, 2015. **181**: p. 207-213.
50. Tang, X., et al., Identification of the release and effects of AHLs in anammox culture for bacteria communication. Chemical Engineering Journal, 2015. **273**: p. 184-191.
51. Lotti, T., et al., Physiological and kinetic characterization of a suspended cell anammox culture. Water Research, 2014. **60**: p. 1-14.
52. Li, H., et al., Short- and long-term effects of manganese, zinc and copper ions on nitrogen removal in nitritation-anammox process. Chemosphere, 2018. **193**: p. 479-488.
53. Chen, H., et al., Enhancement of anammox performance by Cu(II), Ni(II) and Fe(III) supplementation. Chemosphere, 2014. **117**: p. 610-616.
54. Kimura, Y. and K. Isaka, Evaluation of inhibitory effects of heavy metals on anaerobic ammonium oxidation (anammox) by continuous feeding tests. Applied Microbiology and Biotechnology, 2014. **98**(16): p. 6965-6972.
55. Li, J., et al., Enhanced performance and kinetics of marine anammox bacteria (MAB) treating nitrogen-rich saline wastewater with Mn(II) and Ni(II) addition. Bioresource Technology, 2018. **249**: p. 1085-1091.
56. Waters, C.M. and B.L. Bassler, Quorum sensing: Cell-to-cell communication in bacteria, in Annual Review of Cell and Developmental Biology. 2005. p. 319-346.
57. Camilli, A. and B.L. Bassler, Bacterial small-molecule signaling pathways. Science, 2006. **311**(5764): p. 1113-1116.
58. Shrout, J.D. and R. Nerenberg, Monitoring Bacterial Twitter: Does Quorum Sensing Determine the Behavior of Water and Wastewater Treatment Biofilms? Environmental Science & Technology, 2012. **46**(4): p. 1995-2005.
59. Van Teeseling, M.C.F., et al., Anammox Planctomycetes have a peptidoglycan cell wall. Nature Communications, 2015. **6**.
60. Strous, M., et al., Missing lithotroph identified as new planctomycete. Nature, 1999. **400**(6743): p. 446-449.
61. De Clippeleir, H., et al., Long-chain acylhomoserine lactones increase the anoxic ammonium oxidation rate in an OLAND biofilm. Applied Microbiology and Biotechnology, 2011. **90**(4): p. 1511-1519.

62. Sun, Y., et al., Metagenomics-based interpretation of AHLs-mediated quorum sensing in Anammox biofilm reactors for low-strength wastewater treatment. Chemical Engineering Journal, 2018. **344**: p. 42-52.
63. Tang, X., et al., Metabolomics uncovers the regulatory pathway of acyl-homoserine lactones-based quorum sensing in anammox consortia. Environmental Science & Technology, 2018.
64. Strous, M., et al., Deciphering the evolution and metabolism of an anammox bacterium from a community genome. Nature, 2006. **440**(7085): p. 790-794.
65. Wett, B., et al., Expanding DEMON Sidestream Deammonification Technology Towards Mainstream Application. Water Environment Research, 2015. **87**(12): p. 2084-2089.
66. Liu, Y. and J.H. Tay, The essential role of hydrodynamic shear force in the formation of biofilm and granular sludge. Water Research, 2002. **36**(7): p. 1653-1665.
67. Wells, G.F., et al., Comparing the Resistance, Resilience, and Stability of Replicate Moving Bed Biofilm and Suspended Growth Combined Nitritation–Anammox Reactors. Environmental Science & Technology, 2017. **51**(9): p. 5108-5117.
68. Fernandez, I., et al., Biofilm and granular systems to improve Anammox biomass retention. Biochemical Engineering Journal, 2008. **42**(3): p. 308-313.
69. Guo, J., et al., Metagenomic analysis of anammox communities in three different microbial aggregates. Environmental Microbiology, 2016. **18**(9): p. 2979-2993.
70. Gilbert, E.M., et al., Comparing different reactor configurations for Partial Nitritation/Anammox at low temperatures. Water Research, 2015. **81**: p. 92-100.
71. Klaus, S., et al., Startup of a Partial Nitritation-Anammox MBBR and the Implementation of pH-Based Aeration Control. Water Environment Research, 2017. **89**(6): p. 500-508.
72. Arnaldos, M., et al., From the affinity constant to the half-saturation index: Understanding conventional modeling concepts in novel wastewater treatment processes. Water Research, 2015. **70**: p. 458-470.
73. Bothe, H., S. Ferguson, and W.E. Newton, Biology of the Nitrogen Cycle. 2006: Elsevier Science.
74. H.-D., P. and N. D.R., Characterization of two ammonia-oxidizing bacteria isolated from reactors operated with low dissolved oxygen concentrations. Journal of Applied Microbiology, 2007. **102**(5): p. 1401-1417.
75. Philips, S., H.J. Laanbroek, and W. Verstraete, Origin, causes and effects of increased nitrite concentrations in aquatic environments. Reviews in Environmental Science and Biotechnology, 2002. **1**(2): p. 115-141.
76. In 'T zandt, M.H., et al., The hunt for the most-wanted chemolithoautotrophic spookmicrobes. FEMS Microbiology Ecology, 2018. **94**(6): p. fiy064-fiy064.
77. Nowka, B., H. Daims, and E. Spieck, Comparison of Oxidation Kinetics of Nitrite-Oxidizing Bacteria: Nitrite Availability as a Key Factor in Niche Differentiation. Applied and Environmental Microbiology, 2015. **81**(2): p. 745-753.
78. Park, M.-R., H. Park, and K. Chandran, Molecular and Kinetic Characterization of Planktonic Nitrospira spp. Selectively Enriched from Activated Sludge. Environmental Science & Technology, 2017. **51**(5): p. 2720-2728.
79. Akaboci, T.R.V., et al., Effects of extremely low bulk liquid DO on autotrophic nitrogen removal performance and NOB suppression in side- and mainstream one-stage PNA. Journal of Chemical Technology & Biotechnology, 2017.
80. Malovanyy, A., J. Trela, and E. Plaza, Mainstream wastewater treatment in integrated fixed film activated sludge (IFAS) reactor by partial nitritation/anammox process. Bioresource Technology, 2015. **198**: p. 478-487.
81. Szatkowska, B., et al., A one-stage system with partial nitritation and Anammox processes in the moving-bed biofilm reactor. Water Science and Technology, 2007. **55**(8-9): p. 19-26.

82. Li, J., et al., Long-term partial nitrification in an intermittently aerated sequencing batch reactor (SBR) treating ammonium-rich wastewater under controlled oxygen-limited conditions. Biochemical Engineering Journal, 2011. **55**(3): p. 215-222.
83. Akaboci, T.R.V., et al., Assessment of operational conditions towards mainstream partial nitritation-anammox stability at moderate to low temperature: Reactor performance and bacterial community. Chemical Engineering Journal, 2018. **350**: p. 192-200.
84. Trojanowicz, K., E. Plaza, and J. Trela, Pilot scale studies on nitritation-anammox process for mainstream wastewater at low temperature. Water Sci Technol, 2016. **73**(4): p. 761-8.
85. Blum, J.-M., M.M. Jensen, and B.F. Smets, Nitrous oxide production in intermittently aerated Partial Nitritation-Anammox reactor: oxic N2O production dominates and relates with ammonia removal rate. Chemical Engineering Journal, 2018. **335**: p. 458-466.
86. Kuypers, M.M.M., H.K. Marchant, and B. Kartal, The microbial nitrogen-cycling network. Nature Reviews Microbiology, 2018. **16**: p. 263-276.
87. Zhan, X., Z. Hu, and G. Wu, Greenhouse Gas Emission and Mitigation in Municipal Wastewater Treatment Plants. 2018: IWA Publishing.
88. Dotro, G., et al., A review of the impact and potential of intermittent aeration on continuous flow nitrifying activated sludge. Environmental Technology, 2011. **32**(15): p. 1685-1697.
89. Sun, Y., et al., Enhanced biological nitrogen removal and N2O emission characteristics of the intermittent aeration activated sludge process. Reviews in Environmental Science and Bio/Technology, 2017.
90. Yu, R., et al., Mechanisms and Specific Directionality of Autotrophic Nitrous Oxide and Nitric Oxide Generation during Transient Anoxia. Environmental Science & Technology, 2010. **44**(4): p. 1313-1319.
91. Pan, M., et al., Characteristics of nitrous oxide (N2O) emission from intermittently aerated sequencing batch reactors (IASBRs) treating slaughterhouse wastewater at low temperature. Biochemical Engineering Journal, 2014. **86**: p. 62-68.
92. Castro-Barros, C.M., et al., Effect of aeration regime on N2O emission from partial nitritation-anammox in a full-scale granular sludge reactor. Water Research, 2015. **68**: p. 793-803.
93. Li, X., et al., Status, Challenges, and Perspectives of Mainstream Nitritation-Anammox for Wastewater Treatment. Water Environment Research, 2018. **90**(7): p. 634-649.
94. Sinha, B. and A.P. Annachhatre, Partial nitrification - operational parameters and microorganisms involved. Reviews in Environmental Science and Bio/Technology, 2007. **6**(4): p. 285-313.
95. Xu, G., et al., The challenges of mainstream deammonification process for municipal used water treatment. Applied Microbiology and Biotechnology, 2015. **99**(6): p. 2485-2490.
96. Jin, R.-C., et al., The inhibition of the Anammox process: A review. Chemical Engineering Journal, 2012. **197**: p. 67-79.
97. Poot, V., et al., Effects of the residual ammonium concentration on NOB repression during partial nitritation with granular sludge. Water Res, 2016. **106**: p. 518-530.
98. Agrawal, S., et al., Success of mainstream partial nitritation/anammox demands integration of engineering, microbiome and modeling insights. Current Opinion in Biotechnology, 2018. **50**: p. 214-221.
99. Poot, V., et al., Effects of the residual ammonium concentration on NOB repression during partial nitritation with granular sludge. Water Research, 2016. **106**: p. 518-530.
100. Henze, M., et al., Biological wastewater treatment: Principles, Modeling and Design. 2008: IWA publishing.

101. Zhu, G., et al., Biological Removal of Nitrogen from Wastewater, in Reviews of Environmental Contamination and Toxicology, D.M. Whitacre, Editor. 2008, Springer New York: New York, NY. p. 159-195.
102. Laureni, M., et al., Mainstream partial nitritation and anammox: long-term process stability and effluent quality at low temperatures. Water Res, 2016. **101**: p. 628-39.
103. Miao, Y., et al., Partial nitrification-anammox (PNA) treating sewage with intermittent aeration mode: Effect of influent C/N ratios. Chemical Engineering Journal, 2018. **334**: p. 664-672.
104. Qiu, Y., H.-C. Shi, and M. He, Nitrogen and Phosphorous Removal in Municipal Wastewater Treatment Plants in China: A Review. International Journal of Chemical Engineering, 2010. **2010**: p. 10.
105. Burton, F.L., et al., Wastewater Engineering: Treatment and Resource Recovery. 2013: McGraw-Hill Education.
106. Sun, S.-P., et al., Effective biological nitrogen removal treatment processes for domestic wastewaters with low C/N ratios: a review. Environmental Engineering Science, 2010. **27**(2): p. 111-126.
107. Gilbert, E.M., et al., Low Temperature Partial Nitritation/Anammox in a Moving Bed Biofilm Reactor Treating Low Strength Wastewater. Environmental Science & Technology, 2014. **48**(15): p. 8784-8792.
108. Li, X., et al., Nitrogen removal by granular nitritation–anammox in an upflow membrane-aerated biofilm reactor. Water Research, 2016. **94**: p. 23-31.
109. Yeshi, C., et al., Mainstream partial nitritation and anammox in a 200,000 m3/day activated sludge process in Singapore: scale-down by using laboratory fed-batch reactor. Water Sci Technol, 2016. **74**(1): p. 48-56.
110. O'shaughnessy, M., Mainstream deammonification. 2015: Water Environment Research Foundation Alexandria, VA.
111. Li, X., et al., Inhibition of nitrite oxidizing bacterial activity based on low nitrite concentration exposure in an auto-recycling PN-Anammox process under mainstream conditions. Bioresource Technology, 2019. **281**: p. 303-308.
112. Wang, C., et al., Achieving mainstream nitrogen removal through simultaneous partial nitrification, anammox and denitrification process in an integrated fixed film activated sludge reactor. Chemosphere, 2018. **203**: p. 457-466.
113. Dai, W., et al., Toward energy-neutral wastewater treatment: A membrane combined process of anaerobic digestion and nitritation–anammox for biogas recovery and nitrogen removal. Chemical Engineering Journal, 2015. **279**: p. 725-734.
114. Chen, R., et al., Successful operation performance and syntrophic micro-granule in partial nitritation and anammox reactor treating low-strength ammonia wastewater. Water Research, 2019. **155**: p. 288-299.
115. Hu, Z., et al., Nitrogen Removal by a Nitritation-Anammox Bioreactor at Low Temperature. Applied and Environmental Microbiology, 2013. **79**(8): p. 2807-2812.
116. Lackner, S., et al., Influence of seasonal temperature fluctuations on two different partial nitritation-anammox reactors treating mainstream municipal wastewater. Water Sci Technol, 2015. **72**(8): p. 1358-63.
117. Wang, K. 2018; Available from: http://www.sohu.com/a/270608809_698856.
118. De Clippeleir, H., et al., One-stage partial nitritation/anammox at 15 A degrees C on pretreated sewage: feasibility demonstration at lab-scale. Applied Microbiology and Biotechnology, 2013. **97**(23): p. 10199-10210.
119. Lotti, T., et al., Pilot-scale evaluation of anammox-based mainstream nitrogen removal from municipal wastewater. Environmental Technology, 2015. **36**(9): p. 1167-1177.
120. Hoekstra, M., et al., Towards mainstream Anammox; lessons learned from pilot-scale research at WWTP Dokhaven. Environmental Technology, 2018: p. 1-29.

121. Wett, B., et al., Going for mainstream deammonification from bench to full scale for maximized resource efficiency. Water Science and Technology, 2013. **68**(2): p. 283-289.
122. Elmitwalli, T.A., et al., Treatment of domestic sewage in a two-step anaerobic filter/anaerobic hybrid system at low temperature. Water Research, 2002. **36**(9): p. 2225-2232.
123. Henze, M., et al., Activated sludge models ASM1, ASM2, ASM2d and ASM3. 2000: IWA publishing.
124. Sobieszuk, P. and K.W. Szewczyk, Estimation of (C/N) Ratio for Microbial Denitrification. Environmental Technology, 2006. **27**(1): p. 103-108.
125. Han, M., et al., Impact of carbon to nitrogen ratio and aeration regime on mainstream deammonification. Water Science and Technology, 2016. **74**(2): p. 375-384.
126. Xie, G.-J., et al., Achieving high-level nitrogen removal in mainstream by coupling anammox with denitrifying anaerobic methane oxidation in a membrane biofilm reactor. Water Research, 2018. **131**: p. 196-204.
127. Cai, C., et al., Nitrate reduction by denitrifying anaerobic methane oxidizing microorganisms can reach a practically useful rate. Water Research, 2015. **87**: p. 211-217.
128. Ettwig, K.F., et al., Nitrite-driven anaerobic methane oxidation by oxygenic bacteria. Nature, 2010. **464**: p. 543.
129. Weber, K.A., L.A. Achenbach, and J.D. Coates, Microorganisms pumping iron: anaerobic microbial iron oxidation and reduction. Nature Reviews Microbiology, 2006. **4**: p. 752.
130. Yang, Y., et al., Nanostructured pyrrhotite supports autotrophic denitrification for simultaneous nitrogen and phosphorus removal from secondary effluents. Chemical Engineering Journal, 2017. **328**: p. 511-518.
131. Rivett, M.O., et al., Nitrate attenuation in groundwater: A review of biogeochemical controlling processes. Water Research, 2008. **42**(16): p. 4215-4232.
132. Nielsen, J.L. and P.H. Nielsen, Microbial Nitrate-Dependent Oxidation of Ferrous Iron in Activated Sludge. Environmental Science & Technology, 1998. **32**(22): p. 3556-3561.
133. Park, J.Y. and Y.J. Yoo, Biological nitrate removal in industrial wastewater treatment: which electron donor we can choose. Applied Microbiology and Biotechnology, 2009. **82**(3): p. 415-429.
134. Di Capua, F., et al., Electron donors for autotrophic denitrification. Chemical Engineering Journal, 2019. **362**: p. 922-937.
135. Zhang, Y., et al., Nutrient removal through pyrrhotite autotrophic denitrification: Implications for eutrophication control. Science of The Total Environment, 2019. **662**: p. 287-296.
136. Nerenberg, R., The membrane-biofilm reactor (MBfR) as a counter-diffusional biofilm process. Current Opinion in Biotechnology, 2016. **38**: p. 131-136.
137. Du, R., et al., Performance and microbial community analysis of a novel DEAMOX based on partial-denitrification and anammox treating ammonia and nitrate wastewaters. Water Research, 2017. **108**: p. 46-56.
138. Le, T., et al., Impact of carbon source and COD/N on the concurrent operation of partial denitrification and anammox. Water Environment Research, 2019. **91**(3): p. 185-197.
139. Ge, S., et al., Nitrite accumulation under constant temperature in anoxic denitrification process: The effects of carbon sources and COD/NO3-N. Bioresource Technology, 2012. **114**: p. 137-143.
140. Yang, X., S. Wang, and L. Zhou, Effect of carbon source, C/N ratio, nitrate and dissolved oxygen concentration on nitrite and ammonium production from denitrification process by Pseudomonasstutzeri D6. Bioresource Technology, 2012. **104**: p. 65-72.

141. Si, Z., et al., Rapid nitrite production via partial denitrification: pilot-scale operation and microbial community analysis. Environmental Science: Water Research & Technology, 2018. **4**(1): p. 80-86.
142. Qian, W., et al., Long-term effect of pH on denitrification: High pH benefits achieving partial-denitrification. Bioresource Technology, 2019. **278**: p. 444-449.
143. Wang, X., et al., Evaluating the potential for sustaining mainstream anammox by endogenous partial denitrification and phosphorus removal for energy-efficient wastewater treatment. Bioresource Technology, 2019. **284**: p. 302-314.
144. Du, R., et al., Synergy of partial-denitrification and anammox in continuously fed upflow sludge blanket reactor for simultaneous nitrate and ammonia removal at room temperature. Bioresource Technology, 2019. **274**: p. 386-394.
145. Pfluger, A.R., et al., Lifecycle Comparison of Mainstream Anaerobic Baffled Reactor and Conventional Activated Sludge Systems for Domestic Wastewater Treatment. Environmental Science & Technology, 2018. **52**(18): p. 10500-10510.
146. Nhat, P.T., et al., Application of a partial nitritation and anammox system for the old landfill leachate treatment. International Biodeterioration & Biodegradation, 2014. **95**: p. 144-150.
147. Wang, Z., et al., Continuous-flow combined process of nitritation and ANAMMOX for treatment of landfill leachate. Bioresource Technology, 2016. **214**: p. 514-519.
148. Wang, C.-C., et al., Simultaneous partial nitrification, anaerobic ammonium oxidation and denitrification (SNAD) in a full-scale landfill-leachate treatment plant. Journal of Hazardous Materials, 2010. **175**(1-3): p. 622-628.
149. Lieu, P.K., et al., Single-Stage Nitrogen Removal Using Anammox and Partial Nitritation (SNAP) for Treatment of Synthetic Landfill Leachate. Japanese Journal of Water Treatment Biology, 2005. **41**(2): p. 103-112.
150. Wang, S., et al., Anaerobic ammonium oxidation in traditional municipal wastewater treatment plants with low-strength ammonium loading: Widespread but overlooked. Water Research, 2015. **84**: p. 66-75.
151. Lv, Y., et al., Autotrophic nitrogen removal discovered in suspended nitritation system. Chemosphere, 2010. **79**(2): p. 180-185.
152. Zhang, Z., et al., Start-up of the Canon process from activated sludge under salt stress in a sequencing batch biofilm reactor (SBBR). Bioresource Technology, 2010. **101**(16): p. 6309-6314.
153. Yan, J., et al., Mimicking the oxygen minimum zones: stimulating interaction of aerobic archaeal and anaerobic bacterial ammonia oxidizers in a laboratory-scale model system. Environmental Microbiology, 2012. **14**(12): p. 3146-3158.
154. Fitzgerald, C.M., et al., Ammonia-oxidizing microbial communities in reactors with efficient nitrification at low-dissolved oxygen. Water Research, 2015. **70**: p. 38-51.
155. Stahl, D.A. and J.R. De La Torre, Physiology and diversity of ammonia-oxidizing archaea. Annual review of microbiology, 2012. **66**: p. 83-101.
156. Van De Graaf, A.A., et al., Autotrophic growth of anaerobic ammonium-oxidizing micro-organisms in a fluidized bed reactor. Microbiology 1996. **142**(8): p. 2187-2196.
157. Apha, Standard Methods for the Examination of Water and Wastewater. twentieth ed. 1998, Washington DC, USA: American Public Health Association.
158. Langille, M.G.I., et al., Predictive functional profiling of microbial communities using 16S rRNA marker gene sequences. Nature Biotechnology, 2013. **31**: p. 814.
159. Kim, D.-J., D.-I. Lee, and J. Keller, Effect of temperature and free ammonia on nitrification and nitrite accumulation in landfill leachate and analysis of its nitrifying bacterial community by FISH. Bioresource Technology, 2006. **97**(3): p. 459-468.

160. Ngo, H.-H., W. Guo, and W. Xing, Applied technologies in municipal solid waste landfill leachate treatment. Water and wastewater treatment technologies–applied technologies in municipal solid waste landfill, 2008.
161. Strous, M., et al., The sequencing batch reactor as a powerful tool for the study of slowly growing anaerobic ammonium-oxidizing microorganisms. Applied Microbiology and Biotechnology, 1998. **50**(5): p. 589-596.
162. Zhou, S., et al., The relationship between anammox and denitrification in the sediment of an inland river. Science of The Total Environment, 2014. **490**: p. 1029-1036.
163. Li J, S.K., Healy M, Zhan X, Rodgers M, Nutrient removal from slaughterhouse wastewater in an intermittently aerated sequencing batch biofilm reactor, in IWA Biofilm Technologies Conference. 2008: Singapore.
164. Tsoy, O.V., et al., Nitrogen Fixation and Molecular Oxygen: Comparative Genomic Reconstruction of Transcription Regulation in Alphaproteobacteria. Frontiers in Microbiology, 2016. **7**: p. 1343.
165. Xiao, P., et al., Effect of trace hydrazine addition on the functional bacterial community of a sequencing batch reactor performing completely autotrophic nitrogen removal over nitrite. Bioresource Technology, 2015. **175**: p. 216-223.
166. Pereira, A.D., et al., Microbial communities in anammox reactors: a review. Environmental Technology Reviews, 2017. **6**(1): p. 74-93.
167. Gupta, R.S. and E. Lorenzini, Phylogeny and molecular signatures (conserved proteins and indels) that are specific for the Bacteroidetes and Chlorobi species. BMC Evolutionary Biology, 2007. **7**: p. 71-71.
168. Gonzalez-Martinez, A., et al., Performance and bacterial community dynamics of a CANON bioreactor acclimated from high to low operational temperatures. Chemical Engineering Journal, 2016. **287**: p. 557-567.
169. Xu, J.-J., et al., Roles of MnO2 on performance, sludge characteristics and microbial community in anammox system. Science of The Total Environment, 2018. **633**: p. 848-856.
170. Wang, L., et al., Thermomonas carbonis sp. nov., isolated from the soil of a coal mine. International journal of systematic and evolutionary microbiology, 2014. **64**(11): p. 3631-3635.
171. Van Loosdrecht, M.C., et al., Experimental methods in wastewater treatment. 2016: IWA Publishing.
172. Khramenkov, S.V., et al., A novel bacterium carrying out anaerobic ammonium oxidation in a reactor for biological treatment of the filtrate of wastewater fermented sludge. Microbiology, 2013. **82**(5): p. 628-636.
173. Rios-Del Toro, E.E., N.E. Lopez-Lozano, and F.J. Cervantes, Up-flow anaerobic sediment trapped (UAST) reactor as a new configuration for the enrichment of anammox bacteria from marine sediments. Bioresource Technology, 2017. **238**: p. 528-533.
174. Francis, C.A., J.M. Beman, and M.M.M. Kuypers, New processes and players in the nitrogen cycle: the microbial ecology of anaerobic and archaeal ammonia oxidation. The Isme Journal, 2007. **1**: p. 19.
175. Schleper, C., Ammonia oxidation: different niches for bacteria and archaea? The Isme Journal, 2010. **4**: p. 1092.
176. Limpiyakorn, T., et al., Abundance of amoA genes of ammonia-oxidizing archaea and bacteria in activated sludge of full-scale wastewater treatment plants. Bioresource Technology, 2011. **102**(4): p. 3694-3701.
177. Liu, Y., et al., Autotrophic nitrogen removal in membrane-aerated biofilms: Archaeal ammonia oxidation versus bacterial ammonia oxidation. Chemical Engineering Journal, 2016. **302**: p. 535-544.

178. Reeve, P.J., et al., Effect of feed starvation on side-stream anammox activity and key microbial populations. Journal of Environmental Management, 2016. **171**: p. 121-127.
179. Gonzalez-Martinez, A., et al., Archaeal populations in full-scale autotrophic nitrogen removal bioreactors operated with different technologies: CANON, DEMON and partial nitritation/anammox. Chemical Engineering Journal, 2015. **277**: p. 194-201.
180. Cho, S., et al., Nitrogen removal performance and microbial community analysis of an anaerobic up-flow granular bed anammox reactor. Chemosphere, 2010. **78**(9): p. 1129-1135.
181. Sauder, L.A., et al., Cultivation and characterization of Candidatus Nitrosocosmicus exaquare, an ammonia-oxidizing archaeon from a municipal wastewater treatment system. The Isme Journal, 2017. **11**: p. 1142.
182. Srithep, P., P. Pornkulwat, and T. Limpiyakorn, Contribution of ammonia-oxidizing archaea and ammonia-oxidizing bacteria to ammonia oxidation in two nitrifying reactors. Environmental Science and Pollution Research, 2018. **25**(9): p. 8676-8687.
183. Zhu, X., et al., Ammonia oxidation pathways and nitrifier denitrification are significant sources of N2O and NO under low oxygen availability. Proceedings of the National Academy of Sciences, 2013. **110**(16): p. 6328-6333.
184. Hu, H.-W., D. Chen, and J.-Z. He, Microbial regulation of terrestrial nitrous oxide formation: understanding the biological pathways for prediction of emission rates. FEMS Microbiology Reviews, 2015. **39**(5): p. 729-749.
185. He, Q., et al., Impact of dissolved oxygen on the production of nitrous oxide in biological aerated filters. Frontiers of Environmental Science & Engineering, 2017. **11**(6): p. 16.
186. Harris, E., et al., Isotopic evidence for nitrous oxide production pathways in a partial nitritation-anammox reactor. Water Research, 2015. **83**: p. 258-270.
187. Myhre, G., et al., Anthropogenic and natural radiative forcing, in Climate Change 2013: The Physical Science Basis. Contribution of Working Group I to the Fifth Assessment Report of the Intergovernmental Panel on Climate Change, T.F. Stocker, D. Qin, G.-K. Plattner, M. Tignor, S.K. Allen, J. Boschung, A. Nauels, Y. Xia, V. Bex and P.M. Midgley, Editor. 2013: Cambridge, United Kingdom and New York, NY, USA. p. 658-740.
188. Desloover, J., et al., Strategies to mitigate N2O emissions from biological nitrogen removal systems. Current Opinion in Biotechnology, 2012. **23**(3): p. 474-482.
189. Wan, X., J.E. Baeten, and E.I.P. Volcke, Effect of operating conditions on N2O emissions from one-stage partial nitritation-anammox reactors. Biochemical Engineering Journal, 2019. **143**: p. 24-33.
190. Kampschreur, M.J., et al., Nitrous oxide emission during wastewater treatment. Water Research, 2009. **43**(17): p. 4093-4103.
191. Chandran, K., et al., Nitrous oxide production by lithotrophic ammonia-oxidizing bacteria and implications for engineered nitrogen-removal systems. Biochemical Society Transactions, 2011. **39**(6): p. 1832-1837.
192. Annavajhala, M.K., et al., Comammox Functionality Identified in Diverse Engineered Biological Wastewater Treatment Systems. Environmental Science & Technology Letters, 2018. **5**(2): p. 110-116.
193. Quan, X., et al., Nitrous oxide emission and nutrient removal in aerobic granular sludge sequencing batch reactors. Water Res, 2012. **46**(16): p. 4981-90.
194. Garcia-Ochoa, F. and E. Gomez, Bioreactor scale-up and oxygen transfer rate in microbial processes: An overview. Biotechnology Advances, 2009. **27**(2): p. 153-176.
195. Wunderlin, P., et al., Mechanisms of N2O production in biological wastewater treatment under nitrifying and denitrifying conditions. Water Research, 2012. **46**(4): p. 1027-1037.
196. Ma, C., et al., Pathways and Controls of N2O Production in Nitritation–Anammox Biomass. Environmental Science & Technology, 2017. **51**(16): p. 8981-8991.

197. Su, Q., et al., Low nitrous oxide production through nitrifier-denitrification in intermittent-feed high-rate nitritation reactors. Water Research, 2017. **123**: p. 429-438.
198. Peng, L., et al., N2O production by ammonia oxidizing bacteria in an enriched nitrifying sludge linearly depends on inorganic carbon concentration. Water Research, 2015. **74**: p. 58-66.
199. Law, Y., et al., N2O production rate of an enriched ammonia-oxidising bacteria culture exponentially correlates to its ammonia oxidation rate. Water Research, 2012. **46**(10): p. 3409-3419.
200. Lv, Y., et al., Effect of the dissolved oxygen concentration on the N2O emission from an autotrophic partial nitritation reactor treating high-ammonium wastewater. International Biodeterioration & Biodegradation, 2016. **114**: p. 209-215.
201. Peng, L., Y. Liu, and B.-J. Ni, Nitrous oxide production in completely autotrophic nitrogen removal biofilm process: A simulation study. Chemical Engineering Journal, 2016. **287**: p. 217-224.
202. Rathnayake, R.M.L.D., et al., Effects of dissolved oxygen and pH on nitrous oxide production rates in autotrophic partial nitrification granules. Bioresource Technology, 2015. **197**: p. 15-22.
203. Okabe, S., et al., N2O emission from a partial nitrification-anammox process and identification of a key biological process of N2O emission from anammox granules. Water Research, 2011. **45**(19): p. 6461-6470.
204. Sabba, F., et al., Hydroxylamine Diffusion Can Enhance N2O Emissions in Nitrifying Biofilms: A Modeling Study. Environmental Science & Technology, 2015. **49**(3): p. 1486-1494.
205. Henkel, J., Oxygen transfer phenomena in activated sludge. 2010: TU Darmstadt.
206. Huang, T., et al., Ammonia-oxidation as an engine to generate nitrous oxide in an intensively managed calcareous Fluvo-aquic soil. Scientific Reports, 2014. **4**: p. 3950.
207. Avrahami, S., R. Conrad, and G. Braker, Effect of Soil Ammonium Concentration on N₂O Release and on the Community Structure of Ammonia Oxidizers and Denitrifiers. Applied and Environmental Microbiology, 2002. **68**(11): p. 5685-5692.
208. Burgess, J.E., et al., Dinitrogen oxide production by a mixed culture of nitrifying bacteria during ammonia shock loading and aeration failure. Journal of Industrial Microbiology and Biotechnology, 2002. **29**(6): p. 309-313.
209. Yang, S., et al., Effects of step-feed on long-term performances and N2O emissions of partial nitrifying granules. Bioresource Technology, 2013. **143**: p. 682-685.
210. Yang, Q., et al., N2O production during nitrogen removal via nitrite from domestic wastewater: main sources and control method. Environmental Science & Technology, 2009. **43**(24): p. 9400-9406.
211. Åmand, L., G. Olsson, and B. Carlsson, Aeration control – a review. Water Science and Technology, 2013. **67**(11): p. 2374-2398.
212. Christensson, M., et al., Experience from start-ups of the first ANITA Mox Plants. Water Science and Technology, 2013. **67**(12): p. 2677-2684.
213. Rosenwinkel, K.-H. and A. Cornelius, Deammonification in the Moving-Bed Process for the Treatment of Wastewater with High Ammonia Content. Chemical Engineering & Technology, 2005. **28**(1): p. 49-52.
214. Baquero-Rodríguez, G.A., et al., A Critical Review of the Factors Affecting Modeling Oxygen Transfer by Fine-Pore Diffusers in Activated Sludge. Water Environment Research, 2018. **90**(5): p. 431-441.
215. Vogelaar, J.C.T., et al., Temperature effects on the oxygen transfer rate between 20 and 55°C. Water Research, 2000. **34**(3): p. 1037-1041.
216. Lee, J., Development of a model to determine mass transfer coefficient and oxygen solubility in bioreactors. Heliyon, 2017. **3**(2): p. e00248.

217. Wang, X. and D. Gao, In-situ restoration of one-stage partial nitritation-anammox process deteriorated by nitrate build-up via elevated substrate levels. Scientific Reports, 2016. **6**: p. 37500.
218. Joss, A., et al., Combined Nitritation–Anammox: Advances in Understanding Process Stability. Environmental Science & Technology, 2011. **45**(22): p. 9735-9742.
219. Baker, S.C., et al., Molecular Genetics of the GenusParacoccus: Metabolically Versatile Bacteria with Bioenergetic Flexibility. Microbiology and Molecular Biology Reviews, 1998. **62**(4): p. 1046-1078.
220. Van Kessel, M.a.H.J., et al., Complete nitrification by a single microorganism. Nature, 2015. **528**: p. 555.
221. Daims, H., et al., Complete nitrification by Nitrospira bacteria. Nature, 2015. **528**: p. 504.
222. Chan, Y.J., et al., A review on anaerobic–aerobic treatment of industrial and municipal wastewater. Chemical Engineering Journal, 2009. **155**(1): p. 1-18.
223. Malovanyy, A., et al., Combination of upflow anaerobic sludge blanket (UASB) reactor and partial nitritation/anammox moving bed biofilm reactor (MBBR) for municipal wastewater treatment. Bioresource Technology, 2015. **180**: p. 144-153.
224. He, S., et al., Effects of temperature on anammox performance and community structure. Bioresource Technology, 2018. **260**: p. 186-195.
225. T., L., K. R., and V.L. M.C.M., Effect of temperature change on anammox activity. Biotechnology and Bioengineering, 2015. **112**(1): p. 98-103.
226. Xiaoyong Hui, Y.Z. The treatment of monosodium glutamate manufacturing wastewater. 2010; Available from: http://membranes.com.cn/xingyedongtai/gongyexinwen/2015-01-19/8190.html.
227. Epa-U.S. Overview of Greenhouse Gases. 2017; Available from: https://www.epa.gov/ghgemissions/overview-greenhouse-gases.

Publications

Peer-reviewed journal paper:

Songkai Qiu, Yuansheng Hu, Rui Liu, Xiaolin Sheng, Lujun Chen, Guangxue Wu, Hongying Hu, Xinmin Zhan. Start up of partial nitritation-anammox process using intermittently aerated sequencing batch reactor: Performance and microbial community dynamics. **Science of The Total Environment**, 2019. 647: p. 1188-1198.

Manuscripts in preparation:

[1] **Songkai Qiu**, Rui Liu, Lvjun Chen, Xinmin Zhan. What's the possible way for successful mainstream partial nitritation-anammox application? (Ready to submit)
[2] **Songkai Qiu**, Zebing Li, Yuansheng Hu, Rui Liu, Xiaolin Sheng, Lujun Chen, Xinmin Zhan. The mechanisms of oxygen transfer rate and nitritation activity in regulating the N_2O generation via nitritation. (Ready to submit)
[3] **Songkai Qiu**, Zebing Li, Xiaolin Sheng, Rui Liu, Lujun Chen, Alexandre Barretto de Menezes, Xinmin Zhan. A novel system with precise oxygen input control: application of the partial nitritation-anammox process. (Ready to submit, but subject to patent application)
[4] **Songkai Qiu**, Zebing Li, Xiaolin Sheng, Rui Liu, Lujun Chen, Xinmin Zhan. Mainstream partial nitritation-anammox in a novel reactor with precise oxygen input control. (Ready to submit, but subject to patent application)

Disclosure:

A Simple Process for Autotrophic Nitrogen-removal (SPAN) from wastewater. (In progress)

Conference presentations:

[1] **Songkai Qiu**, Xinmin Zhan. Mechanisms of oxygen transfer rate and nitritation activity in regulating the N_2O generation via nitritation. The 8th Annual General Meeting (AGM) of the Ireland Chinese Association of Environment, Resources & Energy (ICAERE), 2019, Galway, Ireland. (Oral presentation)
[2] **Songkai Qiu**, Xinmin Zhan. A novel reactor with precise and straightforward oxygen-input control: application of partial nitritation-anammox process. The 7th Annual General Meeting (AGM) of the Ireland Chinese Association of Environment, Resources & Energy (ICAERE), 2018, Dublin, Ireland. (Oral presentation)
[3] **Songkai Qiu**, Xinmin Zhan. Occurrence of anammox in an intermittently aerated partial nitrification reactor. The 15th IWA World Conference on Anaerobic Digestion - Towards a more sustainable world, 2017, Beijing, China. (Oral presentation)
[4] **Songkai Qiu**, Xinmin Zhan. Metagenomic insights into the microbial community structures in an intermittently aerated partial nitrification reactor. The 6th Annual

General Meeting (AGM) of the Ireland Chinese Association of Environment, Resources & Energy (ICAERE), 2017, Galway, Ireland. (Oral presentation)

[5] **Songkai Qiu**, Xinmin Zhan. Strategies for Start-up and Maintenance of Efficient Partial Nitrification in an Intermittently Aerated SBR. 2016 - Livestock Waste Conference, 2016, Galway, Ireland. (Poster presentation)